UNIVERSITY OF CALIFORNIA, SAN DIEGO
SAN DIEGO STATE UNIVERSITY

Synthesis of Macrocycles and Their Biological Evaluation as Antitumor and Antibacterial Agents

A dissertation submitted in partial satisfaction of the
requirements for the degree Doctor of Philosophy

in

Chemistry

by

Po-Shen Pan

Committee in charge:

University of California, San Diego

Professor William Fenical

Professor Andrew Kummel

Professor Yitzhak Tor

San Diego State University

Professor Shelli R. McAlpine, Chair

Professor Thomas E. Cole

Professor Terrence G. Frey

2008

The Dissertation of Po-Shen Pan is approved, and it is acceptable in quality and form for publication on microfilm:

_____

_____

_____

_____

_____

_____
Chair

University of California, San Diego

San Diego State University

2008

DEDICATION

To mom and dad, and my Stephanie

TABLE OF CONTENTS

LIST OF ABBREVIATIONS

Bn	Benzyl
Boc	N-*tert*-butoxycarbonyl
DCM	Dichloromethane
DEPBT	3-(Diethoxyphosphoryloxy)-1,2,3- benzotriazin-4(3*H*)-one
DIPEA	*N*,*N*-Diisopropylethylamine
DMF	*N*,*N*-Dimethylformamide
Fmoc	9-fluorenylmethoxycarbonyl
HATU	O-(7-azabenzatrizol-1-yl)-*N*,*N*,*N*',*N*'-Tetramethyluronium hexafluorophosphate
HPLC	High-performance liquid chromatography
NMR	Nuclear Magnetic Resonance Spectrometry
Oxone	Potassium peroxymonosulfate
TBAF	Tetrabutylammonium fluoride
TBTU	2-(1H-Benzotriazole-1-yl)-1,1,3,3-tetramethyluronium tetrafluoroborate
THF	Tetrahydrofuran
TLC	Thin Layer Chromatography
TFA	Trifluoroacetic acid
TIPS	Triisopropyl Silyl
Z	Carboxybenzyl

LIST OF FIGURES

ACKNOWLEDGEMENTS

I would like to express my gratitude to all those who gave me the possibility to complete this thesis.

First, I am deeply grateful to my Ph. D advisor Professor Shelli R. McAlpine whose help, stimulating suggestions, and encouragement helped me in all the time of my research. Throughout my dissertation-writing period, she provided encouragement, sound advice, good company, and lots of good ideas. It is difficult to overstate my gratitude to her for the enthusiasm and inspiration, which was always there when I needed it.

I am indebted to my many colleagues for providing a stimulating and fun environment in which to learn and grow. I am especially grateful to Rodrigo, my dear friend, with his encouragement, I started to love learning chemical biology. It is such a pleasure working with him, and I will never forget the "paint ball" game we went to - that was really fun! I am also very grateful to Vasko, my dear friend, who helped me to solve countless biology related problems. I am sorry to drag you on Saturday to prove read my dissertation until 4am the next day. I will never forget the time we spent smoking cigar at Sydney opera house!! Thank you Erin, who's not only my colleague but also my shopping supervisor! Her suggestions on shopping were amazing and inspirational; you've saved me so many times! I am very grateful to Stephanie for her help with revising my dissertation. We've spent the good time in Australia, especially you convinced me to take vodka shots! I am very grateful to Melinda, William, Rob S and Leslie who also help me on revising my dissertation. Special thank to my brother, Eddie,

you have been a huge support throughout my study. I really enjoy the time we spent talking not only on professional matters but also about our childhood memories, it is an unspeakable experience to have you here.

My former colleagues supported me in my research work. I want to thank them for all their help, support, and valuable suggestions for my work. Thank you Chris Carroll, Ricardo Corral, Irene Medina, and Jennifer Robinson. Especially I am obliged to Lisa Liotta as she was a "mother figure" in the lab. You taught me how to get through the difficult times and take them as the challenge with an optimistic attitude. I also want to thank Ahmet Kekec, you are not only my colleague, but my dear friend. You guys have made my study at San Diego State a very unforgettable journey over all those years.

I would like to give my special thanks to my fiancé Mei-Hua (Stephanie) whose patient and love enabled me to complete this work. You helped me get through the difficult times, and for all the emotional support. I am especially thankful to your help with my dissertation editing. I wish you the best for your journey to become the most outstanding designer ever, even though I know you already are! I love you.

I cannot end without expressing my utmost gratitude to my mom and dad. You raised me, supported me, and loved me. Without your encouragement and support, I would never have made it. This dissertation is dedicated to you.

Chapter 2 and 3, in part, has been published as it may appear in "Identification of Sansalvamide a analog potent against pancreatic cancer cell lines", ***Bioorganic and Medicinal Chemistry Letters,*** *17*, **2007**, 5072-5077. Po-Shen Pan, Kathleen L. McGuire and Shelli R. McAlpine. The dissertation author was the primary author of this paper.

Chapter 4, in full, is a reprint of the material, as it appears in "Novel antibiotics: C-2 symmetrical macrocycles inhibiting Holliday junction DNA binding by *E. coli* RuvC", ***Bioorganic and Medicinal Chemistry,*** *14*, **2006**, 4731-4739. Po-Shen Pan, Fiona A. Curtis, Chris L. Carroll, Irene Medina, Lisa Liotta, Gary J. Sharples, and Shelli R. McAlpine. The dissertation author was the primary author of this paper.

VITA

1994-1998 Fu-Jen Catholic University
Department of Applied Chemistry
Bachelor of Science in Chemistry

1998-2000 National Chao-Tung University
Department of Applied Chemistry
Master of Science in Chemistry

2000-2002 Industrial Technology Research Institute Taiwan
IC packaging material department
Research Associate

2003-2008 University of California at San Diego /San Diego State University
Department of Chemistry and Biochemistry
Joint Doctor of Philosophy in Chemistry

PUBLICATIONS

Referred Publications

** Denotes PI on papers, order of authors indicates relative intellectual contributions, where first author contributed the most after the PI contribution*

12 **A Comprehensive Study of Sansalvamide A Derivatives: Their Structure-Activity Relationships and Their Binding Mode to Hsp90** **2008**
Po-Shen Pan†, Robert C. Vasko†, Stephanie A. Lapera, Melinda R. Davis, William S. Disman, David Vander Velde, Palk Thepchatri, James Snyder, and Shelli R. McAlpine*,
Journal of Medicinal Chemistry, **2008**, submitted

11 **Structure-Activity of Sansalvamide A Derivatives and Their Apoptotic Activity in the Pancreatic Cancer Cell Line PL-45** **2008**
Rodrigo A. Rodriguez, **Po-Shen Pan**, Robert C. Vasko, Chung-Mao Pan, and Shelli R. McAlpine*
Journal of the Mexican Chemical Society, **2008,** *in press*

10 **New Class of Potent Decapeptide Macrocycles** **2007**
Melinda R. Davis, Thomas J. Styers, Rodrigo A. Rodriguez, **Po-Shen Pan**, Robert C. Vasko, and Shelli R. McAlpine*,
Organic Letters, *v10*, p177-180, **2007**

9 **Synthesis and Cytotoxicity of FR235222 Derivatives** **2007**
Erinprit K. Singh, Suchitra Ravula, Chung-Mao Pan, **Po-Shen Pan**, Stephanie A. Lapera, and, and Shelli R. McAlpine*, **2007**
Bioorganic & Med. Chem. Lett, *18,* p2549-2554, **2008**

8 **Identification of Sansalvamide A analog potent against pancreatic cancer cell lines** **2007**
Po-Shen Pan, Kathleen L. McGuire, and Shelli R. McAlpine*
Bioorganic & Med. Chem. Lett*, 17, p5072-5077,* **2007**

7 **Synthesis of second generation Sansalvamide A derivatives: Novel Templates as Potential Anti-tumor Agents** **2007**
Rodrigo Rodriguez, **Po-Shen Pan**, Chung-Mao Pan, Suchitra Ravula, Stephanie Lapera, Erin Singh, Thomas J. Styers, Julia Cajica, Joseph D. Brown, Emily Parry, Katerina Otrubova, and Shelli R. McAlpine*
Journal of Organic Chemistry*, v72,* p1980-2002, **2007**

6 **Synthesis of Sansalvamide A derivatives and their cytotoxicity in colon cancer cell line HT-29** **2006**
Thomas J. Styers, Ahmet Kekec, Rodrigo Rodriguez, Joseph D. Brown, Julia Cajica, Chris L. Carroll, **Po-Shen Pan**, Irene Medina, Ricardo Corral, Jennifer V. C. Johnston, Emily Parry, Stephanie Lapera, Katerina Otrubova, Kathleen L. McGuire,* and Shelli R. McAlpine*
Bioorganic and Medicinal Chemistry*, v14,* p5625-5631, **2006**

5 **Novel Antibiotics: C-2 symmetrical macrocycles inhibiting Holliday Junction DNA binding by E. coli RuvC** **2006**
Po-Shen Pan, Fiona A. Curtis, Chris L. Carroll, Irene Medina, Lisa A. Liotta, Gary J. Sharples, and Shelli R. McAlpine*
Bioorganic and Medicinal Chemistry*, v14,* p4731-4739, **2006**

4 **Synthesis and novel structure-activity relationships of potent Sansalvamide A derivatives** **2006**
Katerina Otrubova, Thomas J. Styers, **Po-Shen Pan**, Rodrigo Rodriguez, Kathleen L. McGuire,* and Shelli R. McAlpine*
Chemical Communications, p1033-1034, **2006**

3 **High-yielding macrocyclization conditions used in the synthesis of novel Sansalvamide A Derivatives macrocyclization conditions** **2006**
Thomas J. Styers, Rodrigo Rodriguez, **Po-Shen Pan**, and Shelli R. McAlpine*
Tetrahedron Letters, *v47*, p515-517, **2006**

2 **Synthesis and Cytotoxicity of Novel Sansalvamide A derivatives** **2005**
Chris L. Carroll, Jennifer V. C. Johnston, Ahmet Kekec, Joe Brown, Emily Parry, Julia Cajica, Irene Medina, Kristina M. Cook, **Po-Shen Pan**, and Shelli R. McAlpine*
Organic Letters, *v7* p3481-3484, **2005**

1 **Novel Antibiotics: second generation macrocyclic peptides designed to trap holliday junctions**
Lisa A. Liotta, Irene Medina, Jennifer L. Robinson, Chris L. Carroll, **2004**
Po-Shen Pan, Ricardo Corral, Jennifer V. C. Johnston, Kristina M. Cook, Fiona A. Curtis, Gary J. Sharples and Shelli R. McAlpine*
Tetrahedron Letters, *v45*, p8447-8450 **2004**

FIELDS OF STUDY

Major Field: Organic Synthesis

Studies In Chemistry

Professor Shelli R. McAlpine

ABSTRACT OF THE DISSERTATION

Synthesis of Macrocycles and Their Biological Evaluation as

Antitumor and Antibacterial Agents

by

Po-Shen Pan

Doctor of Philosophy in Chemistry

University of California, San Diego, 2008
San Diego State University, 2008

Professor Shelli R. McAlpine, Chair

Chapter 1

The history of the cyclic peptides was briefly introduced. The syntheses of cyclic peptides via solid-phase strategy as well as solution-phase strategy were also discussed. The aims of this research are listed at the end of this chapter.

Chapter 2 and 3

Seven Sansalvamide A derivatives have been synthesized and sixty-four Sansalvamide A peptide derivatives were tested by using ^{3}H thymidine inhibition assays in two pancreatic cancer cell lines (PL45 and BxPC-3) to evaluate their **S**tructure-**A**ctivity **R**elationships (SAR). Six compounds show greater cytotoxicity against pancreatic cancer cell lines than the commonly used drug, 5-FU, and demonstrate potency on par with treatments used for other cancers. Four compounds have low micromolar IC_{50} values against BxPC-3 and PL45 and are ~20 fold more active than the parent natural product Sansalvamide A peptide (San A). SAR studies show the inclusion of a single *N*-methyl and/ or D-amino acid appears to be critical for presenting the active conformation of the five San A peptide derivatives to their biological target(s).

Chapter 4

Holliday junctions (HJs) are formed as transient DNA intermediates during site-specific and homologous recombination. Trapping HJs leads to bacterial cell death by preventing proper segregation of the resulting interlinked chromosomes, making them ideal targets for potential new antibiotics. Macrocyclic peptides designed to trap this intermediate were synthesized in the hopes of designing compounds capable of antibacterial activity. Ten macrocycles, both hexameric and octameric peptides, proved they were capable of trapping HJs in vitro. Those macrocycles containing tyrosine residues proved most effective. These data demonstrate that C-2 symmetrical macrocycles offer excellent synthetic targets for the development of novel antibiotic

agents. Furthermore, the active compounds provide valuable tools for probing different pathways of recombinational exchange.

Chapter 5

Triostin A is a bicyclic octadepsipeptide, a member of the quinoxaline family of antitumor agents, and can efficiently block both transcription and replication via specific binding at GC positions in the minor groove of dsDNA. Its derivative, Azatandem, was shown to possess antitumor potency. Our efforts to improve the preparation of such derivatives have provided a unique synthetic approach via use of the KAHA (α-**K**eto**a**cid-**H**ydroxyl**a**mine) ligation reaction to furnish the bicyclic core. This proposed strategy will provide structurally diverse Triostin A derivatives in an efficient manner.

Chapter 1

Introduction

1.1 History of Cyclic Peptides

Cyclic peptides are primarily derived from natural products found in marine sponges, tunicates, fungi bacteria and other lower animal forms.[1, 2] Many cyclic peptides are found to exhibit multiple types of biological activity including: antibacterial, antiviral, anti-inflammatory and immunosuppression. Compared to linear peptides, cyclic peptides are generally more resistant to enzymatic degradation by amino peptidases and carboxy peptidases. In addition, the cyclic structure reduces the freedom of peptide conformation and allows the cyclic peptide to have a higher binding affinity, which eventually increases its biological potency. Thus, cyclic peptides provide promising lead compounds for drug development.[1, 3-5] Described here are two examples of exceptional drugs on the market that are well-established cyclic peptides. These drugs are currently vital compounds that are considered imperative in their respective fields for treatment and as such they both represent examples of the future of cyclic peptide drugs.

Cyclosporine A, a cyclic peptide drug on the market (Neoral™) (**Figure 1.1**),[6] is a metabolite produced by *Tolypocladium inflatum* that isolated in was 1970 at Sandoz (now Novartis). In 1976 it was found to have very potent immunosuppressant activity. Cyclosporine A was approved by the FDA in 1983. It is the primary drug of choice for

organ transplant patients, as it suppresses the immune response and decreases the risk of the organ rejection. Its mechanism of action involves interrupting the signaling pathway that is required to activate T cells.[7] The annual sale of cyclosporin A is approximately one billion US dollars and is considered as one of the most successful examples of cyclic peptides as drugs.

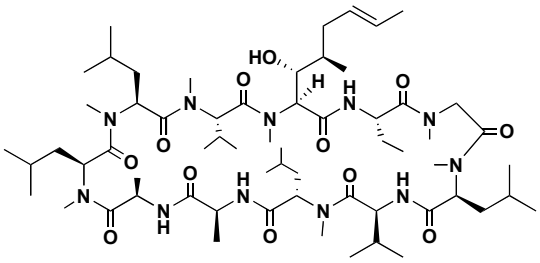

Figure 1.1. Cyclosporine A.

Another well known cyclic peptide drug is Vancomycin (Vancocin™)[8] (**Figure 1.2**). It was found and isolated from the soil microbe *Amycolatopsis orientalis* from the jungle of Borneo in 1956,[9] and was later introduced to the market by Eli Lilly in 1958[9]. It is a glycopeptide that possesses antibiotic activity against Gram-positive bacteria, and is considered to be the "last resort treatment" and used when other antibiotics have failed. Its mechanism of action involves preventing the synthesis of the peptidoglycan layer of the cell wall, thus inhibits the growth of the Gram-positive bacteria because it can no longer synthesize its cell wall.

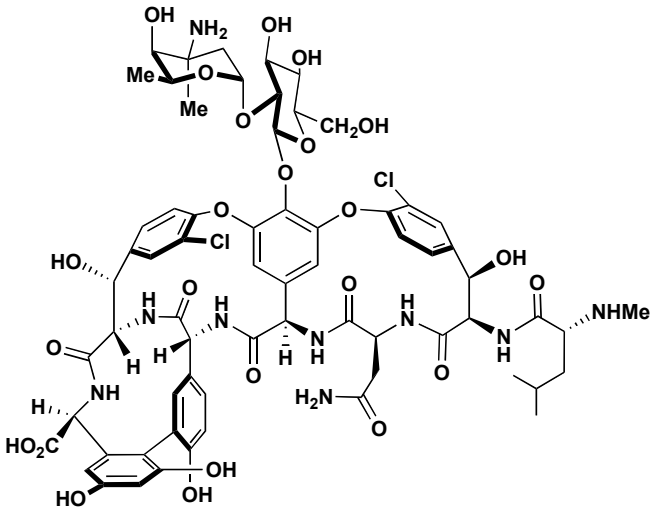

Figure 1.2. Vancomycin.

1.2 Synthesis of Cyclic Peptide

Macrocyclization strategy for cyclic peptides can be summarized into 3 different categories: (1) "Side-chain-to-side-chain" strategy,[4, 10] (2) "Side-Chain to-End" Strategy,[4, 11] and (3) "Head-to-Tail" Strategy.[4, 12] In category 1: "side-chain to side-chain" strategy, macrocyclization is carried out between the side chains of the linear precursor. The most straightforward route to achieve side-chain to side-chain macrocyclization is to incorporate properly protected Asp and Lys amino acids into the linear precursor backbone so that conventional peptide coupling reaction can be performed to yield cyclic product after the protecting groups of Asp and Lys are removed. An example of side-chain to side-chain strategy was reported by Rana and co-workers.[12] They reported the design and the synthesis of cyclic peptide (**Figure 1.3**), which interrupts the HIV-1 Tat - (TAR) RNA interactions leading to the inhibition of HIV-1 gene expression.[13].[12]

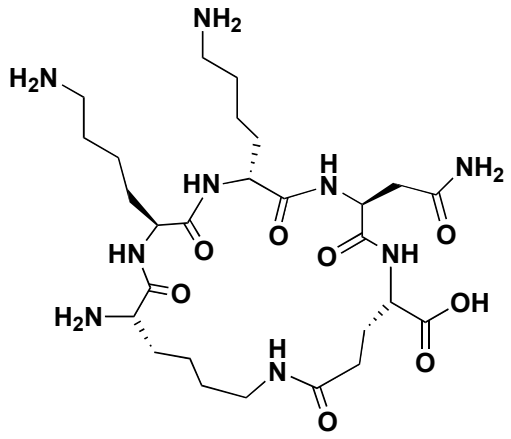

Figure 1.3. Macrocycle Synthesized via Side-Chain-to Side-Chain Strategy.

In the "Side-Chain to-End" Strategy,[4] macrocyclization is carried out between the side chain to the *N*-or *C*-terminus. Yamasaki and co-workers reported a solution-phase synthesis of an endothelin antagonis cyclic peptide, RES-701-1 (**Figure 1.4)** via this method. [11]

Figure 1.4. Macrocycle (RES701-1) Synthesized via Side-Chain-to End Strategy.

In the "Head-to-Tail" Strategy, macrocyclization is carried out between the *N*-and *C*-termini.[4] This head to tail approach is the most commonly used strategy to synthesize cyclic peptides. This chapter will focus mainly on this strategy and how it is applied during solid-phase peptide synthesis and solution-phase synthesis. An example of cyclic peptide, Tyrocidine A, was synthesized via this strategy (**Figure 1.5**).[14]

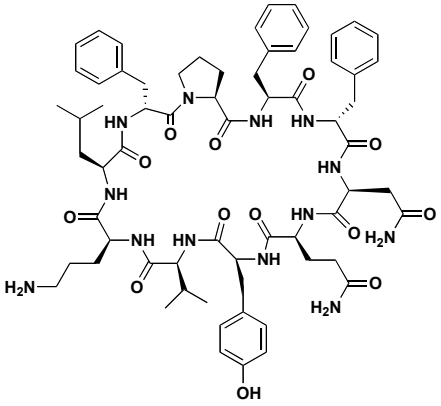

Figure 1.5. Macrocycle Tyrocidine A Synthesized via Head-to-Tail Strategy.

1.2.1 Solid-Phase Synthesis of Macrocyclic Peptides via Head to Tail Strategy

Solid-phase peptide synthesis was first introduced by Merifield et al in 1963,[15] and since then this technology has been significantly developed with the introduction of new protecting groups, and solid supports, both of which offering variety of options to synthetic chemists for their specific needs. Since 1990 there has been an increasing amount of research that utilizes on "on-resin" cyclization. One main aspect of this approach is to remove the cyclic peptide products after the macrocyclization procedure is completed. This on-resin cyclization can be sorted into three different categories based on their linking strategies (**Figure 1.6**). A detailed discussion of these strategies is shown described.

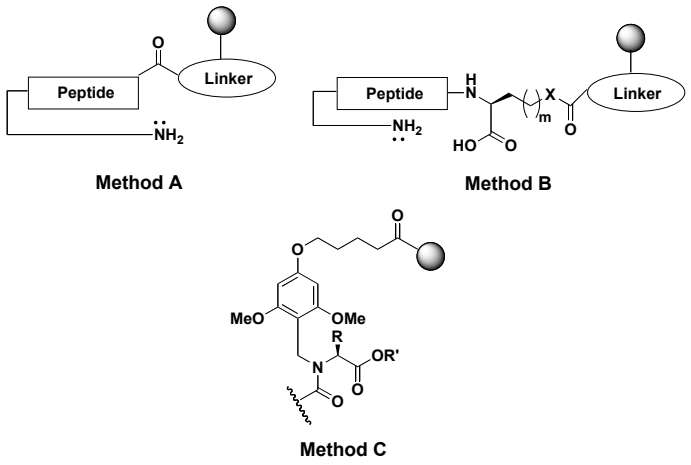

Figure 1.6. **Methods for Solid-Phase Synthesis of Cyclic Peptides.**

Strategy A: This approach, called "cleavage-by strategy", involves the *C*-terminus of the linear precursor linked to the solid support through an electrophilic linkers that is labile simultaneously as the peptide cyclizes. The cleavage of the final cyclic peptides from the solid support occurrs immediately after the macrocyclization reaction. An example that utilized this methodology was reported by Kaiser and co-workers, where they developed an oxime-based linker resin (shown in **Figure 1.7**) to synthesize macrocycles.[16]

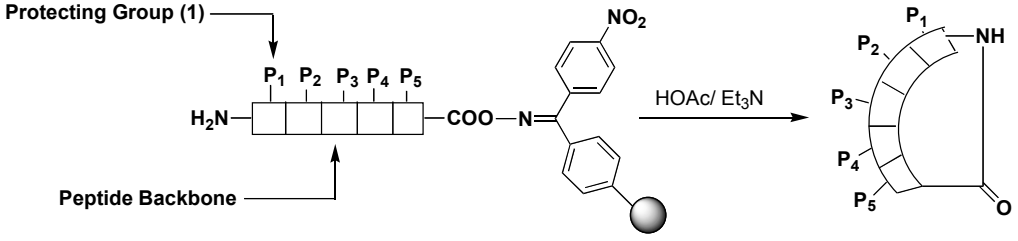

Figure 1.7. **"Cleavage-by" Macrocyclization.**

Due to the electrophilic nature of these linkers, this approach was initially only compatible with synthesizing using Boc-protected amino acids. An alternative linker

strategy called "safety-catch linker" was developed to overcome this limitation.[17] The safety-catch linkers can be regarded as the protected version of eletrophilic linkers where they are very robust and uncleavable during the preparation of linear precursor. These linkers can later be re-activated by removing the protecting group to perform final macrocyclization reaction. Smythe and co-workers[18] utilized this strategy to synthesize cyclic peptide shown in **Figure 1.8**.

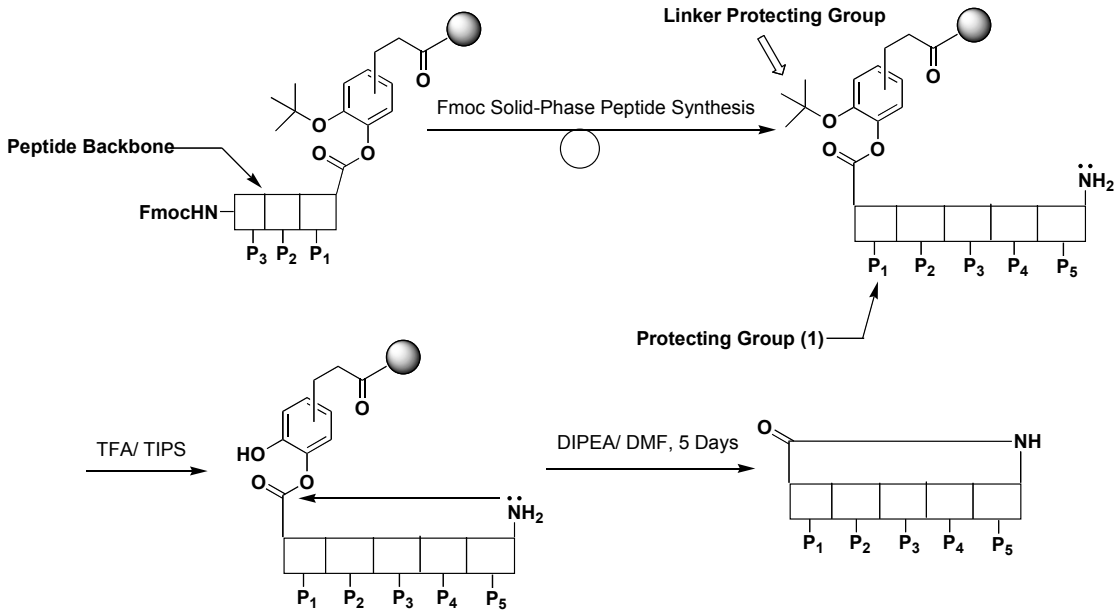

Figure 1.8. **Synthesis of Macrocycles via Safety-Catch Linker Strategy.**

Strategy B: In this approach, polar amino acid polar side chain such as Asp, Glu, Cys, Ser, Tyr, or Lys are utilized to attach the peptide to the solid support. The final cyclized product is removed from the solid support under proper cleavage conditions after cyclization. This strategy minimizes the risks of dimerization and oligomerization, which is often observed when using the other linker strategies during macrocyclization.

This is perhaps due to the fact that cyclization occurs more rapidly using method B because the activated *C*-terminus is farther away from the linker connection, which provides a clearer pathway for the nucleophile to react with the electrophile. Unfortunately, this effective cyclization strategy requires the presence of polar side chains within the linear precursor backbone. In order to overcome this limitation, an alternative "silicon-based linker strategy" was developed.[19] This method allows the non-polar residues (i.e. Phe) to attach to the support, thus allowing synthetic chemists to attach non-polar amino acid onto the solid support through the chemical manipulations. Silverman and co-workers utilized this methodology to synthesize the Sansalvamide A cyclic peptide.[20] Their synthetic strategy is shown in **Figure 1.9**.

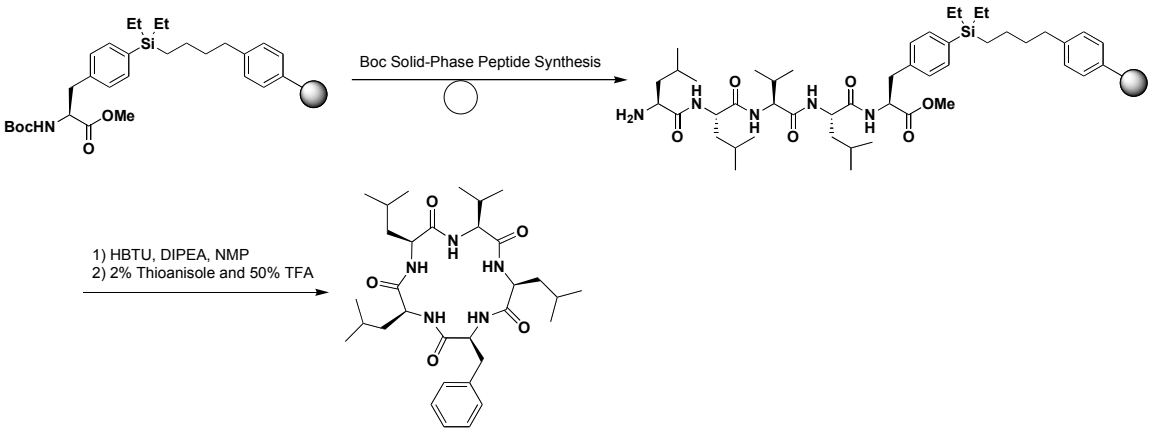

Figure 1.9. **Synthesis of Macrocycle via "Silicon-based linker strategy".**

Strategy C: In this method, the linear peptide substrates are linked directly to the solid support through their backbone (not side chain). An example of this method is called backbone amide linker (BAL) strategy.[21] In this strategy, the *C*-terminal amino acid is linked to the resin via its α-nitrogen atom. BAL strategy allows one to select, theoretically, any linear peptide sequence in any position of cyclization (except proline at the *C*-terminus). This method is particularly appealing to synthetic chemists since it is well known that particular amino acids at positions of cyclization can drastically altered the yield of macrocyclization reaction. Bourne and co-workers utilized BAL strategy to synthesize a library of cyclic peptides targeted at the Somatostatin receptor (**Figure 1.10**).[21]

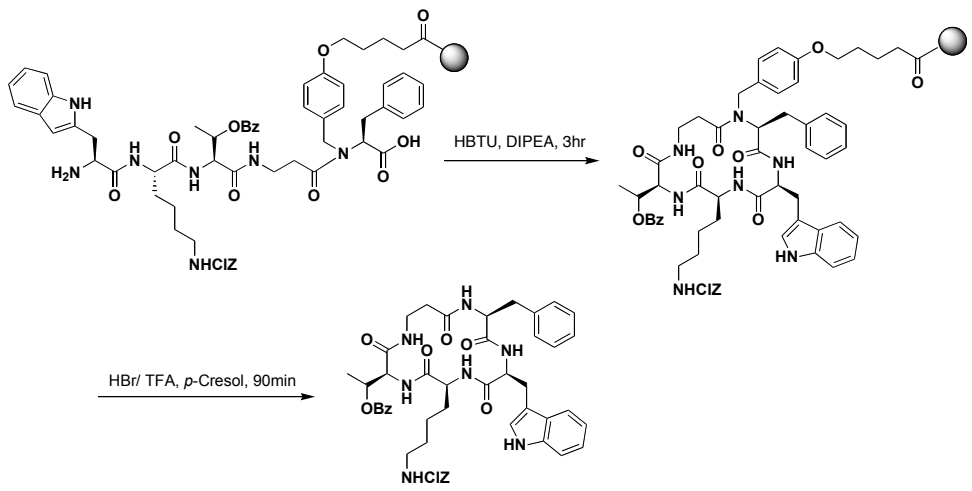

Figure 1.10. **Synthesis of Macrocycle via "Backbone-Amide Linker" strategy.**

1.2.2 Solution-Phase Synthesis of Macrocyclic Peptides via Head to Tail Strategy

Up until the late 1960's, head-to-tail cyclic peptides were synthesized only in solution. Despite the significant advancement of on-resin cyclization technology, solution-phase chemistry still remains as the general synthetic method for making head to tail cyclic peptides to date.[1, 4] Compare to on-resin cyclization, solution-phase cyclization do not require the attachment of the first amino acid to the solid support or optimizing the cleaving procedure, and most importantly, it can be used to prepare the cyclic peptides in large scale.

There are a number of factors that are known to impact the yield of solution-phase head-to-tail cyclization including, selection of the solvent,[22] selection of the ring-closing site,[23] and the conformation of the linear precursor.[24] Throughout the synthesis of aureobasidin A, Kurome and co-workers found that the selection of the solvent played a significant role in final cyclization step[22]. By using PyBrop as the coupling reagent and DIPEA as the base, cyclization performed in CH_2Cl_2 gave 45% isolated yield (**Figure 1.11**) whereas the reaction performed in DMF gave no desired product.

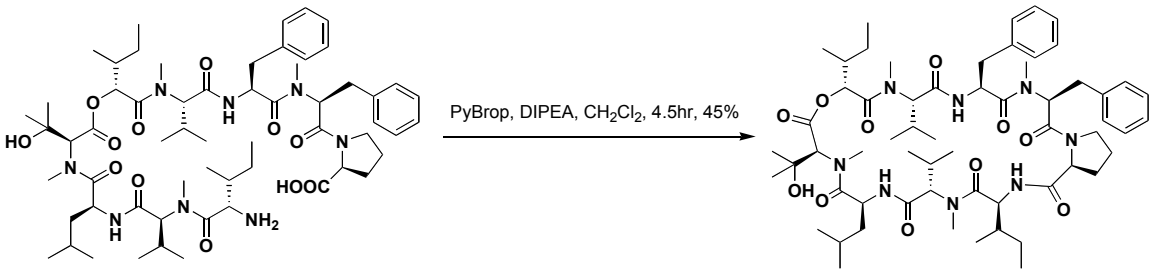

Figure 1.11. **Solvent Effect Towards Synthesis of Aureobasidin A.**

This interesting result was further investigated by the ^{1}H-NMR study in $CDCl_3$ or DMSO-d_6, the Rotating frame nuclear overhauser effect spectroscopy (ROESY) spectra indicated that linear precursor in $CDCl_3$ may possess a bent conformation (figure 1.12), which was expected in CH_2Cl_2; on the other hand, the one in DMSO-d_6 possess a linear stretched conformation (**Figure 1.12**) that was expected in DMF. Thus, it is reasonable to conclude that the one in the bent conformation is in the better position to form cyclized product, as opposed to the stretched conformation that would be present in DMF. This data explains why the reaction only proceeds in CH_2Cl_2.

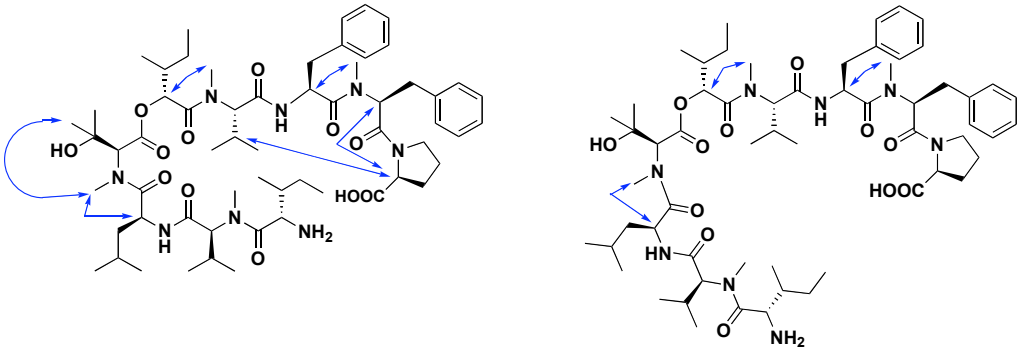

in $CDCl_3$ in DMSO-d_6

Figure 1.12. **Conformation Study of Linear Precursor via 2-D NMR Experiment.**

Despite the importance of selecting an appropriate reaction solvent, choosing a suitable ring-closing site is also an important component in the success of cyclization. There are some criteria of choosing an appropriate ring-closing site including as the selection of an unhindered amino acid (i.e. glycine) at either end of the linear precursor or avoiding a cysteine at the *C*-terminus which may cause serious racemization during cyclization.[25] An interesting example regarding the importance of selecting a suitable ring-closing-site was observed during the synthesis of dendroamide A. Dendroamide A is a cyclic peptide isolated by Moore and co-workers from the terrestrial cyanobacterium *Stigonema dendroideum Fremy* in 1996.[26] It possesses a significant ability to reverse multi-drug resistance in tumor cells. In 2000, Pattenden and co-workers completed the first total synthesis of this molecule.[27] Later, Smith,[28] Kelly,[29] and Shin[30] also completed the total synthesis of dendroamide A. Pattenden et al. carried out the cyclization at site A obtained 91% cyclization yield, Kelly et al selected the cyclization at site B obtained 56%, while Shin et al. did the cyclization at site C obtained 81% cyclization yield. Calculated by CONFLEX® 5, Matsumoto and co-workers found that the distance between *C* and *N*-

terminus for site A linear precursor was 3.73Å, while the distance between *C*- and *N*-terminus for site B was 3.93 Å, and finally, the distance between *C*- and *N*- terminus for site C linear precursor was 3.72Å.[24] This study demonstrated the importance of selecting a suitable ring-closing site for the efficient cyclization reaction.

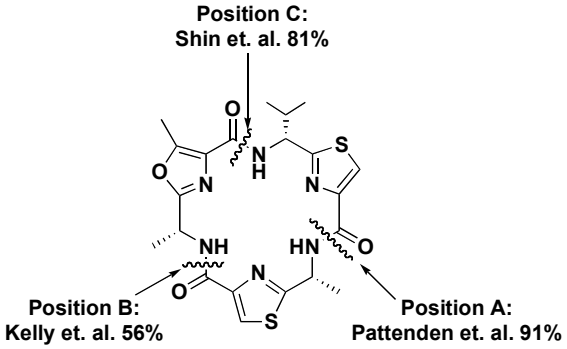

Figure 1.13. **Synthesis of Dendroamide A via Different Ring-Closing Site.**

In addition to the elements described above, conformation of the linear precursor also plays an important role in the success of solution phase head to tail macrocyclization. Wenger and co-workers utilized this conformational approach to design and synthesize cyclosporine A in good yield (62%).[24] (**Figure 1.14**) The success of this work came from the intramolecular hydrogen bonding that directed the linear precursor into a stabilized pre-organized conformation. Through this conformation, the *C*- and *N*-terminus of the linear precursor were brought into a close proximity, thus facilitated the formation of the final product.

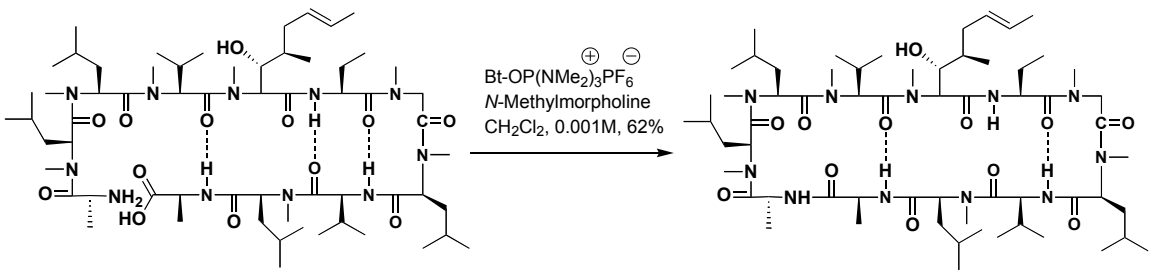

Figure 1.14. **Conformation-Directed Macrocyclization of Cyclosporine A.**

1.3 Recent Compounds Relevant and Important in Drug Discovery

Natural cyclic peptides are the class of molecules that appeared in large structural diversity with a broad spectrum of biological activities, such as antibacterial, anti-inflammatory, antiviral, immunosuppressive, and anticancer activities. Due to their wide range of pharmacological applications, the design and synthesis of the cyclic peptide analogs based on natural products continue to be a growing area in drug discovery. However, the design of novel potent cyclic peptides based on natural products remains a great challenge. Understanding the structure-activity relationship of these molecules based on the role of each amino acid and their cyclized conformations is a requirement when designing potent molecules. Two major strategies in developing novel potent cyclic peptides are: (1) design and synthesize cyclic peptide analogs based on existing natural cyclic peptides model or (2) cyclize linear lead peptide to enhance its biological stability and activity. These strategies are discussed below.

Strategy (1) was utilized in the synthesis of Tamandarin B, a cytotoxic depsipeptide that was isolated from an unidentified Brazilian marine ascidian of the family Didemnidae by Fenical and co-workers in 1996. It's structure was also elucidated by Fenical and co-workers in 2000 (**Figure 1.15**).[31] It shows potent inhibitory growth activity against several human tumor cell lines[31-33] and is considered as a promising lead compound for chemotherapeutic development. The first synthesis of Tamandarin B was accomplished by Joullié and co-workers in 2001.[32] Later, a series of Tamandarin B analogues were synthesized and their structure-activity relationship indicated that its biological activity was highly dependent on the structure of the side chain.[33] Although most of the structural modifications within the depsipeptide backbone were tolerated, it was found that replacing a proline residue at the position 4 with a less structurally rigid alanine residue dramatically diminished its biological activity with GI_{50} = 3.90 nM in HeLa cervical cancer cells (tamandarin B), and GI_{50} = 1180 nM in HeLa cells (alanine containing analog). The presence of a proline at position 4 along with leucine at position 3 appears to induce a β-turn formation that holds the cyclic backbone into a strict conformation. This conformation, in turn, correlates with its potent biological activity.[34]

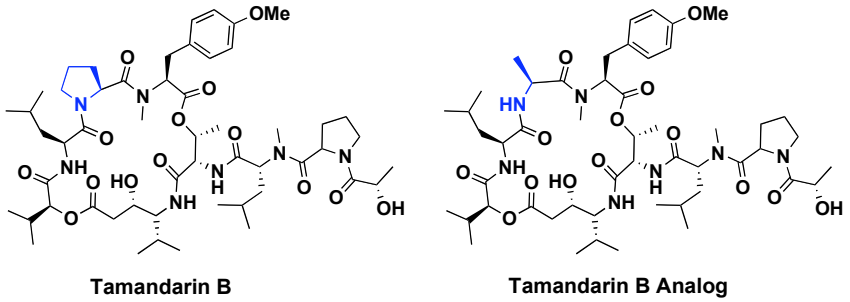

Figure 1.15. Tamandarin B and its Analog.

Strategy (2) was utilized by Brassart-Pasco and co-workers.[35] They used the cytotoxic CNYYSNS linear peptide, which originated from Tumstatin, as a lead in their design of the cyclic peptide YSNSG. This cyclic peptide comprised of a glycine (G) residue along with four residues known to form a β-turn: tyrosine (Y), serine (S), asparagines (N), and serine (S), where a β-turn was shown to be a crucial element in the biological activity of the linear peptide CNYYSNS (**Figure 1.16**).[35] 2-D NMR experiments (TOCSY, and NOESY) and molecular modeling (Molecular Dynamics Simulations) proved that the incorporation of a glycine moiety permitted peptide cyclization to constrain the β-turn and hold the cyclic backbone in the conformation that gave the appropriate conformation for cytotoxicity, generating a cyclic compound that possess a greater percent inhibition of tumor cell growth compared to its linear counterpart. Upon intraperitoneal injection (I.P injection) of the linear peptide, CNYYSNS and the cyclic peptide, YSNSG into the melanoma tumor, the cyclic peptide showed a greater in-vivo inhibitory effect on tumors compared to the linear peptide. The YSNSG cyclic peptide inhibited in-vivo tumor cell growth by 46% while linear CNYYSNS only inhibited in vivo cell growth by 27%. Their work indicated that cytotoxicity and stability could be improved upon generating the cyclic peptide from a

similar linear precursor, and that this improved cytotoxicity was due to the conformational constraint placed on the side chains within the macrocycle.

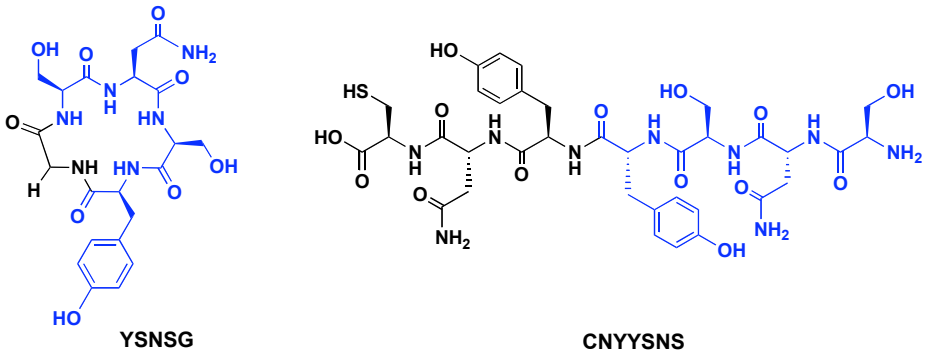

Figure 1.16. YSNSG and CNYYSNS.

In summary, the research discussed above has shown the capability of macrocycles to inhibit cancer cell proliferation. Given the success of other natural product macrocycles of similar or larger molecular weights such as Vancomycin, Cyclosporine A, FK506, and 17AAG,[36-39] the compounds discussed in this thesis, though currently in the preliminary developmental stage, show potential as future chemotherapeutic agents. That is, the promising cancer cell growth inhibition data shown for these macrocyclic compounds and the current success of other macrocycles of similar or larger size, demonstrate the effectiveness of a macrocyclic scaffold as a tool in the development of new antitumor agents.

1.4 Aims of this Research

Given cyclic peptides possess a wide spectrum of biological activity and the design of the potent macrocycles remains a significant challenge, the aim of this research will focus on:

1. Synthesizing cyclic peptide derivatives using either solution-phase or solid-phase via the head-to-tail strategy.
2. Evaluation of biological activity of the synthesized macrocycles through ^{3}H labeled thymidine incorporation assays.

1.5 REFERENCES

1. Davies, J. S. "The Cyclization of Peptides and Depsipeptides", *J. Pept. Sci* **2003**, *9*, 471-501.

2. Fusetani, N. M., S. "Bioactive Sponge Peptides", *Chem. Rev* **1993**, *93*, 1793-1806.

3. Wipf, P. "Synthetic Studies of Biologically Active Marine Cyclopeptides", *Chem. Rev.* **1995,** *95*, 2115-2134.

4. Katsara, M. T., T.; Deraos, S.; Deraos, G.; Matsoukas, M-T.; Lazoura, E.; Matsoukas. J.; Apostolopoulos, V, "Round and Round we Go: Cyclic Peptides in Disease", *Curr. Med. Chem.* **2006,** *13*, 2221-2232.

5. Humphrey, J. M.; Chamberlin, A. R. "Chemical synthesis of natural product peptides:coupling methods for the incorporation of non-coded amino acids into peptides", *Chem. Rev.* **1997,** *97*, 2243-2266.

6. Corey, E. J. C., B.; Kürti, L. "*Molecules and Medicine*", John Wiley & sons, Inc: New Jersey, 2007; p 124.

7. Jin, L. H., S. C. "Crystal structure of Human Calcuineurin Complexed with Cyclosporin A and Human Cyclophilin", *Proc. Natl. Acad. Sci. USA*. **2002,** *99*, 13522-13526.

8. Corey, E. J. C., B.; Kürti, L. "*Molecules and Medicine"* John Wilely & Sons, Inc.: New Jersey, 2007; p 138.

9. Kahne, D. L., C.; Lu, W.; Walsh, C. "Glycopeptide and Lipoglycopeptide Antibiiotics", *Chem. Rev,* **2005,** *105*, 425-448.

10. Satoh, T. L., S.; Friedman, T. M.; Wiaderkiewicz, R.; Korngold, R.; Huang, Z. "Synthetic Peptides Derived from the Fourth Domain of CD4 Angagonize CD4 Function and Inhibit T Cell Activation", *Biochem. Biophys. Res. Commun.* **1996,** *224*, 438-443.

11. Shibata, K. S., T.; Soga, S.; Mizukami, T.; Yamada, K.; Hanai, Nobuo.; Yamasaki, M. "Improvement of Biological Activity and Proteolytic Stability of Peptides by Coupling with a Cyclic Peptide", *Bioorg. Med. Chem. Lett.* **2003,** *13*, 2583-2586.

12. Tamilarasu, N. H., L.; Rana, T. M. "Design, Synthesis, and Biological Activity of a Cyclic Peptide: An Inhibitor of HIV-1 tat-TAR Interactions in Human Cells", *Bioorg. Med. Chem. Lett.* **2000,** *10*, 971-974.

13. Hwang, S. T., N.; Ryan, K.; Huq, I.; Richter, S.; Still, W. C.; Rana, T. M. "Inhibition of Gene Expression in Human Cells Through Small Molecule-RNA Interactions", *Proc. Natl. Acad. Sci. USA*. **1999,** *96*, 12997-13002.

14. Ohno, M. I., N. "Synthesis of Tyrocidine A", *J. Am. Chem. Soc.* **1966,** *88*, 376-378.

15. Merrifield, R. B. "Solid Phase Peptide Synthesis. I. The Synthesis of a Tetrapeptide", *J. Am. Chem. Soc.* **1963,** *85*, 2149-2154.

16. DeGrado, W. F. K., E. T. "Solid-Phase Synthesis of Protected Peptides on a Polymer-Bound Oxime: Presentation of Segments Comprising the Sequence of a Cytotoxic 26-Peptide Analogue", *J. org. Chem.* **1982,** *47*, 3258-3261.

17. Ravn, J. B., G.T.; Smythe, M. L. "A Safety Catch Linker for Fmoc-Based Assembly of Constrained Cyclic Peptides", *J. Pept. Sci.* **2005,** *11*, 572-578.

18. Bourne, G. T. G., S. W., McGeary, R. P.; Meutermans, W. D. F.; Jones, Alun.; Marshall, G. R.; Alewood, P. F.; Smythe, M. L. "The Development and Application of a Novel Safety-Catch Linker for Boc-Based Assembly of Libraries of Cyclic Peptides", *J. Org. Chem.* **2001,** *66*, 7706-7713.

19. Plunkett, M. J. E., J. A. "A Silicon-Based Linker for Traceless Solid-Phase Synthesis", *J. Org. Chem.* **1995,** *60*, 6006-6007.

20. Liu, S. G., W.; Lo, D.; Ding, X-Z.; Ujiki, M.; Adrian, T. E.; Soff, G. A.; Silverman, R. B. "N-Mehtylsansalvamide A Peptide Analogues. Potent New Antitumor Agnets", *J. Med. Chem.* **2005,** *48*, 3630-3638.

21. Bourne, G. T. G., S. W.; Meutermans, W. D. F.; Smythe, M. L. "Synthesis of a Cyclic Peptide Library based on the Somatostatin Sequence using Backbone Amide Linker Approach", *Lett. Pept. Sci.* **2001,** *7*, 311-316w.

22. Kurome, T. I., K.; Inoue, T.; Ikai, K. Takesako, K. Kato, I.; Shiba, T. "Total Synthesis of an Antifungal Cyclic Depsipeptide Aureobasidin A", *Tetrahedron* **1996,** *52*, 4327-4346.

23. Matsumoto, T. M., E.; Shioiri, T. "Investigation of Macrocyclization sites for the Synthesis of Dendroamide A-an Approach from a Conformational search", *Tetrahedron.* **2007,** *63*, 8571-8575.

24. Blankenstein, J. Z., J. "Conformation-Directed Macrocyclization Reactions", *Eur. J. Org. Chem.* **2005**, 1949-1964.

25. Kovacs, J. M., G. L.; Johnson, R. H.; Cover, R. E. Ghatak, U. R. "Racemization of Amino Acid Derivatives. Rate of Racemization and Peptide Bond Formation of Cysteine Active Esters", *J. Org. Chem.* **1970,** *35*, 1810-1815.

26. Ogino, J. M., R. E.; Patterson, G. M. L.; Smith, C. D. "Dendroamides, New Cyclic Hexapeptides from a Blu-Green Algae. Multidrug Resistance of Dendroamide", *J. Nat. Prod.* **1996,** *59*, 581-586.

27. Bertram, A. P., G. "self-Assembly of Amino Acid-Based Thiazoles and Oxazoles. Total Synthesis of Dendroamide A, a Cyclic Hexapeptide from the Cyanobacterium Stigonema dendroideum", *Synlett.* **2000**, 1519-1521.

28. Xia, Z. S., C. D. "Total Synthesis of Dendroamide A, a Novel Cyclic Peptide that Reverse Multiple Drug Resistance", *J. org. Chem.* **2001,** *66*, 3459-3466.

29. You, S.-L. K., J. W. "Total Synthesis of Dendroamide A: Oxazole and Thiazole Construction Using an Oxodiphosphonium Salt", *J. Org. Chem.* **2003,** *68*, 9506-9509.

30. Yonezawa, Y. T., N.; Shin, C-G. "New Total Synthesis of Dendroamide A from Dehydrodi- and Tripeptides", *Heterocycyles* **2005,** *65*, 95-105.

31. Vervoort, H. F., W. "Tamandarins A and B: New Cytotoxic Depsipeptides from a Brazilian Ascidian of the Family Didemnidae", *J. Org. Chem.* **2000,** *65*, 782-792.

32. Liang, B. R., D. J.; Protonovo, P. S.; Joullie´, M. M. "Total Syntheses and Biological Investigations of Tamandarins A and B and Tamandarin A Analogs", *J. Am. Chem. Soc.* **2001,** *123*, 4469-4474.

33. Adrio, J. C., C.; Manzanares, I.; Joullie´, M. M. "Total Synthesis and Biological Evaluation of Tamandarin B Analogues", *J. Org. Chem.* **2007,** *72*, 5129-5138.

34. Adrio, J.; Cuevas, C.; Manzanares, I.; Joullié, M. M. "Total Synthesis and Biological Evaluation of Tamandarin B Analogues", *J. Org. Chem.* **2007,** *72*, 5129-5138.

35. Thevenard, J. F., N.; Ramont, L.; Prost, E.; Nuzillard, J.; Dauchez, M.; Yezid, H.; Alix, A. J. P.; Maquart, F.; Monboisse, J. Brassart-Pasco, S. "Structural and Antitumor Properties of the YSNSG Cyclopeptide Derived from Tumstatin", *Chem. Biol.* **2006,** *13*, 1307-1315.

36. Schulte, T. W.; Neckers, L. M. "The benzoquinone ansamycin 17-allylamino-17-demethoxygeldanamycin binds to Hsp90 and shares important biologic activities with geldanamycin", *Cancer Chemother Pharmacol.* **1998,** *42*, 273-279.

37. Liu, J.; Farmer, J. D.; Lane, W. S.; Friedman, J.; Weissman, I.; Schreiber, S. "Calcineurin is a common target of cyclophilin-cyclosporin A and FKBP-FK506 complexes", *Cell* **1991,** 66, 807-815.

38. Hruby, V. J. "Designing peptide receptor agonists and antagonists", *Nature Reviews. Drug Discovery* **2002,** *1*, 847-858.

39. Grünewald, J.; Marahiel, M. A. "Chemoenzymatic and Template-Directed Synthesis of Bioactive Macrocyclic Peptides", *Microbiology and Molecular Biology Reviews* **2006,** *70*, 121-146.

Chapter 2

Synthesis of Sansalvamide A Derivatives

2.1 Peptides as Drugs

In this chapter I'll be describing the synthesis of 7 Sansalvamide A derivatives and my completed molecules are shown in Figure 2.3. Rational drug design utilizing natural products as templates offers a powerful methodology for new drug discovery[1] and offer particularly relevant templates. Moreover, the continuous discovery of novel naturally occurring peptides has encouraged the development of peptide drugs. Peptide drugs are used as HIV protease inhibitors,[2] osteoporosis treating drugs,[3] antibiotics,[4] immunosuppressant,[5] and anti-tumor agents.[6, 7] To date there are 720 clinically used peptide drugs or candidates; 38% of these are in clinical trials, 56% are in advanced preclinical phases and 5% are on the market.[8] Moreover, peptides are relatively straightforward to synthesize, have commercially available chemical diversity, and can be rapidly assembled. However, the appeal of using peptides as drugs is diminished because they require a relatively large molecular structure to define their three dimensional conformation, and they are rapidly cleared from the body (with half-lives often measurable in minutes). Furthermore, membrane transport is also a challenge due to the hydrophilicity of peptides.[9] These obstacles have made cyclic peptides very attractive lead drug candidates because they tend to have greater binding affinity for protein targets than their linear counterparts. Because cyclic peptides are constrained, they require fewer amino acids to define their 3-D structure. In addition, they are more lipophilic than linear counterpart, which facilitates their membrane transportation.[10] Further, they degrade

slower than linear peptides because proteases have difficulty cleaving amide bonds located in a macrocycle.[11, 12] Thus, there is great potential in developing macrocyclic peptides into drug candidates. Sansalvamide A (**Figure 2.1**) was isolated from a marine fungus (*Fusarium sp*.) in 1999 by Fenical *et al*. off the coast of San Salvadore island in the Bahamas. Initial testing showed that it exhibits antitumor activity in the NCI's 60 cell line panel (IC_{50} = 42.5μM).[10, 13, 14] Its novel cyclic depsipeptide structure presents a unique alternative to many chemotherapeutic agents currently on the market, thus, making it a promising structure for further development.

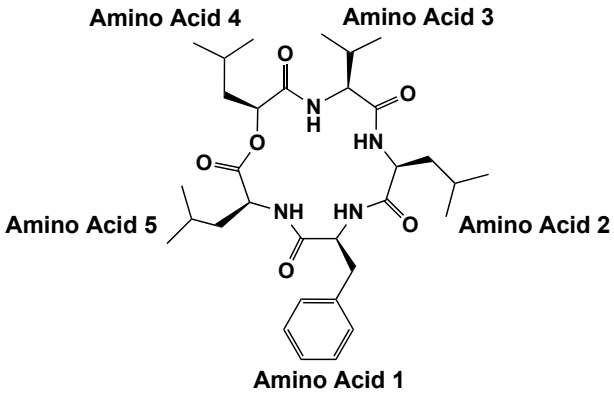

Figure 2.1 Sansalvamide A Depsipeptide.

San A depsipeptide was first synthesized by Silverman et al. in 2000,[15, 16] and initial testing by Silverman has demonstrated its potency against pancreatic, colon, breast, prostate, and melanoma cancers.[17, 18] Recent work by our group has shown that San A peptide derivatives are potent against the drug-sensitive colon cancer cell line HT-29. This clearly indicates the potential of this class of compounds as a platform useful in targeting multiple cancers.

2.2 General Synthesis Strategy

San A is composed of four L-amino acids and one α-hydroxy-acid. However, only the peptide analogues, involving the exchange of the hydroxy acid in position 4 with an amino acid, were synthesized because initial testing of the San A peptide showed greater potency than the San A depsipeptide.[15] The peptide analogues also have the advantage of being more stable by resisting degradation to ring opening saponification by lipases, and the peptide core structure can serve as a scaffold where substituents can be interchanged around this general core structure (**Figure 2.1**). A convergent approach, involving two fragments (**Figure 2.2**), is amenable to inserting L-and D-amino acids systematically, thus allowing the incorporation of diversity around the peptide backbone via a relatively standard synthetic route.[19-21] This method is a general, rapid, high-yield approach that enables large-scale synthesis needed for extensive biological studies.

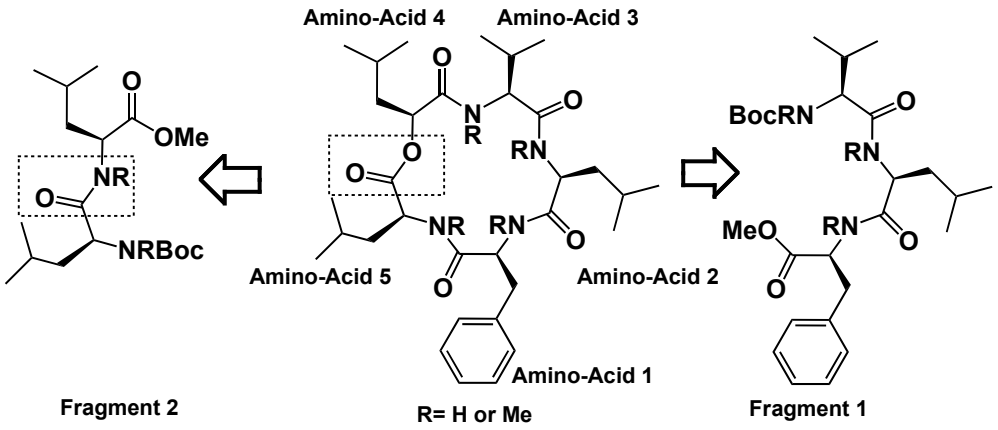

Figure 2.2 Retrosynthetic Strategy via a Convergent Approach.

A variety of L and D-amino acids were used (**Figure 2.3**) to construct a library of San A analogues that could later be utilized to study the molecule's structure activity relationship (SAR). The amino acids that I used to construct seven San A analogues are shown in blue while amino acids used by my colleagues are shown in black.

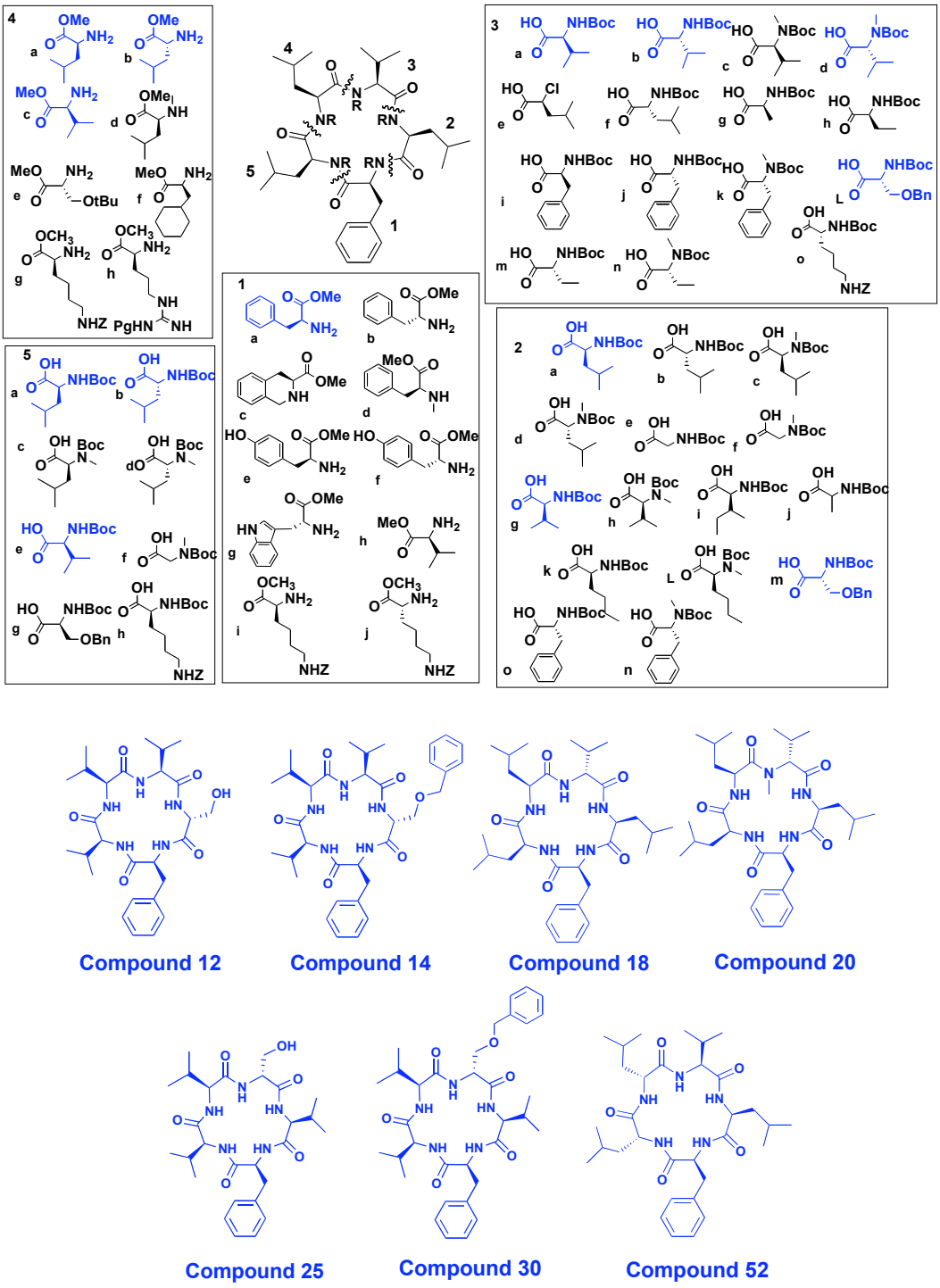

Figure 2.3 Amino Acids used in San A Synthesis. Compounds and Synthesized using Amino Acids (in blue) Above Include 12, 14, 18, 20, 25, 30, 52.

The analogues were designed to explore alterations at individual positions in order to explore a relationship with potency. Structure activity relationships (SAR) of San A analogues were compiled for a series of compounds and will be discussed in successive chapters.

It has been theorized by Garland Marshall[22] and others[23, 24] that *N*-methyl groups lock the macrocycle into a favorable conformation that might potentially improve the binding affinity of the molecule to the biological target.

I have synthesized seven San A derivatives, which are **12**, **14**, **18**, **20**, **25**, **30**, and **52**. These seven derivatives were part of a larger group of analogs that explored the effects of *N*-methyl and D-amino acids on biological activity. A number of compounds were made by colleagues that explored the role of relative and absolute configurations at positions 1 and 2. In compound **18**, which was differentiated from the San A peptide **1** (**Figure 2.3**) by incorporating amino acid 3b (D-valine) and compound **20**, which contained amino acid 3d (*N*-methyl-D-valine) were designed to explore the effect of stereochemistry on cytotoxicity at position 3. There are two deviations from the San A peptide **1** in compound **52**: D-leucines were incorporated into positions 4 and 5. In compounds **25** and **30**, L-valines were used in position 2, 4, and 5 rather than L-leucines seen in the San A peptide **1** to explore the effect of lowering the molecular weight while maintaining stereochemistry and similar steric constraints compared to **1**. Further, incorporating a D-serine (compound **25**) or a Benzyl protected D-serine (compound **30**) at position 3 provides compounds that would explore how changing the compound's

hydrophobicity altered its cytotoxicity. The same rational was applied to the design of compound **12** and compound **14**, with the D-serine or benzyl protected serine incorporated into position 2, and L-valines at positions 3, 4, and 5. By comparing the potency of compounds **25** and **12** to **1** one could establish the importance of a polar moiety at positions 2 and 3. Further, by comparing the cytotoxicity of **30** and **14** to **1**, **25**, and **12** it will be possible to establish the importance of hydrophobic elements at positions 2 and 3.

2.2.1 Synthesis of Fragment 1

A solution phase synthesis strategy was used in part because of the hydrophobic nature of most of the amino acids used in the construction of San A analogues and to facilitate large scale synthesis of biologically active derivatives. Deprotected tripeptides (Fragment 1) were synthesized using the conditions outlined in **Figure 2.4**. Compounds **18**, **20**, and **52** were made using the same starting dipeptide, 1a-2a. Residue 1a, H-L-phenylalanine-methyl ester, was coupled with residue 2a, Boc-L-leucine-OH. This coupling reaction involved 1.0 equivalents of the free acid (residue 1), 1.1 equivalents of the free amine, (residue 2), 1.1 equivalents of the coupling agent 2(1-H-benzotriazole-1-yl)-1,1,3-tetramethyluronium tetrafluoroborate (TBTU), and 4 equivalents of diisopropylethylamine (DIPEA). All starting materials were dissolved in anhydrous methylene chloride to a concentration of 0.1 M. The reactions were allowed to run for approximately 30 minutes to 1 hour and monitored via TLC. After the reaction was

completed, the crude reaction products were isolated by diluting the crude reaction with excess ethyl acetate followed by washing with 0.1M $HCl_{(aq)}$ to remove excess free amine, then washing with saturated sodium bicarbonate three times to remove coupling agent by product and excess coupling agent. The resulting dipeptide was isolated upon drying the combined organic layers over sodium sulfate, filtering, and concentrating down via rotary evaporator. ^{1}H NMR was used to identify the product and verify its purity. The reaction resulted in the dipeptide 1a-2a (95% yield).

Following the synthesis of this dipeptide, 20% trifluoroacetic acid (TFA) in methylene chloride (0.1M) with anisole (2 equivalents) were used to remove the *t*-butoxycarbonyl (Boc) protecting group on the amine of residue 2 to obtain the dipeptide 1a-2a-NH_2. Reactions were monitored via Thin Layer Chromatography (TLC). To be noted, TLC samples were obtained with methylene chloride along with DI water in order to remove excess TFA. Upon completion (ca. 30 minutes, verified by TLC), the crude amine deprotected dipeptides were concentrated and quantitative yields were assumed based on ^{1}H NMR. The same procedure was utilized to synthesize dipeptides 1a-2g-NH_2, and 1a-2m-NH_2 (yields for 1a-2g and 1a-2m coupling shown in (**Figure 2.4**).

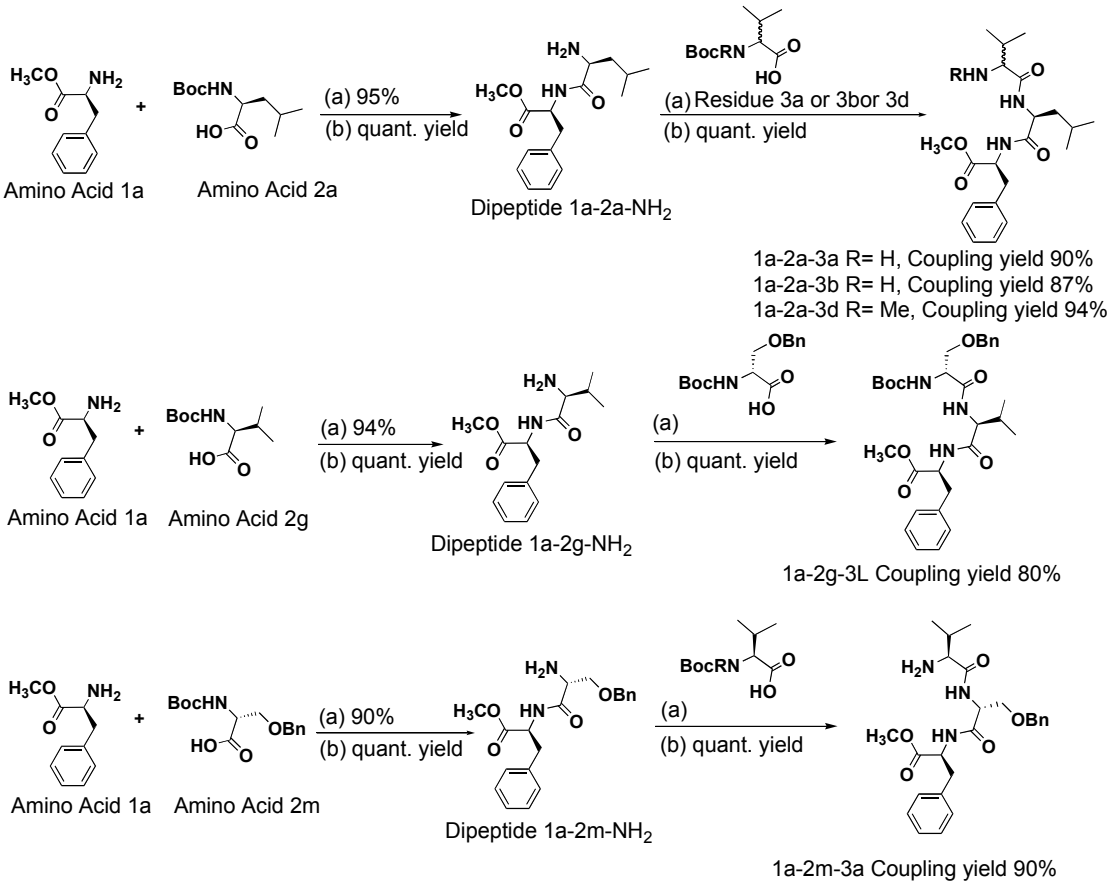

Conditions: (a) TBTU (1.1eq), DIPEA (4.0 eq), CH_2Cl_2 (0.1M);
(b) anisole (2.0 eq), 20% TFA, CH_2Cl_2 (0.1M)

Figure 2.4 Synthesis of Fragment 1

Three different amino acids were then used to couple to the free-amine dipeptides to generate five different tripeptides. The dipeptide 1a-2a-NH_2 was coupled with residue 3a (Boc-L-valine-OH (1.0 equivalents)), with residue 3b (Boc-*N*-methyl-D-valine-OH (1.0 equivalent)), with residue 3d (Boc-*N*-Me-D-Val-OH (1.0 equivalent)), and dipeptide 1a-2g-NH_2 was coupled with residue 3L (Boc-D-Bn-Ser-OH (1.0 equivalent)), and dipeptide 1a-2m-NH_2 was coupled with residue 3a (Boc-L-valine-OH (1.0 equivalents)), in order to obtain the tripeptides: 1a-2a-3a, 1a-2a-3b, 1a-2a-3d, 1a-2g-3L, and 1a-2m-3a,

respectively (for yields see **Figure 2.4)**. These reactions were performed by using 1.1 equivalents of TBTU and 4 equivalents of DIPEA, and anhydrous methylene chloride (0.1M). These reactions were allowed to run for approximately 45 minutes to 1 hour and monitored via TLC. After the reactions were complete, the crude reaction products were isolated by diluting the crude reactions with excess ethyl acetate followed by washing with 0.1M $HCl_{(aq)}$ to remove excess free amine, then washing with saturated sodium bicarbonate three times to remove coupling agent byproduct and excess coupling agent. The resulting pure tripeptides were isolated upon drying the combined organic layers over sodium sulfate, filtering, and concentrating via rotary evaporator. ^{1}H NMR spectroscopy was used to identify the product. These reactions resulted in the tripeptides 1a-2a-3a (90%), 1a-2a-3b (87%), 1a-2a-3d (94%), 1a-2g-3L (80%), and 1a-2m-3a (90%). The amine protecting group of these tripeptides were then removed by using 20% TFA in methylene chloride with anisole (2 equivalents) to yield the free amine (Fragment 1) in quantitative yields.

2.2.2 Synthesis of Fragment 2

The free acid dipeptides (Fragment 2) were synthesized by coupling residue 4 to residue 5 (**Figure 2.5**). Residue 4a (H-L-leucine methyl ester) was coupled with residue 5a (Boc-L-leucine-OH). This coupling reaction involved 1.0 equivalent of the free acid (residue 5); 1.1 equivalents of the free amine (residue 4); 1.1 equivalents of coupling agent TBTU and 4 equivalents of DIPEA in 0.1M anhydrous methylene chloride. The

reaction was allowed to run for approximately 1 hour and monitored via TLC. After the reaction was completed, the crude reaction product was isolated up by diluting the crude reaction with excess ethyl acetate followed by washing with 0.1M $HCl_{(aq)}$ to remove excess free amine, then washing with saturated sodium bicarbonate three times to remove coupling agent byproduct and excess coupling agent. The resulting pure dipeptide was isolated upon drying the combined organic layers over sodium sulfate, filtering, and concentrating down via rotary evaporator. ^{1}H NMR was used to identify the product and verify its purity. The reaction resulted in the dipeptide 4a-5a (92% yield). The same procedure was applied to synthesize and purify 4b-5b (91%), and 4c-5e (94%).

Following the synthesis of these dipeptides, lithium hydroxide (8.0 equivalents) in methanol to a concentration of 0.1M was used to hydrolyze the methyl ester on residue 4 of all three dipeptides to produce the free-acid (**Figure 2.5**). Reactions were allowed to proceed for one to three hours and monitored via TLC. The crude reaction mixtures were dissolved in an excess of methylene chloride and extracted with 1M $HCl_{(aq)}$. The combined organic layers were dried over sodium sulfate, filtered, and concentrated via rotary evaporation. This work-up procedure served as the only purification approach throughout the synthesis of fragment 2. ^{1}H NMR was used to identify the structure of the products. This afforded three pure dipeptides: HO-4a-5a (87% yield), HO-4b-5b (85% yield), and HO-4c-5e (83% yield).

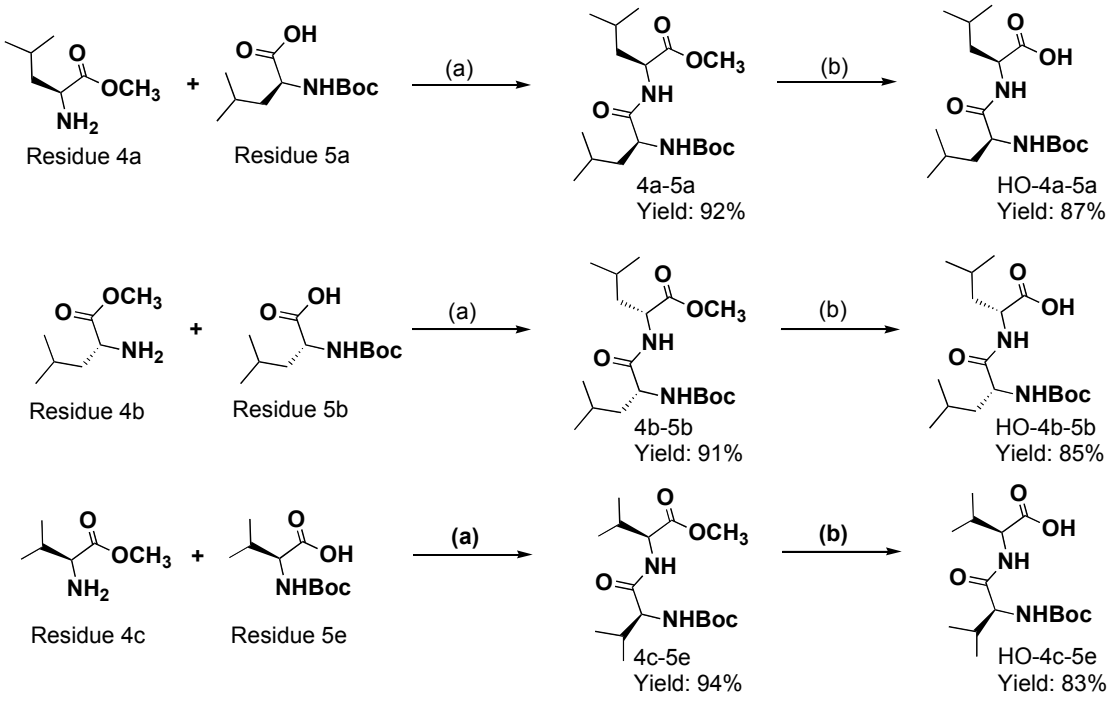

Conditions: (a) TBTU (1.1eq), DIPEA (4.0 eq), CH_2Cl_2 (0.1M);
(b) LiOH (8eq), CH_3OH (0.1M).

Figure 2.5 Synthesis of Fragment 2

2.2.3 Synthesis of Pentapeptides 1a-2a-3b-4a-5a, 1a-2g-3L-4c-5e, 1a-2m-3a-4c-5e, and 1a-2a-3a-4b-5b

Linear pentapeptides 1a-2a-3b-4a-5a, 1a-2g-3L-4c-5e, 1a-2m-3a-4c-5e, and 1a-2a-3a-4b-5b were synthesized using Fragments 1 and 2 (**Figure 2.6**). The dipeptide free-acid, fragment 2 (1.0 equivalent) was coupled with 1.1 equivalents of the tripeptide free-amine (Fragment 1). Free-acid dipeptide HO-4a-5a was coupled with the free-amine 1a-2a-3b-NH_2 (**Figure 2.6a**), free-acid HO-4b-5b was coupled with the free-amine tripeptide 1a-2a-3a-NH_2 (**Figure 2.6b**), free-acid HO-4c-5e was coupled with the free-amine tripeptide 1a-2g-3L-NH_2 (**Figure 2.6c**), and free-acid dipeptide HO-4c-5e was coupled

with the free-amine 1a-2m-3a-NH_2 (**Figure 2.6d**). These reactions were performed by using 0.7 equivalents of TBTU, 0.7 equivalents of 2-(H-7-azabenzotriazol-1-yl)-1,1,3,3-tetramethyluronium hexafluorophosphate (HATU) (0.7 equivalents) and 4.0 equivalents of DIPEA in a solution of anhydrous methylene chloride and acetonitrile (1:1) to 0.1M. Reactions were allowed to proceed for 1-2 hours and monitored via TLC. Upon completion the crude reaction was diluted with ethyl acetate and washed first with 1M $HCl_{(aq)}$ followed by washing with saturated sodium bicarbonate. Three to four washes were required with sodium bicarbonate to remove excess coupling agents and its byproduct. The combined organic layers were dried over sodium sulfate, filtered, and concentrated *via* rotary evaporator. Pure linear pentapeptide was purified by flash column chromatography using silica gel and ethyl acetate-hexanes as the gradient system. Structures of the products and their purity were confirmed by using NMR and LCMS. This resulted in the following protected linear pentapeptides (PLP): Compound **14**-PLP (1a-2m-3a-4c-5e, 71% yield), Compound **18**-PLP (1a-2a-3b-4a-5a, 70% yield), Compound **30**-PLP (1a-2g-3L-4c-5e, 66%), and Compound **52**-PLP (1a-2a-3a-4b-5b, 77% yield).

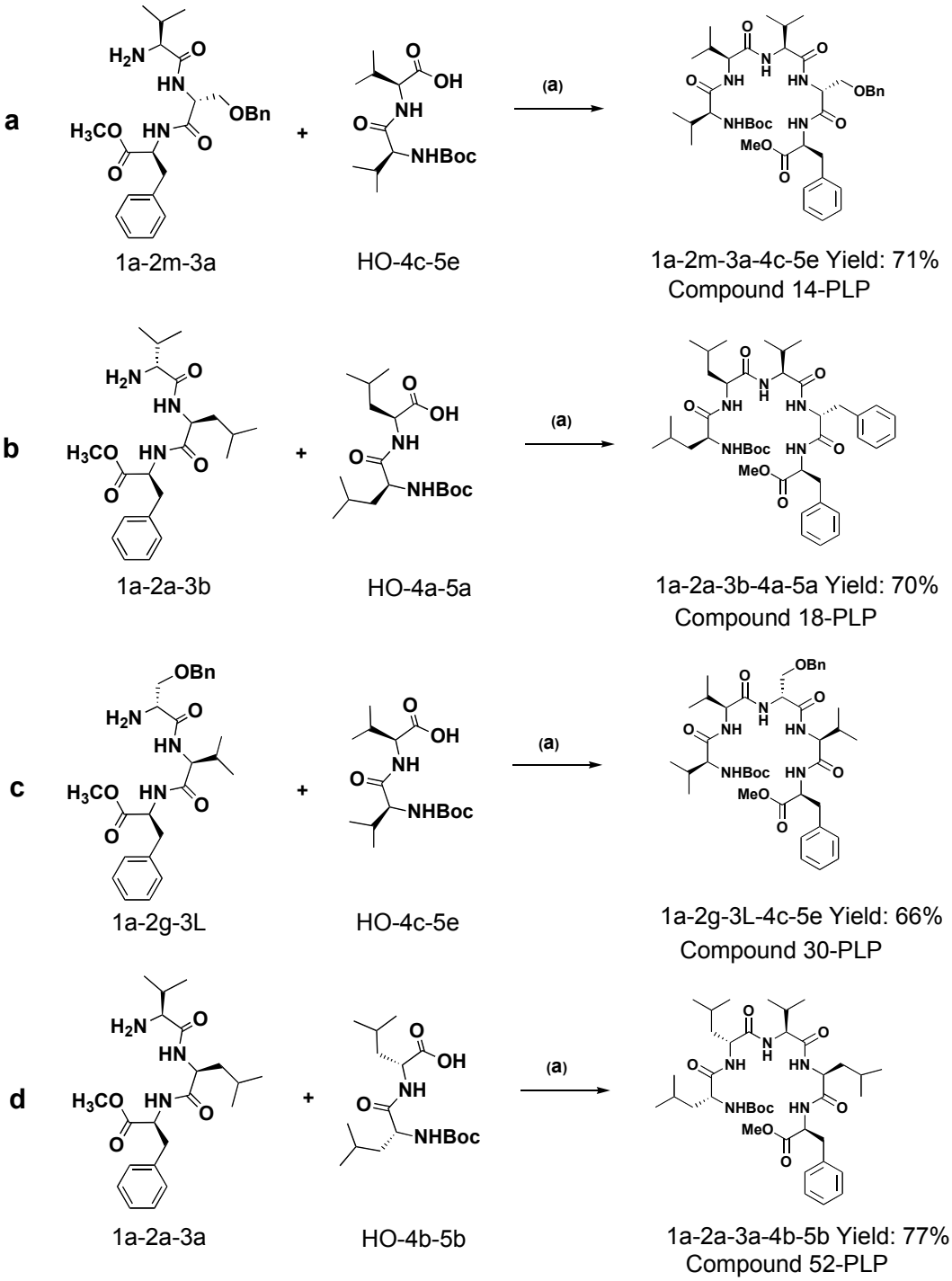

Conditions: (a) Fragment 1 (1.1eq), Fragment 2 (1.0eq), TBTU (0.7eq), HATU(0.7eq), DIPEA (6eq), CH_2Cl_2: CH_3CN (1:1) (0.1M)

Figure 2.6 Convergent Synthesis of Protected Linear Pentapeptides 14-PLP, 18-PLP, 30-PLP, and 52-PLP.

2.3 A linear Approach for the Synthesis of Compound 20

Compound **20** was not synthesized via the convergent two-fragment method. The *N*-methyl amine at position 3 of fragment 1 causes steric hindrance, which results in reduced pentapeptide yields. Since an individual amino acid is much smaller than the dipeptide, coupling a single amino acid to Fragment 1 rather than the Fragment 2 dipeptide improves the overall yield for the pentapeptide synthesis. Since compound **20** contains an *N*-methyl at the position 3, it was synthesized via this linear approach (**Figure 2.7**). The free amine tripeptide 1a-2a-3d-NH_2 (1.1 equivalents) was coupled with the free acid 4a, Boc-L-leucine-OH (1.0 equivalent). In addition to 0.7 equivalents of TBTU, 0.7 equivalents of HATU were used to facilitate coupling of the secondary amine. DIPEA (4.0 equivalents) was then added to the reaction along with anhydrous methylene chloride and acetonitrile (1:1 ratio) resulting in the tetrapeptide 1a-2a-3d-4a (74% yield). The amine protecting group on residue 4a was removed with 20% TFA in methylene chloride (0.1M) with 2 equivalents anisole to yield the free amine 1a-2a-3d-4a-NH_2. In order to form the pentapeptide, the free amine linear tetrapeptide 1a-2a-3d-4a-NH_2 (1.1 equivalents) was coupled with the free acid 5a Boc-L-leucine-OH (1.0 equivalent) with TBTU and HATU (0.7 equivalents each) and DIPEA (4 equivalents) in anhydrous methylene chloride and acetonitrile (1:1 ratio, 0.1M). The reaction was monitored via TLC. Upon completion, the crude reaction mixture was subjected to an acid-base wash followed by flash column chromatography with silica gel and an ethyl acetate-hexane gradient. ^{1}H NMR and LCMS were used to identify the product and its purity. The result was the linear protected pentapeptide: **20**-PLP (1a-2a-3d-4a-5a, 60% yield).

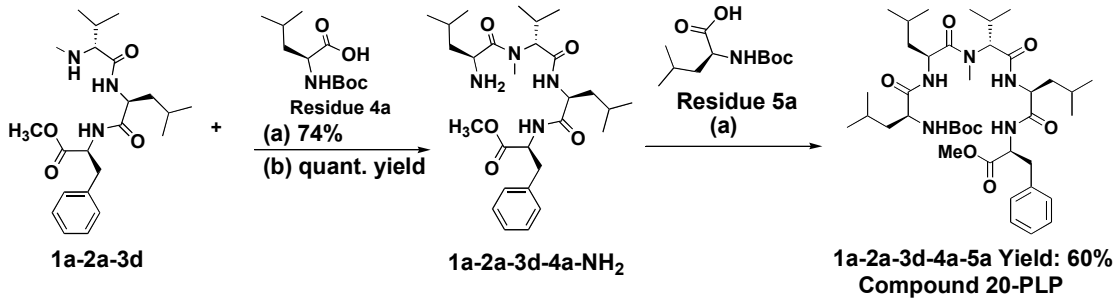

Conditions: (**a**) TBTU (0.7eq), HATU (0.7eq), DIPEA (4.0eq), CH_2Cl_2 : CH_3CN (1:1) 0.1M;
(**b**) 20% TFA, CH_2Cl_2 (0.1M)

Figure 2.7 Linear Approach to the Synthesis of Compound 31-PLP

2.4 Double Deprotection of Linear Pentapeptides

In order to cyclize the linear pentapeptide, both ends must first be deprotected. The Boc protecting group is removed to reveal the free amine at position 5. The methyl ester is then removed to reveal the free acid at postion 1. Two different methods for the double deprotection of the linear pentapeptide and cyclizing the linear precursor *in situ*[25] were utilized in my synthesis of seven San A derivatives.

2.4.1 *In-Situ* Deprotection

The Compound **14**-PLP (1a-2m-3a-4c-5e), **20-**PLP (1a-2a-3d-4a-5a), and **30**-PLP (1a-2g-3L-4c-5e) were acid and amine deprotected using concentrated HCl (8 drops per 0.3 mmols of linear pentapeptide) in tetrahydrofuran (THF) (0.05M). Anisole (2.0 equivalents) was added to the reaction and the resulting reaction was stirred at room temperature. According to TLC and LCMS analysis, which were used to monitor the reaction, it took approximately four days. Interestingly, LCMS data indicated the reaction was ~50% complete after the first day. An additional three drops of concentrated HCl per 0.3 mmol of peptide were added on the second and on the third day resulting in a total of 15 drops of concentrated HCl. On the fourth day, verification of the presence of the free-amine and the free-acid and disappearance of the starting linear protected pentapeptide permitted workup. The reaction was concentrated *in vacuo* and the double deprotected linear peptide (DLP) in quantitative yield was assumed (**Figure 2.8**).

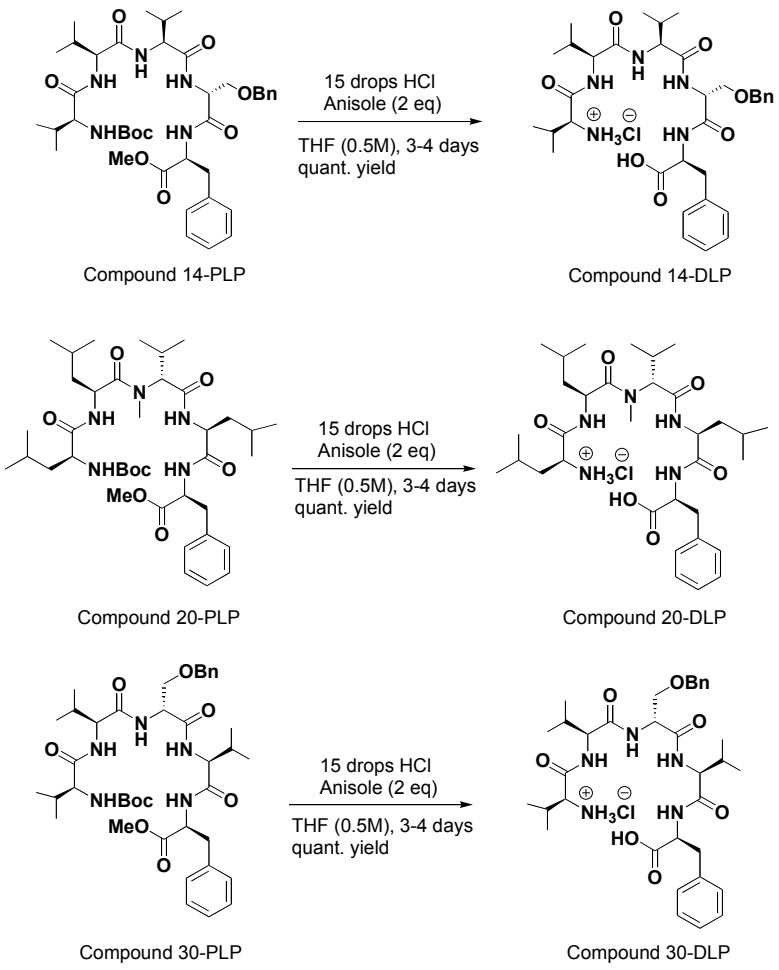

Figure 2.8 ***In situ*** **Deprotection of Protected Linear Pentapeptides 14, 20, 30.**

2.4.2 Stepwise Double Deprotection of Linear Pentapeptide

The *in situ* deprotection method using only HCl is slow, often taking a minimum of 3 days for completion. Thus, an alternate method was developed and utilized for compounds **18**-PLP and **52**-PLP (**Figure 1.9**). Protected linear pentapeptides were first acid deprotected by adding 10 equivalents of lithium hydroxide to 1.0 equivalent of protected linear pentapeptide in methanol (0.1M). These reactions were allowed to

proceed for 3-4 hours and monitored via TLC. Upon completion, the reactions were washed with 10% hydrochloric acid in DI water. In order to remove the excess lithium hydroxide, the aqueous layer was washed multiple times with fresh methylene chloride. The organic layers were then combined, dried over sodium sulfate, filtered, and concentrated via rotary evaporator. ^{1}H NMR and LCMS confirmed structure of products and their purity. This resulted in two free-acid linear pentapeptides (ALP): Compound **18**-ALP (HO-1a-2a-3b-4a-5a, 75% yield) and Compound **52**-ALP (HO-1a-2a-3a-4b-5b, 70% yield).

The Boc group was then removed with 20% TFA in methylene chloride (0.1M) and anisole (2.0 equivalents) to produce the double-deprotected linear pentapeptides (DLP): Compound **18**-DLP (HO-1a-2a-3b-4a-5a-NH_2), and compound **52**-DLP (HO-1a-2a-3a-4b-5b-NH_2). All reactions were verified by LCMS to observe the free–acid and free-amine and as is typical in these deprotection reactions quantitative yields were assumed. Overall, this second method of a stepwise double deprotection resulted in the rapid recovery (~1 day) of a much cleaner product than the *in situ* approach. This was confirmed by LCMS analysis.

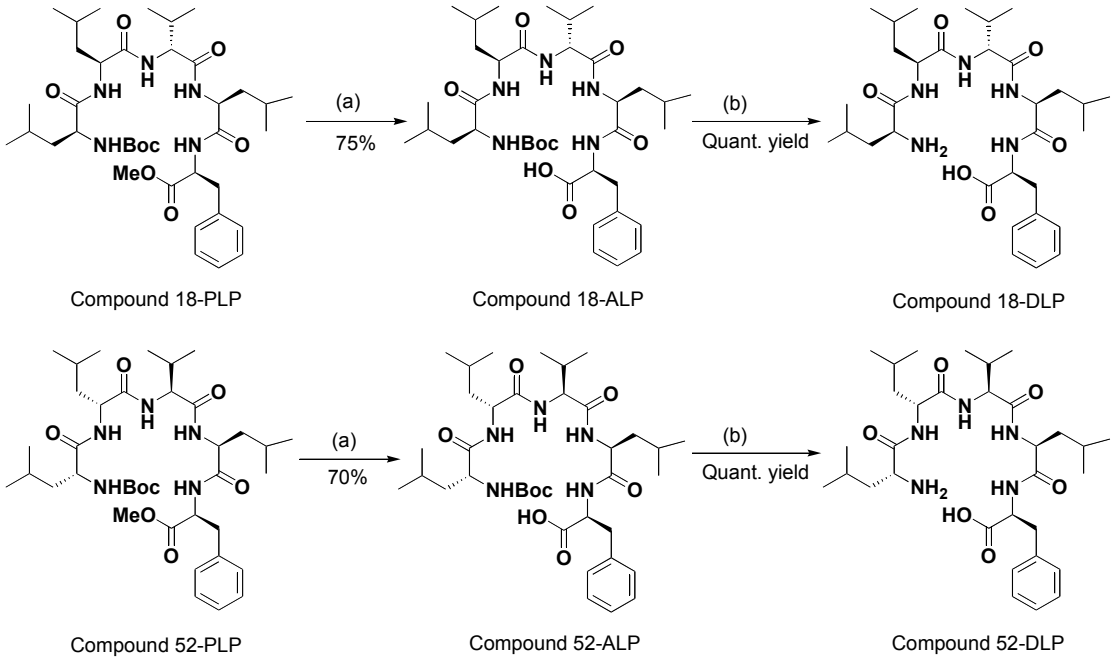

Figure 2.9 Stepwise Linear Double Deprotection of Compounds 18-PLP, 52-PLP.

2.5 Macrocyclization Procedures

The double deprotected linear pentapeptides (DLPs) were concentrated *in vacuo* and combined in a flask with three coupling agents: TBTU and HATU (0.7 equivalents each), DEPBT (3-(diethoxyphosphoryloxy)-1,2,3-benzotriazin-4-(3H)-one) (0.2 equivalents) along with DIPEA (6.0 equivalents) in anhydrous methylene chloride: acetonitrile (1:1 ratio, 0.1M) solution. Reactions were performed at a concentration of 0.007M and monitored via LCMS and were generally allowed to proceed three hours for compounds **18**, **20**, and **52**. Due to solubility problems, dimethyl foramide (DMF) was

added to the reaction mixture of compounds **14** and **30** respectively dropwise, until the reaction became clear. The more dilute reactions (0.0008) that were forming compounds **14** and **30** were allowed to proceed for a longer period of time (5-6 hours). Upon completion, the crude reaction mixtures were washed with saturated ammonium chloride three times. The organic layers were combined, dried over sodium sulfate, and concentrated via rotary evaporator. Flash column chromatography using an ethyl acetate-hexanes gradient over silica gel was used to isolate macrocyclic peptides. These macrocycles underwent further purification by reversed-phase HPLC using DI water: acetonitrile and 0.1% TFA gradient to afford macrocycles: 1a-2m-3a-4c-5e (compound **14**, 11% yield), 1a-2a-3b-4a-5a (compound **18**, 16% yield), 1a-2a-3d-4a-5a (compound **20**, 4% yield), 1a-2g-3L-4c-5e (compound **30**, 9% yield), and 1a-2a-3a-4b-5b (compound **52**, 8% yield). ^{1}H NMR and LCMS confirmed structure of products and their purity (**Figure 2.10**).

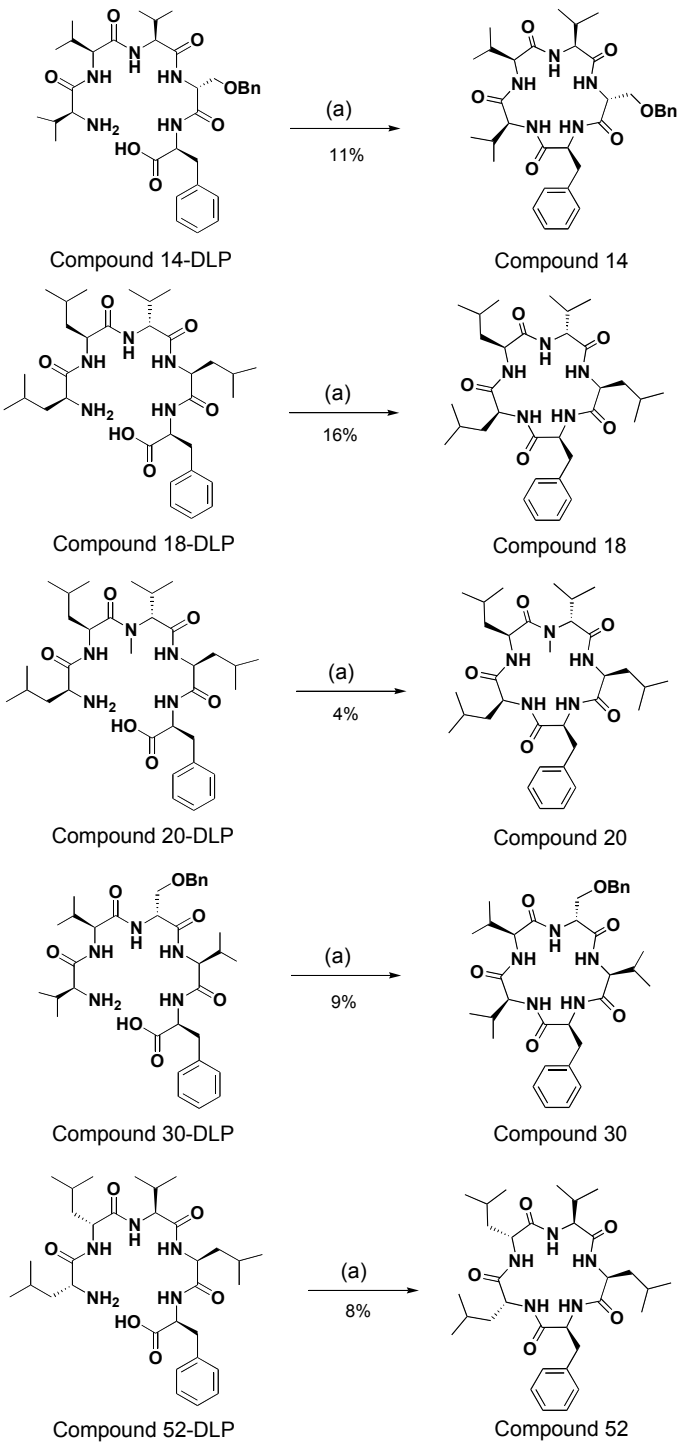

Condition: (a) TBTU (0.7eq), HATU (0.7eq), DEPBT (0.2eq), DIPEA (6eq), CH_2Cl_2: CH_3CN (1:1) to a concentration of 0.004-0.007M

Figure 2.10 Cyclization of Double Deprotected Linear Pentapeptides 14, 18, 20, 30, and 52.

2.6 Cbz Deprotection Procedures

The benzyl protected compound **14** and **30** were deprotected by using the following procedure: compound **14** and **30** were dissolved in ethanol (0.1M), and then Pd-C (10%) was added to the reaction, and then H_2 gas was bubbled into the reaction. The reactions were performed under H_2 at room temperature for 8 hours and monitored by TLC. Upon completion, reactions were filtered through celite to remove the Pd-C. This isolated crude reaction products were then purified by reversed-phase HPLC. ^{1}H NMR and LCMS confirmed structures of the resulting compounds, **12** yield 25% and **25** yield 35% (**Figure 2.11**).

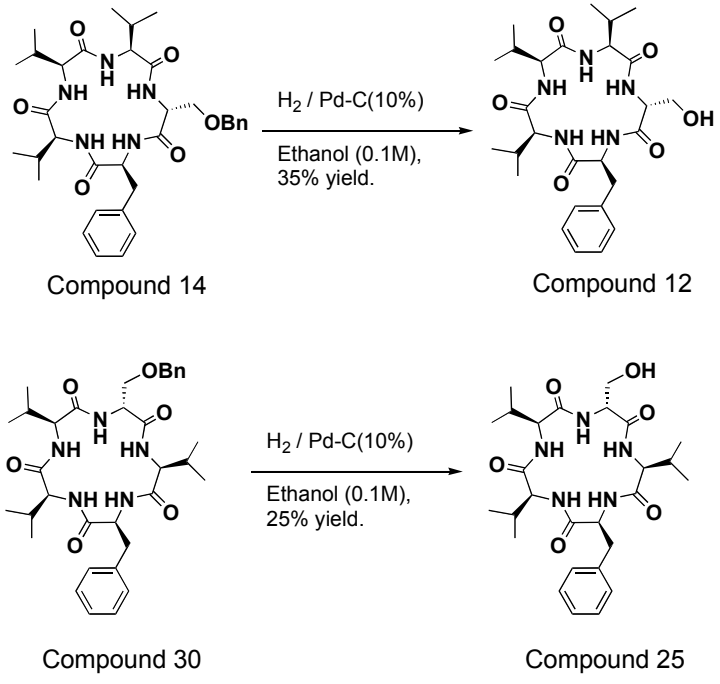

Figure 2.11 Benzyl Deprotection of Compound 14, 30.

2.7 Conclusions

The described work resulted in the completion of seven compounds (**Figure 2.3**), which were added to the existing series of San A analogues that were produced by our laboratory. These compounds have diversity in conformational space (L-versus D-amino acids), and variation in their polarity (hydrophobic versus hydrophilic groups). Overall, the reactions gave pure products, thus providing copious amounts of material that is later used for biological testing. Thus, this work presents a general method for building cyclic pentapeptide libraries that can be used to explore the structure activity relationship (SAR) of San A derivatives. The SAR of these compounds is discussed in Chapter 3. A diverse set of San A analogs that were tested against multiple cancer cell lines will highlight key structural features that are important for cytotoxicity against cancer cells. This data will then be useful in designing new and more potent compounds as future chemotherapeutic agents.

Chapter 2 in part, has been published as it may appear in "Identification of Sansalvamide a analog potent against pancreatic cancer cell lines", ***Bioorganic and Medicinal Chemistry Letters,*** *17*, **2007**, 5072-5077. Po-Shen Pan, Kathleen L. McGuire and Shelli R. McAlpine. The dissertation author was the primary author of this paper.

Chapter 3

Structure-Activity Relationships of Sansalvamide A Analoges

3.1 Models of Carcinogenesis

In this chapter, I will discuss structure-activity relationships data on 64 sansalvamide A derivatives. 7 of which were synthesized by me and described in chapter 2 and 57 of which were made by colleagues. Of the 128 growth inhibition numbers from ^{3}H-labeled thymidine uptake assays discussed here I gathered 88 of the growth inhibition numbers, the rest were gather by my colleagues, Robert C. Vasko. Pancreatic cancer is the fifth most deadly cancer in the U.S. Only 10% of patients are eligible for surgery[26], and less than 20% of pancreatic cancers respond to the current drugs of choice, the most common of which is Gemcitabine (2,2-difluorodeoxycytidine).[27] The five-year survival rate for patients with pancreatic cancers is less than 5%.[28] With such a poor rate of response to current chemotherapeutic methods, there is an immediate need for new and effective pancreatic cancer treatments.

3.2 Peptides as Drugs

Peptides are often considered poor drugs for two reasons: poor cell permeability and rapid degradation within cells.[15, 16] This is because in order for linear peptides to achieve well define **3-D**imensional (3-D) conformations that will bind appropriately to their protein targets, they are often composed of extended sequences of amino acids that

lead to decrease in cell permeability. Cyclic peptides, such as Sansalvamide A (San A), have better "drug-like" qualities than linear peptides because a smaller number of amino acids define a more conformational restrained 3-D structure thus they are more cell permeable than linear peptide drugs. In addition, cyclic peptides degrade much slower than linear peptides because proteases have difficulty cleaving amide bonds located in a macrocycle. San A analogs also have the advantage that they are lipophilic and therefore they have rapid membrane absorption.[10] Finally, cyclic peptides tend to have a greater binding affinity for protein targets than their linear counterparts or smaller molecules because they have restricted bond rotation and are conformationally constrained.[22] In summary, cyclic peptides have commercially available chemical diversity (i.e. amino acids), possess defined 3-D structures that have good binding affinity for protein targets, are effective at penetrating cell membranes, and are relatively stable within cells.[11, 12]

Although major efforts have been made, few truly novel classes of compounds have been identified that have activity against drug-resistant pancreatic cancer tumors.[17] With this in mind, my work elucidates an understanding of the complex structure-activity relationship (SAR) of sixty-four San A derivatives against two drug-resistant pancreatic cancer cell lines (PL45, BxPC-3).[29] This SAR study describes an overview of the cytotoxicity in cell-based assays for the San A clan of molecules and establishes a relationship between the 3-D structures of the active compounds' side chain and their growth inhibition against two cell lines.

We have discovered that there are two factors important for potency: a single *N*-methyl and / or a single D-amino acid. This theory is validated by several current

examples described in the recent literature, where cyclic peptides, specifically pentapeptides, with a single D-amino acid lock the macrocycle into a strict conformation.[22-24] Further, it is well established that these cyclic pentapeptides mimic beta and gamma turns and serve as templates for the appropriate positioning of suitable binding motifs for proteins.[30, 31]

3.3 Positional Approach to Activity

To date, there is still an incomplete understanding of the structure-activity relationship (SAR) of San A, especially in drug-resistant pancreatic cancers. Thus, it is crucial to evaluate the key SARs for targeting drug-resistant pancreatic cancers so that future analogs will have greater potency. Initially, there was no known target for San A in cancer cell lines; therefore a medicinal chemistry approach was used to evaluate structural features that are key to potency. This approach involves synthesizing of compound analogues that have both single and multiple key changes and testing them for potency. The core peptide structure serves as a scaffold and compounds' potency are organized by changes to the amino acids at each position (1-5) around the peptide macrocycle backbone (**Figure 3.1)**. Cell proliferation was monitored by measuring how much ^{3}H-thymidine was incorporated into a cell's DNA. This data can be analyzed to determine a particular compound's activity. ^{3}H-thymidine uptake assays were performed using two distinguishable pancreatic cancer cell lines: PL45 and BxPC-3. Data shown gives percent growth inhibition at 5μM concentrations.

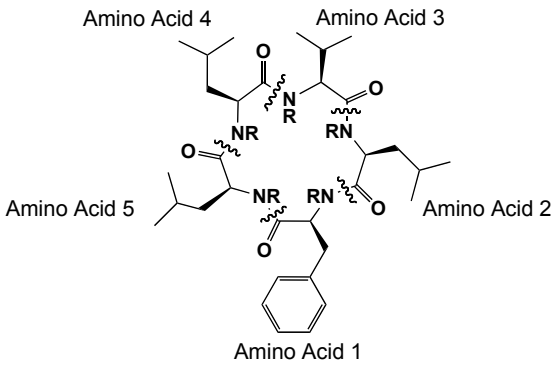

Figure 3.1. Numbering System for San A Peptide Derivatives.

3.3.1 Structure-Activity Relationships (SAR) Position One

Sixty-four San A analogs have been tested for cytotoxicity against two drug-resistant pancreatic carcinoma cell lines (PL45, BxPC-3). The use of two cell lines ensures that our compounds are consistently inhibiting drug-resistant pancreatic cancers. In addition, it clearly establishes the structure-activity relationship (SAR), and determines the key features necessary to inhibit growth of pancreatic cancer cells. Potency exhibited by the San A peptide (compound **1)** is shown so that comparisons can be made between the natural product peptide and our synthetic analogs. The histogram in **Figure 3.2** shows the percent inhibition of growth produced by the addition of compounds (5μM concentration) that have changes at position 1 to two pancreatic cell lines. Any value below or equal to 45% growth inhibition is not considered a lead structure. Compared to compound **1**, two compounds show a moderate increased potency against PL45 and BxPC-3: Compound **2**, which incorporated a D-phenylalanine, and compound **3**, which

incorporated a *N*-methyl-L-phenylalanine at position 1. Compound **4** places a constrained aromatic moiety, an L-tetrahydroisoquinoline amino acid (aa), at position 1. Compound **4** shows a limited improvement on potency compared to compound **1** against both cell lines suggesting that restraining the rotational freedom at position 1 may not be a significant factor in increasing potency. Finally, compounds **5** and **6** were designed to determine whether an H-bonding element would improve the cytotoxicity against pancreatic cancer cell lines (PL45, BxPC-3). **Figure 3.2** shows that compound **5**'s potency is slightly increased against PL45 compared to that of compound **1** but it is not as effective in BxPC-3. Interestingly compound **6** is significantly less potent than compound **1**, possibly due to steric hindrance of the tryptophen residue when San A is binding to its biological target.

Overall, two compounds **2**, and **4** in this series showed improved potency over the compound **1** and greater than 45% growth inhibition against both cell lines. This compound contained a D-phenylalanine, compound **2**, and a L-tetrahydroisoquinoline, compound **4**, at position 1.

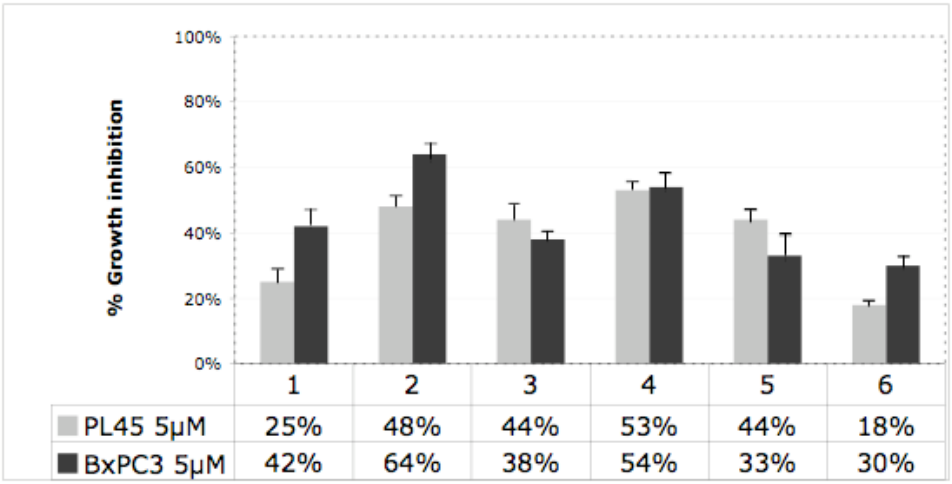

	1	2	3	4	5	6
PL45 5μM	25%	48%	44%	53%	44%	18%
BxPC3 5μM	42%	64%	38%	54%	33%	30%

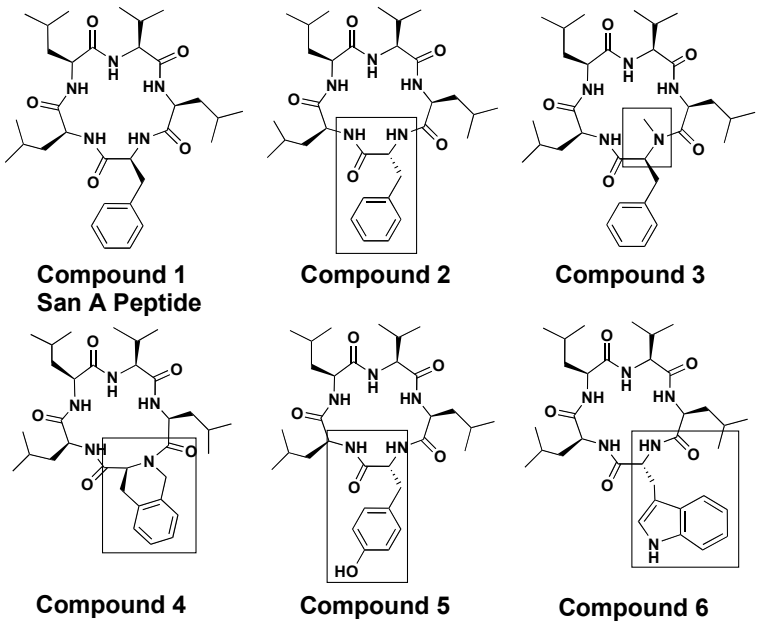

Compound 1
San A Peptide

Compound 2

Compound 3

Compound 4

Compound 5

Compound 6

Figure 3.2. Compounds with Alterations at Position 1. Data is Represented as % Growth Inhibition Relative to 1% DMSO Control. Each Data Point is an Average of 4 wells Performed in Three Assays. All Assays were Allowed to Proceed for 72 hours at 5μM Compound Concentration.

3.3.2 Structure-Activity Relationships (SAR) Position Two

The histogram in **Figure 3.3** shows the percent inhibition of growth by compounds with changes at position 2. There is no improvement in growth inhibition for compound **7**, which incorporated a *N*-methyl-L-leucine at position 2, over compound **1**. Replacing a L-leucine at postion 2 (compound **1**) with a D-leucine at position 2 (compound **8**) slightly decreased potency against BxPC-3, but incorporation of *N*-methyl-D-leucine at position 2 (compound **9**) dramatically decreased the potency against both cell lines. Comparing compound **11**, which incorporates a D-phenyl alanine at position 2 to compound **13**, which incorporates a D-serine at position 2, indicates that a hydrophobic element at position 2 slightly improves the potency against PL45. Yet, both compounds show decreased potency against BxPC-3. Interestingly, placing a *N*-methyl-D-phenyl alanine at position 2 (compound **10**) dramatically reduced the potency against both cell lines. Compound **12** and **14** share similar features except compound **12** incorporates a D-serine at position 2 and compound **14** has a benzyloxy protected D-serine at position 2. Both compounds are inactive compared to compound **1**. Moreover, the potency of compound **12** over both cell lines dropped significantly.

Overall, none of the compound in this series demonstrated a clear improvement in growth inhibition.

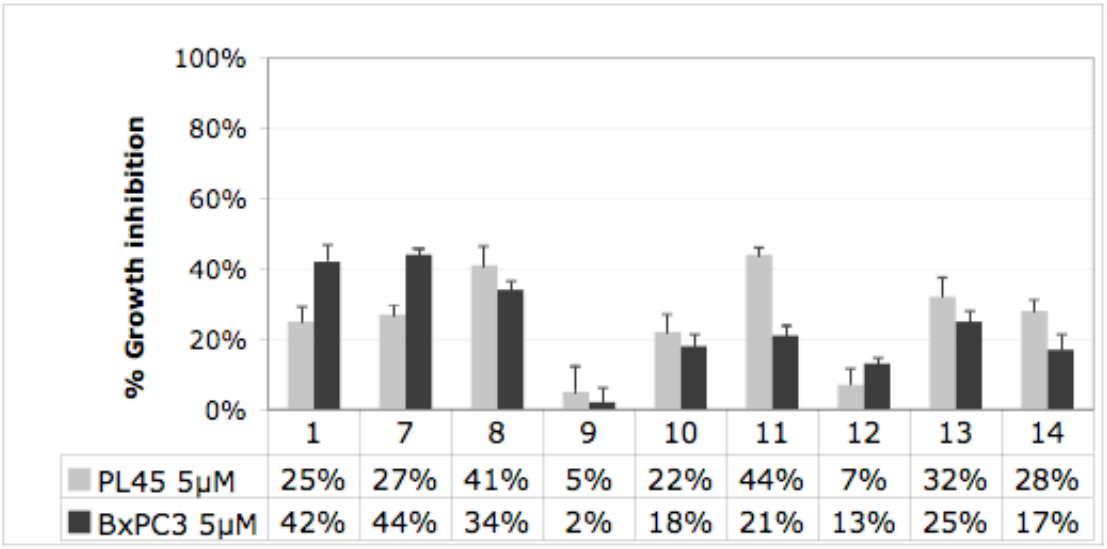

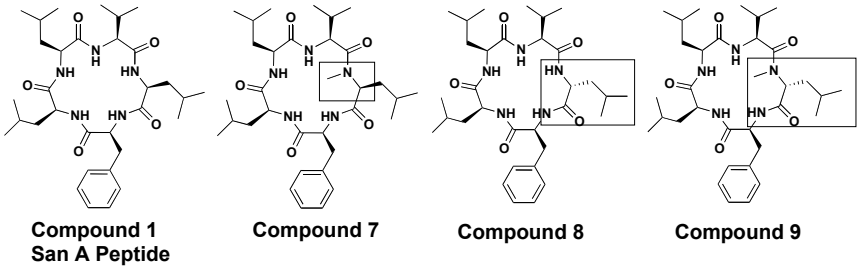

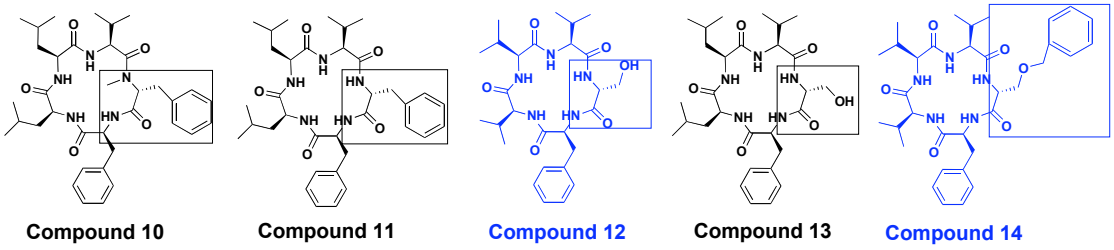

Figure 3.3. Compounds with Alterations at Position 2. Data is Represented as % Growth Inhibition Relative to 1% DMSO Control. Each Data Point is an Average of 4 wells Performed in Three Assays. All Assays were Allowed to Proceed for 72 Hours at 5μM Compound Concentration.

3.3.3 Structure-Activity Relationships (SAR) Position Three

The histogram in **Figure 3.4** shows the percent inhibition of growth by compounds with changes at position 3. Compound **15** incorporates an *N*-methyl-valine at position 3, compound **18** a D-valine, and compound **20**, a *N*-methyl-D-valine at position 3. Only compound **18** shows greater than 45% growth inhibition against both cell lines. In contrast to **1**, which contains an isopropyl moiety at position 3, compounds containing a methyl (compound **16)** or an ethyl (compound **17)** moiety at position 3 are tested. Both of these compounds showed significantly reduced potency against PL45, although, compound **17** still remains active against BxPC-3. Similar to compound **17**, compound **27** contains an ethyl moiety at position 3 along with a D-leucine at position 2 and shows no improvement in potency compared to **1**. Interestingly, placing either a hydrophilic element at position 3 (compound **22**) or a hydrophobic element at position 3 (compound **26**) does not help to increase the potency against either cell lines. This trend was also observed with compounds **25** and **30**. Compound **23** and **24** share an almost identical core structure except compound **23** has an isopropyl moiety at position 3 and **24** has an ethyl moiety at position 3. Both compounds are inactive against PL45; yet, compound **23** shows excellent potency against BxPC-3. Compound **19** which incorporated a D-phenylalanine at position 1, a D-leucine at position 2, and a D-valine at position 3 shows significant potency against PL45. Compounds **21** and **29** involved alterations at both position 2 and 3. Compound **21** showed similar potency compared to **1** against PL45 but showed no potency against BxPC-3. Compound **29** showed greatly decreased potency relative to **1** against BxPC-3; yet, has improved potency against PL45. Analogously,

compounds **24** and **28**, which both contain a D-methylalanine at position 3, were both inactive against both cell lines. Interestingly, **18**, which contains a D-valine at position 3, is excellent against both cell lines, yet **23**, which contains L-valines substituted at positions 2, 4, and 5 in addition to a D-valine at position 3 only showed greater than 45% growth inhibition against BxPC-3.

Overall, only **18** demonstrated a clear and significant improvement in growth inhibition against both cell lines. One compound, **19**, showed greater than 45% growth inhibition against PL45 and one compound **23** showed a significant increase in growth inhibition against BxPC-3.

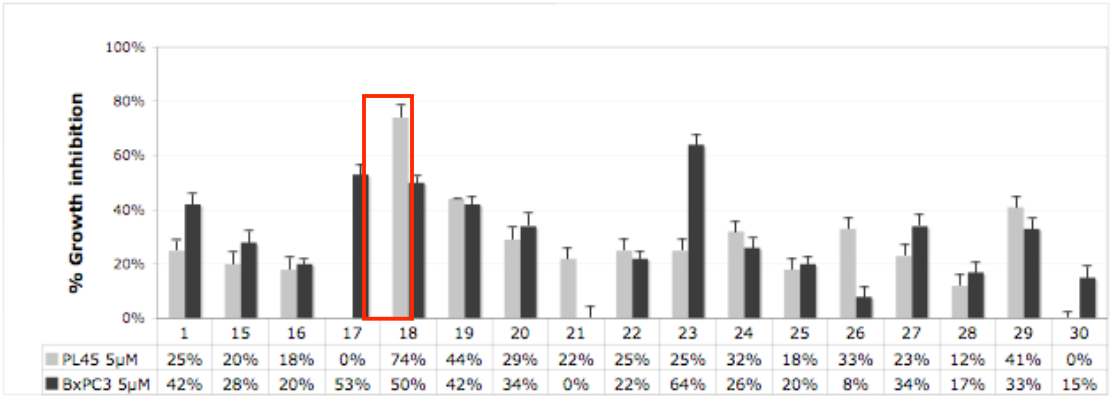

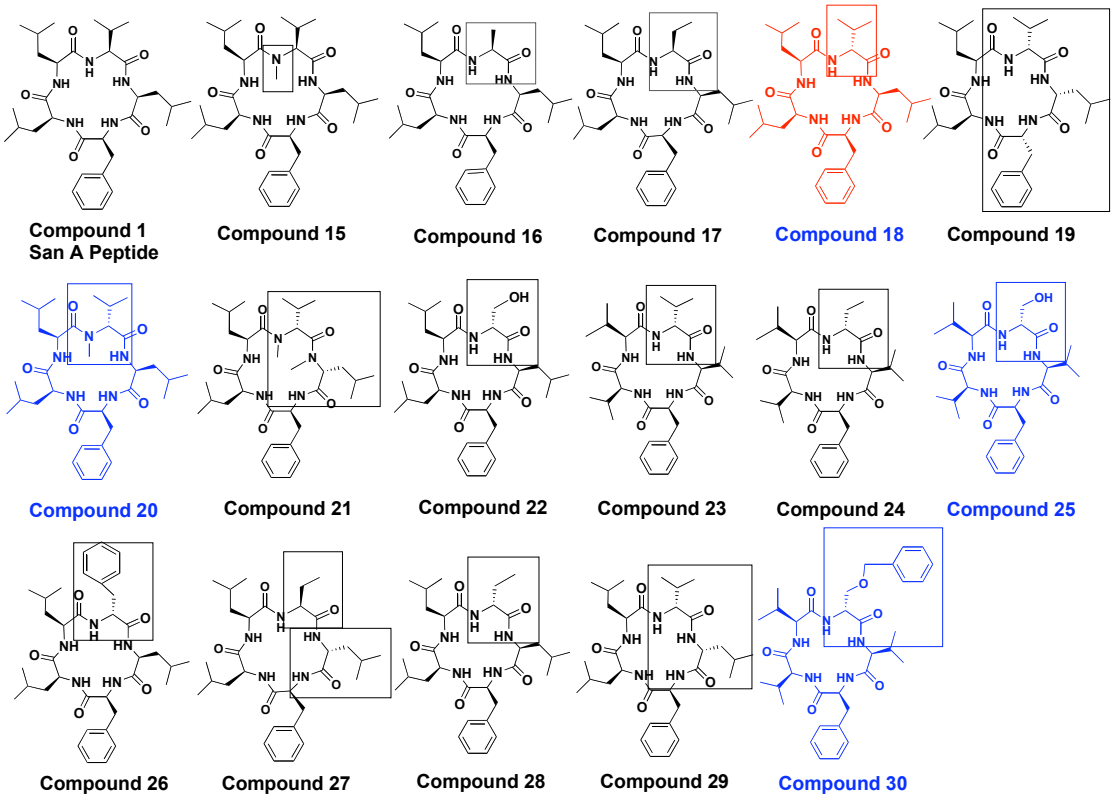

Figure 3.4. Compounds with Alterations in Position 3. Data is Represented as % Growth Inhibition Relative to 1% DMSO Control. Each Data Point is an Average of 4 wells Performed in Three Assays. All Assays were Allowed to Proceed for 72 hours at 5μM Compound Concentration.

3.3.4 Structure-Activity Relationships (SAR) Position Four

The histogram in **Figure 3.5** shows the percent inhibition of growth by compounds with changes at position 4. Compound **31**, which incorporates a D-leucine at position 4, shows excellent inhibition against BxPC-3 but not PL45, whereas compound **32**, which incorporates an *N*-methyl moiety at position 4, showed some promise against PL45, not against BxPC-3. Compound **33**, which has D-leucine at position 4 along with D-phenylalanine at position 1 and a D-leucine at position 3, exhibited greater than 45% growth inhibition against BxPC-3 but not PL45. Compounds **35**, **36**, **37**, **39**, and **44** all contain a lysine at position 4, as well as other changes. All five compounds are uniformly non-toxic against both cell lines. Interestingly, the hydrophobic compound that are structurally related to these five polar compounds, **40**, **41**, **42**, **43**, and **46** respectively, are also non-toxic and show very limited potency against these cell lines. Further, the incorporation of an *N*-methyl D-valine, and a cyclohexyl moiety at position 4 produced compound **34**, which is relatively potent against both cell lines. In addition both compound **38**, and **45** incorporate the same cyclohexyl moiety at position 4 as seen in compound **34**, where **38** incorporates a ethyl moiety at position 3, and **45** contains a *N*-methyl-D-phenyl alanine at position 2. Compound **38** shows the same potency against both cell lines relative to **1** and compound **45** shows similar potency as **34** against PL45 but reduced potency against BxPC-3. Finally, incorporation of a Cbz protected arginine, **47**, at position 4 along with a hydrogen bonding element at position 1 clearly decreases the potency against both cell lines.

Overall, one compound **31**, which has a D-leucine at postion 4, was found to be significantly potent against BxPC-3, and one compound **33**, which has D-leucine at position 4 along with D-phenylalanine at 1 and a D-leucine at 3, was found to be potent against both cell lines. Both of these compounds were found to be the most potent against BxPC-3. Only compound **34**, which contains a cyclohexyl moiety at position 4 and a *N*-methyl D-valine at position 3, exhibited greater than 45% growth inhibition against both cell lines.

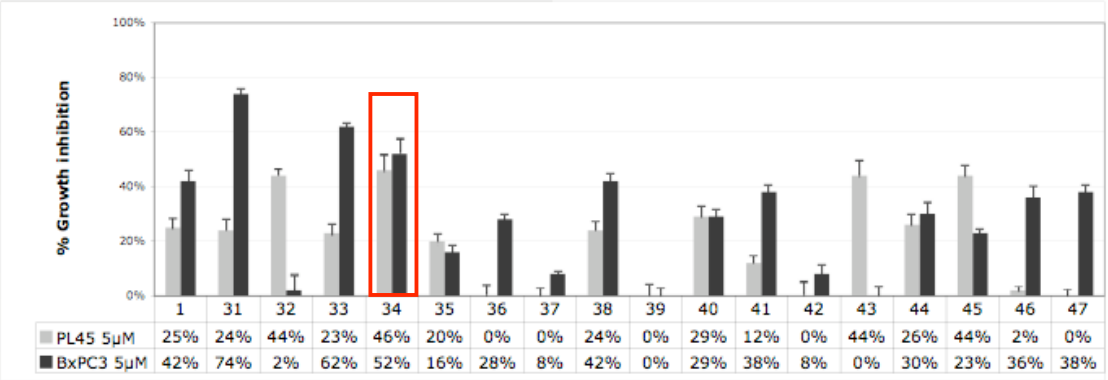

	1	31	32	33	34	35	36	37	38	39	40	41	42	43	44	45	46	47
PL45 5μM	25%	24%	44%	23%	46%	20%	0%	0%	24%	0%	29%	12%	0%	44%	26%	44%	2%	0%
BxPC3 5μM	42%	74%	2%	62%	52%	16%	28%	8%	42%	0%	29%	38%	8%	0%	30%	23%	36%	38%

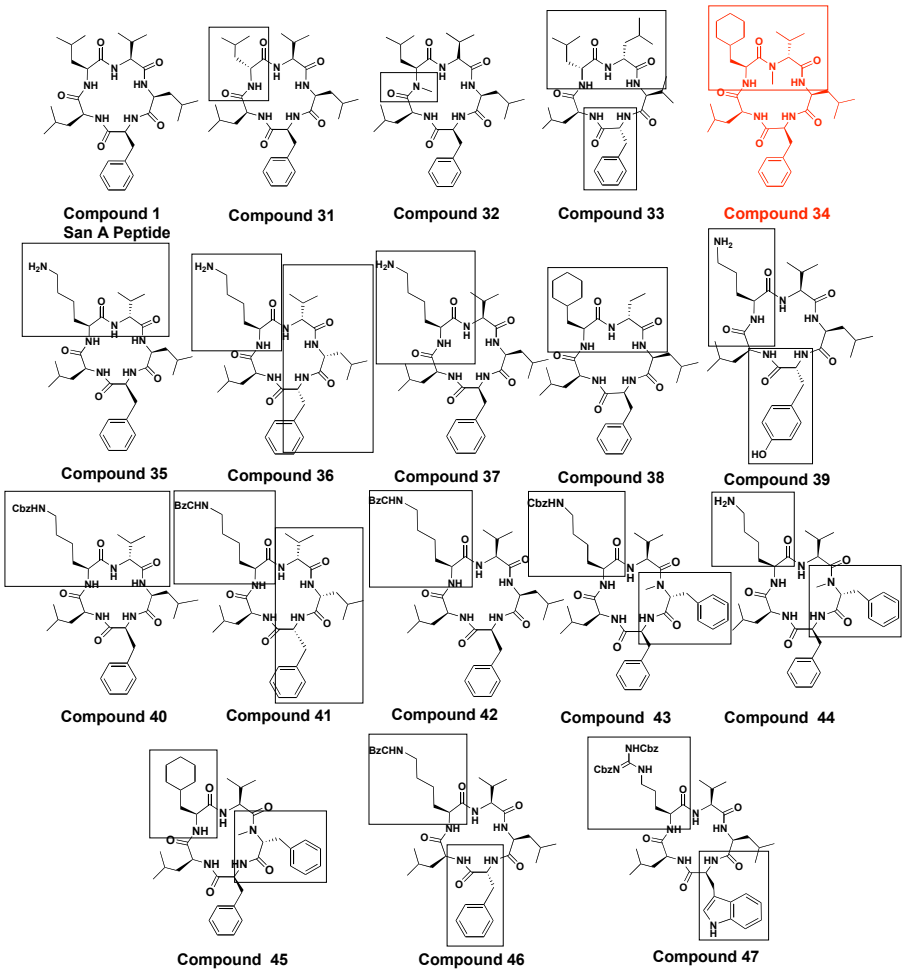

Figure 3.5. Compounds with Alterations at Position 4. Data is Represented as % Growth Inhibition Relative to 1% DMSO Control. Each Data Point is an Average of 4 wells Performed in Three Assays. All Assays were Allowed to Proceed for 72 Hours at 5μM Compound Concentration.

3.3.5 Structure-Activity Relationships (SAR) Position Five

The histogram in **Figure 3.6** shows the percent inhibition of growth by compounds with changes at position 5. Compound **48** incorporates an *N*-methy-L-leucine at position 5, compound **49** a D-leucine, and compound **54** an *N*-methyl D-leucines. Of these three compounds both **48** and **54** exhibit greater than 45% growth inhibition against both cell lines, and **49** is very potent against PL45. In contrast to **49**, structurally similar compound **50**, which contains an *N*-methyl-L-leucine at position 4 and D-leucine at position 5, showed significant potency against BxPC-3 but decreased potency against PL45. Compound **51**, which involved alterations at positions 1, 4, and 5 also showed promising potency against both cell lines. Incorporating a D-leucine at positions 4 and 5 gave compound **52**, which showed excellent growth inhibition against both cell lines. Compounds **55** and **56**, which contain a D-leucine at postion 5 and are structurally similar to compound **49**, showed poor growth inhibition against both cell lines. Compound **57**, which is similar to potent compound **48** also showed poor cytotoxicity against these two cell lines. It is important to note that compounds **56**, and **57**, which both contain the potent residue from **18** (a D-valine at position 3) as well as substitutions at position 5, both have reduced potency compared to the parent compounds **1**, **48**, **18**, or **49**. Thus, combined features do not generate synergistic cytotoxic effects. Compound **58** and compound **64** have almost identical features except compound **58** incorporates an L-lysine at position 5 and compound **64** incorporates a Cbz protected lysine at position 5. Interestingly, only compound **64** shows activity against both cell lines. This indicates perhaps the active site of the biological target is more accessible to the hydrophobic

molecule. This trend was also observed in compound **59**, and **62**. Compound **60**, which contains a *N*-methyl-L-valine at position 3, a D-leucine at position 4 and a D-phenyl alanine at position 5 is the most potent San A derivative discovered to date. It is interesting to note that compound **60** is also the only compound that incorporates a D-phenyl alanine at position 5. This suggests that incorporating a D-aromatic moiety into the molecule at position 5 will help it bind to its biological target. Finally, compound **53**, **61**, and **63** include substitutions at three different positions relative to San A **1**. They were synthesized in order to explore whether multiple specific features that appear to be critical to potency, can be utilized synergistically to improve activity over the parent compound. The growth inhibition data indicates that only compound **53** shows greater than 45% inhibition potency against PL45, while compound **61** and **63** show the same potency against both cell lines relative to **1**.

Overall, six compounds were found to be active (growth inhibition ≥ 45% for both cell lines) in this series: **48**, **51**, **52**, **54**, **60**, and **64**. Three out of six contain at least two D-amino acids: compounds **51**, **52**, **60**. Compound **60**, the most potent compound in all series, is composed of two D-amino acids including a unique D-phenyl alanine at position 5. This information perhaps suggests that having two D-aas next to each other in the core structure may facilitate the San A derivatives in presentation to its biological target by inducing an appropriate conformation. In addition, the compounds that contain hydrophilic elements exhibit greatly reduced potency over both cell lines indicating that hydrophobic elements are the key for the molecule to access the biological target's active site.

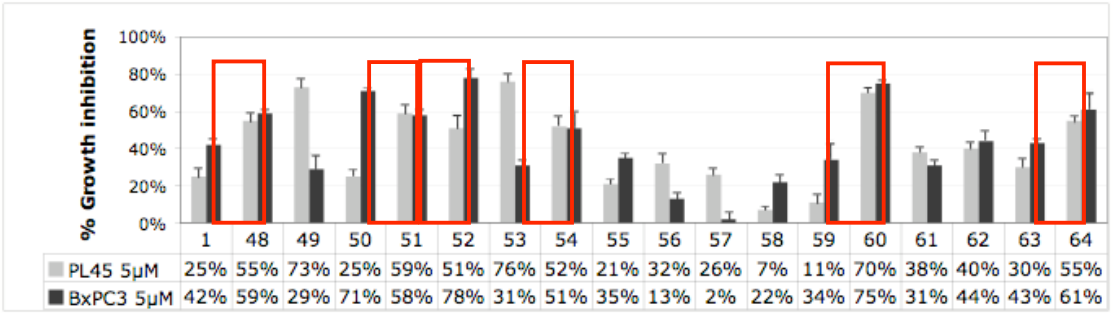

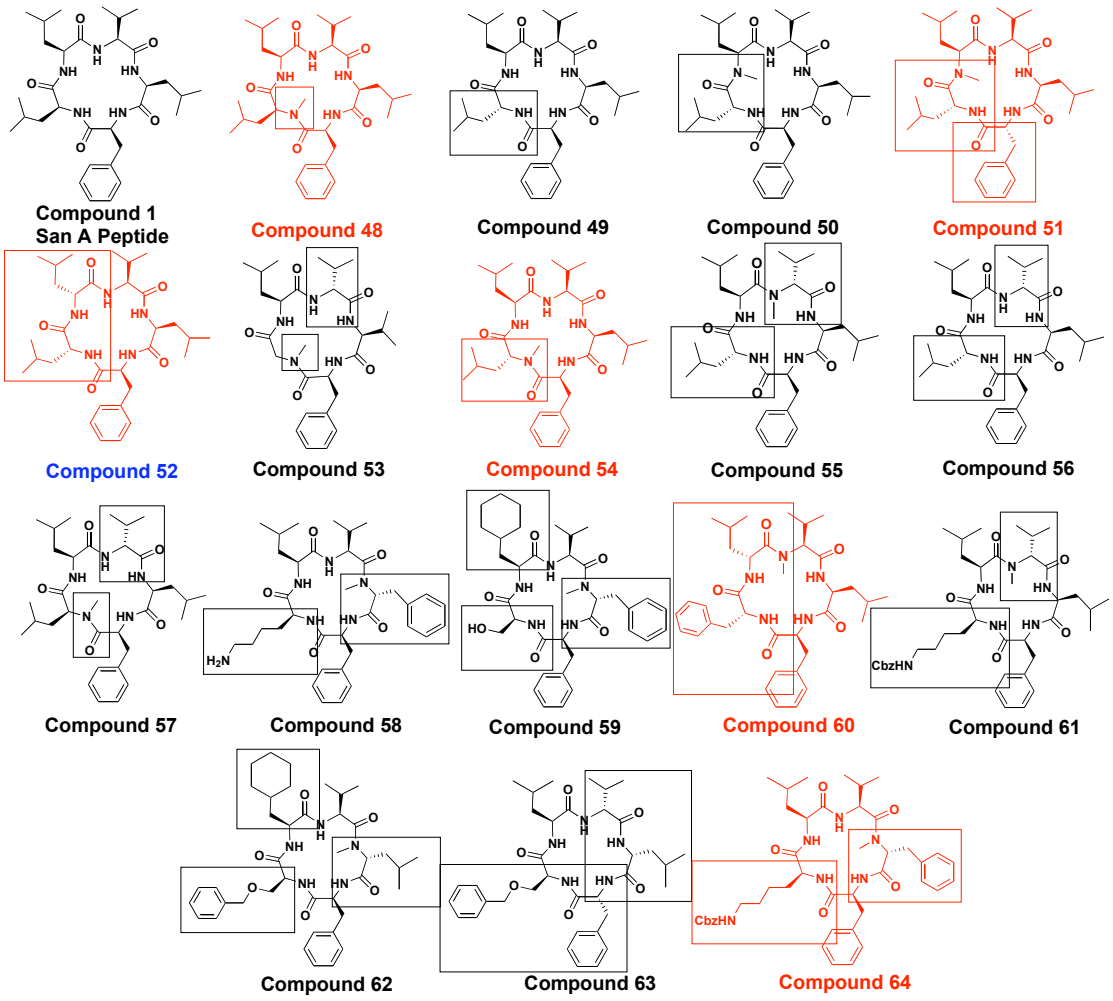

Figure 3.6. Compounds with Alterations at Position 5. Data is Represented as % Growth Inhibition Relative to 1% DMSO Control. Each Data Point is an Average of 4 wells Performed in Three Assays. All Assays were Allowed to Proceed for 72 Hours at 5μM Compound Concentration.

3.3.6 IC_{50} Determination

Inhibition constants were calculated for the most potent compounds by plotting five concentrations (50, 10, 0.5, and 0.1μM) and extracting data from the curves. All relationships are exponential in nature. We have identified 6 compounds **18**, **34**, **52**, **54**, **60**, **64** that show low micromolar potency against pancreatic cancer cell lines. The IC_{50} values for the most potent compounds are shown in **Figure 3.7.** Compound **18**, **54**, **60** and **64** have low micromolar IC_{50} values against BxPC-3 and PL45 and are ~20 fold more active than the parent San A peptide **1**. Compound **52** shows ~14 fold more selectivity against pancreatic cancer than the San A petpdie **1**. Finally, compound **34** has low micromolar activity against PL45 and is ~10 fold more active than the San A peptide **1**.

Gemzar® (Gemcitabine), a current drug on the market, is an anticancer drug used primarily for the treatment of pancreatic cancer. It is used as a control where its activity is compared to the San A derivatives. Although San A analogues **18**, **34**, **52**, **54**, **60**, **64** are less effective than this drug, they show promising result as they all possess low micromolar potency against PL45 and BxPC-3. Since San A is structurally different from Gemzar®, which is a nucleoside analog, it is most likely inhibiting cell growth via a different mechanism. Our preliminary data indicates that San A analogues disrupt Hsp90-IP6K2 binding, which leads to apoptosis.

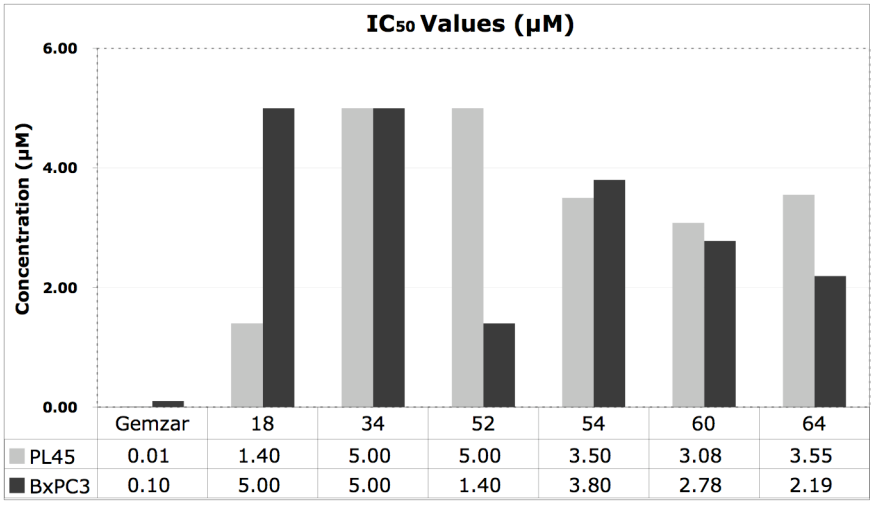

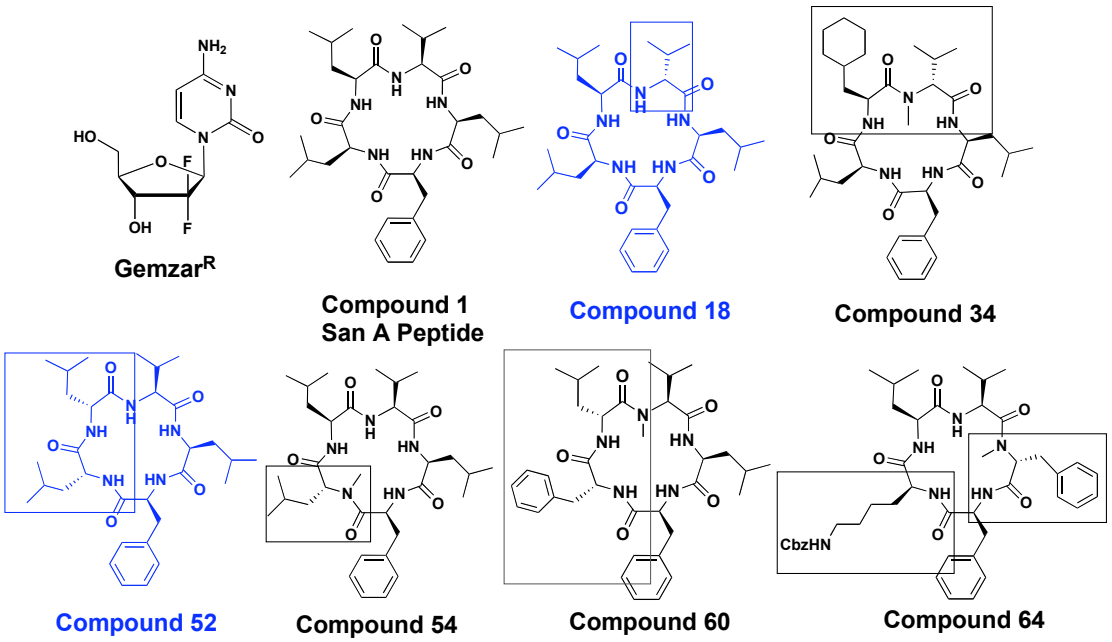

Figure 3.7. IC_{50s} of Potent Compounds. Each Data Point is an Average of 4 wells Performed in Three Assays at 50, 10, 0.5, and 0.1µMs.

3.3.7 Summary of SAR results

The most important features to emerge from this SAR study includes the incorporation of a D-phenylalanine at position 1, a D-valine at position 3, and an *N*-methyl or D-leucine or D-phenylalanine or *N*-methyl D-leucine at position 5. It is important to note that compounds **50** and **51** are both potent against BxPC-3. However, compound **50**, which is structurally very similar to compound **51**, indicated that specific residues at a single position are not the only controlling factor for cytotoxicity, where compound **50** features a *N*-methyl-D-leucine with a L-phenylalanine and compound **51** features a *N*-methyl-D-leucine with a D-phenylalanine at position one. Thus, a single feature or position is not responsible for potency as both compounds maintain cytoxicity in against pancreatic cancer. Rather, as is typical in complex systems, there are several determining factors. It seems that a key connection between potency and structure involves constraining the macrocycle into its preferred and active conformation. Further, because all compounds are cyclic peptides, they have restricted bond rotations, and are conformationally constrained, suggesting that their binding affinity for their target is greater than any small molecule.[22] Recent publications highlight that a single *N*-methyl and/or D-aa is a key structural component required to maintain a dominant conformation in macrocycles with five amino acids.[23, 24] Thus, the inclusion of a single *N*-methyl and/or D-aa, as seen in the six most potent compounds, appears to be critical for presenting its active conformation of San A. In addition, all active compounds are lipophilic. Thus they are rapidly absorbed through membranes.[10] Indeed, any hydrophilic element that was substituted into the macrocycle greatly diminished their potency. Finally, these

macrocycles are relatively straightforward to synthesize and can be made on a multi-gram scale for further biological studies. Given that San A derivatives share no homology to other classes of chemotherapeutic agents and they are potent at levels that are on par with other drugs on the market, these compounds represent promising leads for new cancer therapeutics.

Chapter 3, in part, has been published as it may appear in "Identification of Sansalvamide a analog potent against pancreatic cancer cell lines", ***Bioorganic and Medicinal Chemistry Letters****, 17*, **2007**, 5072-5077. Po-Shen Pan, Kathleen L. McGuire and Shelli R. McAlpine. The dissertation author was the primary author of this paper.

3.4 REFERENCES AND NOTES

1. Lee, K.-H. "Anticancer Drug Design based on Plant-Derived Natural Products", *Journal of Biomedical Science.* **1999**, *6*, 236-250.

2. Potash, M. J.; Bentsman, G.; Muir, T.; Krachmarov, C.; Sova, Pavel.; Volsky, D. J. "Peptide Inhibitors of HIV-1 Protease and Viral Infection of Peripheral Blood Lymphocytes based on HIV-1 Vif ", *Proc. Natl. Acad. Sci. USA.* **1998**, *95*, 13865-13868.

3. Whitfield, J. "Osteoporosis-Treating Parathyroid Hormone Peptides: What are They? What do They do? How might They do It?", *Curr Opin Investig Drugs.* **2006**, *7*, (4), 349-359.

4. Dutton, C. J.; Haxell, M. A.; McArthur, H. A. I.; Wax, R. G. "Peptide Antibiotics: Discovery, Modes of Action and Applications", Marcel Dekker: New York. **2002**, 1-296.

5. Wenger, R. M. "Synthesis of Cyclosporine and Analogues: Structure Requirements for Immunosuppressive Activity", *Angewandte Chemie International Edition.* **2003**, *24*, (2), 77-85.

6. Annabi, B. "Contribution of the 37-kDa Laminin Receptor Precursor in the Anti-Metastatic PSP94-Derived Peptide PCK3145 Cell Surface Binding", *Biochemical and Biophysical Research Communications.* **2006**, *346*, (1), 358-366.

7. Singh, V. K.; Zhou, Y.; Marsh, J. A.; Uversky, V. N.; Forman-Kay, J. D., Liu, J.; Jia, Z. "Synuclein-γ Targeting Peptide Inhibitor that Enhances Sensitivity of Breast Cancer Cells to Antimicrotubule Drugs", *Cancer Research.* **2007**, *67*, 626-633.

8. "Peptide Drugs/ Candidates", *Frost and Sullivan annual report*. **2004**.

9. Borchardt, R. T. "Optimizing Oral Absorption of Peptides using Prodrug Strategies", *Journal of Controlled Release.* **1999**, *62*, 231-238.

10. Belofsky, G. N.; Jensen, P. R.; Fenical, W. "Sansalvamide: A New Cytotoxic Cyclic Depsipeptide Produced by a Marine Fungus of the Genus Fusarium", *Tetrahedron Lett.* **1999**, *40*, 2913-2916.

11. Amidon, G. L.; Lee, H. J. "Absorption of Peptide and Peptidimimetic Drugs", *Ann. Rev. Pharmacol. Toxicol.* **1994**, *34*, 321-341.

12. Wenger, R. M., "Synthesis of Cyclosporin and Analogues: Structural and Conformational Requirements for Immunosuppressive Activity, *Prog. Allergy.* **1986**, *38*, 46-64.

13. Hwang, Y.; Rowley, D.; Rhodes, D.; Gertsch, J.; Fenical, W.; Bushman, F." Mechanism of Inhibition of a Poxvirus Topoisomerase by the Marine Natural Product Sansalvamide A", *Molecular Pharmacology*. **1999**, *55*, 1049-1053.

14. Cueto, M.; Jensen, P. R.; Fenical, W., *N*-Methylsansalvamide, a Cytotoxic Cyclic Depsipeptide from a Marine Fungus of the Genus *Fusarium*, *Fusarium*. *Phytochemistry.* **2000**, *55*, 223-226.

15. Lee, Y.; Silverman, R. B. "Rapid, High-Yield, Solid-Phase Synthesis of the Antitumor Antibiotic Sansalvamide A using a Side-Chain-Tethered Phenylalanine Building Block", *Org. Lett.* **2000**, *2*, 3743-3746.

16. Gu, W.; Liu, S.; Silverman, R. B. "Solid-Phase, Pd-Catalyzed Silicon-Aryl Carbon bond Formation. Synthesis of Sansalvamide A Peptide", *Org. Lett.* **2002**, *4*, 4171-4174.

17. Ujiki, M.; Milam, B.; Ding, X.-Z.; Roginsky, A. B.; Salabat, M. R.; Talamonti, M. S.; Bell, R. H.; Gu, W.; Silverman, R. B.; Adrian, T. E. "A Novel Peptide Sansalvamide A Analogue Inhibits Pancreatic Cancer Cell Growth Through G0/G1 Cell-Cycle Arrest", *Biochemical and Biophysical Research Communications,* **2006**, *340*, 1224-1228.

18. Liu, S.; Gu, W.; D., L.; Ding, X.-Z.; Ujiki, M.; Adrian, T. E.; Soff, G. A.; Silverman, R. B. "*N*-Methylsansalvamide A Peptide Analogues. Potent New Antitumor Agents", *J. Med. Chem.* **2005**, *48*, 3630-3638.

19. Bolla, M. L.; Azevedo, E. V.; Smith, J. M.; Taylor, R. E.; Ranjit, D. K.; Segall, A. M.; McAlpine, S. R. "Novel Antibiotics: Macrocyclic Peptides Designed to trap Holliday Junctions", *Org. Lett.* **2003**, *5*, 109-112.

20. Carroll, C. L.; Johnston, J. V. C.; Kekec, A.; Brown, J. D.; Parry, E.; Cajica, J.; Medina, I.; Cook, K. M.; Corral, R.; Pan, P.-S.; McAlpine, S. R. "Synthesis and Cytotoxicity of Novel Sansalvamide A Derivatives", *Org. Lett.*. **2005**, *7*, 3481-3484.

21. Rodriguez, R.; Pan, P.-S.; Pan, C.-M.; Ravula, S.; Lapera, S.; Singh, E.; Styers, T. J.; Brown, J. D.; Cajica, J.; Parry, E.; Otrubova, K.; McAlpine, S. R. "Synthesis of Second Generation Sansalvamide A derivatives: Novel Templates as Potent Anti-tumor Agents", *J. Org. Chem.* **2007,** *72*, 1980-2002.

22. Zhang, X.; Nikiforovich, G. V.; Marshall, G. R. "Conformational templates for Rational Drug Design: Flexibility of *cyclo*(D-Pro[1]-Ala[2]-Ala[3]-Ala[4]-Ala[5]) in DMSO Solution", *J. Med. Chem.* **2007**, *50*, 2921-2925.

23. Heller, M.; Sukopp, M.; Tsomaia, N.; John, M.; Mierke, D. F.; Reif, B.; Kessler, H. "The Conformation of Cyclo(D-pro-ala-) as a Model for Cyclic Pentapeptides of the DL Type", *J. Am. Chem. Soc.*. **2006**, *128*, 13806-13814.

24. Chatterjee, J.; Mierke, D. F.; Kessler, H. "*N*-Methylated Cyclic Pentaalanine Peptides as Template Structures", *J. Am. Chem. Soc.* **2006**, *128*, 15164-15172.

25. Styers, T. J.; Rodriguez, R.; Pan, P.-S.; McAlpine, S. R. "High-Yielding Macrocyclization Conditions used in the Synthesis of Novel Sansalvamide A Derivatives", *Tetrahedron Lett.* **2006,** *47*, 515-517.

26. Murr, M. M.; Sarr, M. G.; Oishi, A. J.; Heerden, J. A. "Pancreatic Cancer", *CA Cancer J. Clin.* **1994**, *44*, 304-318.

27. Burris, H. A.; Moore, M. J.; Andersen, J.; Greem, M. R.; Rothenberg, M. I.; Modiano, M. R.; Cripps, M. C.; Portenoy, R. K.; Sotorniolo, A. M.; Tarassaoff, P.; Nelson, R.; Dorr, F. A.; Stephens, C. D.; vonHoff, D. *J. "*Improvements in Survival and Clinical Benefits with Gemcitabine as First-Line Therapy for Patients with Advanced Pancreatic Cancer: a Randomized Trial"*, Clin. Oncol.* **1997**, *15*, 2403-2413.

28. Sener, S. F.; Fremgen, A.; Menck, H. R.; Winchester, D. P. "Pancreatic Cancer: Report of Treatment and Survivial Trends for 100,313 Patients Diagnosed from 1985-1995, using the National Cancer Database", *J. Am. Coll. Surg.* **1999**, *189*, 1-7.

29. Two cell lines were chosen to provide evidence that our compounds were targeting a type of cancer that is pancreatic. PL45 is a primary pancreactic ductial adenocarcinoma and BxPC-3 is the cell line of choice for xenograft mouse model studies.

30. Tyndall, J. D.; Pfieiffer, B.; Abbenante, G.; Fairlie, D. P. "Over one hundred Peptide-Activated G Protein-Coupled Receptors Recognized Ligands with Turn Structure"**,** *Chem. Rev.* **2005**, *105*, 793-826.

31. Viles, J. H.; Mitchell, J. B. O.; Gough, S. L.; Doyle, P. M.; Harris, C. J.; Sadler, P. J.; Thornton, J. M. "Multiple Soulition Conformations of the Integrin-Binding Cyclic Pentapeptide Cyclo(-Ser-D-Leu-Asp-Val-Pro-) Analysis of the (φ,ψ) Space Available to the Cyclic Pentapeptides", *Eur. J. Biochem.,* **1996**, *242*, 352-362.

Chapter 4

Holliday Junction Trapping Compounds

4.1 Introduction

In this chapter, I will describe 26 Holiday Junction trapping compounds. 1 of which was synthesized by me, 25 of which were made by my colleagues. All of the *in-vitro* DNA gel shift asssays and *in-vivo* growth inhibition assays were done by the collaborators Fiona A. Curtis and Gary J. Sharples. The emergence of new microbial pathogens, coupled with a dramatic rise in the incidence of drug resistance, poses a considerable challenge to human health.[1-3] We face the possibility of a post-antibiotic era where relatively minor hospital procedures can lead to life-threatening, untreatable infections. To combat this threat, we need new antibiotics that target unique sites in resistant strains of bacteria. The Holliday Junction (HJ) is an intermediate formed during site-specific recombination of replicating DNA.[4] The HJ occurs between two complimentary strands and it possesses C-2 symmetry (**Figure 4.1**). In bacterial DNA, the HJ is generated by the site-specific recombinase, Xer C/D, that controls gene expression and it is resolved by the HJ-specific endonuclease, Ruv C, to complete genetic recombination (**Figure 4.1**). Thus, HJs represent potential targets for a new spectrum of antimicrobials, as their generation and resolution are critical for DNA recombination and repair.

Recombinational processes are vital for accurate chromosomal segregation and DNA repair, they salvage stalled replication forks, and they generate the rearrangements that fuel evolution.[5] Blocking recombination reactions by trapping the HJ intermediate prevents transmission of the genetic material to daughter cells leading to bacterial death. Research by Segall and coworkers has shown bacterial growth inhibition by trapping the HJ intermediate during site-specific recombination.[6] Their studies have identified several linear dodecapeptide lead compounds that trap the HJ and are bactericidal.[7] One of the most potent compounds contains the sequence Lys-Trp-Trp-Cys-Arg-Trp and is dimerized via a disulfide bridge between the cysteine residues.[8] Both this dimerized hexapeptide and the HJ intermediate possesses C-2 symmetry. These linear dodecapeptides inhibit cell growth of Gram-positives bacteria (e.g., *Staphylococcus aureus*) in a dose-dependent manner and represent a new class of antibiotics reminiscent of the quinolone/ fluoroquinolone group, which stabilize a normally transient intermediate.

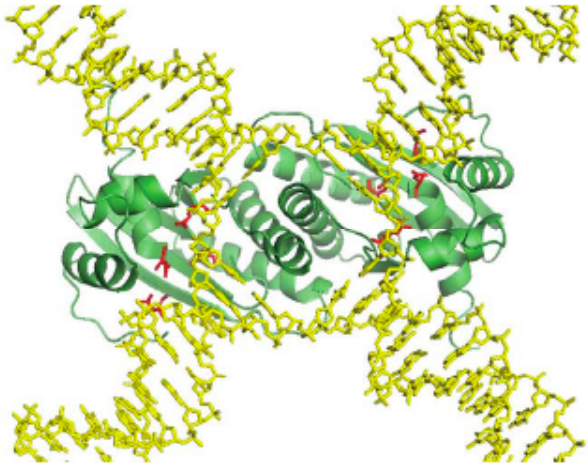

Figure 4.1. Model of *Escherichia coli* RuvC Protein Bound to a Square Planar Holliday Junction. The DNA is Shown in Yellow and the Crystal Structure of Homodimeric RuvC in Green. Residues Important for Catalysis (Asp-7, Glu-66, Asp-138, and Asp-141) are Highlighted in Red. RuvC is Thought to Bind this HJ Conformation During Branch Migration as Part of a RuvABC Complex.

Crystallographic studies indicate that the lead linear dodecapeptides bind at the HJ center.[9] However, these leads are problematic. Since they are not rigid, these dodecapeptides lack distinct structure making it difficult to determine more detailed interactions between the DNA, mediating proteins, and the peptide leads. In addition, their large molecular weights (typically between 1800 and 2000 Daltons) contribute to poor solubility in an aqueous system. The disulfide bridges are also very easily reduced within the intracellular environment and, upon reduction, the compounds do not sustain their active conformation. The goal for this project was to synthesize C-2 symmetrical macrocyclic compounds that trap bacterial HJs and stop site-specific recombination. We anticipate this will result in bacterial cell death and, consequently, a new class of potent antibiotics. The use of macrocyclic structures was chosen to reduce the size of the

compound, which in-turn increases solubility, thus allowing the elucidation of their biological mechanism of action.

4.2

4.2.1 Design of First Generation HJ Trapping Compounds

Our laboratory has synthesized eight first-generation macrocyclic compounds that trap the HJ and the amino acids used to construct these macrocycles are shown in (**Figure 4.2)**. Their biological activity was tested and is discussed later in the chapter. The design of these compounds addressed the issues described above including: poor solubility, stability, rigid conformation and the amino acid units were chosen based on the active linear dodecapeptide leads from the Segall laboratory.[8] The space within the HJ intermediate was measured to be approximately 25Å by 10Å; hence, six to ten amino acids were required to construct macrocycles that fit into this space.[8, 9] In addition, aromatic residues were also selected due to their expected importance in π-stacking with DNA base pairs. Thus our compounds consisted of a macrocyclic scaffold to maintain their structural rigidity, and eliminated the multiple conformations typically seen with linear lead compounds. Our initial design involved a macrocycle with six amino acid residues. This design reduced the molecular weight significantly to 700-850 Daltons (the linear lead peptides possess 1800-2000 Daltons) and, therefore, these macrocycles will have improved solubility in an aqueous system. In addition, since disulfide bridges are easily reduced within the intracellular environment, they were omitted from the design. In

order to be consistent with the HJ binding site and the linear peptide leads, the first generation compounds maintained C-2 symmetry.

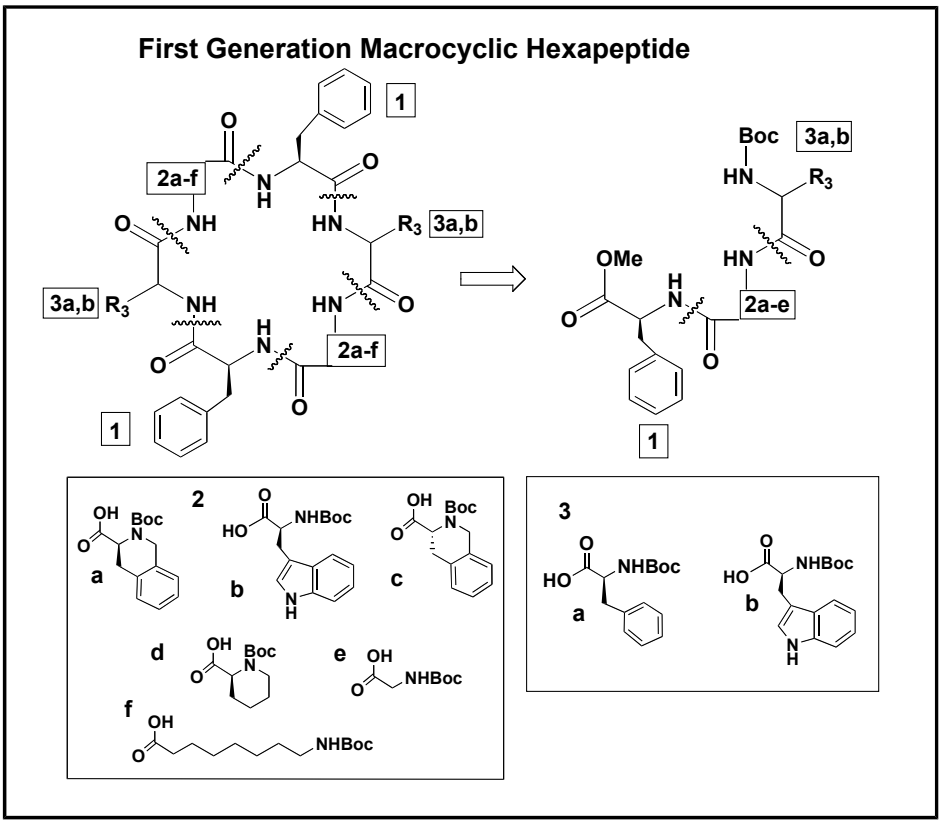

Figure 4.2. Amino Acids used for the Synthesis of First-Generation HJ Trapping Compounds.

4.2.2 Synthesis of First Generation HJ Trapping Compounds

In order to simplify the synthesis of the macrocycles, while allowing easy exchange of amino acids, a combinatorial approach was chosen. This method allowed for easy and rapid assembly, as well as diversity by enabling variation of amino acid residues to be placed at each position.[10] Eight first-generation C-2 symmetrical macrocyclic

hexapeptides were synthesized using hydrophobic amino acids (**Figure 4.3**). Specially, phenylalanine and tryptophan were used because they were present in the lead compounds.[11] The general synthesis procedures for synthesizing first-generation hexameric macrocycles are shown in (**Figure 4.3)**. The acid-protected residue **1** and *N*-Boc-protected residue **2a–f** were coupled using HATU (1.2 eq), and DIPEA (6.0 eq) to give the dipeptide **1-2-Boc** (80–94% yield, 8 examples). Deprotection of the amine on residue **2** using TFA gave the free amine **1-2-NH_2** (assume quantitative yields). Coupling of this dipeptide to amino acid **3a–b** gave the desired tripeptide in good yield (65–94%, 8 examples). The tripeptide was separated into two equal aliquots. The acid was deprotected in one aliquot using sodium hydroxide (6.0 eq) in methanol (0.1M), while the amine was deprotected in the other using 20% TFA in dichloromethane (0.1M). These two tripeptides were coupled together using HATU (1.2 eq), DIPEA (6.0 eq) in acetonitrile (0.1M) yielding eight examples of linear hexapeptides (19–73% yield). These linear hexapeptides were subjected to 20% TFA in dichloromethane (0.1M) to remove the Boc-protecting group of the amine. Upon completion, the reaction was concentrated *in vacuo*, and the free-amine hexapeptide substrates were acid deprotected by adding sodium hydroxide (6.0 eq) in methanol (0.1M). Following acid deprotection, the reaction was concentrated *in vacuo* and subjected to HATU, TBTU, and DEPBT coupling reagents (0.75 equivalents each), and DIPEA (6.0 equivalents) in acetonitrile or dichloromethane (0.005-0.01M). Macrocyclizations took approximately four days due to the dilute concentration and was required to maximize the yield. The final compounds were purified using reversed-phase HPLC and confirmed via LCMS.[10] These eight,

uniquely designed, macrocyclic compounds (**Figure 4.3**) were tested for their ability to trap HJs *in vitro*.

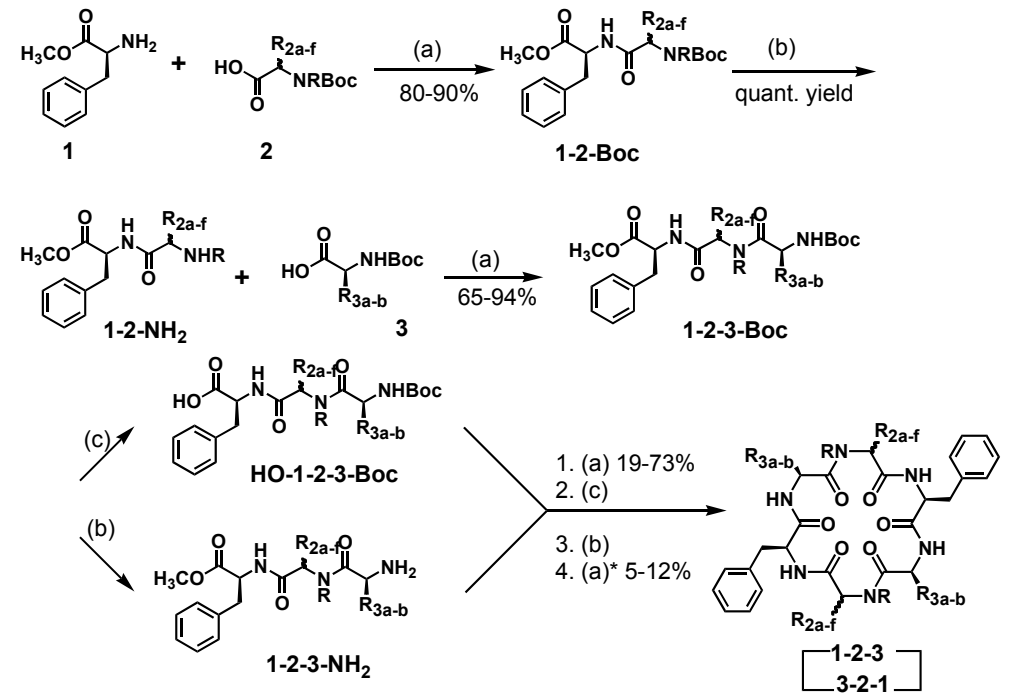

Conditions: (**a**) HATU (1.2 eq), DIPEA (6.0 eq), acetonitrile (0.1M);
(**b**) TFA (20%), dichloromethane (0.1M);
(**c**) NaOH (6.0 eq), MeOH (0.1)M.
*HATU, TBTU, DEPBT were used as coupling agents (0.75 eq each), acetonitrile or dichloromethane (0.005-0.01M).

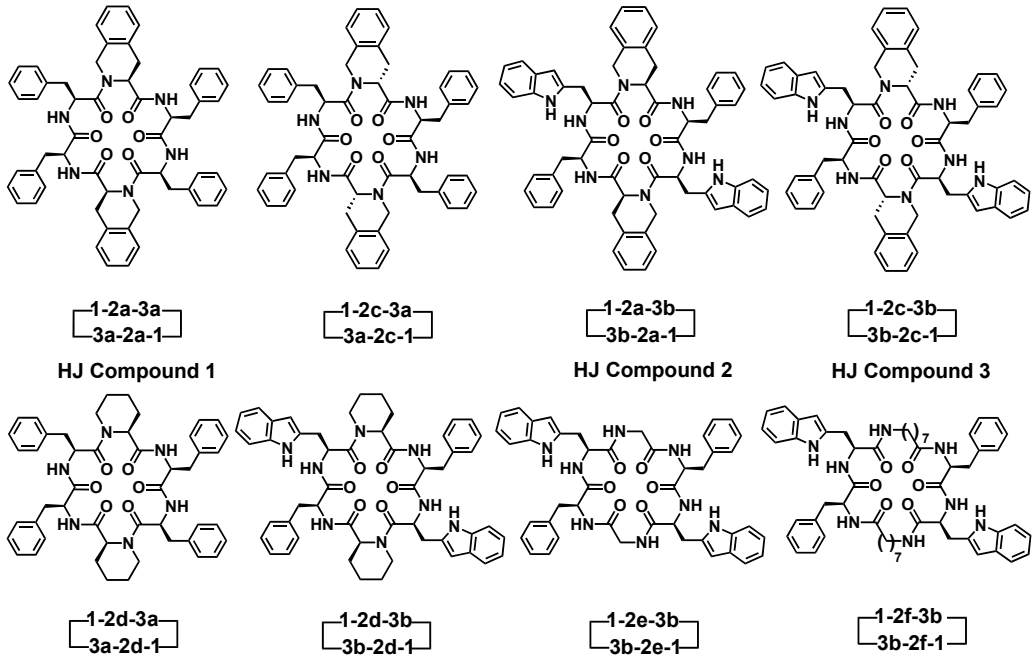

Figure 4.3. Synthesis of Eight First-Generation Hexameric Macrocycles Designed to Trap HJ's.

4.2.3 First-Generation Assays

The eight first-generation hexameric macrocycles were tested for their ability to trap the HJ in an *in-vitro* site-specific recombination assay.[10] Three of these compounds (**Figure 4.4**) successfully trapped the HJ in a manner similar to the linear lead Lys-Trp-Trp-Cys-Arg-Trp. Here we utilized the *Escherichia coli* RuvC protein to probe the effect of these three compounds on homologous recombination reactions in vitro. RuvC is a HJ-specific endonuclease that eliminates 4-way junctions formed by homologous recombination or replication fork resolution.[12] RuvC (200 nM) forms a single complex with a model HJ DNA substrate (0.3 nM) labeled with ^{32}P (**Figure 4.4**, panel 1, lane B). At 1 μM the peptide trapped a significant amount of HJ substrate (panel 1, II), with the free HJ clearly accumulating in the presence of the three macrocycles (**Figure 4.4**, lanes E, H, and K, panel I, band II) when compared to the control reaction (lane N, panel I, band II). Each of the compounds also reduced the number of complexes formed by the structurally unrelated RusA HJ resolvase[13] (data not shown), indicating that inhibition is due to an interaction with the junction rather than specific contacts with the resolving enzyme. These macrocycles can therefore prevent several different enzymes, including those functioning in site-specific[10] and homologous recombination, from gaining access to the Holliday Junction structure. All three compounds (**HJ compd 1**, **HJ compd 2**, **HJ compd 3**) contain phenylalanine coupled to 1,2,3,4-tetrahydroisoquinoline and it is probable that this aromatic group is involved in π-stacking with nucleotide bases. Furthermore, since binding assays were conducted in EDTA, the macrocycles must be

binding the open square planar junction (**Figure 4.1**) rather than the non square planar conformation that predominates in the presence of divalent cations.[14]

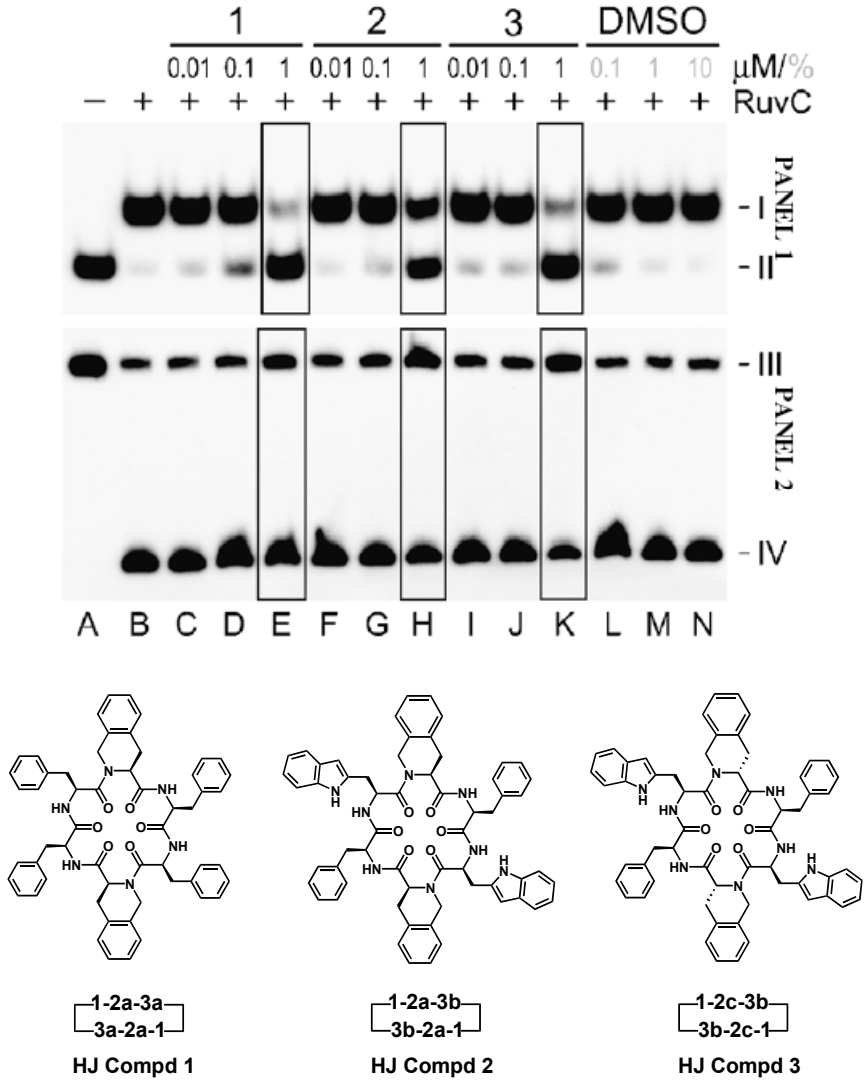

Figure 4.4. Effect of First Generation Compounds on RuvC Binding (panel 1) I, RuvC with HJ DNA; II, Peptide Trapping HJ Substrate. HJ Resolution of ^{32}P-Labeled HJ DNA (panel 2) III, Substrate Prior to Nicking; IV Nicked Duplex.

When the experiments were repeated at 37 ^{o}C with the addition of 10 mM $MgCl_2$, RuvC (100 nM) cleaved the HJ to generate nicked duplexes (**Figure 4.4**, lane B, panel 2, IV). The ability to form this nicked duplex was reduced slightly by the three peptides,

especially with **HJ compd 3** (lanes E, H, and K, compare band III to IV) as seen by the change in the proportions of substrate and product (compare band III to IV, respectively). Similar results were obtained with the linear Trp-Arg-Trp-Tyr-Cys-Arg peptide blocking HJ cleavage by RuvC.[6-8, 15, 16] The relatively poor inhibition seen with both the linear and the cyclic peptides may be due to a failure to bind effectively to the non-square planar conformation favored under these reaction conditions.

4.3

4.3.1 Design of Second-Generation HJ Trapping Compounds

The goals for the second-generation compounds were to improve both the binding affinity to the HJ and the growth inhibition of bacteria. Hydrophobic residues, which appear in both linear and cyclic lead compounds, appear to play an important role in DNA intercalation and/or base stacking interactions at the junction cross-over. The first-generation peptides were composed entirely of hydrophobic residues, making them fairly insoluble and unable to hydrogen-bond via side-chain residues to either DNA or proteins bound to the HJ. This may explain why the first-generation compounds succeeded at trapping HJs, but failed to show any bactericidal effect (data not shown). It is also unclear how many residues participate in binding to the HJ. The first-generation contained only six amino acids, but according to the crystal structure approximately six to ten amino acid residues could potentially 'fit' into the HJ binding site. The second-generation incorporated tyrosine and lysine residues into the macrocycles in order to improve their hydrogen bonding properties, while maintaining their π-stacking ability (**Figure 4.5**). In

addition, testing macrocyclic hexapeptides along with cyclic octapeptides explores potential ‘fits’ in the HJ. The synthesis of sixteen second-generation macrocycles including one I synthesized, were completed using the same conditions described for the first-generation and the amino acids shown (**Figure 4.5)**. Interestingly, we observed that only when a tyrosine was included at position 7 was the cyclization of the octapeptides successful.

Several second-generation compounds contained the 1,2,3,4-tetrahydroisoquinoline moiety, which was present in effective compounds from the first-generation. In addition to macrocyclic hexapeptides, C-2 symmetric octapeptides were also synthesized in order to investigate the effect of size on binding and immobilizing the HJ. Solid-phase synthesis was employed for compounds containing polar residues. This enabled facile and rapid synthesis of these macrocyclic compounds with easily cleavable protecting groups on polar side-chains.

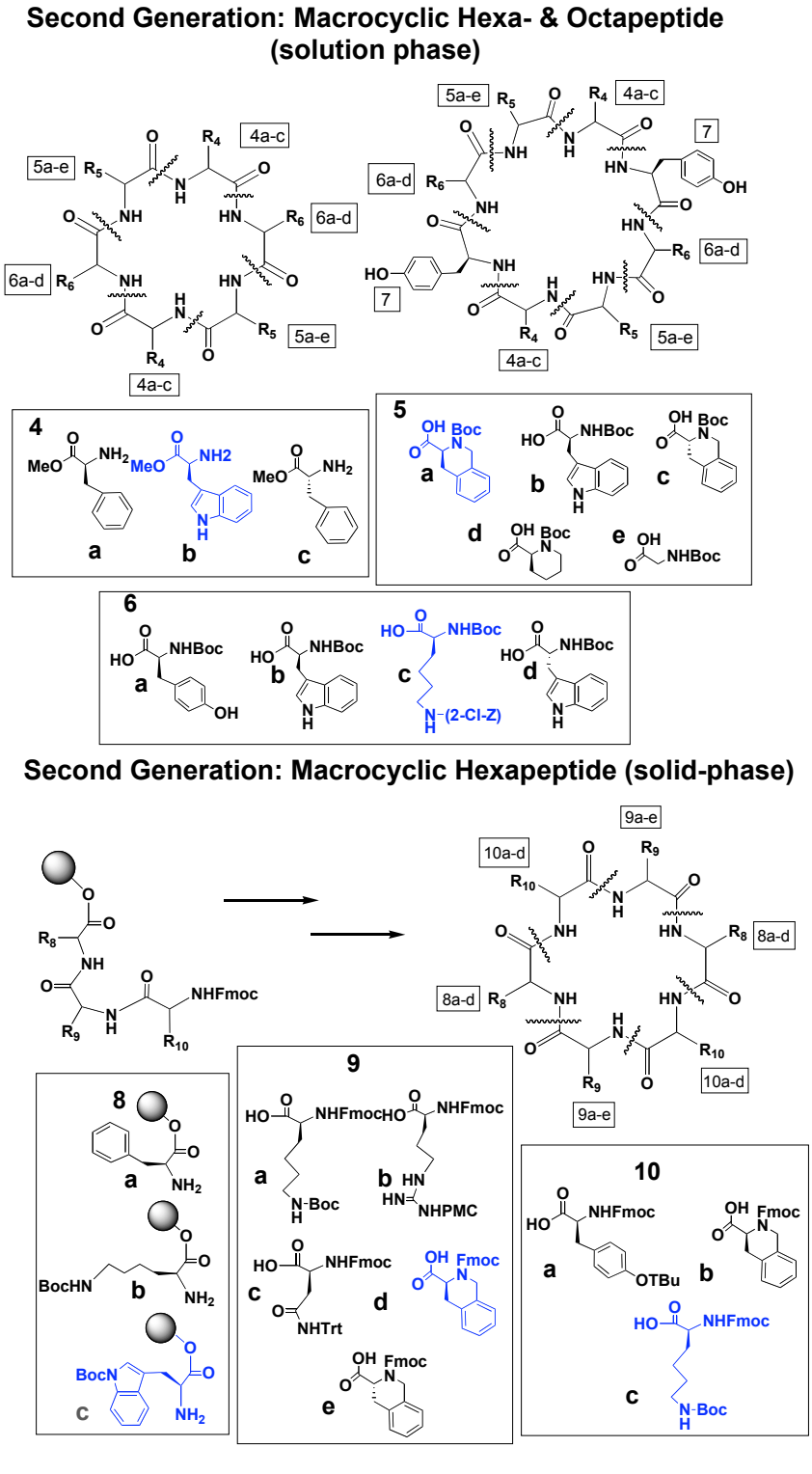

Figure 4.5. Amino Acids used for the Synthesis of Second-Generation HJ Trapping Compounds. The Amino Acids in Blue were used to Construct HJ Compd 10.

4.3.2 Solution-Phase Synthesis of Second-Generation HJ Trapping Compounds

General approach of synthesizing second-generation hexameric and octameric macrocycles as well as their structures are shown in **(Figure 4.6).**. Using the same approach outlined for the first-generation, the tripeptides were synthesized in good yields (65–85%). These tripeptides were converted into linear hexapeptides (7 examples, 63–94% yields) and cyclized (7 examples, 8–25% yields).[17] The synthesis of the tetrapeptide was completed by deprotecting the tripeptide amine using TFA and coupling it to residue 7 (**Figure 4.6**). In a similar fashion to the hexapeptides, the tetrapeptide was separated into two equal aliquots, whereupon one aliquot was acid deprotected and the other was amine deprotected. The subsequent coupling of the tetrapeptide free acid and free amine using multiple coupling agents gave four examples of linear octapeptides (36–68% yield). The octapeptides were cyclized using the same conditions as those used for the macrocyclic hexapeptides, yielding four examples (18–25% yield). These final compounds were purified using reversed-phase HPLC and confirmed via LCMS.[18] Their ability to block the formation of a RuvC–HJ complex was assayed *in vitro*.

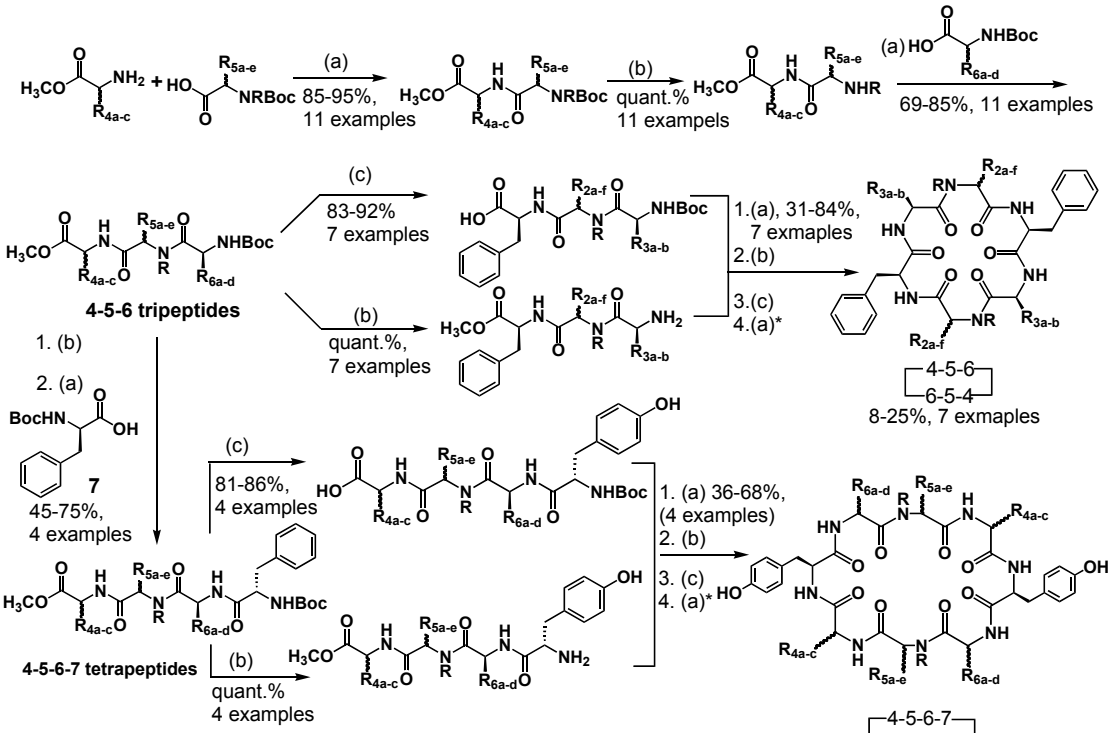

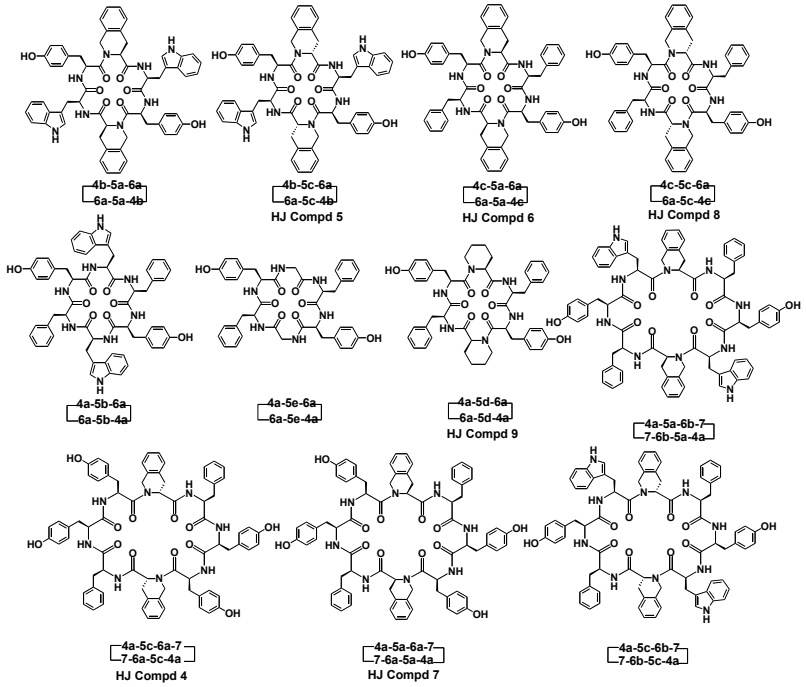

Figure 4.6. Solution-Phase Synthesis of Second-Generation Macrocycles that Trap the HJ.

4.3.3 Solution-phase Synthesis of HJ compd 10

My efforts to synthesize **HJ compd 10** using a solution-phase approach are shown in (**Figure 4.7).** Amino acid 4b was coupled to 5a by using TBTU (1.2 eq), DIPEA (3.0 eq) in acetonitrile (0.1M) at room temperature to give 4b-5a-Boc with 94%. The Boc protecting group of dipeptide 4b-5a was then removed by using 20% TFA in dichloromethane (0.1M) to give 4b-5a-NH_2 with assumed quantitative yield. 4b-5a-NH_2 was coupled to residue 6c by using TBTU (1.2 eq), DIPEA (3.0 eq) in acetonitrile (0.1M) at room temperature to give tripeptide, 4b-5a-6c, with 85% yield. This tripeptide was then separated into two equal aliquots, whereupon one aliquot was acid deprotected (98% yield) and the other was amine deprotected (assumed quantitative yield). The subsequent coupling of the tripeptide free acid and free amine using TBTU (0.8 eq), HATU (1.0 eq), DIPEA (6.0 eq) in acetonitrile (0.1M) to furnish acid and amine protected linear hexapeptide 4b-5a-6c-4b-5a-6c with 60% yield. This double protected linear hexapeptide was then amine deprotected by using 20% TFA in dichloromethane, (assumed quantitative yield) and acid deprotected using sodium hydroxide (8.0 eq) in methanol (80% yield). This provided a double deprotected linear hexapeptide. The double deprotected linear hexapeptide was then converted to a hexameric macrocycle by using TBTU (0.6 eq), HATU (1.0 eq), DEPBT (0.8 eq), and DIPEA (6.0 eq) in acetonitrile (0.007M) at room temperature to give $[4b\text{-}5a\text{-}6c]_2(2\text{-}Cl\text{-}Z)_2$ with 15% yield.

After completing the synthesis of the **HJ compd 10** (**4b-5a-6c-4b-5a-6c**), palladium catalyzed hydrogenation was attempted under various conditions.

Unfortunately, only one lysine was deprotected. Furthermore, attempts by several group members on three unique cyclized macrocycles containing two Cl-Cbz protected lysines also failed, suggesting that the exploration of alternative conditions was needed. After, numerous attempts using other conditions to cleave the Cl-Cbz protecting group from the lysine side-chains we decided to find another route for this molecule. Thus, our laboratory initiates a solid-phase strategy to synthesize second-generation compounds containing polar-side chains. Detailed information on this strategy will be discussed later in the chapter.

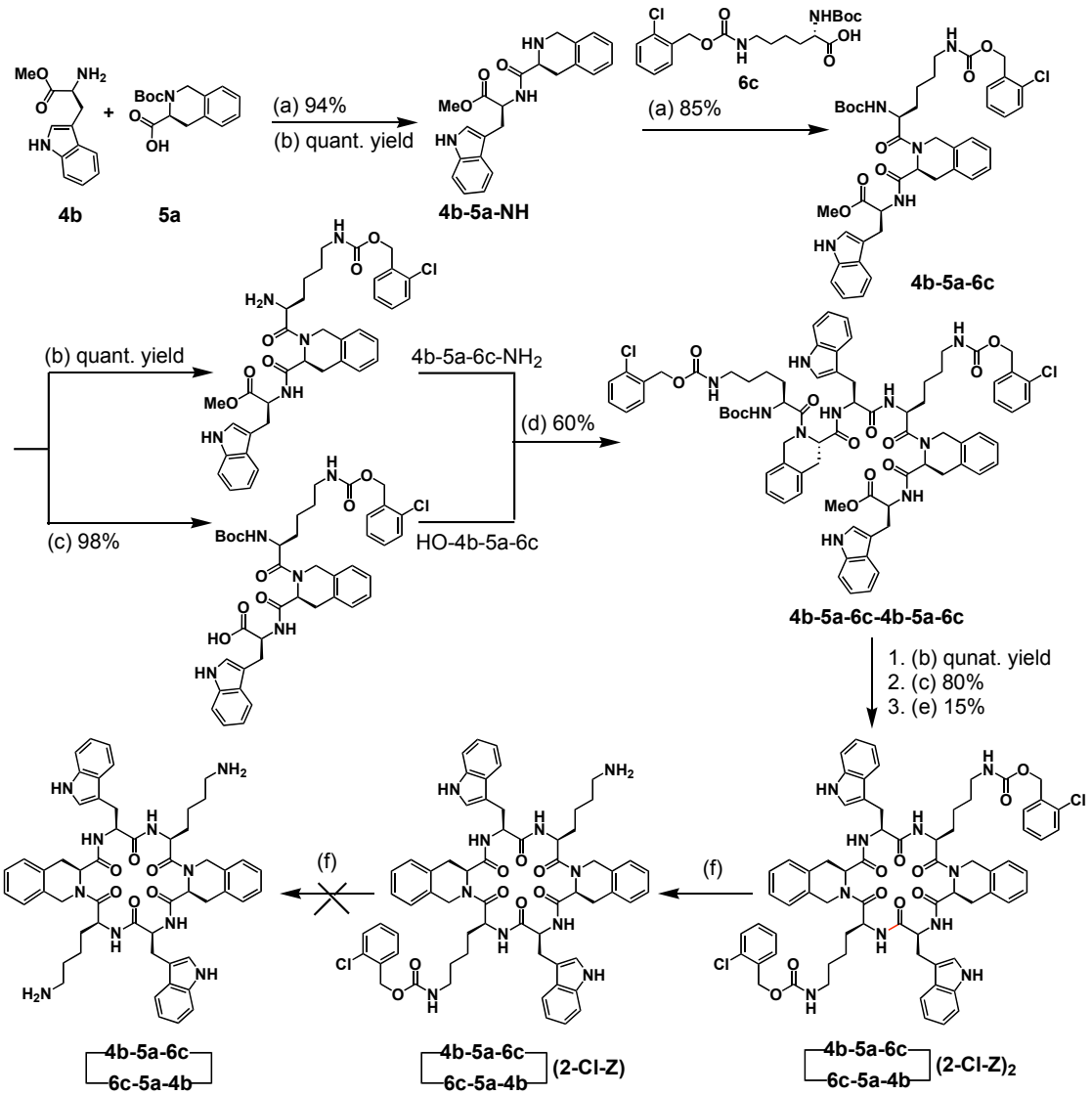

Conditions: (a) TBTU (1.2 eq), DIPEA (3.o eq), acetonitrile (0.1M);
(b) 20% TFA, CH_2Cl_2 (0.1M);
(c) NaOH (8.0 eq), CH_3OH (0.1M);
(d) TBTU (0.8 eq), HATU (1.0 eq), DIPEA (6.0 eq), acetonitrile (0.1M);
(e) TBTU (0.6 eq), HATU (1.0 eq), DEPBT (0.8 eq), acetonitrile (0.007M);
(f) 6.0 M HCl, MeOH (0.1 M.

Figure 4.7. Solution-Phase Approach of Synthesizing HJ Compd 10 (4b-5a-6c) Macrocycle.

4.3.4 Assays of Solution-Phase Second-Generation HJ Trapping Compounds

RuvC is a HJ-specific endonuclease, which functions during homologuous recombination.[12] To determine whether these second-generation macrocycles function in blocking HJs, biological assays were performed to test their impact on DNA binding by *Escherichia coli* RuvC. Initially, six of the second-generation macrocycles synthesized by our laboratory were tested in the RuvC-junction binding assay (**HJ compds 4–9**) by professor . In RuvC–HJ binding experiments, a significant amount of HJ accumulated in the presence of all macrocycles at 1 μM **(Figure 4.8. band II). HJ Compds 7** and **9** were particularly effective in preventing the formation of a complex between 200 nM RuvC and 0.3 nM ^{32}P labeled HJ DNA (lanes K and O) when compared to the control (lane C). These two macrocycles appear to be at least as potent in trapping the HJ as one of the lead peptides (lane Q). It is important to note that all six compounds tested bind to the HJ complex and all six compounds contain tyrosine. The presence of tyrosine appears to be critical for the HJ interaction, which is demonstrated not only by this data but also by the compounds synthesized by solid-phase (**Figure 4.9**). We estimate that a hexapeptide can be readily accommodated within the central space of a HJ. (**Figure 4.1**). Multiple interactions probably contribute to the stability of DNA binding and their tight association will either present a steric hindrance to protein access or restrict the ability of recombinases to fold the DNA structure correctly for the catalysis process. The octapeptides should also fit within the center of HJs, although clearly they will be more constrained in their mode of DNA binding. **HJ Compd 7**, an octapeptide (**Figure 4.8**, lane K), was more effective at blocking RuvC binding to the HJ than a structurally

similar **HJ compd 6** (lane I). Thus, both hexapeptides and octapeptieds trap HJ's. Intercalation between nucleotide bases may be more important for these larger macrocycles. Further details on these interactions require an HJ–peptide co-crystal structure. However, our success at synthesizing compounds that trapped HJ's and our ability to determine important structural features required for binding is a fundamental discovery.

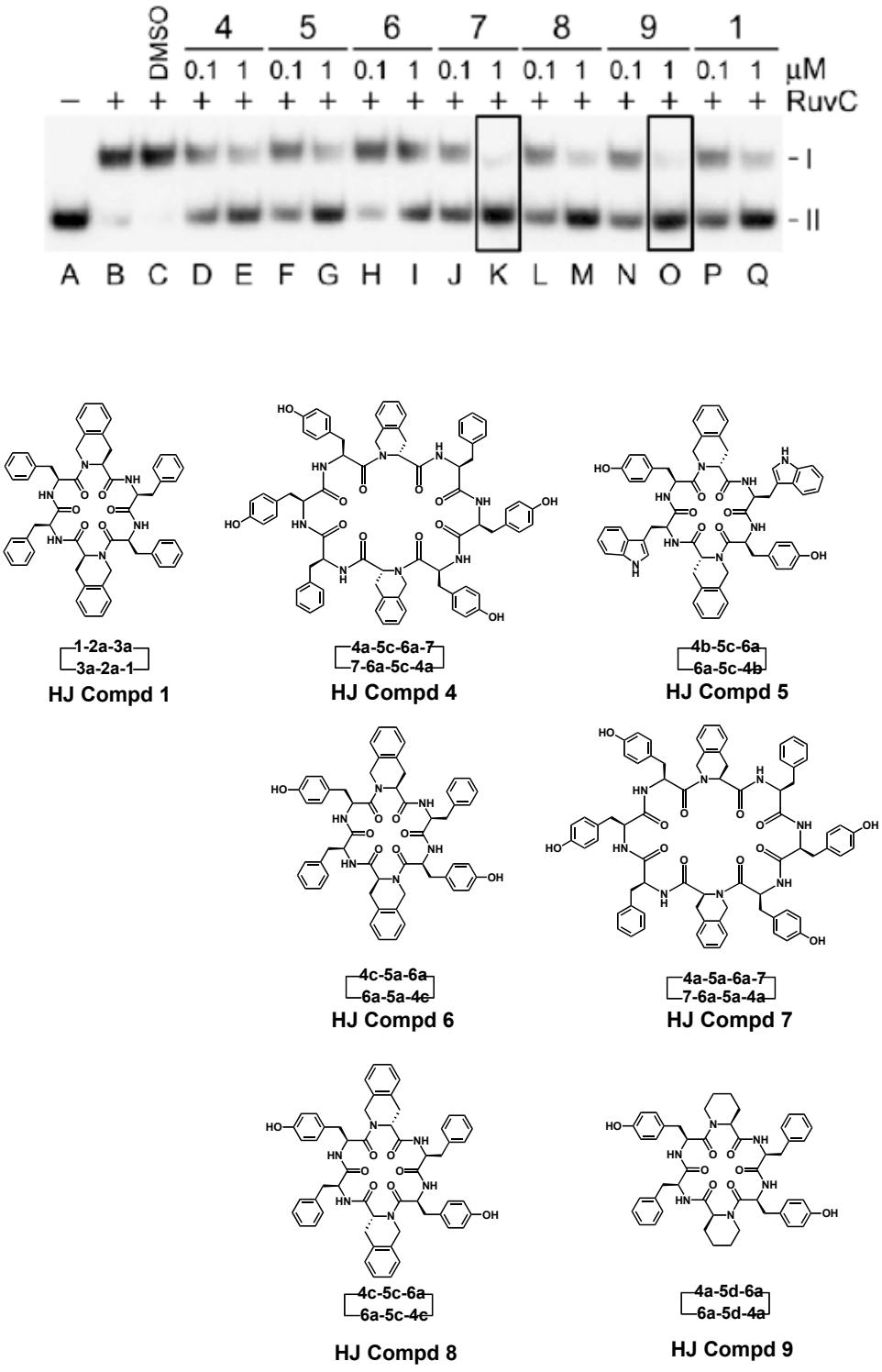

Figure 4.8. Effect of Second-Generation Compounds on RuvC Binding to 32P-labeled HJ DNA. I, RuvC with HJ DNA; II, Peptide Trapping HJ Substrate.

4.3.5 Assays of Solution-Phase Second-Generation HJ Trapping Compounds

In addition to the assays of the solution-phase second-generation HJ trapping compounds, growth inhibition experiments were conducted on Gram-negative (*Escherichia coli*) and Gram-positive (*S. epidermidis*) bacteria. **HJ Compd 9** was tested, as it was highly effective in trapping HJs. However, at 5 μM this peptide had no negative effect on the growth or survival of a wild-type *Escherichia coli* strain (data not shown). The inability of **HJ compd 9** to inhibit bacterial growth may be in part due to its hydrophobicity. Their hydrophobic nature may serve to limit passage across bacterial cell walls.

4.3.6 Solid-phase Approach of Synthesizing Second-Generation HJ Compd 10 (Initial Approach)

An efficient synthesis of peptides using polar amino acids, such as lysine, often utilizes solid-phase chemistry. A convergent solid-phase approach was first chosen to synthesize hexameric macrocycle. (**Figure 4.9**). Starting with resin-bound residues **8a–c**, addition of TBTU, DIPEA, and residues **9a-e-Fmoc** gave the resin-bound dipeptide **8-9-Fmoc**. We coupled residue **9** a second time to ensure the reaction had gone to completion.[20] Deprotection of the amine on residue **9** using piperidine in DMF gave the free amine **8-9-NH_2**. Coupling of this dipeptide to monomer **10a–c** gave the desired tripeptide **HO-8-9-10** in good yields (94% when cleaved).[20] Emulating the solution-phase

approach, the tripeptide was separated into two equal aliquots. The acid was formed by cleaving the compound from the bead in the first aliquot using 0.5% TFA in methylene chloride. The amine was deprotected in the second aliquot using 20% piperidine in DMF. The free acid tripeptide, now in solution, was coupled to the resin-bound tripeptide amine. This yielded a hexapeptide bound to the resin.

Subsequent amine deprotection and cleavage from the bead yielded a double deprotected linear hexapeptide. Unfortunately, this double deprotected hexapeptide was obtained in low yield. We discovered this outcome was due to the fact that the tripeptide free acid coupled in low yields to resin-bound tripeptide amine. This low-yielded coupling reaction occurs when any multi amino acid chain is coupled to solid phase. In order to address this issue, the synthetic strategy was redesigned.

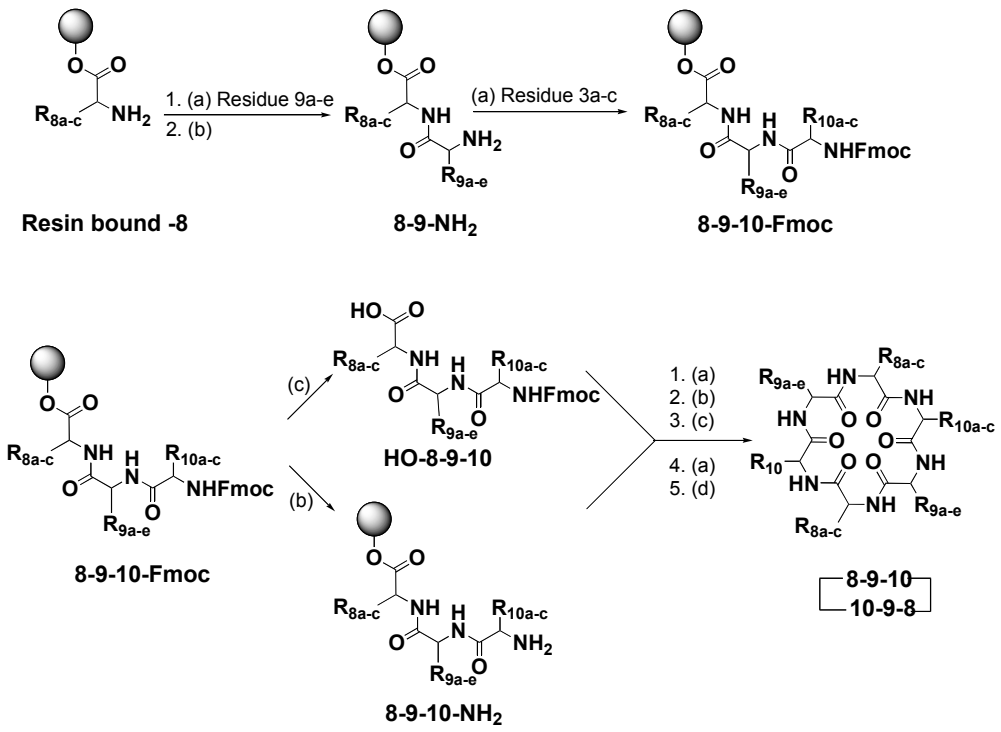

Conditions: (a) Coupling agents (3 eq), DIPEA (3.0 eq), CH_2Cl_2;
(b) Piperdine(20%), DMF;
(c) 0.5% TFA in CH_2Cl_2 (d) 20% TFA, CH_2Cl_2, anisole (2.0eq).

Figure 4.9. Initial Solid-Phase Approach of Synthesizing Second-Generation Macrocycles.

4.3.7 Synthesis of Second-Generation HJ Compd 10 (Final Approach)

Given the difficulties encountered using a convergent approach, our laboratory synthesized the same compound using a linear approach. This approach was utilized by me to synthesize **HJ compd 10 (Figure 4.10)**. The resin-bound amino acid **8c** was coupled to a *N*-Fmoc-protected residue **9d**. Double coupling of resin **9d** was carried out to ensure complete formation of the dimer.[20] Upon deprotection of the amine on residue **9d**, residue **10c** was coupled to the dipeptide. Double coupling was utilized to ensure

complete formation of the tripeptide. Subsequent deprotection and coupling reactions were performed until the hexapeptide was formed. Cleavage of this hexapeptide to give the double deprotected linear hexamer and analysis by LCMS showed pure product.

The reaction was concentrated *in-vacuo* and subjected to HATU (0.8 eq), TBTU (0.8 eq), and DEPBT (1.0 eq) coupling reagents (2.6 equivalents total), and DIPEA (8.0 eq) in dichloromethane. The final macrocyclizations took four days due to the low concentration (0.01 M) required to maximize the yield. The one-pot ring-closing gave better yields (15%) than those seen when the convergent approach was utilized (10% average). The compounds were purified using reversed-phase HPLC and confirmed via LCMS. Finally, deprotection of the peptide side chains was completed using 95% TFA in methylene chloride. **HJ compd 10** was purified by HPLC and confirmed via LCMS.

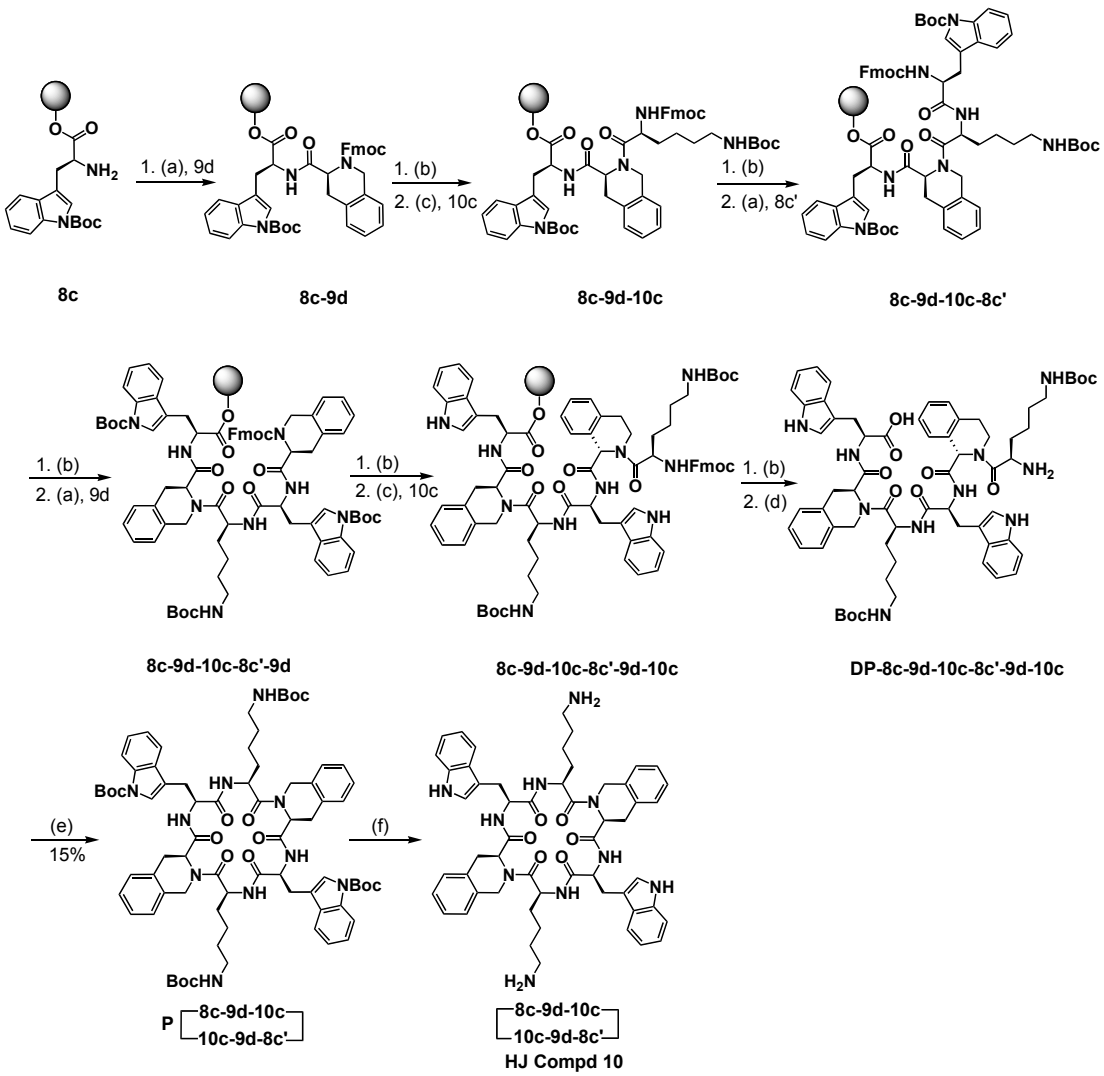

Conditions: (a) TBTU (3.1 eq), DIPEA (3.5 eq), DMF, rt, 2 X 15 min;
(b) 20% piperidine, DMF, rt, 2 X 30 min;
(c) HATU (3.1 eq), DIPEA (4.0 eq), DMF, rt, 2 X 20 min;
(d) 1% TFA, dichloromethane, rt, 40 min;
(e) TBTU (0.8 eq), HATU (0.8 eq), DEPBT (1.0 eq), DIPEA (8.0 eq), acetonitrile (0.01 M);
(f) 20% TFA,dichloromethane (0.1M), anisole (2.0 eq), rt, 5h.

Figure 4.10. Synthesis of Second-Generation Macrocycle HJ Compd 10 using Solid-Phase Final Approach.

A total of seven lysine (or arginine) containing second-generation hexameric macrocycles were synthesized by this approach and their structures were shown in **Figure 4.11**.

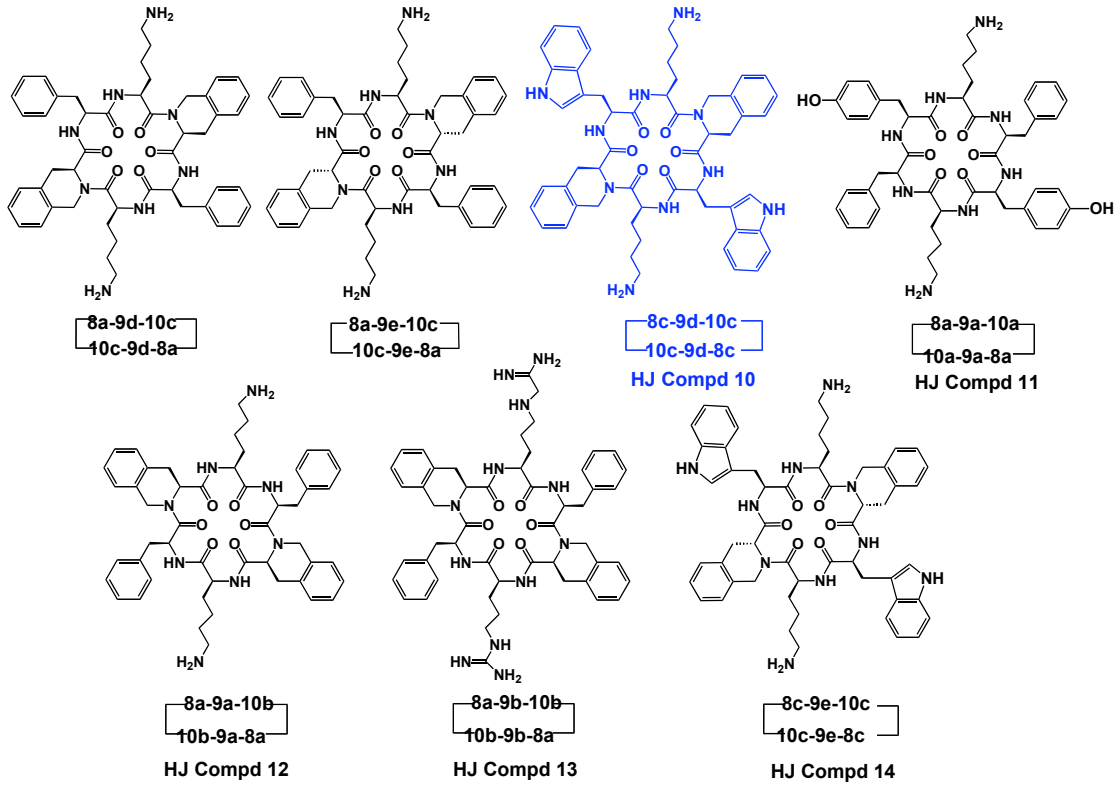

Figure 4.11. Second-Generation Hexameric Macrocycles Synthesized by Revised Solid-Phase Approach.

4.4

4.4.1 Assays of Solid-phase Second-Generation HJ Trapping Compounds

Five macrocycles (compounds **10–14**) that contained lysine or arginine, were tested for their ability to block HJs in the *in-vitro* RuvC–HJ DNA binding assay. Among the five tested, one significantly reduced the ability of RuvC (200 nM) to form complexes

with the radioactively labeled HJ substrate at 0.3 nM (**Figure 4.12**, lane G, compound **11**, band III). Remarkably, this compound was the only one that contained a tyrosine, which is consistent with earlier observations of solution-phase compounds that trap HJs (**Figure 4.8**). Therefore, the incorporation of tyrosine in macrocycles for effective HJ trapping appears to be a critical feature and may be due to tyrosine's ability to π-stack as well as hydrogen bond with nucleotide bases. To determine the ideal 'fit' for trapping HJs, additional experiments comparing hexapeptides versus octapeptides on HJ binding are in progress. Although macrocycle **11** traps HJs, when it was tested for antibacterial activity in *E. coli* and *S. epidermidis* bacteria, no growth inhibition was detected (data not shown). One possible explanation for this is that compound **11** does not bind sufficient quantities of HJs to kill bacteria. Alternatively, it may be unable to gain entry through the cell wall. Regardless of this issue, compound **11** provides an excellent tool for elucidating molecular pathways that involve HJ intermediates.

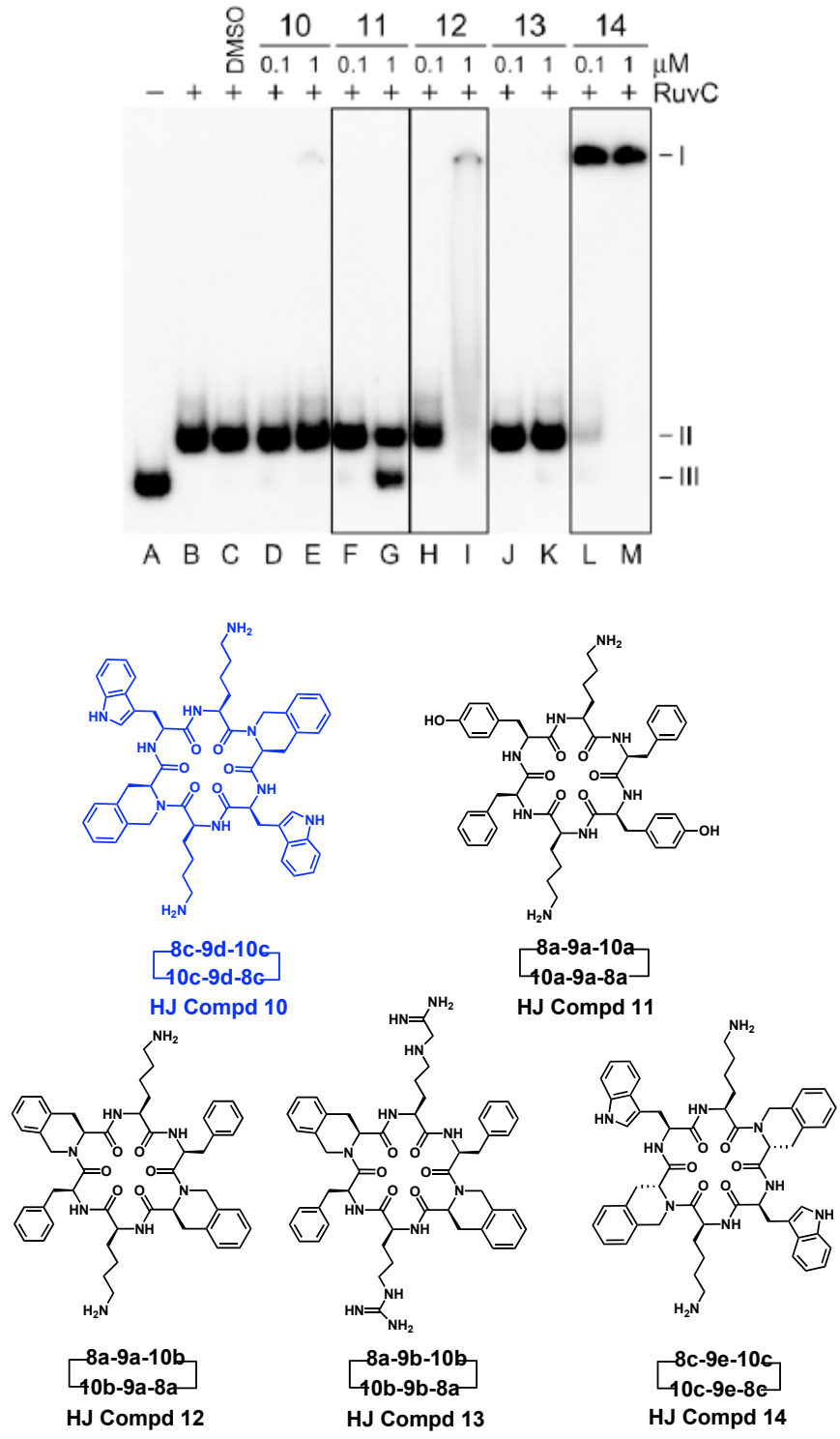

Figure 4.12 RuvC Gel-Shift Assay of Solid-Phase Compounds, Band I, Non-Specific Binding to DNA; II, RuvC with HJ DNA; III, Peptide Trapping HJ Substrate.

4.4.2 Non-Specific DNA Binding Assay

In **Figure 4.12**, **HJ compd 12** and **14** disrupted the formation of RuvC–HJ complexes, although in this case the HJ substrate remains trapped in the wells of the polyacrylamide gel (band I, (**Figure 4.12)**, lanes I and M). This may be indicative of non-specific binding with multiple peptides assembling on the DNA thus preventing its entry into the gel matrix. To confirm this possibility, the solid-phase macrocycles were examined for their ability to bind to ^{32}P-labeled single-stranded (ss) and double-stranded (ds) DNA substrates (0.3 nM) in the absence of RuvC protein (**Figure 4.13**). **HJ compd 10**, **11**, and **12** did not appear to bind stably to ss DNA or ds DNA. However, **HJ compd 14** bound to both ss and ds DNA, trapping all of the substrate at the top of the well (**Figure 4.13**, lanes L). Compound **12** formed a much less stable association with ss and ds DNA, with at least some of the complexes being able to enter the gel (**Figure 4.13**, lane H). These results correlate with those obtained using the HJ DNA substrate (**Figure 4.12**). The following conclusions for the five solid-phase **HJ compd 10–14** can be drawn: (i) **HJ compd 10** and **13** do not block RuvC binding to the HJ, which is consistent with their inability to bind at the center of the **HJ intermediate**; (ii) **HJ compd 11** fails to bind to unbranched DNA in (**Figure 4.13)** but does block RuvC binding to HJ's, indicating genuine HJ specificity, (iii) **HJ compd 12** and **14** bind to DNA non-specifically as seen by trapping of HJ, ss or ds DNA at the gel origin (**Figures 4.12 and 4.13**). The lack of discrimination in binding to ss or ds DNA seen with these two peptides implies that the nucleic acid interaction does not require base stacking in the helical form of DNA. It is unclear at this stage whether contacts are made with the phosphodiester

backbone or with the purine/ pyrimidine bases. Clearly, addition of positively charged residues can generate compounds with reduced branched DNA specificity and even closely related molecules (e.g., **HJ compd 10** and **13**) that appear unable to interact with DNA at all. Comparison of the different properties associated with the structure of these compounds will assist the rational design of future macrocycles. All five compounds were tested for antibacterial activity in *E. coli* and *S. epidermidis* bacteria. No growth inhibition was detected with wild-type *E. coli* (data not shown). However, two of the peptides (**HJ compd 12** and, to a significantly lesser degree, **HJ compd 14**) did inhibit the growth of *S. epidermidis* when dilutions were spotted on a lawn of bacteria (**Figure 4.14**). Surprisingly, it was **HJ compd 12**, which forms a relatively unstable association with ss and ds DNA, that had a significant effect on bacterial growth. Further work is needed to characterize how these macrocycles interact with DNA and how this correlates with their ability to inhibit the growth of Gram-positive bacteria. In conclusion, **HJ compd 11** displays high specificity for the HJ as demonstrated by its ability to reduce the efficiency of RuvC binding to the non square planar and inability to bind unbranched DNA molecules.

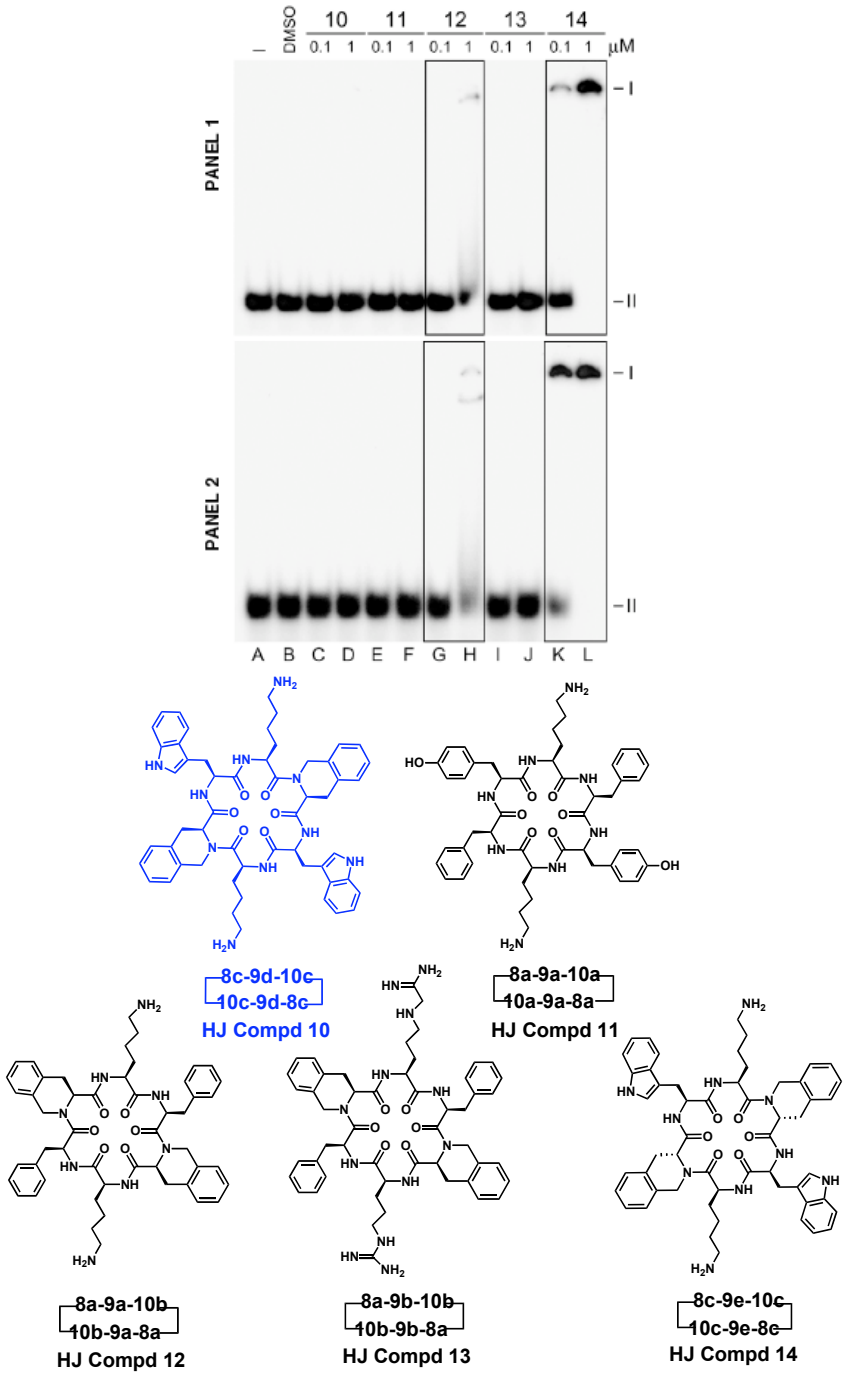

Figure 4.13. Gel-Shift Assay Showing the Binding of Solid-Phase Compounds (10-14) to ^{32}P-labeled dsDNA (panel 1) I, Double-Stranded DNA Trapped by Peptide; II, Double-Stranded DNA not Trapped by Peptide. ssDNA (panel 2) I, Single Stranded DNA Trapped by Peptide; II, Single-Stranded DNA not Trapped by Peptide.

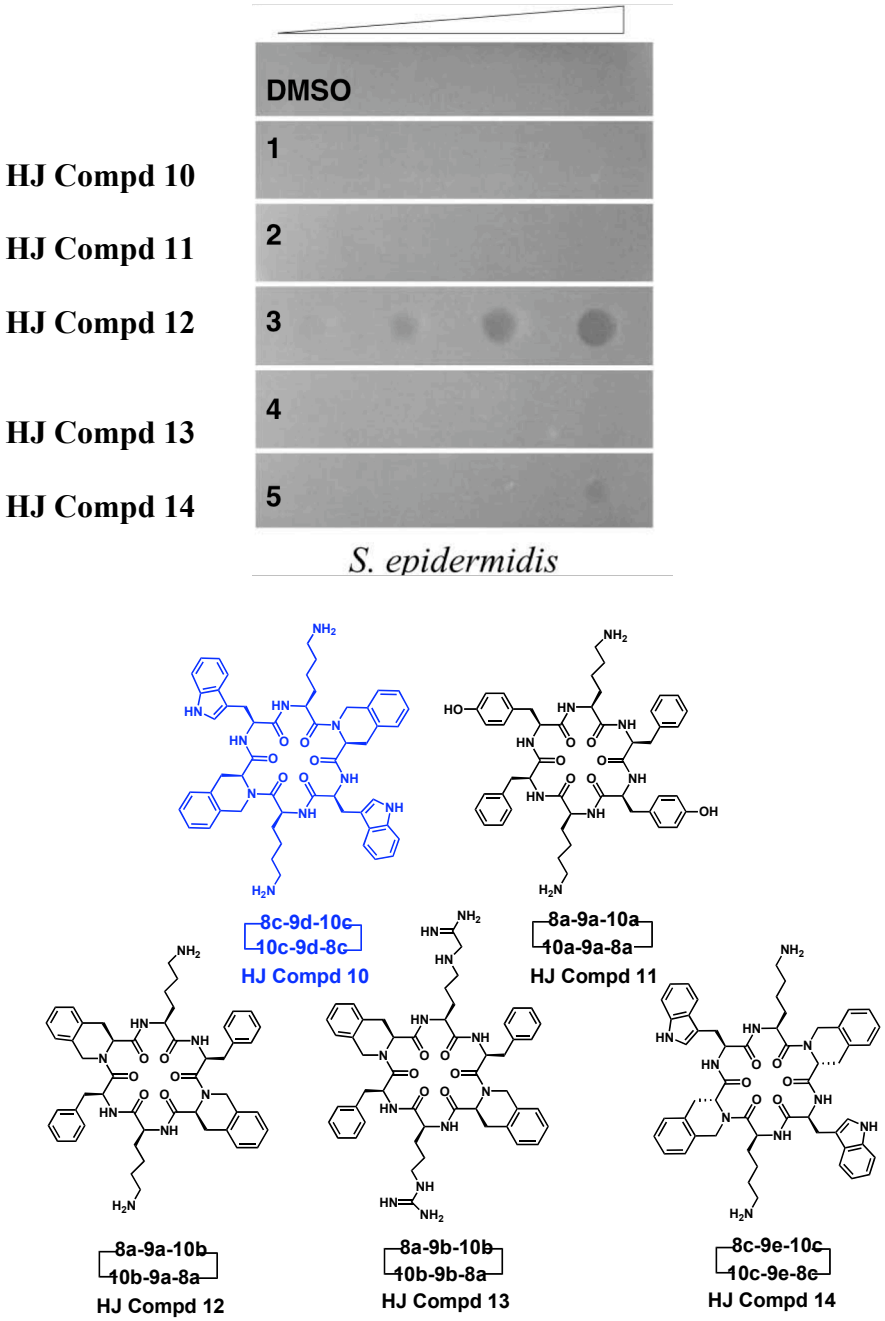

Figure 4.14. Inhibition of the Growth of *S. epidermidis* by Compounds HJ Compd 12 and HJ Compd 14. 2.5 µl of Peptide Dilutions in LB broth (0.625, 1.25, 2.5 and 5 µM) were Spotted onto an Lawn of Bacteria in a 0.6% Agarose Overlay. Control Samples of DMSO were used at Dilutions of 1.25, 2.5, 5 and 10%.

4.4.3 Conclusions

Overall, I synthesized one second-generation compound **HJ compd 10** by using two different synthetic approaches (**Figure 4.7**, and **Figure 4.10**). There are four areas of significance in this described project. First, I described the synthesis and associated biological assays on a new class of compounds. Synthesis of two generations of compounds yielded critical information that will assist further development of this structural class as a tool for studying pathways involving HJs during DNA repair. In addition, we have macrocycles that may lead to the development of new antibiotics. Using assays with the RuvC resolvase, we demonstrate that macrocycles successfully trap HJ's *in vitro*. The second important aspect of this work is the substitution of polar residues such as lysine within these macrocycles. These polar residues do not play a critical role in HJ binding, but do improve compound solubility. A third, and fundamental discovery, described here is the structure–activity relationship: (i) compounds containing tyrosine were highly effective at trapping HJs, and (ii) both hexapeptides and octapeptides were able to trap HJ's. This discovery regarding the hexa- versus octa-peptides demonstrates that an ideal fit within HJs may be reliant on the hydrophobic residues π-stacking with the nucleotides rather than just the macrocycle size, as the peptides bind specifically to HJs, rather than the recombinases that target HJ's, we hypothesize that π-stacking residues, in combination with those that can also form H-bonds (e.g., tyrosine), are the key element in trapping HJs. Further work is needed to determine the precise structural requirements for trapping HJs and increasing antimicrobial potency. We anticipate that a third generation of macrocycles,

incorporating tyrosines, hydroxy tetrahydroquinolines, and hydroxy tryptophans will help uncover the structure–activity relationship crucial for HJ binding. Studies to determine if these compounds kill bacteria and whether they do so via trapping HJs are on going and will be reported in due course. Fourth, perhaps the most important aspect of this work is the discovery of new macrocyclic compounds that provide an insight on recombination pathways that proceed via this HJ intermediate. The discovery of structurally constrained compounds with reasonable solubility affords the opportunity to see HJ–peptide interactions via X-ray crystallography.

Chapter 4, in full, is a reprint of the material, as it appears in "Novel antibiotics: C-2 symmetrical macrocycles inhibiting Holliday junction DNA binding by *E. coli* RuvC", ***Bioorganic and Medicinal Chemistry,*** *14*, **2006**, 4731-4739. Po-Shen Pan, Fiona A. Curtis, Chris L. Carroll, Irene Medina, Lisa Liotta, Gary J. Sharples, and Shelli R. McAlpine. The dissertation author was the primary author of this paper.

4.5 REFERENCES AND NOTES

1. Neu, H. C. "The Crisis in Antibiotic Resistance" *Science.* **1992**, *257*, 1064.

2. Shortridge, V. D.; Doern, G. V.; Brueggemann, A. B.; Beyer, J. M.; Flamm, R. K. "Prevalence of Macrolide Resistance Mechanisms in *Streptococcus pneumoniae* Isolates from a Multicenter Antibiotic Resistance in Surveillance Study Conducted in the United States in 1994-1995", *Clin. Infect. Dis.* **1999**, 29, 1186-1188.

3. Kaufman, M. "Worries Rise Over Effect of Antibiotics in Animal Feed", *Washington Post.* **2000**, March 17th, Page A1.

4. Blakely, G.; May, G.; McCulloch, R.; Arciszewska, L. K.; Burke, M.; Lovett, S. T.; Sherratt, D. J. "Two Related Recombinases are Required for Site-Specific Recombination at *dif* and *cer* in E. coli K12", *Cell.* **1993**, *75*, 351-361.

5. Nash, H. A. "Site-specific recombination: Integration, Excision, Resolution, and Inversion of Defined DNA Segments in E. coli and Salmonella", ASM Press: Washington, D.C. **1996**; 2363-2376.

6. Klemm, M.; Cheng, C.; Cassell, G.; Shuman, S.; Segall, A. M. "Peptide Inhibitors of DNA Cleavage by Tyrosine Recombinases and Topoisomerases", *J. Mol. Bio.* **2000**, *299*, 1203-1216.

7. Cassell, G.; Klemm, M.; Pinilla, C.; Segall, A. M. "Dissection of Bacteriophage λ Site-Specific Recombination using Synthetic Peptide Combinatorial Libraries", *J. Mol. Biol.* **2000**, *299*, 1193-1202.

8. Ghosh, K.; Lau, C. K.; Guo, F.; Segall, A. M.; Van Duyne, G. D. "Peptide trapping of the Holliday Junction Intermediate in Cre-loxP Site-Specific Recombination", *J. Biol. Chem.* **2005**, *280*, (9), 8290-8299.

9. Gopaul, D. N.; Guo, F.; VanDuyne, G. D. "Structure of the Holliday Junction Intermediate in Cre−loxP Site-Specific Recombination", *EMBO J.* **1998,** *17*, 4175-4187.

10. Bolla, M. L.; Azevedo, E. V.; Smith, J. M.; Taylor, R. E.; Ranjit, D. K.; Segall, A. M.; McAlpine, S. R. "Novel Antibiotics: Macrocyclic Peptides Designed to trap Holliday Junctions", *Org. Lett.* **2003**, *5*, 109-112.

11. Bursavich, M. G.; West, C. W.; Rich, D. H. "From Peptide to Non-Peptide Peptidomimetics: Design and Synthesis of New Piperdine Inhibitors of Aspartic Peptidases", *Org. Lett.* **2001**, *3*, 2317-2320.

12. Sharples, G. J. "The X-philes: Structure-Specific Endonucleases that Resolve Holliday Junctions", *Mol. Microbiol.* **2001**, *39*, 823-834.

13. Sharples, G. J.; Curtis, F. A.; McGlynn, P.; Bolt, E. L. "Holliday Junction Binding and Resolution by the Rap Structure-Specific Endonucelase of Phage Lambda", *J. Mol. Biol.* **2004**, *340*, 739-751.

14. Duckett, D. R.; Murchie, A. H.; Diekmann, S.; Kitzing, E. V.; Kemper, B.; Lilley, D. M, "The Structure of the Holliday Junction, and its Resolution", *Cell.* **1988**, *55*, 79-89.

15. Boldt, J. L.; Pinilla, C.; Segall, A. M. "Reversible Inhibitors of Lambda Integrase-Mediated Recombination Efficiently trap Holliday Junction Intermediates and form the Basis of a Novel Assay for Junction Resolution. *J. Biol. Chem.* **2004**, *279*, (5), 3472-3483.

16. Kepple, K. V.; Boldt, J. L.; Segall, A. M. "Holliday Junction-Binding Peptides Inhibit Distinct Junction-Processing Enzymes", *Proc. Natl. Acad. Sci. USA.* **2005,** *102*, (19), 6867-6872.

17. Hexapeptide macrocycles synthesized by McAlpine Laboratory: (1) 4 = a, a., 6 = a, (2) 4 = a, 5 = b, 6 = a, (3) 4 = a, 5 = c, 6 = a, (4) 4 = a, 5 = d, 6 = a, (5) 4 = a, 5 = e, 6 = a, (6) 4 = b, 5 = a, 6 = a, (7) 4 = a, 5 = a, 6 = c, (8) 4 = b; 5 = a, c., (9) 4 = b, 5 = c, 6 = c, (10) 4 = a, 5 = c, 6 = c, (11) 4 = b, 5 = c, 6 = a, (12) 4 = c, 5 = a, 6 = d, (13) 4 = c, 5 = c, 6 = d; Octapeptide macrocycles synthesized by McAlpine Laboratory: (1) 4 = a, a., 6 = a, 7 (2) 4 = a, 5 = b, 6 = a, 7 (3) 4 = a, 5 = c; 6 = a, a., 5 = d, 6 = a, 7.

18. Liotta, L. A.; Medina, I.; Robinson, J. L.; Carroll, C. L.; Pan, P.-S.; Corral, R.; Johnston, J. V. C.; Cook, K. M.; Curtis, F. A.; Sharples, G. J.; McAlpine, S. R. "Novel Antibiotics: Second Generation Macrocyclic Peptides Designed to trap Holliday Junctions", *Tetrahedron Lett.* **2004**, *45*, 8447-8450.

19. Chelucci, G. F.; M.; Giacomelli, G. "Synthesis of 1-Substituted 2-[(2S)-2-Pyrrolidinyl]pyridine from L-Proline", *Synthesis.* **1990**, 1121-1122.

20. Ninhydrin tests typically demostrated a very light blue color after coupling. Upon a second coupling they gave yellow beads.

21. Dunderdale, H. J.; Sharples, G. J.; Lloyd, R. G.; West, S. C. "Cloning, Overexpression, Purification and Characterization of the E. coli RuvC Holliday Junction Resolvase", *J. Biol. Chem.* **1994**, *269*, 5187-5194.

Chapter 5

Synthesis of Triostin A analogue: Azatandem

5.1 Introduction and Background of Triostin A

In this chapter, I will describe the partial synthesis of Azatandem. Compounds that I have synthesized are coded in blue and the other work done in this chapter, coded in black, was done Rodrigo Rodriguez and Chumg-Mao Pan. The Triostin Triostin A (**1a, Figure 5.1**) was isolated in 1961 from a strain of *Streptomyces aureus* designated S-2 210.[1, 2] Acid hydrolysis studies have shown that Triostin A was composed of quinoxaline-2-carboxylic acid, D-serine, L-alanine, *N*-methyl-L-cysteine and *N*-methyl-L-valine residues (**1a**, **Figure 5.1**).[3] NMR studies demonstrated this cyclic octadepsipeptide structure possessed a disulfide linkage.[4, 5] Studies have also indicated that Triostin A had significant antibiotic and anticancer activity.[1, 6] It has been proven that its toxicity involves bisintercalation into the DNA minor groove whereupon the DNA-Triostin A complex then blocks transcription enzymes, such as RNA polymerase, during transcription, eventually leading to apoptosis.[7, 8] The crystal structure of a DNA-Triostin A complex (**Figure 5.1b**) showed that the depsipeptide ring is a roughly rectangular shape with the disulfide bridge pointing away from the DNA binding site.[9] In addition this complex showed that the orientation of the D-Ser amino group allows for the chromophores to project parallel to each other at right angles from the peptide backbone, bracketing a CG base-pair in the minor groove of DNA.[9] The valine side-chains lay at the opposite corners of the rectangle to the quinoxaline chromophores, with the *N*-methyl

groups pointing in towards the nucleic acid surface. Alanine (on the long sides of the rectangle) also has both its carbonyl groups and methyl side-chains pointing towards DNA.[10, 11]

(a)

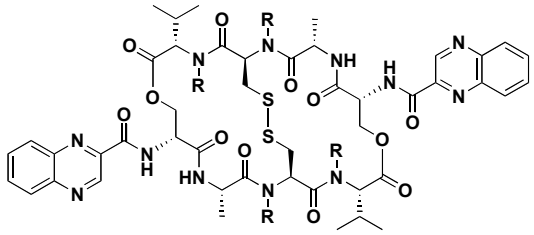

Triostin A (1a): R = Me
TANDEM (1b): R = H

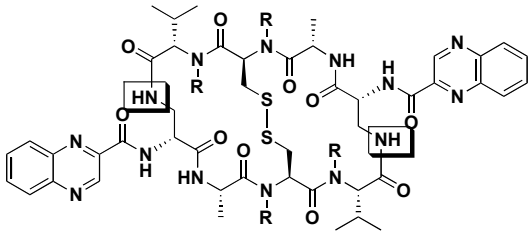

Azatriostin A (2a): R = Me
Azatandem (2b): R = H

(b)

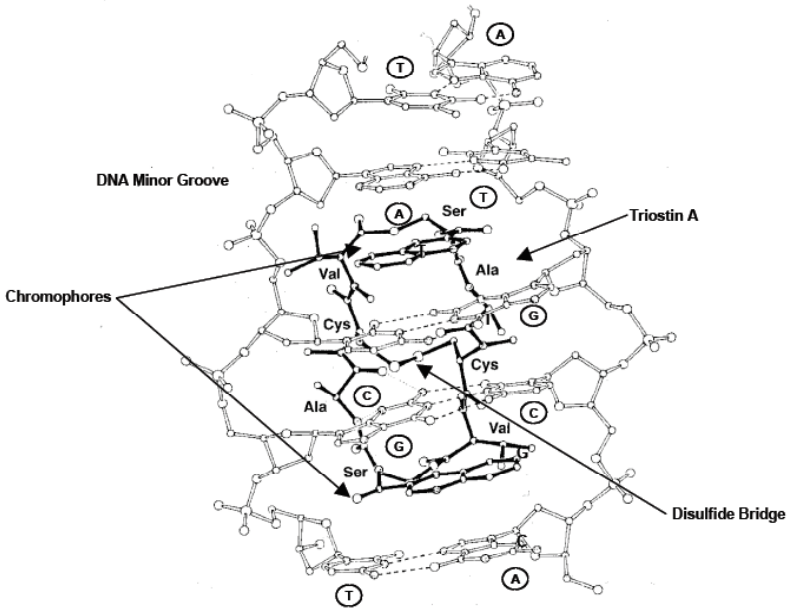

Figure 5.1. a.) Triostin A Derivatives. b.) DNA-Triostin A Complex (Triostin A is Shown in Solid Bonds and the DNA Minor Groove is Shown in Outline Bonds.)

Structural features that contribute to DNA binding have also been studied. The *N*-demethylated analogue TANDEM (**T**riostin **A** ***N*-DEM**ethylated, **1b**, **Figure 5.1**), maintains bifunctional intercalation, however, unlike Triostin A, it binds with high affinity to AT-rich DNA.[12] It was suggested that the structural change induced by the removal of the *N*-methyl groups exposes the NH-amide groups of L-Ala, and these could interact with the 2-keto groups of thymine.[13] [*N*-MeCys^3, *N*-MeCys^7]TANDEM or CysMeTANDEM has been shown to bind in a very similar manner to TANDEM, in that both of these derivatives bisintercalate into DNA with approximately the same affinity as that of TANDEM.[14, 15] It has also been suggested that the *N*-methyl groups of Cysteine play a minor part in the binding to DNA, as they have been shown to project away from the minor groove, rather it is the *N*-methyl on valine that alters the conformation of Triostin A so that it targets C-G rich sequences.[13, 15, 16] In addition, studies have indicated that the only role of disulfide linkage is to hold the structure rigid and hence improve binding strength by reducing unfavorable entropic effects.[13, 16, 17]

Furthermore, Azatriostin (**2a**, **Figure 5.1**) differs from Trisotin A **1a** by replacing the D-serine amino acid with D-*β*-aminoalanine, which converts the ester linkage in Triostin A to an amide linkage in Azatriostin. This cyclic octapeptide **2a** still maintains DNA bisintercalation as its primary mechanism of action.[18]

Finally, Azatandem **2b** differs from TANDEM **1b** by replacing the D-serine amino acid with D-*β*-aminoalanine providing an amide versus ester linkage in the cyclic

peptide backbone. This compound was first synthesized by Dietrich[19] in solid-phase and its biological activity is currently under investigation.

5.2 Determination of the ring closing site of Triostin A derivatives

In order to identify the key features of Triostin A and its analogues (**Figure 5.1**) that are responsible for binding affinity and sequence selectivity, different synthetic strategies have been reported.[18-25] However, these efforts were hindered by the difficulty in synthesizing Triostin A analogues, thus hampering the progress of this research. Here we describe a new synthetic strategy for Azatriostin and Azatandem derivatives, where this efficient construction will allow us to gain insight on the structure-activity relationship of Triostin A.

The most important issue in the synthetic strategy is the ring closure step. Previous studies have indicated that the ring closing step is key to success in the synthesis of the Triostin derivatives.[25] There are four potential sites for macrocyclization (**A**-**D**, **Figure 5.2**). Alphabetical order (**A**-**D**) represents the order in which the synthetic strategies were undertaken.[18, 20, 25-27]

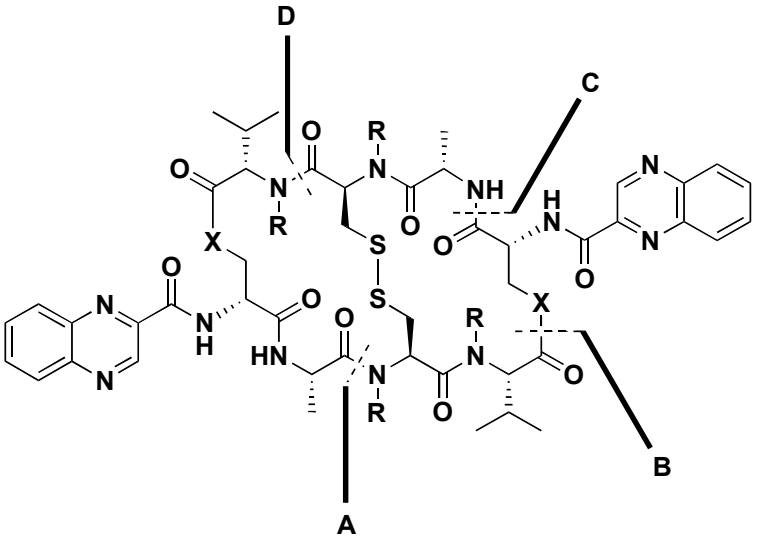

Triostin A (1a): R = Me, X= O
TANDEM (1b): R = H, X = O

Azatriostin A (2a): R = Me, X = NH
Azatandem (2b): R = H, X = NH

Figure 5.2. Potential Sites for Cyclization Reaction.

5.2.1 Site A: Olsen's Approach

Olsen and co-workers began an investigation into the synthetic approach of the natural product by focusing on TANDEM **1b**.[20] The initial synthesis involved a linear route to a tetradepsipeptide precursor in which Boc-Cys(Acm)-Val-OH was coupled to Cbz-D-Ser-Ala-OTce through an ester bond to the side-chain of serine. In a convergent approach, this tetrapeptide precursor was subsequently deprotected at either the cysteine α-amino group or the alanine carboxyl group, and then dimerized to give the linear octadepsipeptide **3** (**Figure 5.3**). Cyclization was carried out at **site A** (**Figure 5.2**) by using NHS-DCC under basic conditions to form **5**. This bis-Cbz-protected cyclic peptide was then subjected to Acm-deprotection and oxidation with iodine in

methanol/dichloromethane to form the disulfide bridged cyclic peptide **6**. Finally, deprotection and acylation with 2-quinoxaloyl chloride gave TANDEM **1b**.

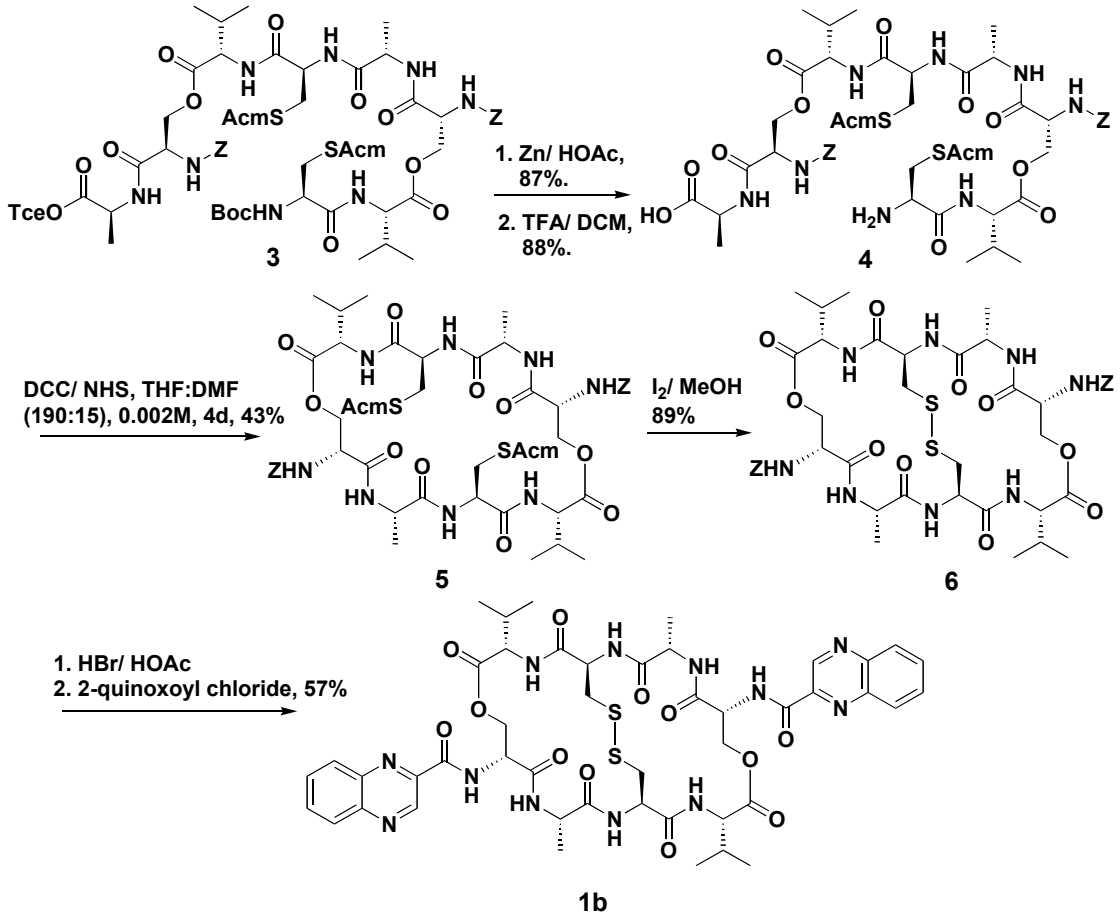

Figure 5.3. Olsen's Synthesis of TANDEM (Z = Cbz protecting group)

Olsen's synthesis was the first example of making TANDEM. However, this methodology suffered from racemization during the formation of the linear octa-depsipeptide.

5.2.2 Site B: Boger's Approach

Not only was the formation of the depsipeptide bond (**Site B**, **Figure 5.2**) as the final step a less attractive synthetic pathway, due to the lower nucleophilicity of the alcohol, the depsipeptide is also less stable than the peptide derivative, Azatriostin. Further, the conditions required for such a ring closure would be a potential source of significant racemization of the terminal valine and/or dehydration and racemization of the serine residue. However, with the synthesis of Azatriostin (**2a**, **Figure 5.1**) this was not a concern because the D-β-aminoalanine was less prone to recemization than the serine residue. Further, the amide linkage formed by the D-β-aminoalanine would be significantly more stable than the ester linkage.

With these issues in mind, Boger chose to synthesize Azatriostin **2a** using site **B** and his strategy is described in **Figure 5.4.**[18] The initial synthesis involved a linear route to a tetrapeptide precursor, in which Ala-MeCys(Acm)-MeVal-OMe was coupled to N^{α}-Boc-N^{β}-Teoc-D-3-Amino-Ala-OH through a standard peptide coupling procedure. In a convergent approach, this tetrapeptide precursor was subsequently deprotected at either the D-β-aminoalanine α-amino group or the valine carboxyl group, and then dimerized to give the linear octapeptide (**7, Figure 5.4**). Subsequent deprotection at the *N*-terminus and *C*-terminus of the linear octaepeptide **7** was then followed by Acm-deprotection and oxidation with iodine in methanol/ dichloromethane to form the disulfide bridged peptide **10**. Cyclization was carried out at site **B** by using EDCI-HOAt under basic conditions to form the core cyclic peptide. Finally, deprotection and coupling with 2-quinoxaloyl acid

produced Azatriostin **2a**. Interestingly, an alternative approach involving dimerization of the tetrapeptide through the disulfide bridge followed by macrocyclization also proved to be successful in constructing the core bicyclic peptide structure.[18] Interestingly, cyclization of the linear octapeptide prior to the disulfide bridge formation proved to be challenging due to the instability of the amide cyclized intermediate, therefore this synthetic strategy is less satisfactory.

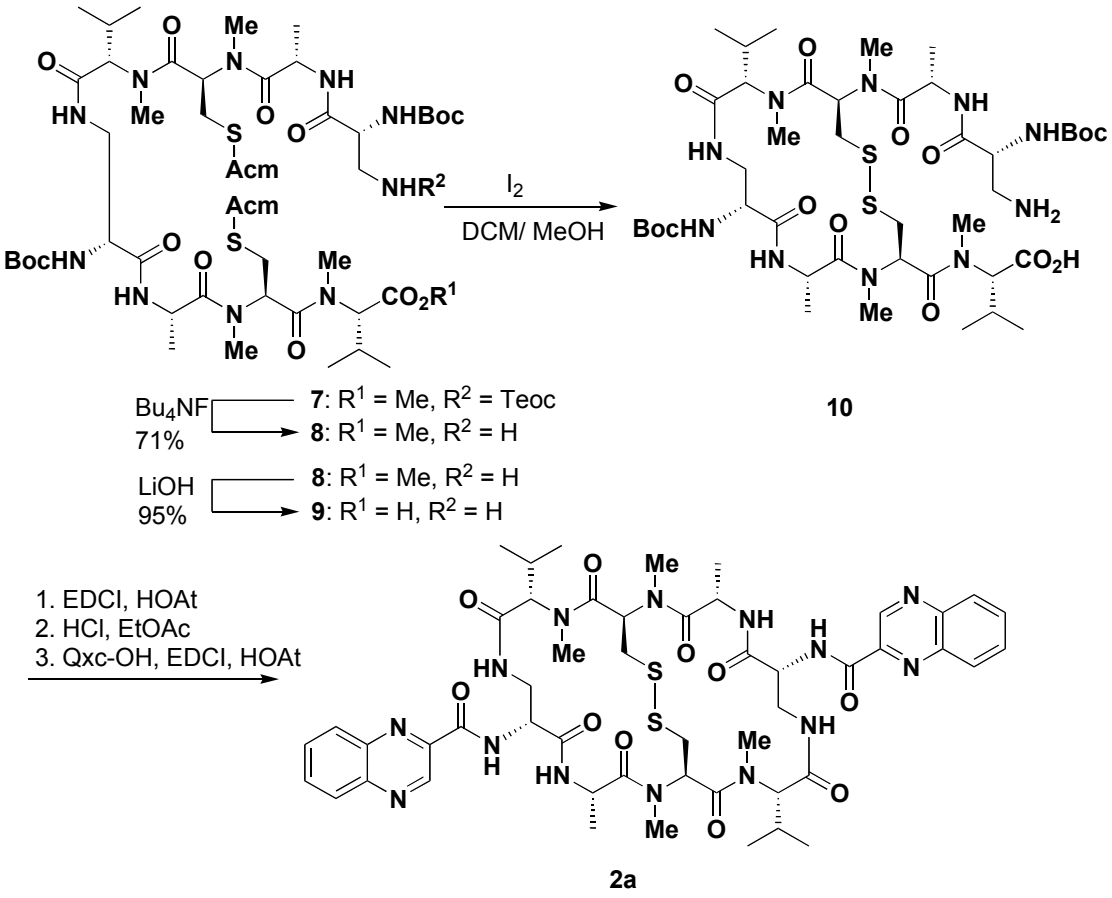

Figure 5.4. Boger's Synthesis of Azatriostin 2a

All synthetic intermediates generated by Boger could be purified by acid/base liquid-liquid extractions, and this simple method of purification makes Boger's approach

an attractive one. This novel methodology offers an attractive route for synthesizing an Azatriostin library because it requires fewer synthetic and purification steps than Olsen's strategy to complete the synthesis but overall both Boger and Olsen's strategy gave comparable yield about 40%.[18, 20]

5.2.3 Site C: Diederichsen's Approach

Diederichsen and co-workers formed a ring closure using DIC/HOAt between serine and alanine (**Site C**, **Figure 5.5**),[26] which gave an excellent yield of 82% for the bis-Cbz-protected bicyclic peptide **14**. It is speculated that this high yielding bicyclic peptide formation occurred due to the fact that the free acid at the *C*-terminus and the free amine at the *N*-terminus were oriented in an ideal close proximity to one another, thus resulting in a high yielding macrocyclization.[26]

Formation of the cysteine-valine bond (**Site D**, **Figure 5.2**) is a possibility, but this would involve the activation of the terminal cysteine carboxyl group prior to macrocyclization, which is known to lead to racemization.[27] Given this issue, this synthetic route was eventually abandoned.

Out of the 3 viable strategies, **A**-**C**, (**D** was not viable) Diederichsen's approach (site **C**) gave the highest yield with a yield of 82% for cyclization compared to 46% and 39% for A, and B sites respectively. Its success mainly relied upon the disulfide bridge linkage to hold the linear octadepsipeptide's free acid *C*-terminus and free amine *N*-

terminus in close proximity needed so that macrocyclization could occur in a favorable manner. However, utilizing the disulfide bridge requires a lengthy inefficient linear synthetic approach and not appropriate for constructing multiple Triostin A derivatives.

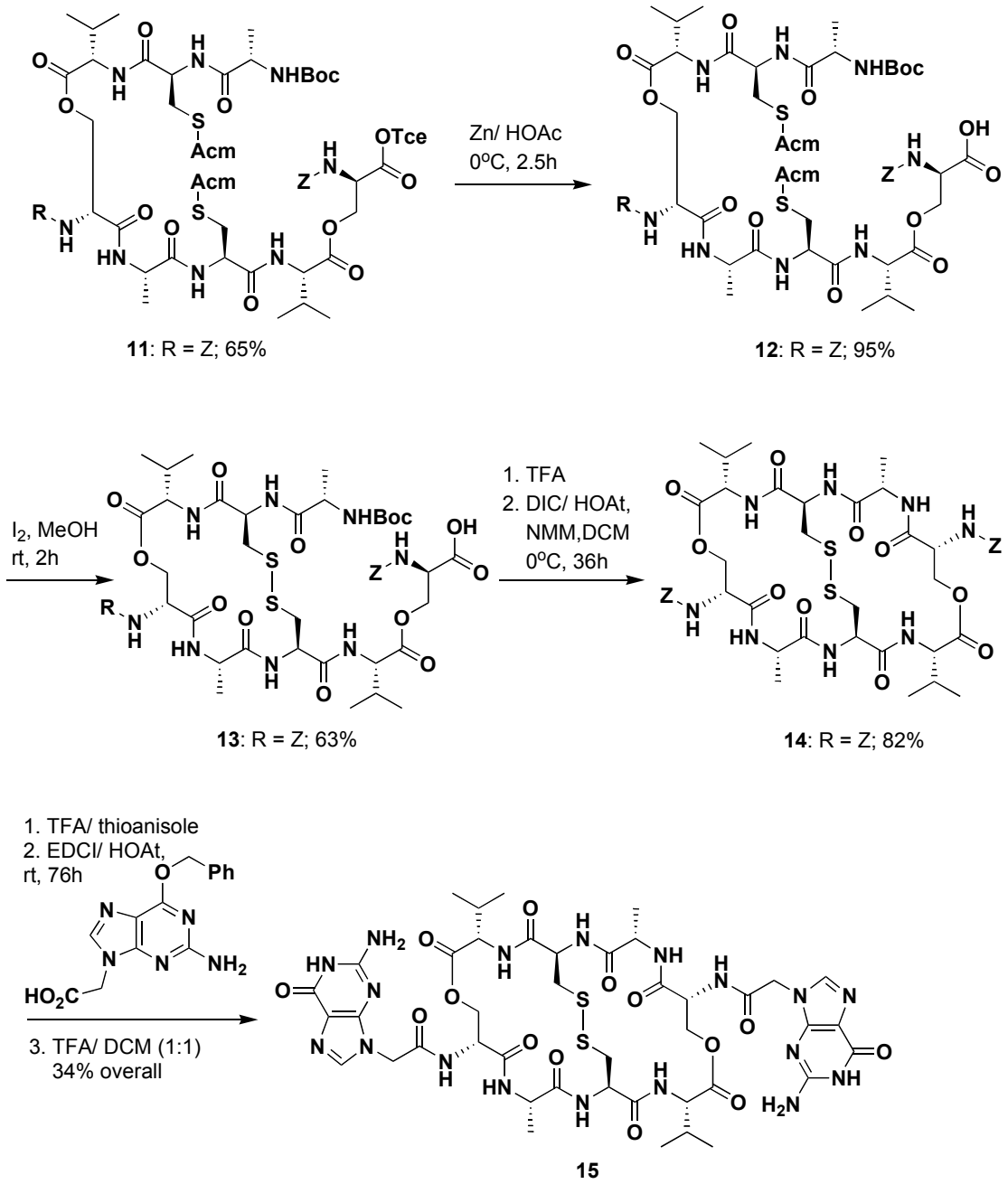

Figure 5.5. Diederichsen's Synthesis of TANDEM Derivative 15. (Z = Cbz)

5.3 Synthetic Strategies of Azatandem

Given that both **B** and **C** provided the final Triostin derivatives in good yields when they utilized the disulfide bridge to templating the ring closing reaction, site **B** was considered as an option in making Azatandem via a KAHA (α-**K**eto**a**cid-**h**ydroxyl**a**mine) ligation.[28] The KAHA ligation reaction (**Figure 5.6**) is a chemoselective process that forms peptide bonds between two unprotected amino acid fragments.[28] This reaction performed under mild conditions (neutral or slightly acidic) at a wide range of concentrations (1.0M-0.001M). Specifically, it was proposed that the KAHA ligation would efficiently generates the macrocycle in good yields by making use of the disulfide bridge as an anchor (**24**, **Figure 5.7**).

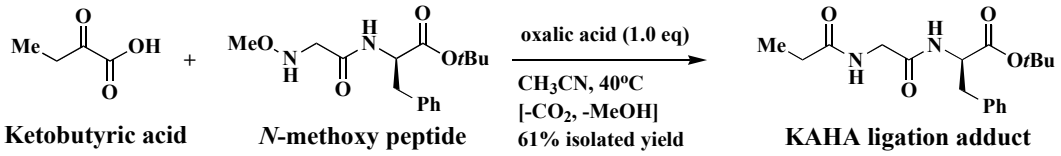

Figure 5.6. KAHA ligation reaction.

5.3.1 Retrosynthetic Strategy of Azatandem 2b

The overall retro-synthetic strategy of Azatandem **2b** is shown in **Figure 5.7**. We anticipate that Azatandem **2b** could be accessed from **25** via KAHA ligation[28] (**Figure 5.7**) between α-ketoacid and methoxylamine. **25** would be derived from the Pd-catalyzed hydrogenation of **24**, while **24** would be formed by dimerization of **23** via disulfide

bridge formation. Tetrapeptide **23** would be obtained by coupling **21** to **22** via peptide bond formation followed by TIPS deprotection, tosylation, and S_N2 methoxylamine formation. **22** would be formed by standard peptide coupling of **16** to H-Cys(Acm)-OMe followed by acid deprotection. TIPS protected dipeptide **16** could be furnished from commercially available Boc-D-Ser-OH and H-Ala-OMe via chemoselective peptide bond formation.

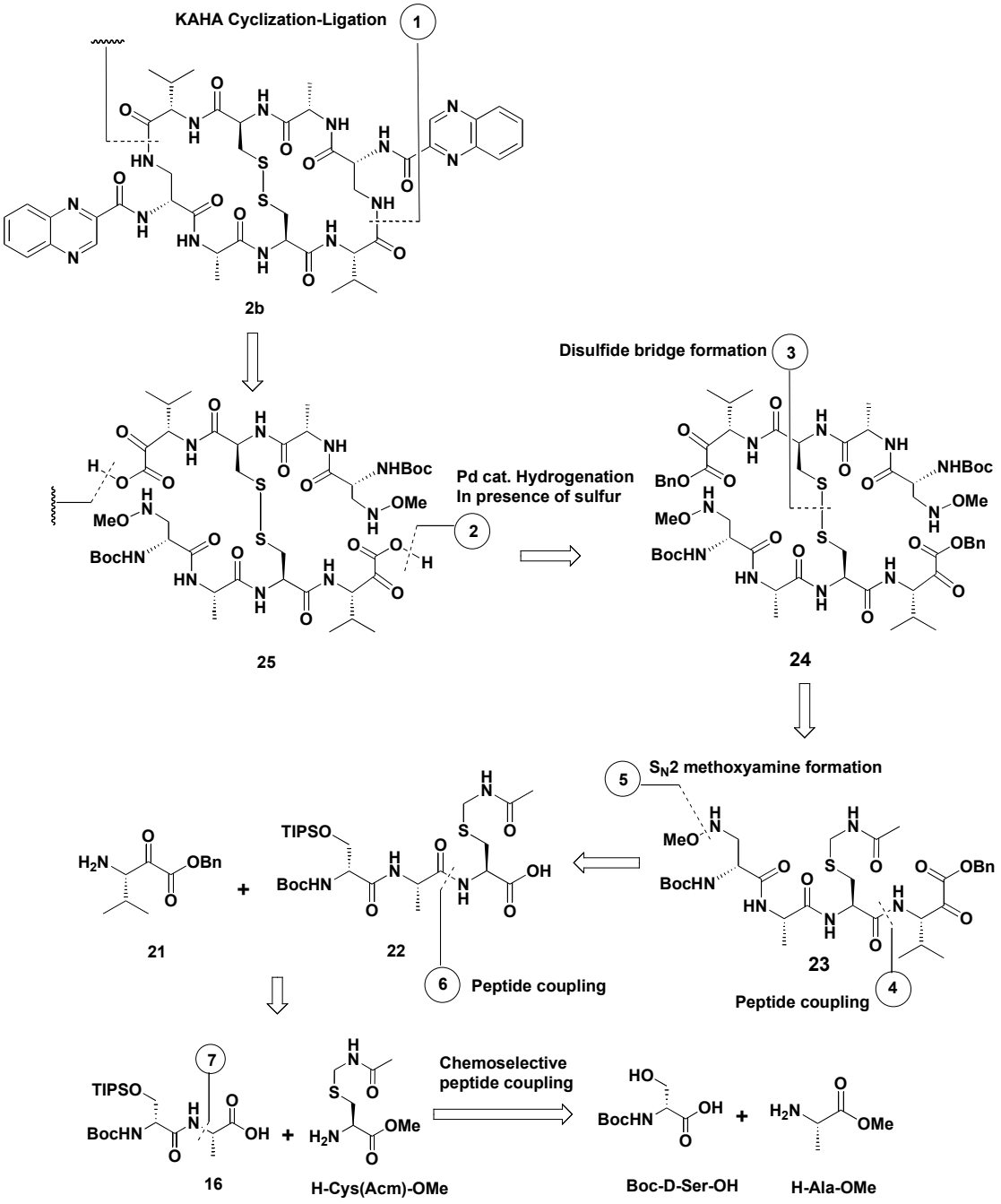

Figure 5.7. Retrosynthetic Strategy of Azatandem 2b.

5.3.2 Synthesis of Azatandem 2b

The overall synthetic strategy of Azatandem **2b** for this research is shown in **Figure 5.8**, and will be discussed in detail in the following sections.

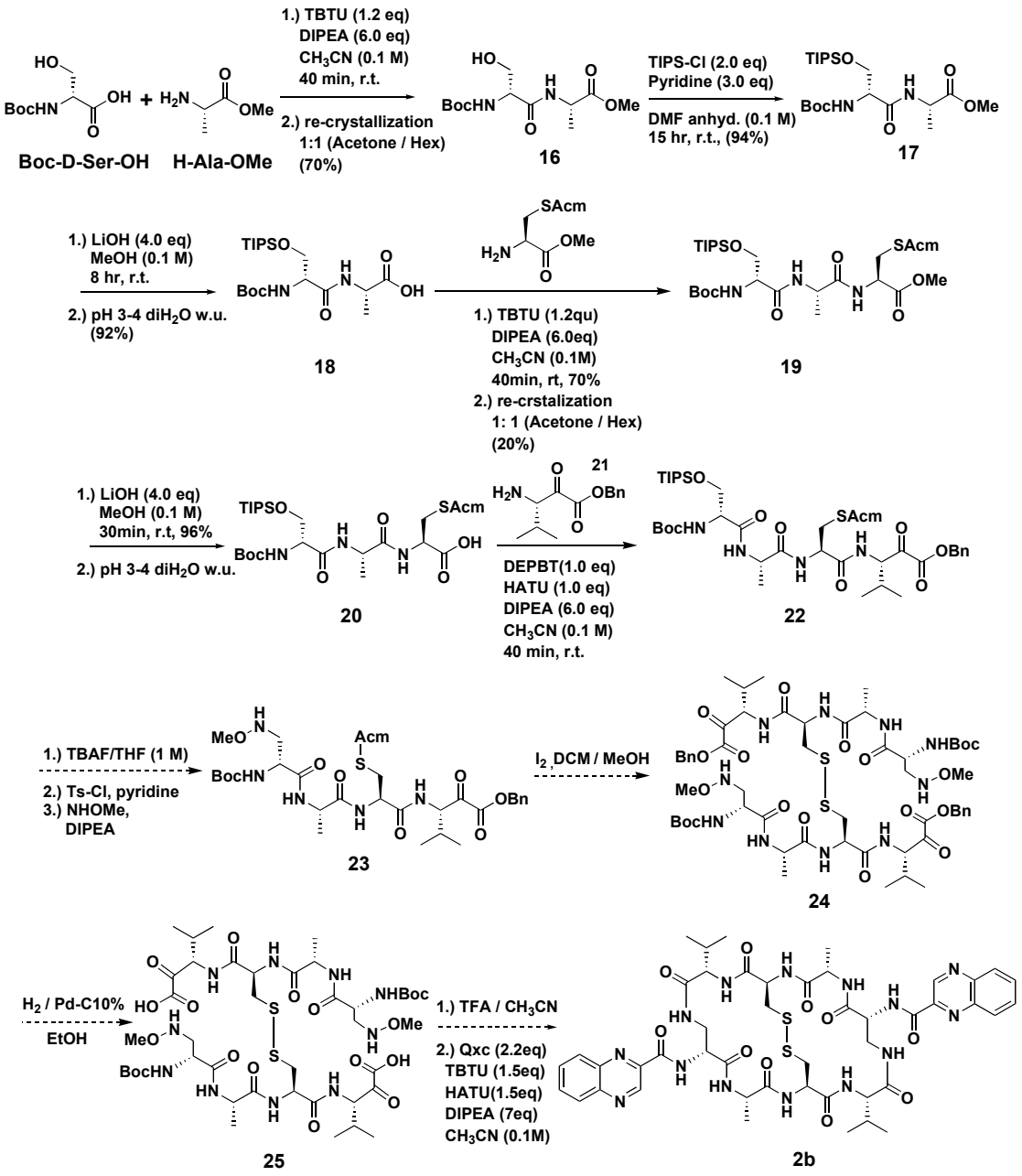

Figure 5.8. Synthetic Strategy for Azatandem 2b.

5.4 Synthesis of 16

The H-Ala-OMe was coupled to Boc-D-Ser-OH using TBTU (1.2eq) and DIPEA (6.0eq) in acetonitrile (0.1M) to give crude (**16, Figure 5.9)**. Crude **16** was first purified via flash column chromatography followed by recrystallization in Acetone: Hexane (1:1 ratio) to give pure dipeptide **16** with a 70% yield.

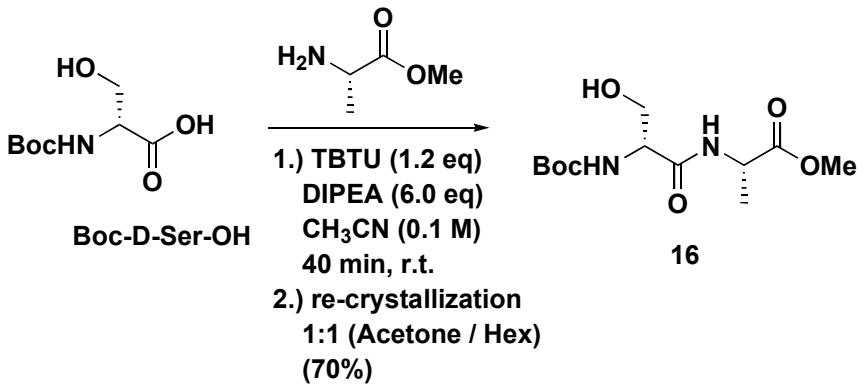

Figure 5.9. Synthesis of 16.

5.5 Synthesis of 20

The dipeptide **16** was subjected to TIPS-Cl (2.0eq) and pyridine (3.0eq) in dry DMF (0.1M) for 15 hours under argon at room temperature (**Figure 5.10**). The crude product was purified by flash column chromatography to furnish pure **17** with a 94% yield. Substrate **17** was then acid deprotected by adding LiOH (4eq) in methanol (0.1M) at room temperature for 8 hours. The crude product was extracted with dichloromethane/DI water (pH = 3-4) to give **18** as white solid in 92% yield. It is important to maintain a pH = 3-4 of the aqueous layer, because slight decomposition of

the reaction product was observed if the aqueous layer had lower pH values. Compound **18** was then coupled to H_2N-Cys(Acm)-OMe by using TBTU (1.2eq) and DIPEA (6.0eq) in acetonitrile (0.1M) for 40 minutes at room temperature. The crude product was then recrystalized in acetone/hexane (1:1 ratio) resulting in compound **19** with a 70% yield. Compound **19** was acid deprotected by the protocol described above used for compound **18**, to produce **20** with a 96% yield.

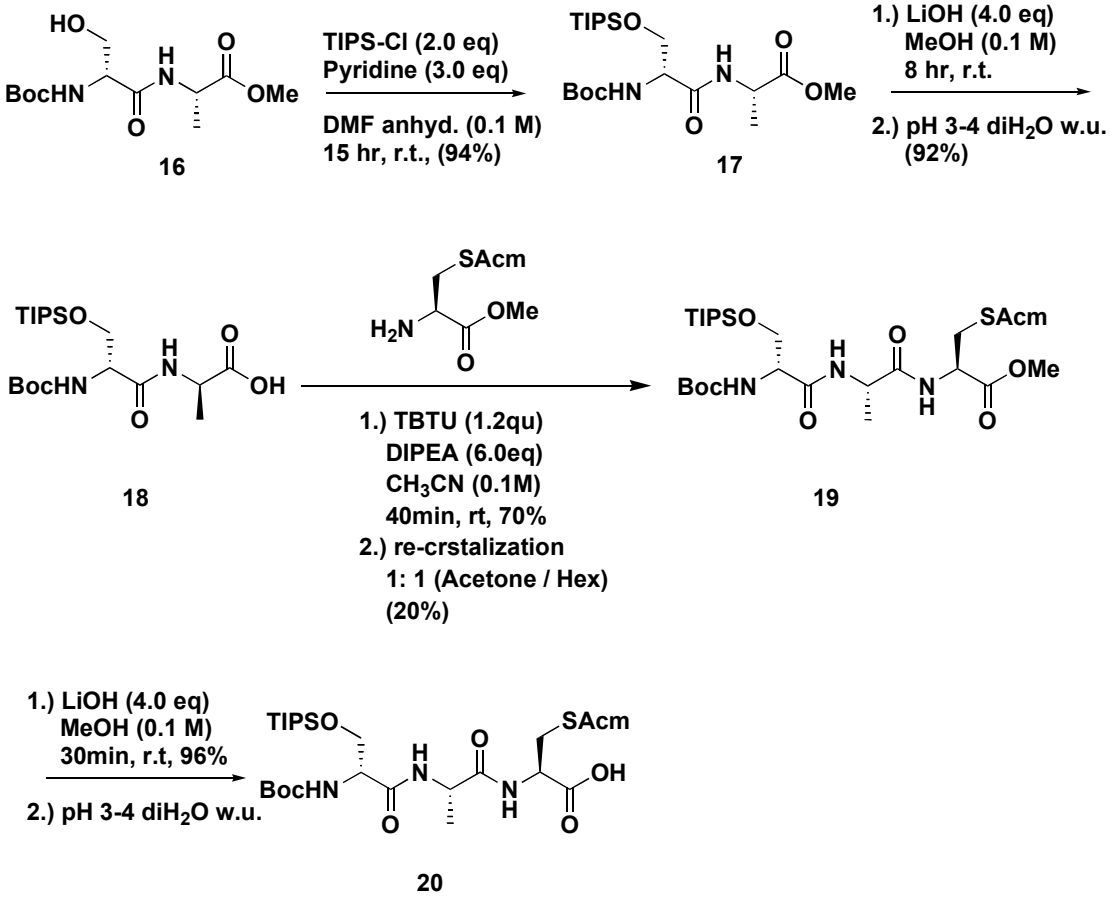

Figure 5.10. Synthesis of 20.

5.6 Synthesis of 21

5.6.1 Phosphorous ylide approach

Two approaches toward the synthesis of α-ketoester **21** were carefully evaluated. Wasserman's phosphorous ylide strategy for synthesizing the amino acid based α-ketoacid.[29] One example of this strategy is shown in **Figure 5.11**.[29] Boc-Phe-OH was coupled to (cyanomethy1ene)triphenylphosphorane **26** to form the cyano keto phosphoranes **27** with an 80% yield. An oxidation procedure was then performed to furnish the α-Keto Ester **28** with an 89% yield.

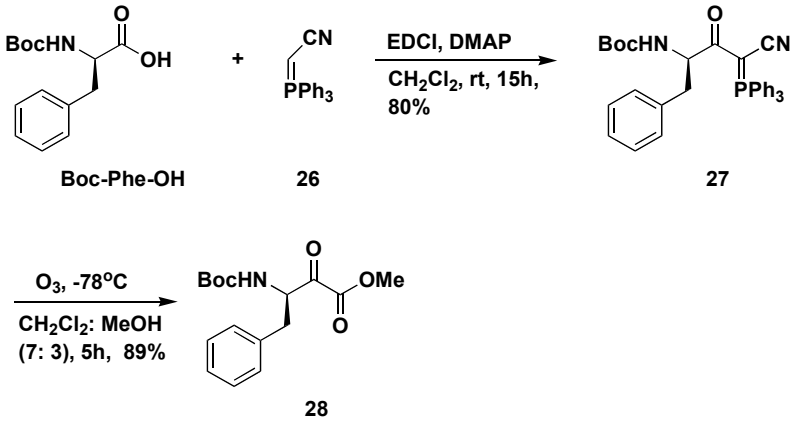

Figure 5.11. Synthesis of α-Keto Ester 28.

Wasserman's phosphorous ylide approach provided an efficient strategy to synthesize amino acid based α-keto acids, esters, and amides.[29] The success, however, suffered from two main obstacles. First, the rate of coupling between the carboxylic acid

and cyanophosphorane ylide **27** was low regardless of the acid used; second, the rate of oxidation to form α-ketoester (i.e. **28)** was very slow depending on the reaction.

5.6.2 Sulfur ylide Approach

Inspired by Wasserman's work, Bode's group has made advances towards synthesizing amino acid-based α-keto acids or esters by utilizing sulfur ylide chemistry.[28] This sulfur ylide approach involved the coupling of the sulfonium salt to carboxylic acid of the peptide substrate to yield the sulfur ylide intermediate (**30, 32, Figure 5.12)**. Oxidation of this sulfur ylide intermediate in an alcohol containing solvent system furnishes the amino acid-based α-keto esters (**33, Figure 5.12)**. It should be noted that the reaction time needed to complete the sulfur ylide formation (**30**, and **32**, **Figure 5.12**) is less than the formation of phosphorous ylide.[28] Furthermore, oxidation of sulfur ylides to form α-ketoester by oxone is faster than oxidation of phosphorous ylide by ozone.[28]

Two different synthetic strategies toward the formation of amino acid-based α-keto esters were analyzed. Bode's sulfur ylide approach was chosen for this research because of its feasibility. The synthetic details including yields are discussed in the following section.

Sulfonium salt **29** was coupled to the Boc-Val-OH (1.0 eq) by using TBTU (1.1eq) and DIPEA (4eq) in dichloromethane (0.1M) to form **30** in good yield (90%) (**Figure 5.12**). The same conditions were also applied to form **32** in good yield (95%).

We have observed that the sulfur ylide **32** tends to form white crystals as a pure product, while sulfur ylide **30** tends to form yellow oil. Due to this unique difference, **32** was purified by simple recrsytalization while **30** was purified by flash column chromatography. The ease of purification has made **32** a preferred precursor for the synthesis of **21**. Thus, the sulfur ylide **32** was subjected to oxone (2.2eq) in a mixture of benzyl alcohol, dichloromethane, and acetone (3:7:10 ratio) at a 0.2M reaction concentration. This reaction was monitored every 30 minutes until the reaction was complete. We have noticed that the composition ratio of the solvent system plays an important role in the success of this reaction. It is speculated that the appropriate composition of the solvent system may help to stabilize the reaction intermediate during the reaction process. The subsequent crude reaction products was then purified by flash column chromatography and identified by ^{1}H NMR. The purified product **33** is a light-yellow oil material with a 55% yield. Compound **33** was then subjected to the standard Boc removal condition to yield **21** with assumed quantitative yield.

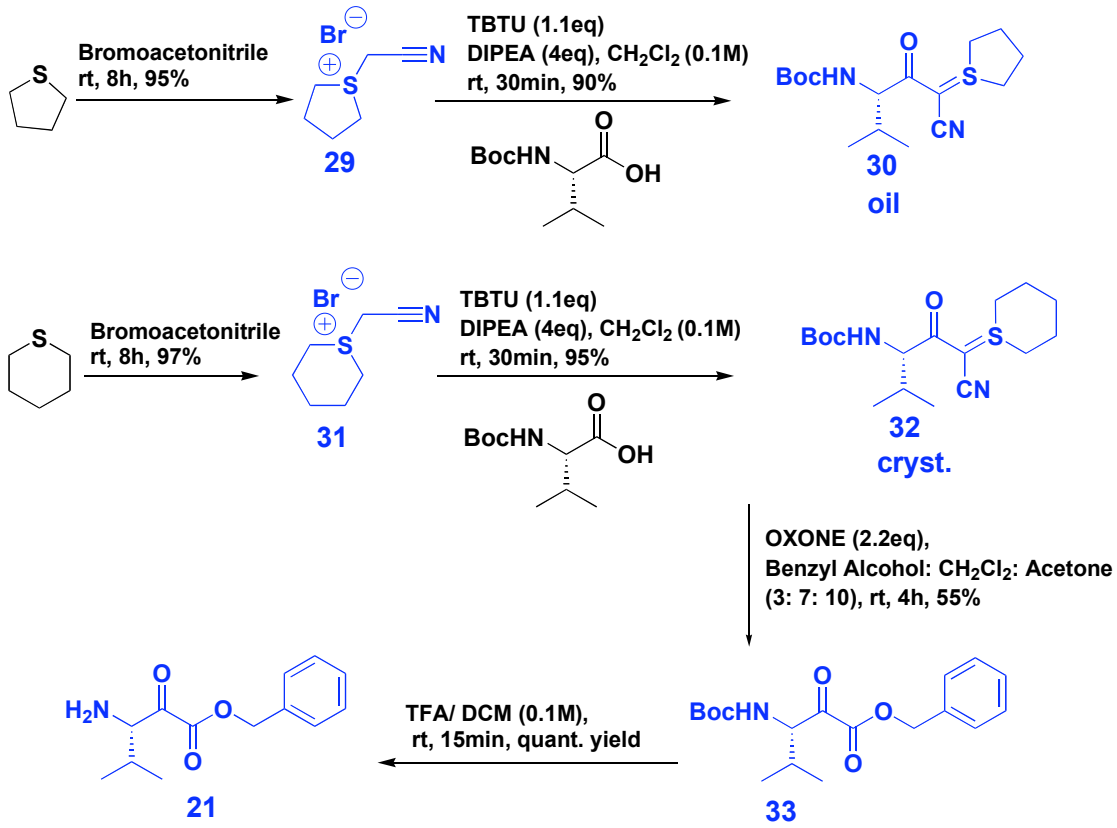

Figure 5.12. Synthesis of 21

5.7 Proposed Synthesis of 22

Formation of tetrapeptide **22** could be accomplished by coupling between compound **20** and compound **21** via standard peptide coupling condition (**Figure 5.13**). Once the expecting tetrapeptide **22** is formed, subsequent reactions can be performed to yield the key intermediate **23**.

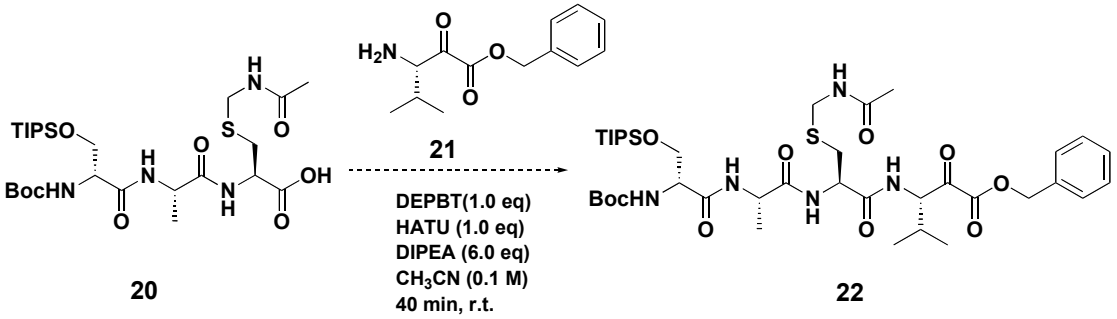

Figure 5.13. Proposed Synthesis of 22

5.8 Proposed Synthesis of 23

Conversion of **22** to **23** involved: (a) removal of the TIPS protecting group of the D-serine moiety, (b) tosylation of the unmasked hydroxyl group of the D-serine moiety, and (c) S_N2 displacement reaction to furnish the methoxylamine embedded tetrapeptide **23** (**Figure 5.14**). Preliminary results of these three individual chemical transformations are described in the following sections.

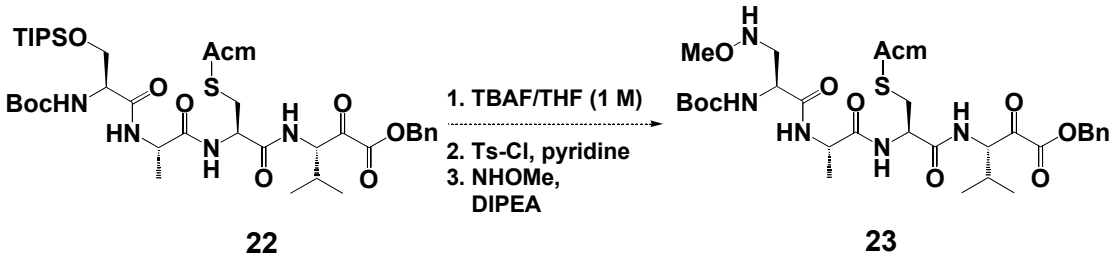

Figure 5.14. Proposed Strategy for Synthesizing 23.

5.8.1 TIPS removal reaction

The dipeptide substrate **17** was dissolved in anhydrous THF in a plastic reaction vessel and followed by the addition of TBAF into the reaction. After one minute, the reaction was quenched and ^{1}H NMR was used to confirm the structure of **34** (**Figure 5.15**) with a 90% yield.

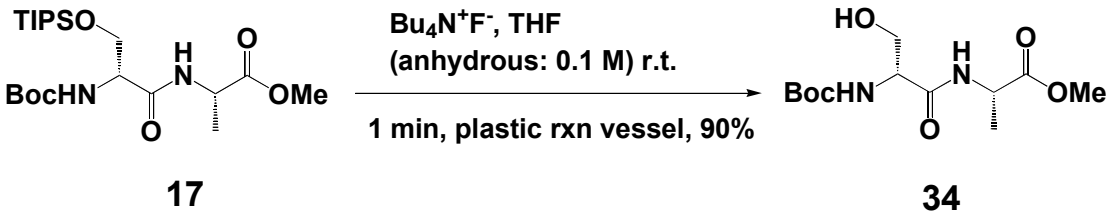

Figure 5.15. TIPS Deprotection Conditions.

5.8.2 Synthesis of Methoxylamine 37

Substrate **35** was dissolved in anhydrous dichloromethane (0.1M) and followed by treatment with pyridine (2.0 eq) and tosyl chloride (1.5eq) (**Figure 5.16**). The reaction was allowed to proceed for 28 hours under argon at room temperature. Upon completion, the crude reaction product was purified via recrystalization to furnish **36** with an 80% yield. The tosylated intermediate **36** was dissolved in acetonitrile (0.1M) then treated with DIPEA (2.0 eq) and *N*-methoxy amine (1.2eq) (**Figure 5.16**). The crude reaction product was purified by flash column chromatograpy and ^{1}H NMR was used to confirmed the structure of **37** with a 67% yield.

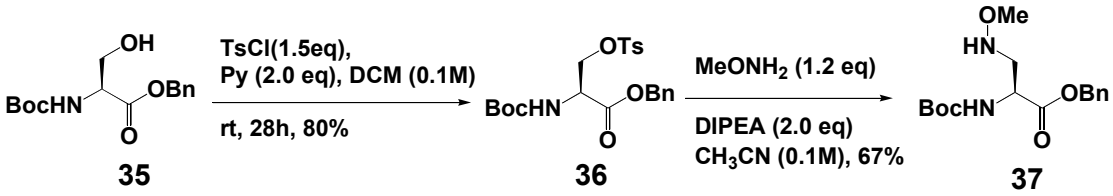

Figure 5.16. Synthesis of Methoxylamine 37.

In summary, conditions for TIPS deprotection, toslation, and methoxylamine formation are developed. These conditions can be applied to convert **22** to **23** (**Figure 5.8**) in the future.

5.9 Proposed Synthesis of 24.

Once the key intermediate **23** is obtained, direct dimerization of **23** via disulfide bond formation[30] (**Figure 5.17**) will be performed to furnish **24**.

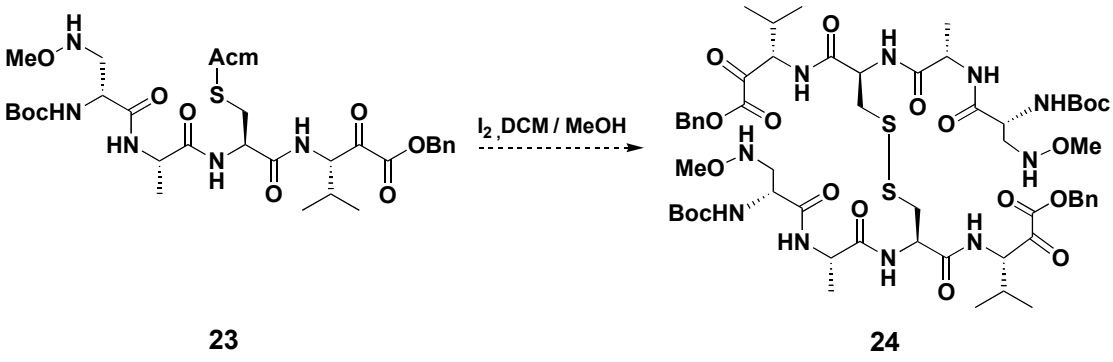

Figure 5.17. Proposed Condition to Synthesize 24.

Preliminary studies of disulfide bond formation are shown in **Figure 5.18**. Substrate **38** was dissolved in methanol and added drop-wise over 30 minutes to a

solution of dichloromethane/methanol (9:1 ratio) and iodine. The reaction was carried out at room temperature for 14 hours to furnish **39**. From our results, it appears the concentration of the reaction is the key factor in the success of the disulfide bridge formation. Improved yield may be achieved by optimizing the reaction concentration and the reaction times. Further, the rate of reaction is solvent dependent,[30] thus finding an optimal solvent system may be an alternative way to increase the overall yield of the reaction.

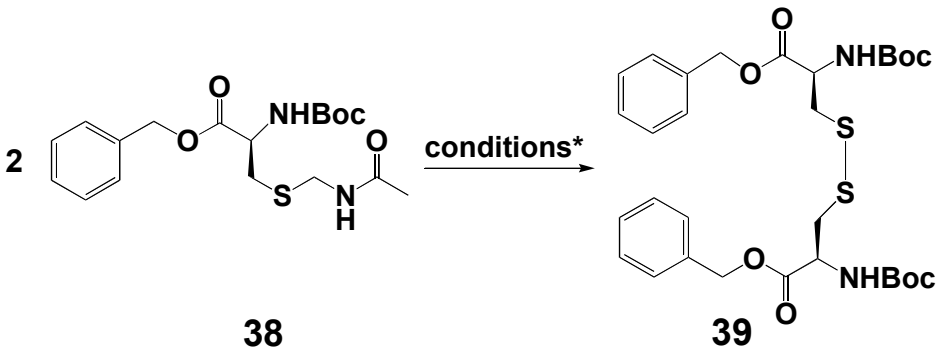

Conditions: a.) I_2(3.0 eq), DCM:MeOH=9:1, 0.0007M, 14h, 20%
b.) I_2(3.0 eq), DCM:MeOH=9:1, 0.1M, 14h, 60%

Figure 5.18. Conditions for Disulfide Bond Formation.

5.10 Proposed Synthesis of 25

Once the key intermediate **24** is obtained, a benzyl deprotection reaction (**Figure 5.19**) will be performed to furnish **25**. This is a challenging step given that sulfur is notorious for deactivating palladium catalyst in the hydrogenation process.[31]

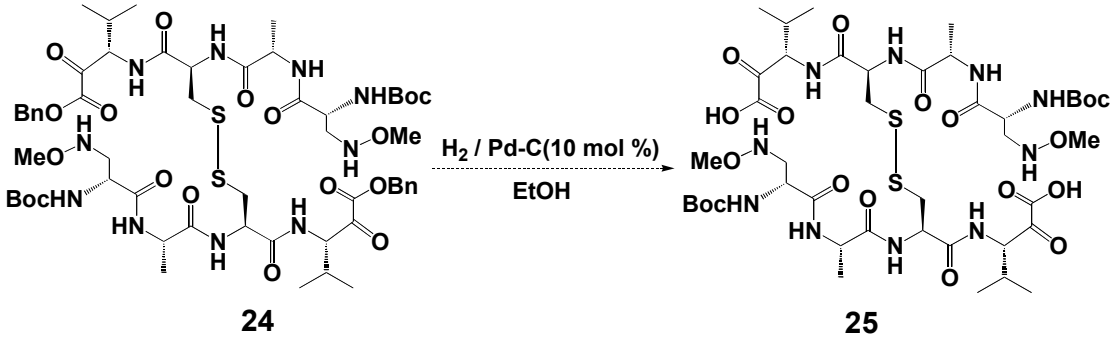

24 25

Figure 5.19. Synthesis of 25

The model reactions were performed and the conditions are shown in **Figure 5. 20**. In conditions (**a)** and (**b)**, three and six equivalents of 10 mol% Pd-C catalyst were applied respectively. Neither one of these conditions converted the starting material **40** to the desired product **41**. In condition (**c**), 33 equivalents of 10 mol % Pd-C catalyst was applied. These data indicate that even with the large excess of palladium, the benzyl protected starting material **40** still cannot be fully converted to the desired product **41**. An alternative strategy to remove the benzyl-protecting group from a sulfur containing substrate is described in the next section.

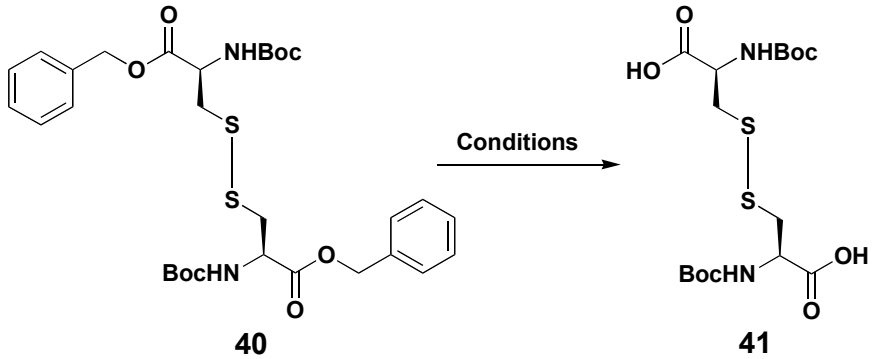

40 41

Conditions: a.) H_2, Pd-C (10 mol %) (3eq) in Ethanol (0.1M), 14h, rt,
b.) H_2, Pd-C (10 mol %) (6eq) in Ethanol (0.1M), 14h, rt
c.) H_2, Pd-C (10 mol %) (33eq) in Ethanol (0.1M), 14h, rt.

Figure 5.20. Hydrogenation for Disulfide Bridged Compound 41.

Kobayashi's group has developed the **P**olymer-**I**ncarcerated (PI) method to immobilize palladium catalysts onto polymers.[32] This polymer-incarcerated palladium (PI Pd) possesses excellent activity in hydrogenation of various olefins, benzyl ethers, and nitro and aromatic compounds. Most importantly, PI Pd is highly resistant to poisoning by sulfur and can be recovered completely by simple filtration. Kobayashi's methodology provides a promising insight to remove the benzyl-protecting group of the sulfur containing substrate, and this approach should potentially be incorporated into our synthetic strategy.

5.11 Proposed Synthesis of 2b

Once the key intermediate **25** was obtained, the KAHA ligation will be performed to form the core bicyclic product (**Figure 5.21**). Furthermore, Boc protecting groups of this bicyclic product are expecting to be removed under KAHA ligation conditions. Finally the core bicyclic product will be subjected to a general peptide coupling with quinoxaline-2-carboxylic acid (Qxc) to furnish the final product **2b**.

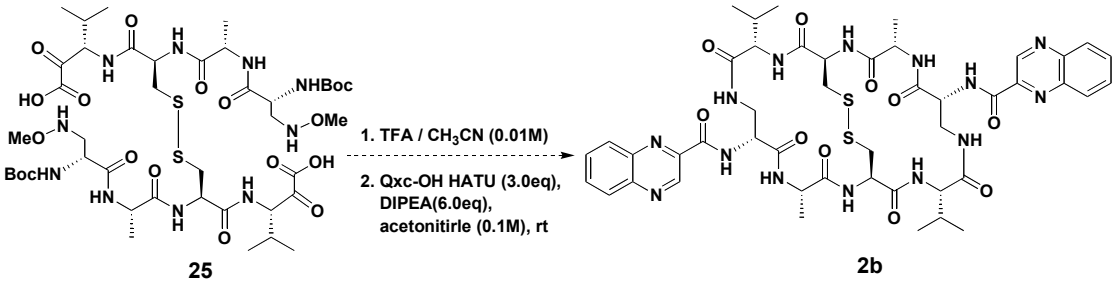

Figure 5.21. Proposed Synthesis of 2b

5.12 Summary

In summary, α-ketoester **21** was synthesized by me and TIPS protected tripeptide **22** was synthesized by my colleague Rodrigo Rodriguez. The conditions for the disulfide bond formation from **23** to give **24** and the conversion of **22** to **23** have also been briefly investigated by my colleague Chung-Mao Pan. These conditions will be utilized in the synthesis of Azatandem **2b**, and the successful completion of Azatandem will be report in due course.

5.13 REFERENCES AND NOTES

1. Kuroya, M.; Ishida, N.; Katagiri, K.; Shoji, J.; Yoshida, T.; Mayama, M.; Sato, K.; Matsuura, S.; Niinome Y.; Shiratori, O. "Studies on Quinoxaline Antibiotics", *J. Antibiot.* **1961**, Ser. A *14:* 324-329.

2. Shoji, J.; Katagiri, K. "Studies on Quinioxaline Antibiotics. III. New Antibiotics, Triostin A, B and C", *J. Antibiot.* **1961**, Ser. A *14*: 335-339.

3. Otsuka, H.; Shoji, J. "Degradative Study on Quinoxaline Antibiotics", *J. Antibiot.* **1963**, Ser. A *16*: 52-54.

4. Otsuka, H.; Shoji, J. "The Structure of Triostin C", *Terahedron.* **1965**, *21*, 2931-2938.

5. Shoji, J.; Tori, K.; Otsuka, H. "Configuration of *N*, β-Dimethylleucine, a Constituent Amino Acid of Triostin C", *J. Org. Chem.* **1965**, *30*, 2772-2776.

6. Matsuura, S. "Studies on Quinoxaline Antibiotics. IV. Selective Antibumor Activity of Each Quinoxaline Antibiotic", *J. Antibiot.* **1965**, Ser. A *18*: 43-46.

7. Ward, D. C.; Reich, E.; Goldberg, I. H. "Base Specificity in the Interaction of Polynucleotides with Antibiotic Drugs", *Science.* **1965**, *149*, 1259-1263.

8. Sato, K.; Shiratori, O.; Katagiri, K. "The Mode of Action of Quinoxaline Antibiotics. Interaction of Quinomycin A with Deoxyribonucleic Acid", *J. Antibiot.* **1967**, *20*, 270-276.

9. Wang, A. H.; Ughetto, G.; Quigley, G. J.; Hakoshima, T.; van der Marel, G. A.; van Boom, J. H.; Rich, A. "The Molecular Structure of a DNA-Triostin A Complex", *Science.* **1984**, *225*, 1115-1121.

10. Takusagawa, F. "The Role of the Cyclic Depsipeptide Rings in Antibiotics", *J. Antibiot.* **1985**, 38, 1596-1604.

11. Addess, K. J.; Feigon, J. "Sequence Specificity of Quinoxaline Antibiotics: 1. Solution Structure of a 1:1 Complex Between Triostin A and $[d(GACGTC)]_2$ and Comparison with the Solution Structure of the [*N*-$MeCys^3$,*N*-$MeCys^7$]TANDEM-$[d(GATATC)]_2$ Complex", *Biochemistry.* **1994**, *33*, 12386-12396.

12. Lee, J.S.; Waring, M. J. "Interaction Between Synthetic Analogues of Quinoxaline Antibiotics and Nucleic acids. Changes in Mechanism and Specificity Related to Structural Alterations", *Biochem. J.* **1978**, *173*, 129-144.

13. Low, C.M.; Fox., K. R.; Olsen, R.K.; Waring, M. J. "DNA Sequence Recognition by Under-Methylated Analogues of Triostin A", *Nucleic Acids Res.* **1986**, *14*, 2015-2033.

14. Waterloh, K.; Olsen, R. K.; Fox, K.R. "Bifunctional intercalator [*N*-MeCys^3,*N*-MeCys^7]TANDEM Binds to the Dinucleotide TpA", *Biochemistry.* **1992**, *31*, 6246-6253.

15. Addess, K. J.; Gilbert., D. E.; Olsen, R. K.; Feigon, J. "Proton NMR Studies of [*N*-MeCys^3, *N*-MeCys^7]TANDEM Binding to DNA Oligonucleotides: Sequence Specific Binding at the TpA Site", *Biochemsitry.* **1992**, *31*, 339-350.

16. Addess, K. J.; Sinsheimer, J. S.; Feigon, J. "Solution Structure of a Complex Between [*N*-MeCys^3, *N*-MeCys^7]TANDEM and [d(GATATC)]$_2$", *Biochemistry.* **1993**, *32*, 2498-2508.

17. Kim, Y.B.; Kim, Y. H.; Park, J. Y.; Kim, S. K. "Synthesis and Biological Activity of New Quinoxaline Antibiotics of Echinomycin Analogues", *Bioorg. Med. Chem. Lett.* **2004**, *14*, 541-544.

18. Boger, D. L.; Lee, J. K. "Development of a Solution-Phase Synthesis of Minor Groove Binding bis-Intercalators based on Triostin A Suitable for Combinatorial Synthesis", *J. Org. Chem.* **2000**, *65*, 5996-6000.

19. Dietrich, B.; Diederichsen, U. "Synthesis of Cyclopeptidic Analogues of Triostin A with Quinoxalines or Nucleobases as Chromophores", *Eur. J. Org. Chem.* **2005**, *1*, 147-153.

20. Ciardelli, T. L.; Olsen, R. K. "Synthesis of Des-*N*-tetramethyltriostin A, a Bicyclic Octadepsipeptide Related to the Quinoxaline Antibiotics", *J. Am. Chem. Soc.* **1977**, *99*, 2806-2807.

21. Chakravarty, P. K.; Olsen, R. K. "Synthesis of Triostin A", *Tetrahedron Lett.* **1978**, *19*, 1613-1616.

22. Shin, M.; Inouye, K.; Otsuka, H. "Synthetic Studies on Quinoxaline Antibiotics. II. Synthesis of Triostin A", *Bull. Chem. Soc. Jpn.* **1984**, *57*, 2203-2210.

23. Higuchi, N.; Kyogoku, Y.; Shin, M.; Inouye, K. "Origin of Slow Conformer Conversion of Triostin A and Interaction Ability with Nucleic Acid Bases", *Int. J. Pept. Protein. Res.* **1983**, *21*, 541-545.

24. Shin, M.; Inouye, K.; Higuchi, N.; Kyogoku, Y. "Synthetic Studies on Quinoxaline Antibiotics. III. Synthesis of Nortriostin A, a Triostin A Analog

Lacking *N*-Methyl Groups on the Cystine and Valine Residues", *Bull. Chem. Soc. Jpn.* **1984**, *57*, 2211-2215.

25. Malkinson, J. P.; Anim, M. K.; Zloh, M.; Searcey, M.; Hampshire, A. J.; Fox, K.R. "Efficient Solid-Phase-based Totoal Synthesis of the Bisintercalator TANDEM", *J. Org. Chem.* **2005**, *70*, 7654-7661.

26. Lorenz, K. B.; Diederichsen, U. "Solution-Phase Synthesis of Nucleobase-Substituted Analogues of Triostin A", *J. Org. Chem.* **2004**, *69*, 3917-3927.

27. Han, Y.; Albericio, F.; Barany, G. "Occurrence and Minimization of Cysteine Racemization During Stepwise Solid-Phase Peptide Synthesis", *J. Org. Chem.* **1997**, *62*, 4307-4312.

28. Bode, J.W.; Fox, R. M.; Baucom, K.D. "Chemoselective Amide Ligations by Decarboxylative Condensations of *N*-alkylhydroxylamines and α-Ketoacids", *Angew. Chem. Int. Ed.* **2006**, *45*, 1248-1252.

29. Wasserman, H. H.; Ho, W. -B. "(Cyanomethylene)phosphoranes as Novel Carbonyl 1,1-Dipole Synthesis: an Efficient Synthesis of α-keto Acids, Esters, and Amides", *J. Org. Chem.* **1994**, *59*, 4364-4366.

30. Kamber, B.; Hartmann, A.; Eisler, K.; Riniker, B.; Rink, H.; Sieber, P.; Rittel, W. "The Synthesis of Cystine Peptides by Iodine Oxidation of *S*-Trityl-cysteine and *S*-Acetamidomethyl-Cysteine Peptides", *Helv. Chim. Acta.* **1980**, *63*, 899-915.

31. Nasri, N. S.; Jones, J. M.; Dupont, V.A.; Williams, A. "A Comparative Study of Sulfur Poisoning and Regeneration of Precious-Metal Catalysts", *Energy and Fuels.* **1998**, *12*, 1130-1134.

32. Okamoto, K.; Aklyama, R.; Kobayashi, S. "Recoverable, Reusable, Highly Active, and Sulfur-Tolerant Polymer Incarcerated Palladium for Hydrogenation", *J. Org. Chem.* **2004**, *69*, 2871-2873.

Conclusions and Future Directions

In the Sansalvamide A project, I have synthesized seven compounds (**Figure 2.3**), which were included to the existing library of San A analogues that were synthesized by our laboratory. These compounds not only have diversity in conformational space (L-versus D-amino acids) but also vary in their polarity (hydrophobic versus hydrophilic groups). Using ^{3}H-labeled thymidine incorporation assays, my colleague Robert V. Vasko and I have found 6 potent compounds, including **18**, **34**, **52**, **54**, **60**, **64,** all of which possess growth inhibitory activity above 50% against PL45 and BxPC-3 pancreatic cancer cell lines. IC_{50} studies of theses potent compounds conducted by Robert V. Vasko and I showed low micromolar potency against PL45 and BxPC-3. Compound **18**, **54**, **60** and **64** are about 20 fold more active than the parent San A peptide **1**. Compound **52** exhibit approximately 14 fold greater cytotoxicity against pancreatic cancer than the San A peptide **1**. Finally, compound **34** has low micromolar activity against PL45 and is approximately 10 fold more active than the San A peptide **1**. In addition, Gemzar® (Gemcitabine), a current drug on the market that is used to treat pancreatic cancer, was used as a control of IC_{50} studies. The result indicated that San A analogues **18**, **34**, **52**, **54**, **60**, **64** are less effective than this drug. However, they show promising potential as they all possess low micromolar potency against PL45 and BxPC-3. Since San A analogues show no structure homology to Gemzar®, it is most likely inhibiting cell growth through a different biological pathway. The preliminary data from McAlpine laboratory shows that San A analogues disrupt Hsp90-IP6K2 binding, which leads to apoptosis. Further studies

such as computational docking studies will be conducted in order to elucidate the mode of action of San A analogues.

In the Holliday junction project, I utilized a solution-phase and a solid-phase approach of synthesizing a macrocycle, and have successfully synthesized one second-generation compound **HJ compd 10** via a solid-phase approach. Contrary to original predictions, biological assays conducted by the colleagues Fiona A. Curtis and Gary A. Sharples indicated that incorporation of polar residues such as lysine within HJ trapping macrocycles do not play a critical role in HJ binding, except improve the solubility of the compounds. Further, these bioassays concluded that (i) compounds containing tyrosine were highly effective at trapping HJs, and (ii) both hexapeptides and octapeptides were able to trap HJ's. These findings indicate that the binding of HJs may not relying on the size of the macrocycles but rather the π-stacking between the aromatic residues and the nucleotides. Further work such as synthesizing a third generation of macrocycles, incorporating tyrosines, hydroxy tetrahydroquinolines, and hydroxy tryptophans are needed to determine the precise structural and conformation requirements for trapping HJs.

In the Azatandem project, I have synthesized α-ketoester **21**, and my colleague Rodrigo Rodriguez has synthesized TIPS protected tripeptide **22.** The conditions for the disulfide bond formation from **23** to give **24** and the conversion of **22** to **23** have also been briefly investigated by my colleague Chung-Mao Pan. These conditions will be utilized in the synthesis of Azatandem **2b**. Further investigation including deprotection

condition of benzyl protecting group with the appearance of sulfur element as well as cyclization of the disulfide linked octapeptide precursor via KAHA ligation reaction are needed and the results will be report in due course.

Chapter 6

Experimental methods and supporting spectra

6.1. General remarks

All coupling reactions were performed under argon atmosphere with the exclusion of moisture. All reagents were used as received. anhydrous methylene chloride Dri Solv (EM), anhydrous tetrahydrofuran, Andydrous dimethylformamide, and anhydrous acetonitrile Dri Solv (EM) were obtained from VWR, and were packed under nitrogen with a septum cap. Diisopropylethylamine (DIPEA) was purchased from Aldrich, packaged under nitrogen in a sure seal bottle. The coupling agent HATU came from: Applied Biosystems at 850 Lincoln Center Dr. Foster City, CA 94404, USA. Tel.: +1-800-327-3002 and the coupling agents TBTU NovaBiochem. DEPBT [3(diethoxyphosphoryloxy)-1,2,3-benzotriazine-4(3H)] was purchased from Aldrich (order number 49596-4). The ^{1}H NMR spectra were recorded on the Varian at 200MHz or 400MHz or 500 MHz. LCMS was performed at San Diego State University using HP1100 Finnigan LCQ. Flash column chromatography used 230–400 mesh 32–74 lm 60Å silica gel from Bodman Industries.

6.2. Peptide synthesis

General peptide synthesis

All peptide coupling reactions were carried out under argon with dry solvent, using methylene chloride, acetonitrile, or DMF depending on the solubility of the reactants. The amine (1.1 equivalents) and acid (1 equivalent) were weighed into a dry flask along with DIPEA (between 4.0 equivalents to 6.0 equivalents for Sansalvamide A derivatives, 3.0 equivalents to 6.0 equivalents for HJ compounds), and TBTU* (1.1 equivalents for Sansalvamide A derivatives and 1.2 equivalents for HJ compounds). Anhydrous solvent was added to generate a 0.1M solution. The solution was stirred at room temperature and reactions were monitored via TLC. Reactions were run for 45 minutes before checking via TLC. If reaction was not complete additional 0.25 equivalents of coupling agents were added. If reaction was complete then work-up was done by diluting the crude material with excess ethyl acetate followed by washing with 0.1M $HCl_{(aq)}$ to remove excess free amine, then washing with saturated sodium bicarbonate three times to remove coupling agent by product and excess coupling agent(s). Organic layers were combined, dried over sodium sulfate, filtered and concentrated. Flash chromatography using a gradient of ethyl actetate-hexane gave our desired peptide.

*Some coupling reactions would not go to completion using only TBTU and therefore ~0.25 equivalents of HATU, and/or DEPBT were used. In a few cases up to 1.1 equivalents of all three coupling reagents were used.

General solid-phase peptide synthesis

Peptide couplings were carried out for 15 min in DMF using a 2.5-fold excess (over resin loading) of protected amino acid, activated with TBTU (3.1 equivalents with the appearance of primary amine substrate) or HATU (3.1 equivalents with the appearance of secondary amine substrate), in the presence of a DIPEA (between 3.5 equivalents to 4.0 equivalents). Each coupling was repeated and completion monitored using the Kaiser test for free amines. Unsuccessful couplings were further repeated until a negative Kaiser test was obtained. Fmoc protecting group was removed using 20% (v/v) piperidine in DMF for 30 minutes, two times. Upon each procedure, the resin-bond materials were washed with copious DMF, CH_2Cl_2 and MeOH three times.

General solid-phase peptide cleavage

The resin-bound peptide was washed thoroughly with DMF, CH_2Cl_2, and then 50% (v/v) MeOH in CH_2Cl_2 three times. The peptide was removed from the solid support by using 1% TFA in CH_2Cl_2 for 2 hours at room temperature. The TFA was removed under reduced pressure. The crude product was purified by reverse-phase HPLC, and characterized via LCMS.

General amine deprotection

Amines were deprotected using 20% TFA in methylene chloride (0.1M) with two equivalents of anisole. The reactions were monitored by TLC, where the TLC sample was first worked up in a mini-workup using DI water and methylene chloride to remove TFA. Reactions were allowed to run for 1-2 hours and then concentrated *in vacuo*.

General acid deprotection

Acids were deprotected using lithium hydroxide (between 8.0 equivalents to 10.0 equivalents) for Sansalvamide A derivatives, sodium hydroxide (between 6.0 equivalents to 8.0 equivalents) for HJ compounds in methanol (0.1 M). The peptide was placed in a flask, along with lithium hydroxide and methanol and stirred overnight. Within 12 hours the acid was usually deprotected. Work-up of reactions involved the acidification of reaction solution using $HCl_{(aq)}$ to pH = 1. The aqueous solution was extracted three times with methylene chloride, and the combined organic layer was dried, filtered and concentrated *in vacuo*.

In-situ double deprotection of linear pentapeptide

Pentapeptides were acid and amine deprotected using concentrated HCl (8 drops per 0.3mmols of linear pentapeptide) in THF (0.05M). Anisole (2 equiv) was added to the reaction and the reaction was stirred at room temperature. The reaction typically took

4 days, but TLC and LCMS were used to monitor the reaction every 12 hours. LCMS data typically indicated the reaction was ~50% complete after the first day. Addition of four drops of concentrated HCl per 0.3 mmol of pentapeptide, stirring at room temperature overnight and checking the reaction via LCMS usually showed ~75% completion. On the fourth day verification of the presence of the free amine and free acid and disappearance of the starting linear protected pentapeptide permitted workup. The reaction was concentrated in vacuo to yield double deprotected linear peptide.

Stepwise double deprotection of linear pentapeptide

Protected linear pentapeptides were first acid deprotected by adding 10 equivalents of lithium dydroxide to 1.0 equivalent of protected linear pentapeptide in methanol (0.1M). These reactions were allowed to run for 3-4 hours and monitored via TLC. Once the TLC indicated the acid had been deprotected, the reactions were worked up with 10% $HCl_{(aq)}$. The aqueous layer was washed three to four times with fresh methylene chloride. The organic layers were then combined, dried over sodium sulfate, filtered, and concentrated via rotary evaporator to yield acid deprotected linear pentapeptide. The Boc protecting group of the acid deprotected linear pentapeptide was then removed with 20% TFA in methylene chloride (0.1M) and anisole (2.0 equivalents) to produce the double deprotected linear pentapeptides.

Macrocyclization procedure A (Sansalvamide A derivatives)

The crude, dry, double deprotected peptides (free acid and free amine) were combined in a flask with three coupling agents: TBTU and HATU (0.7 equivalents each), DEPBT (0.2 equivalents) along with DIPEA (0.6 euqivalents) in anhydrous methylene chloride: acetonitrile (1:1 ratio, 0.007M). After 1 hour, TLC and LCMS (where the LCMS sample was worked up prior to injection) indicated that a product spot was developing. The comparison Rf value in the product spot on TLC was the protected linear pentapeptide. The reactions were always complete after 2 hours, and monitoring the starting material deprotected pentapeptide via LCMS was the easiest method of determining completion. Upon completion, the reaction was worked up by washing with saturated ammonium chloride. After back extraction of aqueous layers with large quantities of methylene chloride, the organic layers were combined, dried, filtered and concentrated. All macrocycles were purified by flash column chromatography with an ethyl acetate/hexane gradient on silica gel. Finally, when necessary reverse phase HPLC was used for additional purification using a gradient of acetonitrile and DI water with 0.1% TFA.

Macrocyclization procedure B (HJ solution-phase)

All hexa- and octa-peptides were deprotected using 20% TFA in dichloromethane (0.1M) and the presence of the free amine was verified using LCMS. The reaction was then neutralized with sodium hydroxide. Upon neutralization, NaOH was added (4

equivalents) to bring the pH up to 11. The acid deprotection was verified via LCMS. Upon acid deprotection the reaction was concentrated in vacuo and the crude, dry, double deprotected peptide (free acid and free amine) was dissolved in a minimum of dry acetonitrile. Three coupling agents were initially used: DEPBT (0.8 equivalents), HATU (1.0 equivalent), and TBTU (0.6 equivalents). These coupling agents were dissolved in a calculated volume of dry 50% acetonitrile and 50% methylene chloride that would give a 0.01 M solution when including the volume used for the deprotected peptide. The coupling agents were then added to the deprotected peptide solution. Five to six equivalents of DIPEA were then added to the reaction to ensure the pH was kept at or greater than 8. If the solution was not clear, DMF or methylene chloride was added but not more than 20% of the volume used for the overall reaction. Note: in some cases methylene chloride addition improved the solution clarity more than DMF, this depended on the number of methyl groups on the compound (i.e., the hydrophobicity). With at least one methyl group it was found that methylene chloride was a better solvent than DMF for clarity; with no methyl groups, DMF was the better solvent. After 24 h, TLC and LCMS (where the LCMS sample was worked up prior to injection) were taken, if no clear distinct product spot was visible, then typically PyAOP was added (0.5 equiv), and sometimes, depending on reaction clarity, 0.5 equiv of HATU were also added. The comparison for Rf value in the product spot on TLC was the protected linear hexa- or octapeptide. The reaction was allowed to run another 24 h, and checked again by TLC and LCMS. If the reaction still failed to show a clear product spot, then 0.25 equiv of DEPBT were added and the reaction continued for 24–48 h. At this point we found the reaction always demonstrated a product spot, although it was sometimes difficult to

determine if it was complete (monitoring the starting material deprotected hexa- or octapeptide via LCMS was the easiest method). Upon completion, the reaction was worked up by washing with ammonium chloride. After back extraction of aqueous layers with methylene chloride, organic layers were combined, dried over sodium sulfate, filtered, and concentrated. All macrocycles were purified using reverse phase HPLC, and a gradient of acetonitrile and DI water with 0.1% TFA.

Macrocyclization procedure C (HJ solid-phase)

The crude, dry, double deprotected peptides (free acid and free amine) were combined in a flask with three coupling agents: TBTU and HATU (0.8 equivalents each), DEPBT (1.0 equivalent) along with DIPEA (3.0 euqivalents) in anhydrous acetonitrile (0.01M). The reactions were normally complete after 4 hours, and monitoring the starting material deprotected linear peptide via LCMS was the easiest method of determining completion. Upon completion, the reaction was worked up by washing with saturated ammonium chloride. After back extraction of aqueous layers with large quantities of methylene chloride, the organic layers were combined, dried, filtered and concentrated. All macrocycles were purified by flash column chromatography with an ethyl acetate/hexane gradient on silica gel. Finally, when necessary reverse phase HPLC was used for additional purification using a gradient of acetonitrile and DI water with 0.1% TFA.

Cbz Deprotection procedure

The benzyl-protected compounds were dissolved in ethanol (0.1M), and the Pd-C (10%) was added to the reaction, and then H_2 gas was bubbled into the reaction at room temperature for 8 hours. The reactions were monitored by TLC every 2 hours. Upon completion, reaction was filtered through celite to remove the Pd-C. The semi-pure crude materials were then purified by reverse phase HPLC. The desired products were characterized by LCMS.

6.3. Biological Assays

Thymidine incorporation assay

Cytotoxicity of Sansalvamide A molecules in pancreatic cancers BxPc-3 and PL45 was measured using a thymidine incorporation assay. A 75mm^2 tissue culture plate of either BxPc-3 or PL45 was grown for 72hr to a sub confluent monolayer. Cells were washed with 1x PBS and detached with 0.25% Trypsin-EDTA. Cells were re-suspended in fresh medium, counted, and seeded at 2500cells/well onto a 96 well plate. The plate was incubated for 6 hours at 37^{o}C to allow full cell attachment. Drug was added at appropriate concentration with DMSO as vehicle to create a final 1% DMSO concentration. DMSO without drug was also added to wells at a 1% final concentration to serve as 100% growth determination. After 56 additional hours of incubation at 37^{o}C 1μCi of tritium labeled thymidine was added to each well. After 16 more hours of incubation at 37^{o}C the cells were harvested and captured on glass fiber filter paper using

a Brandel 290 PHD multiwell cell harvester. The glass fiber filter paper was then transferred to 6.5ml scintillation vials to which 2ml of ScinitVerse™ was added. Each scintillation vial's tritium content was then quantified using a Beckman LS 5000 TD. Quantification was recorded as counts per minute (CPM). CPM counts were then converted to percent growth inhibition values by dividing the CPM values for the wells to which drug was added, by the average of all the CPM values for the wells to which 1% DMSO was added and then subtracting that value from one. Each drug was plated in 3 separate 4 well experiments and compared to 3 separate 4 well experiments of 1% DMSO. Error is recorded as ± SEM which falls within 5% of the growth inhibition value.

6.4. Synthesis of Sansalvamide A derivatives

Compounds 12, 14

Dipeptide1a-2m

Dipeptide **1a-2m** was synthesized following the General Peptide Synthesis procedure, utilizing 430 mg (2.03 mmol, 1.2 equiv) of amine **1a**, 500 mg (1.65 mmol, 1.0 equiv) of acid **2m**, 0.86 mL (3 equiv) of DIPEA, and 790 mg (2.47 mmol, 1.5 equiv) of TBTU. The crude reaction was purified by column chromatography (silica gel, EtOAc/Hex) to yield the dipeptide (740 mg, 98% yield): R_f 0.6 (EtOAc/Hex 1:1); ^{1}H NMR (200 MHz, $CDCl_3$) δ 1.4 (s, 9H), 3.0-3.2 (m, 2H), 3.4-3.8 (m, 2H), 3.6 (s, 3H), 4.2 (br, 1H), 4.4 (dd, *J*= 14Hz, 11Hz, 8Hz, 2H), 4.8 (q, *J*= 10Hz, αH), 5.3 (br, 1H), 6.9 (br, 1H), 7.0-7.4 (m, 10H).

Dipeptide 1a-2m-NH_2

Dipeptide **1a-2m-NH_2** was synthesized following the General Amine Deprotection procedure. This dipeptide was taken on to the next reaction without further purification or characterization (578 mg, assume quantitative yield).

Tripeptide 1a-2m-3a

Tripeptide **1a-2m-3a** was synthesized following the General Peptide Synthesis procedure, utilizing 1000 mg (2.8 mmol, 1.3 equiv) of amine **1a-2m**, 460 mg (2.1 mmol, 1.0

equiv) of acid **3a**, 1.47 mL (4 equiv) of DIPEA, 670 mg (2.1 mmol, 1.0 equiv) of TBTU, and 399 mg (1.05 mmol, 0.5 equiv) of HATU. The crude reaction was purified by column chromatography (silica gel, EtOAc/Hex) to yield the tripeptide (870 mg, 75% yield): R_f 0.5 (EtOAc/Hex 1:1); ^{1}H NMR (200 MHz, $CDCl_3$) δ 0.8-1.0 (dd, *J*= 11Hz, 7Hz, 6H), 1.4 (s, 9H), 2.0-2.2 (m, 1H), 3.0-3.2 (m, 2H), 3.4-4.0 (m, 2H), 3.6 (s, 3H), 3.8-4.0 (m, αH), 4.5 (dd, *J*= 12Hz, 8Hz, 2H), 4.6 (m, αH), 4.8 (q, *J*= 8Hz, αH), 5.0 (br, 1H), 6.7 (br, 1H), 6.9 (br, 1H), 7.0-7.4 (m, 10H).

Tripeptide 1a-2m-3a-NH_2

Tripeptide **1a-2m-3a-NH_2** was synthesized following the General Amine Deprotection procedure. This dipeptide was taken on to the next reaction without further purification or characterization (713 mg, assume quantitative yield).

Dipeptide 4c-5e

Dipeptide **4c-5e** was synthesized following the General Peptide Synthesis procedure, utilizing 920 mg (5.5 mmol, 1.2 equiv) of amine **4c**, 1000 mg (4.6 mmol, 1.0 equiv) of acid **5e**, 2.4 mL (3 equiv) of DIPEA, and 2210 mg (6.9 mmol, 1.5 equiv) of TBTU. The crude reaction was purified by column chromatography (silica gel, EtOAc/Hex) to yield the dipeptide (1440 mg, 94% yield): R_f 0.5 (EtOAc/Hex 35:65); ^{1}H NMR (200 MHz, $CDCl_3$) δ 0.9-1.0 (dd, *J*= 12Hz, 7Hz, 12H), 1.4 (s, 9H), 2.0-2.2 (m, 2H), 3.7 (s, 3H), 3.8-4.0 (dd, *J*= 11Hz, 7Hz, αH), 4.5 (dd, *J*= 10Hz, 7Hz, αH), 5.0 (br, 1H), 6.4 (br, 1H)

Dipeptide HO-4c-5e

Dipeptide **HO-4c-5e** was synthesized following the General Acid Deprotection procedure. This dipeptide was taken on to the next reaction without further purification or characterization (1340 mg, 93% yield).

Pentapeptide 1a-2m-3a-4c-5e

Pentapeptide **1a-2m-3a-4c-5e** was synthesized following the General Peptide Synthesis procedure, utilizing 400 mg (0.87 mmol, 1.1 equiv) of amine **1a-2m-3a**, 250 mg (0.79 mmol, 1.0 equiv) of acid **4c-5e**, 0.69 mL (5 equiv) of DIPEA, 152 mg (0.47 mmol, 0.6 equiv) of TBTU, and 300 mg (0.79 mmol, 1.0 equiv) of HATU. The crude reaction was purified by column chromatography (silica gel, EtOAc/Hex) to yield the pentapeptide (310 mg, 52% yield): R_f 0.4 (EtOAc/Hex 1:1); ^{1}H NMR (500 MHz, DMSO-d_6) δ 0.8 (dd, J= 10Hz, 6Hz, 18H), 1.4 (s, 9H), 1.8-2.0 (m, 2H), 2.8-3.0 (m, 2H), 3.4 (d, J= 5Hz, 2H), 3.6 (s, 3H), 3.8 (t, J= 6Hz, αH), 4.2 (dd, J= 12Hz, 6Hz, αH), 4.3 (m, αH), 4.4 (s, 2H), 4.5 (m, αH), 4.6 (m, αH), 6.8 (d, J= 6Hz, 1H), 7.1-7.3 (m, 10H), 7.6 (d, J= 6Hz, 1H), 7.8 (d, J= 6Hz, 1H), 8.0 (d, J= 6Hz, 1H), 8.4 (d, J=6Hz, 1H).

Pentapeptide HO-1a-2m-3a-4c-5e-NH_2

Pentapeptide **HO-1a-2m-3a-4c-5e-NH_2** was synthesized following the *In-situ* double deprotection of linear pentapeptide procedure. The crude product was confirmed by LCMS and was taken on to the macrocyclization without further purification. LCMS: m/z calcd for $C_{34}H_{49}N_5O_7$ (M+1) =641.37, found 641.2

Macrocycle 1a-2m-3a-4c-5e (Compound 14)

Macrocycle **1a-2m-3a-4c-5e** was synthesized following the Macrocyclization procedure A, utilizing 500 mg (0.78 mmol, 1.0 equiv) of linear pentapeptide, 0.82 mL (6.0 equiv) of DIPEA, 175 mg (0.55 mmol, 0.7 equiv) of TBTU, 207 mg (0.55 mmol, 0.7 equiv) of HATU, and 47 mg (0.16 mmol, 0.2 equiv) of DEPBT. The crude reaction was purified by reverse phase HPLC to yield the macrocycle (53 mg, 11% yield): R_f 0.5 (EtOAc/Hex 3:1); LCMS *m*/*z* calcd for $C_{34}H_{47}N_5O_6$ (M + 1) 622.77, found 621.9.

Deprotected macrocycle 1a-2m-3a-4c-5e (Compound 12)

Deprotected Macrocycle **1a-2m-3a-4c-5e** was synthesized following the Cbz Deprotection procedure. Utilizing 75mg (0.012 mmols, 1.0 equivalents) of protected macrocycle, 10% Palladium-Carbon (cat. Amount). The crude reaction was purified by reverse phase-HPLC to yield the deprotected macrocycle. (0.3mg, 3.7 % yield.) LCMS: m/z calcd for $C_{27}H_{41}N_5O_6$ (M+1) = 532.5, found 533.0

Compound 18

Dipeptide 1a-2a

Dipeptide **1a-2a** was synthesized following the General Peptide Synthesis procedure, utilizing 475.8 mg (2.206 mmol, 1.1 equiv) of amine **1a**, 500 mg (500 mmol, 1.0 equiv) of acid **2a**, 1400 μL (4 equiv) of DIPEA, and 708.3 mg (2.206 mmol, 1.1 equiv) of TBTU. The crude reaction was purified by column chromatography (silica gel, EtOAc/Hex) to yield the dipeptide (716.5 mg, 91% yield): R_f 0.7 (EtOAc/Hex 1:1); ^{1}H NMR (200 MHz, $CDCl_3$) δ 0.9-1.0 (dd, J= 10Hz, 5Hz, 6H), 1.5 (s, 9H), 1.5-1.7 (m, 3H), 3.0-3.2 (m, 2H), 3.7 (s, 3H), 4.0- 4.2 (m, αH), 4.5-4.7 (br, αH), 4.8-4.9 (br, 1H), 6.4-6.5 (br, 1H) 7.1-7.4 (m, 5H).

Dipeptide 1a-2a-NH_2

Dipeptide **1a-2a-NH_2** was synthesized following the General Amine Deprotection procedure. This dipeptide was taken on to the next reaction without further purification or characterization (534 mg, 100% yield).

Tripeptide 1a-2a-3b

Tripeptide **1a-2a-3b** was synthesized following the General Peptide Synthesis procedure, utilizing 631 mg (2.199 mmol, 1.1 equiv) of amine **1a-2a-NH_2**, 427 mg (1.899 mmol, 1.0 equiv) of acid **3b**, 1400 μL (4 equiv) of DIPEA, and 756 mg (2.399 mmol, 1.2 equiv) of TBTU. The crude reaction was purified by column chromatography (silica gel,

EtOAc/Hex) to yield the tripeptide (800 mg, 86% yield): R_f 0.5 (EtOAc/Hex 1:1); ^{1}H NMR (200 MHz, $CDCl_3$) δ 0.9-1.0 (m, 12H), 1.57 (s, 9H), 1.6- 1.7 (m, 3H), 2.1-2.3 (m, 1H), 3.1-3.4 (m, 2H), 3.8 (s, 3H), 3.9-4.0 (m, αH), 4.5 (m, αH), 4.8-5.0 (q, *J*= 6Hz, αH), 5.0 (br, 1H), 6.6 (br, 1H), 6.8 (br, 1H), 7.2-7.4 (m, 5H).

Tripeptide 1a-2a-3b-NH_2

Tripeptide **1a-2a-3b-NH_2** was synthesized following the General Amine Deprotection procedure. This dipeptide was taken on to the next reaction without further purification or characterization (744 mg, assume quantitative yield).

Dipeptide 4a-5a

Dipeptide **4a-5a** was synthesized following the General Peptide Synthesis procedure, utilizing 401 mg (2.2 mmol, 1.1 equiv) of amine 4a, 500 mg (2.0 mmol, 1.0 equiv) of acid, 1.4 mL (8 equiv) of DIPEA, and 708 mg (2.2 mmol, 1.0 equiv) of TBTU. The crude reaction was purified by column chromatography (silica gel, EtOAc/Hex) to yield the dipeptide (679 mg, 95% yield): R_f 0.5 (EtOAc/Hex 1:1); ^{1}H NMR (200 MHz, $CDCl_3$) δ 0.9-1.0 (m, 12H), 1.4 (s, 9H), 1.6-1.8 (m, 6H), 3.7 (s, 3H), 4.0- 4.1 (br, αH), 4.5-4.7 (m, αH), 4.8-4.9 (br, 1H), 6.4 (br, 1H).

HO-4a-5a

Dipeptide **HO-4a-5a** was synthesized following the General Acid Deprotection procedure. This dipeptide was taken on to the next reaction without further purification or characterization (631 mg, 98% yield).

Pentapeptide 1a-2a-3b-4a-5a

Pentapeptide **1a-2a-3b-4a-5a** was synthesized following the General peptide Synthesis procedure. Utilizing 500 mg (1.09 mmols, 1.1 equivalents) of amine 1a-2a-3b, 310mg (1.0 mmols, 1.0 equivalents) of acid 4a-5a, 0.86 mL (5.0 equivalents) of DIPEA, 190 mg (0.58 mmol, 0.6 equivalents) of TBTU, and 370 mg (1.0 mmol, 1.0 equivalents) HATU. The crude reaction was purified by column chromatography (silica gel, EtOAc/Hex) to yield the pentapeptide (670mg, 45% yield). R_f: 0.5 (EtOAc: Hex 1:1). ^{1}H NMR (500 MHz, DMSO-d_6): δ 0.8-1.0 (m, 24H), 1.4 (s, 9H), 1.5-1.8 (m, 6H), 2.1-2.3 (br, 1H), 3.0-3.2 (m, 2H), 3.7 (s, 3H), 4.2 (br, 2αH), 4.4-4.5 (br, 2αH), 4.8 (q, *J*= 8Hz, αH), 5.0 (br, 1H), 6.7 (br, 1H), 7.1 (br, 2H), 7.1-7.3 (m, 5H).

Pentapeptide HO-1a-2a-3b-4a-5a-NH_2

Pentapeptide **HO-1a-2a-3b-4a-5a-NH_2** was synthesized following the Stepwise double deprotection of linear pentapeptide procedure. The crude product was confirmed by LCMS and was taken on to the macrocyclization without further purification. LCMS: m/z calcd for $C_{32}H_{53}N_5O_6$ (M+1) =604.40, found 604.3.

Macrocycle 1a-2a-3b-4a-5a (Compound 18)

Macrocycle **1a-2a-3b-4a-5a** was synthesized following the Macrocyclization procedure A, utilizing 120 mg (0.20 mmol, 1.0 equiv) of linear pentapeptide, 0.21 mL

(6.0 equiv) of DIPEA, 45 mg (0.14 mmol, 0.7 equiv) of TBTU, 53 mg (0.14 mmol, 0.7 equiv) of HATU, and 12 mg (0.04 mmol, 0.2 equiv) of DEPBT. The crude reaction was purified by reverse phase HPLC to yield the macrocycle (29 mg, 16% yield): R_f 0.5 (EtOAc/Hex 3:1); LCMS *m*/*z* calcd for $C_{32}H_{51}N_5O_6$ (M + 1) 586.38, found 586.5.

Compound 20

Dipeptide 1a-2a

Dipeptide **1a-2a** was synthesized following the General Peptide Synthesis procedure, utilizing 475.8 mg (2.206 mmol, 1.1 equiv) of amine **1a**, 500 mg (500 mmol, 1.0 equiv) of acid **2a**, 1400 μL (4 equiv) of DIPEA, and 708.3 mg (2.206 mmol, 1.1 equiv) of TBTU. The crude reaction was purified by column chromatography (silica gel, EtOAc/Hex) to yield the dipeptide (716.5 mg, 91% yield): R_f 0.7 (EtOAc/Hex 1:1); ^{1}H NMR (200 MHz, $CDCl_3$) δ 0.9-1.0 (dd, *J*= 11Hz, 7Hz, 6H), 1.5 (s, 9H), 1.5-1.7 (m, 3H), 3.0 3.2 (m, 2H), 3.7 (s, 3H), 4.0- 4.2 (m, αH), 4.5-4.7 (br, αH), 4.8-4.9 (br, 1H), 6.4-6.5 (br, 1H) 7.1-7.4 (m, 5H).

Dipeptide 1a-2a-NH_2

Dipeptide **1a-2a-NH_2** was synthesized following the General Amine Deprotection procedure. This dipeptide was taken on to the next reaction without further purification or characterization (534 mg, 100% yield).

Tripeptide 1a-2a-3d

Tripeptide **1a-2a-3d** was synthesized following the General Peptide Synthesis procedure, utilizing 631 mg (2.161 mmol, 1.1 equiv) of amine **1a-2a**, 454 mg (1.962 mmol, 1.0 equiv) of acid **3d**, 1400 μL (4 equiv) of DIPEA, 378 mg (1.176 mmol, 0.6 equiv) of TBTU, and 448 mg (1.176 mmol 0.6 equiv) of HATU. The crude reaction was purified by column chromatography (silica gel, EtOAc/Hex) to yield the tripeptide (822 mg, 83% yield): R_f 0.5 (EtOAc/Hex 2:3); ^{1}H NMR (200 MHz, $CDCl_3$) δ 0.8-1.0 (m, 12H), 1.4 (s, 9H), 1.5-1.8 (m, 2H), 2.2- 2.4 (m, 1H), 2.7-2.9 (s, 3H), 3.1-3.2 (d, *J*= 13Hz, 2H), 3.7 (s, 3H), 4.0 (m, αH), 4.3 (m, αH), 4.8 (m, αH), 6.2 (br, 1H), 6.4-6.6 (br, 1H), 7.0-7.4 (m, 5H).

Tripeptide 1a-2a-3d-NH_2

Tripeptide **1a-2a-3d-NH_2** was synthesized following the General Amine Deprotection procedure. This dipeptide was taken on to the next reaction without further purification or characterization (649 mg, quantitative yield).

Tetrapeptide 1a-2a-3d-4a

Tripeptide **1a-2a-3d-4a** was synthesized following the General peptide Synthesis procedure. Utilizing 590 mg (2.1 mmols, 1.3 equivalents) of amine 1a-2a-3d, 480mg (1.62 mmols, 1.0 equivalents) of acid 4a, 1.13 mL (4 equivalents) of DIPEA, 480 mg (1.5 mmols, 0.8 equivalents) of TBTU, and 300mg (0.81mmols, 0.8 equivalents) of HATU,

The crude reaction was purified by column chromatography (silica gel, EtOAc/Hex) to yield the tripeptide (730mg, 81% yield). *Rf*: 0.6 (EtOAc: Hex 1:1) ^{1}H NMR (200 MHz, $CDCl_3$): δ 0.8-1.0 (m, 18H), 1.3-1.8 (m, 13H), 2.2-2.4 (m, 1H), 2.9 (s, 3H), 3.1-3.2 (m, 2H), 3.6 (s, 3H), 4.3-4.4 (m, 2αH), 4.5-4.6 (q, *J*= 7Hz, αH), 4.7-4.8 (q, *J*= 7Hz, αH), 5.2-5.4 (d, *J*= 11Hz, 1H), 6.4-6.5 (d, *J*= 12Hz, 1H), 6.6-6.7 (d, *J*=12Hz, 1H), 7.1-7.3 (m, 5H).

Tetrapeptide 1a-2a-3d-4a-NH_2

Tripeptide **1a-2a-3d-4a-NH_2** was synthesized following the General amine deprotection. This dipeptide was taken on to the next reaction without further purification or characterization. (598mg, Assume quantitative yield).

Pentapeptide 1a-2a-3d-4a-5a

Pentapeptide **1a-2a-3d-4a-5a** was synthesized following the General peptide synthesis procedure. Utilizing 500 mg (1.09 mmols, 1.1 equivalents) of amine 1a-2a-3d-4a, 310mg (1.0 mmol, 1.0 equivalents) of acid 5a, 0.86 mL (5 equivalents) of DIPEA, 190 mg (0.58 mmol, 0.6 equivalents) of TBTU, and 370 mg (1.0 mmol, 1.0 equivalents) HATU. The crude reaction was purified by flash column chromatography (silica gel, EtOAc/Hex) to yield the pentapeptide (893mg, 60% yield). *Rf*: 0.5 (EtOAc: Hex 1:1). ^{1}H NMR (500 MHz, $CDCl_3$): δ 0.8-1.0 (m, 24H), 1.1-1.9 (m, 18H), 2.3-2.4 (br, 1H), 3.0-3.2 (m, 2H), 3.7 (s, 3H), 4.1-4.2 (br, αH), 4.3-4.4 (br, αH), 4.4-4.5 (br, αH), 4.7-4.8 (br, αH), 4.9-5.0 (br, αH), 6.4-6.5 (br, 1H), 7.1-7.3 (m, 5H), 7.4 (t, *J*= 8Hz, 1H), 7.6 (t, *J*= 8Hz, 1H), 7.8 (t, *J*=7Hz, 1H), 8.1 (t, *J*= 7Hz, 1H).

Pentapeptide HO-1a-2a-3d-4a-5a-NH_2

Pentapeptide **HO-1a-2a-3d-4a-5a-NH_2** was synthesized following the ***In-situ* double deprotection of linear pentapeptide** procedure. The crude product was confirmed by LCMS and was taken on to the macrocyclization without further purification. LCMS: m/z calcd for $C_{33}H_{55}N_5O_6$ (M+1) =618.42, found 618.6.

Macrocycle 1a-2a-3d-4a-5a (Compound 20)

Macrocycle **1a-2a-3d-4a-5a** was synthesized following the Macrocyclization procedure A, utilizing 120 mg (0.20 mmol, 1.0 equiv) of linear pentapeptide, 0.21 mL (6.0 equiv) of DIPEA, 45 mg (0.14 mmol, 0.7 equiv) of TBTU, 53 mg (0.14 mmol, 0.7 equiv) of HATU, and 12 mg (0.04 mmol, 0.2 equiv) of DEPBT. The crude reaction was purified by reverse phase HPLC to yield the macrocycle (3 mg, 4% yield): R_f 0.6 (EtOAc/Hex 3:1); LCMS *m*/*z* calcd for $C_{33}H_{53}N_5O_5$ (M + 1) 600.3, found 600.7.

Compounds 25, 30

Dipeptide 1a-2g

Dipeptide **1a-2g** was synthesized following the General Peptide Synthesis procedure, utilizing 1100 mg (5.06 mmol, 1.1 equiv) of amine **1a**, 1000 mg (4.6 mmol, 1.0 equiv) of acid **2g**, 3.2 mL (4 equiv) of DIPEA, and 1630 mg (5.06 mmol, 1.1 equiv) of TBTU. The crude reaction was purified by column chromatography (silica gel,

EtOAc/Hex) to yield the dipeptide (1700 mg, 98% yield): R_f 0.5 (EtOAc/Hex 35:65); ^{1}H NMR (200 MHz, $CDCl_3$) δ 1.0 (dd, *J*= 12Hz, 7Hz, 6H), 1.5 (s, 9H), 2.2 (m, 1H), 3.2 (dd, *J*= 10Hz, 6Hz, 2H), 3.8 (s, 3H), 3.8 (dd, *J*= 14Hz, 8Hz, αH), 5.0 (q, *J*= 9Hz, αH), 5.1 (br, 1H), 6.4 (br, 1H), 7.2-7.4 (m, 5H).

Dipeptide 1a-2g-NH_2

Dipeptide **1a-2g-NH_2** was synthesized following the General Amine Deprotection procedure. This dipeptide was taken on to the next reaction without further purification or characterization (566 mg, assume quantitative yield).

Tripeptide 1a-2g-3L

Tripeptide **1a-2g-3L** was synthesized following the General Peptide Synthesis procedure, utilizing 590 mg (2.1 mmol, 1.3 equiv) of amine **1a-2g**, 480 mg (1.62 mmol, 1.0 equiv) of acid **3L**, 1.13 mL (4 equiv) of DIPEA, 480 mg (1.5 mmol, 0.8 equiv) of TBTU, and 300 mg (0.81 mmol, 0.8 equiv) of HATU. The crude reaction was purified by column chromatography (silica gel, EtOAc/Hex) to yield the tripeptide (730 mg, 81% yield): R_f 0.6 (EtOAc/Hex 1:1); ^{1}H NMR (200 MHz, $CDCl_3$) δ 0.7-0.9 (dd, *J*= 15Hz, 9Hz, 6H), 1.4 (s, 9H), 2.0-2.2 (m, 1H), 2.9-2.2 (m, 2H), 3.5-3.9 (m, 2H), 3.6 (s, 3H), 4.2-4.3 (t, *J*= 9Hz, αH), 4.4-4.6 (dd, *J*= 12Hz, 6Hz, αH), 4.7-4.8 (q, *J*= 9Hz, αH), 5.4 (br, 1H), 6.4 (br, 1H), 6.8 (br, 1H), 7.0-7.4 (m, 5H).

Tripeptide 1a-2g-3L-NH_2

Tripeptide **1a-2g-3L-NH_2** was synthesized following the General Amine Deprotection procedure. This dipeptide was taken on to the next reaction without further purification or characterization (598 mg, assume quantitative yield).

Dipeptide 4c-5e

Dipeptide **4c-5e** was synthesized following the General Peptide Synthesis procedure, utilizing 920 mg (5.5 mmol, 1.2 equiv) of amine **4c**, 1000 mg (4.6 mmol, 1.0 equiv) of acid **5e**, 2.4 mL (3 equiv) of DIPEA, and 2210 mg (6.9 mmol, 1.5 equiv) of TBTU. The crude reaction was purified by column chromatography (silica gel, EtOAc/Hex) to yield the dipeptide (1440 mg, 94% yield): R_f 0.5 (EtOAc/Hex 35:65); ^{1}H NMR (200 MHz, $CDCl_3$) δ 0.8-1.0 (dd, *J*= 12Hz, 7Hz, 6H), 1.2 (s, 9H), 2.1-2.3 (m, 2H), 3.7 (s, 3H), 3.8-4.0 (dd, *J*= 11Hz, 8Hz, αH), 4.5-4.6 (dd, *J*= 10Hz, 6Hz, αH), 5 (br, H), 6.4 (br, H).

Acid deprotected dipeptide HO-4c-5e

Dipeptide **HO-4c-5e** was synthesized following the General Acid Deprotection procedure. This dipeptide was taken on to the next reaction without further purification or characterization (1296 mg, 93% yield).

Pentapeptide 1a-2g-3L-4c-5e

Pentapeptide **1a-2g-3L-4c-5e** was synthesized following the General Peptide Synthesis procedure, utilizing 500 mg (1.09 mmol, 1.1 equiv) of amine **1a-2g-3L**, 310 mg (1.0 mmol, 1.0 equiv) of acid **4c-5e**, 0.86 mL (5 equiv) of DIPEA, 190 mg (0.58 mmol, 0.6 equiv) of TBTU, and 370 mg (1.0 mmol, 1.0 equiv) of HATU. The crude reaction was purified by column chromatography (silica gel, EtOAc/Hex) to yield the pentapeptide (670 mg, 45% yield): R_f 0.5 (EtOAc/Hex 1:1); ^{1}H NMR (500 MHz, DMSO-d6) δ 0.7-0.8 (m, 18H), 1.4 (s, 9H), 1.8-2.0 (br, 3H), 2.9-3.0 (m, 2H), 3.5 (s, 3H), 3.8 (br, αH), 4.2 (br, αH), 4.3 (br, αH), 4.4 (br, αH), 4.4 (br, 2H), 4.7 (br, αH), 6.8 (br, 1H), 7.1-7.4 (m, 10H), 7.6 (br, 1H), 7.9 (br, 1H), 8.2 (br, 1H), 8.4 (br, 1H)

Pentapeptide HO-1a-2g-3L-4c-5e-NH_2

Pentapeptide **HO-1a-2g-3L-4c-5e-NH_2** was synthesized following the ***In-situ* double deprotection of linear pentapeptide** procedure. The crude product was confirmed by LCMS and was taken on to the macrocyclization without further purification. LCMS: m/z calcd for $C_{34}H_{49}N_5O_7$ (M+1) = 640.78, found 640.8.

Macrocycle 1a-2g-3L-4c-5e (Compound 30)

Macrocycle **1a-2g-3L-4c-5e** was synthesized following the Macrocyclization procedure, utilizing 130 mg (0.2 mmol, 1.0 equiv) of linear pentapeptide precursor, 0.2

mL (6 equiv) of DIPEA, 80 mg (0.25 mmol, 1.2 equiv) of TBTU, 100 mg (0.26 mmol, 1.3 equiv) of HATU, and 80 mg (0.26 mmol, 1.3 equiv) of DEPBT. The crude reaction was purified by reverse phase HPLC to yield the macrocycle (10 mg, 8% yield): R_f 0.4 (EtOAc/Hex 1:1); LCMS m/z calcd for $C_{34}H_{47}N_5O_6$ (M + 1) 622.77, found 622.3

Deprotected macrocycle 1a-2g-3L-4c-5e (Compound 25)

Deprotected Macrocycle **1a-2g-3L-4c-5e** (Compound 25) was synthesized following the "Cbz Deprotection procedure". Utilizing 5mg (0.009 mmols, 1.0 equivalents) of protected macrocycle, 10% Pladium-Carbon (cat. Amount). The crude reaction was purified by reverse phase-HPLC to yield the deprotected macrocycle. (0.3mg, 3.7 % yield.) LCMS: m/z calcd for $C_{27}H_{41}N_5O_6$ (M+1) = 532.64, found 532.5

Compound 52

Dipeptide 1a-2a

Dipeptide 1a-2a. Dipeptide **1a-2a** was synthesized following the General Peptide Synthesis procedure, utilizing 1904 mg (8.827 mmol, 1.1 equiv) of amine 1**a**, 2000 mg (8.022 mmol, 1.0 equiv) of acid 2**a**, 5,622 µL (4 equiv) of DIPEA, and 3090 mg (9.627 mmol, 1.2 equiv) of TBTU. The crude reaction was purified by column chromatography (silica gel, EtOAc/Hex) to yield the dipeptide (3115 mg, 99% yield): R_f 0.5 (EtOAc/Hex 7:13) ^{1}H NMR (200 MHz, $CDCl_3$) δ 0.9-1.0 (dd, *J*= 12Hz, 9Hz, 6H), 1.5 (s, 9H), 1.5-1.7

(m, 3H), 3.0-3.2 (m, 2H), 3.7 (s, 3H), 4.0-4.2 (m, αH), 4.8-4.9 (m, αH), 4.7-4.9 (br, 1H), 6.4-6.5 (br, 1H) 7.1-7.4 (m, 5H).

Dipeptide 1a-2a-NH_2

Dipeptide **1a-2a-NH_2** was synthesized following the General Amine Deprotection procedure. This dipeptide was taken on to the next reaction without further purification or characterization (2321 mg, quantitative yield).

Tripeptide 1a-2a-3a

Tripeptide **1a-2a-3a** was synthesized following the General Peptide Synthesis procedure, utilizing 360 mg (1.231 mmol, 1.1 equiv) of amine **1a-2a**, 243 mg (1.121 mmol, 1.0 equiv) of acid **3a**, 800 μL (4 equiv) of DIPEA, and 431 mg (1.339 mmol, 1.2 equiv) of TBTU. The crude reaction was purified by column chromatography (silica gel, EtOAc/Hex) to yield the tripeptide (500 mg, 91% yield): R_f 0.5 (EtOAc/Hex 1:1); ^{1}H NMR (200 MHz, $CDCl_3$) δ 0.9-1.0 (m, 12H), 1.57 (s, 9H), 1.6-1.7 (m, 3H), 2.1-2.3 (m, 1H), 3.1-3.4 (m, 2H), 3.8 (s, 3H), 4.0-4.2 (m, αH), 4.5-4.6 (m, αH), 4.8-5.0 (q, *J*= 9Hz, αH), 5.8 (br, 1H), 7.2-7.4 (m, 5H).

Tripeptide 1a-2a-3a-NH_2

Tripeptide **1a-2a-3a-NH_2** was synthesized following the General Amine Deprotection procedure. This dipeptide was taken on to the next reaction without further

purification or characterization (399 mg, quantitative yield).

Dipeptide 4b-5b

Dipeptide **4b-5b** was synthesized following the General Peptide Synthesis procedure, utilizing 400 mg (2.2 mmol, 1.1 equiv) of amine **4b**, 500 mg (2.0 mmol, 1.0 equiv) of acid **5b**, 1.4 mL (4 equiv) of DIPEA, and 770.6 mg (2.4 mmol, 1.1 equiv) of TBTU. The crude reaction was purified by column chromatography (silica gel, EtOAc/Hex) to yield the dipeptide (680 mg, 98% yield); R_f 0.5 (EtOAc/Hex 1:1); ^{1}H NMR (200 MHz, $CDCl_3$) δ 0.8-1.0 (m, 12H), 1.4 (s, 9H), 1.5-1.8 (m, 6H), 3.7 (s, 3H), 4.0 (m, αH), 4.6 (m, αH), 4.8 (br, 1H), 6.4 (br, 1H)

Acid deprotected dipeptide HO-4b-5b

Dipeptide **HO-4b-5b** was synthesized following the General Acid Deprotection procedure. This dipeptide was taken on to the next reaction without further purification or characterization (575 mg, 89.8% yield): ^{1}H NMR (200 MHz, $CDCl_3$) δ 0.7-0.9 (dd, 12H), 1.2-1.6 (m, 2H), 1.4 (s, 9H), 2.0-2.2 (m, 2H), 3.2-3.3 (m, 2H), 3.6 (s, 3H), 3.8 (dd, RH), 4.2 (m, αH), 4.8 (quint, αH), 4.9 (br, 1H), 6.3 (br, 1H), 6.6 (br, 1H), 7.0-7.6 (m, 5H), 8.2 (br, 1H).

Pentapeptide 1a-2a-3a-4b-5b

Pentapeptide **1a-2a-3a-4b-5b** was synthesized following the General peptide Synthesis procedure. Utilizing 500 mg (1.09 mmols, 1.1 equivalents) of amine 1a-2a-3a,

310mg (1.0 mmols, 1.0 equivalents) of acid 4b-5b, 0.86 mL (5 equivalents) of DIPEA, 190 mg (0.58 mmols, 0.6 equivalents) of TBTU, and 370 mg (1.0 mmols, 1.0 equivalents) HATU. The crude reaction was purified by column chromatography (silica gel, EtOAc/Hex) to yield the pentapeptide (1146 mg, 77% yield). R_f: 0.5 (EtOAc: Hex 1:1). ^{1}H NMR (400 MHz, $CDCl_3$): δ 0.7-1.0 (m, 24H), 1.4 (s, 9H), 1.4-1.7 (br, 9H), 1.9-2.1 (br, 1H), 3.0-3.1 (m, 2H), 3.6 (s, 3H), 4.2-4.3 (br, αH), 4.4-4.5 (br, αH), 4.6-4.8 (br, 3αH), 7.0-7.2 (br, 5H), 7.4-7.8 (br, 5H).

Pentapeptide HO-1a-2a-3a-4b-5b-NH_2

Pentapeptide **HO-1a-2a-3a-4b-5b-NH_2** was synthesized following the Stepwise double deprotection of linear pentapeptide procedure. The crude product was confirmed by LCMS and was taken on to the macrocyclization without further purification. LCMS: m/z calcd for $C_{32}H_{53}N_5O_6$ (M+1) =604.40, found 604.3.

Macrocycle 1a-2a-3a-4b-5b

Macrocycle **1a-2a-3a-4b-5b** was synthesized following the Macrocyclization procedure A, utilizing 431 mg (0.71 mmol, 1.0 equiv) of linear pentapeptide HO-1a-2a-3a-4b-5b-NH_2, 0.49 mL (6.0 equiv) of DIPEA, 157 mg (0.14 mmol, 0.7 equiv) of TBTU, 189 mg (0.14 mmol, 0.7 equiv) of HATU, and 41 mg (0.04 mmol, 0.2 equiv) of DEPBT. The crude reaction was purified by reverse phase HPLC to yield the macrocycle (33 mg, 8% yield): R_f 0.4 (EtOAc/Hex 3:1); LCMS *m/z* calcd for $C_{32}H_{51}N_5O_5$ (M + 1) 586.8, found 586.4.

6.5. Synthesis of Holliday Junction Trapping Compound

Compound 4b-5a-6c

Tripeptide **4b-5a-6c** was synthesized following General peptide synthesis procedure. Utilizing 1009 mg (2.88 mmol, 1.1 equivalents) of amine 4b-5a, 1008 mg (2.62 mmol, 1.0 equivalents) of acid 6c, 1.36 mL (3.0 equivalents) of DIPEA, 1200 mg (3.15 mmols, 1.2 equivalents) of TBTU. The crude reaction was purified by flash column chromatography (silica gel, EtOAc/ Hex) to give pure tripeptide 4b-5a-6c (1712 mg, 85% yield). R_f 0.4 (EtOAc/Hex 2:1); ^{1}H NMR (300 MHz, $CDCl_3$) δ 1.3-1.8 (m, 15H), 3.0-3.3 (m, 6H), 3.6 (s, 3H), 4.3 (d, *J*= 9Hz1H), 4.6 (br, 2H), 4.8 (m, αH), 5.0 (t, *J*= 6Hz, 2αH), 5.2-5.4 (m, 3H), 6.4 (d, *J*= 7Hz, 1H), 6.7 (s, 1H), 7.0-7.5 (m, 13H).

Acid deprotected tripeptide HO-4b-5a-6c

Tripeptide **HO-4b-5a-6c** was synthesized following the General Acid Deprotection procedure. This tripeptide was taken on to the next reaction without further purification or characterization (800 mg, 98% yield). LCMS *m*/*z* calcd for $C_{40}H_{46}ClN_5O_8$ (M + 1) 760.30, found 760.20.

Amine deprotected tripeptide 4b-5a-6c-NH_2

Tripeptide 4b-5a-6c-NH_2 was synthesized following the General amine deprotection procedure to give the desired product (522 mg, assumed quantitative yield). LCMS: m/z calcd for $C_{36}H_{40}ClN_5O_6$ (M+1) = 674.27, found 674.5.

Hexapeptide 4b-5a-6c-4b-5a-6c

Hexapeptide 4b-5a-6c-4b-5a-6c was synthesized following General peptide synthesis procedure. Utilizing 701 mg (1.04 mmol, 1.1 equivalents) of amine 4b-5a-6c, 718 mg (0.94 mmol, 1.0 equivalents) of acid 4b-5a-6c, 0.98 mL (6.0 equivalents) of DIPEA, 270 mg (0.86 mmol, 0.8 equivalents) of TBTU, and 410 mg (1.08 mmols, 1.0 equivalents) of HATU. The crude reaction was purified by flash column chromatography (silica gel, EtOAc/ Hex) to give pure hexapeptide 4b-5a-6c-4b-5a-6c (890 mg, 60% yield). R_f 0.4 (EtOAc/Hex 4:1). LCMS: m/z calcd for $C_{76}H_{84}Cl_2N_{10}O_{13}$ (M+1) = 1415.56, found 1415.3.

2-Cl-Z protected 4b-5a-6c-4b-5a-6c macrocycle

2-Cl-Z protected 4b-5a-6c-4b-5a-6c macrocycle was synthesized following Macrocyclization procedure B. Utilizing 1.78 mL (6.0 equivalents) of DIPEA, 443 mg (1.37 mmol, 0.6 equivalents) of TBTU, 870 mg (2.29 mmol, 1.0 equivalents) of HATU and 547 mg (1.83 mmol, 0.8 equivalents) of DEPBT. The crude reaction was purified by

flash column chromatography (silica gel, EtOAc/ Hex) to give pure 2-Cl-Z protected 4b-5a-6c-4b-5a-6c macrocycle (115mg, 15% yield). R_f 0.4 (EtOAc/Hex 4:1). LCMS: m/z calcd for $C_{70}H_{72}Cl_2N_{10}O_{10}$ (M+1) = 1283.48, found 1283.9.

Hexapeptide HO-8c-9d-10c-8c-9d-10c-NH_2

Hexapeptide **HO-8c-9d-10c-8c-9d-10c-NH_2** was synthesized by the following manner: Resin-bond amine deprotected linear hexapeptide was first synthesized following Solid-Phase peptide Synthesis procedure. Then, the amine deprotected linear hexapeptide 8c-9d-10c-8c-9d-10c was cleaved from the resin by peptide cleavage procedure to furnish double deprotected linear hexapeptide HO-8c-9d-10c-8c-9d-10c-NH_2. LCMS: m/z calcd for $C_{74}H_{96}N_{10}O_{15}$ (M+1) = 1366.61, found 1366.3.

HJ compund 10

HJ compd 10 was synthesized by the following manner: linear hexapeptide HO-8c-9d-10c-8c-9d-10c-NH_2 was subjected to Macrocyclization procedure C to form Boc protected 8c-9d-10c-8c-9d-10c macrocycle. This Boc protected macrocycle was purified by flash column chromatography (silica gel, EtOAc/ Hex) with 15% yield. This pure Boc protected macrocycle was subjected to General amine deprotection procedure for 5 hours yielding desired product HJ compound 10. The crude HJ compound 10 was purified by reverse phase HPLC. LCMS (Boc protected 8c-9d-10c-8c-9d-10c macrocycle): m/z calcd

for $C_{74}H_{94}N_{10}O_{14}$ (M+1) = 13476.70, found 1347.7; LCMS (HJ compd 10): m/z calcd for $C_{54}H_{62}N_{10}O_6$ (M+1) = 948.13, found 948.1.

6.6. Synthesis of Triostin A analogue: Azatandem

Compound 29

Tetrahydrosulfide (1.0 eq) was added to the bromoacetonitrile (1.0 eq) at room temperature and stirred for 8 hours to afford crude compound (**29**). The crude material was washed with cold dried acetone three times (10 mL per wash) to gave pure compound **29** with 95% yield. ^{1}H NMR (200 MHz, DMSO-d_6): δ 2.2-2.4 (sextet, *J*= 11Hz, 4H), 3.4-3.8 (m, 4H), 4.6-4.7 (br, 2H).

Compound 30

Compound **29** (1.1 eq) was coupled to the Boc-Val-OH (1.0 eq) by using TBTU (1.1 eq) and DIPEA (4.0 eq) in dichloromethane (0.1M) at room temperature for 30 min. The reaction was monitored via TLC every 10 minutes. Upon completion, the crude material was diluted with excess of dichloromethane and washed with saturated ammonium chloride. After back extraction of aqueous layers with dichloromethane, organic layers were combined, dried over sodium sulfate, filtered, and concentrated *in vacuo*. The crude reaction was purified by flash column chromatography (silica gel, EtOAc/ Hex) to give pure compound (**30**), as light yellow liquid with 90% yield. R_f: 0.4

(EtOAc: Hex 1:1) ^{1}H NMR (200 MHz, $CDCl_3$): δ 0.8-1.0 (dd, *J*= 12Hz, 8Hz, 6H), 1.4(s, 9H), 1.8-2.0 (m, 2H), 2.0-2.2 (m, 1H), 2.8-3.0 (m, 2H), 3.4 (t, *J*= 9Hz, 2H), 4.1-4.3 (m, 3H), 5.0 (br, 1H).

Compound 31

Pentahydrosulfide (1.0 eq) was added to the bromoacetonitrile (1.0 eq) at room temperature and stirred for 8 hours to afford crude compound **31**. The crude mateial was washed with cold dried acetone three times (10 mL per wash) to gave pure compound **31** with 95% yield. ^{1}H NMR (200 MHz, DMSO-d_6)**:** δ 1.4-1.6 (br, 2H), 1.8-2.0 (2H), 2.0-2.2 (br, 2H), 3.3-3.5 (br, 2H), 3.6-3.8 (br, 2H), 5.0 (s, 2H).

Compound 32

Compound **31** (1.1 eq) was coupled to the Boc-Val-OH (1.0 eq) by using TBTU (1.1 eq) and DIPEA (4.0 eq) in dichloromethane (0.1M) at room temperature for 30 min. The reaction was monitored via TLC every 10 minutes. Upon completion, the crude material was diluted with excess of dichloromethane and washed with saturated ammonium chloride. After back extraction of aqueous layers with dichloromethane, organic layers were combined, dried over sodium sulfate, filtered, and concentrated *in vacuo*. The crude material was purified by recrystalization in cold EtOAc to give the desired product, compound **32**, as white crystal with 95% yield. R_f: 0.5 (Acetone: EtOAc

1:9) ^{1}H NMR (200 MHz, $CDCl_3$): δ 0.8-1.0 (dd, 6H), 1.4(9H), 1.7-1.9 (m, 3H), 1.9-2.1 (m, 1H), 2.2-2.3 (br, 3H), 3.0-3.1 (br, 2H), 3.3-3.6 (q, 2H), 4.4 (br, αH), 5.2 (br, 1H).

Compound 33

Compuond **32** (1.0 eq) was subjected to oxone (2.2 eq) in a mixture of benzyl alcohol, dichloromethane, and acetone (3:7:10 ratio) at a 0.2M reaction concentration at room temperature for 4 hours. The reaction was monitored by TLC every 30 minutes until the reaction was complete. Upon completion, the crude material was filtered and and concentrated *in vacuo*. The crude reaction was purified by flash column chromatography (silica gel, EtOAc/ Hex) to give pure compound **33** as light yellow liquid with 55% yield. R_f: 0.4 (EtOAc: Hex 2:8). ^{1}H NMR (500 MHz, $CDCl_3$): δ 0.8 (d, *J*= 8Hz, 3H), 0.9 (d, *J*= 8Hz, 3H), 1.4 (s, 9H), 2.2-2.3 (br, 1H), 4.9 (br, αH), 5.1 (br, 1H), 5.2-5.3 (q, *J*= 7Hz, , 2H), 7.3-7.4 (m, 5H).

Compound 21

Compound **21** (299mg) was synthesized following the General amine deprotection procedure. This compound was taken on to the next reaction without further purification (210 mg, Assume quantitative yield).^{1}H NMR (200 MHz, $CDCl_3$)**:** δ 1.9 (d, *J*= 7Hz, 3H), 1.1(d, *J*= 7Hz, 3H), 2.4 (br, 1H), 4.8 (br, αH), 5.3 (s, 2H), 7.2-7.4 (br, 5H), 8.2-8.6 (br, 2H).

6.7. Supporting Spectra

^{1}H NMR for Sansalvamide A derivatives

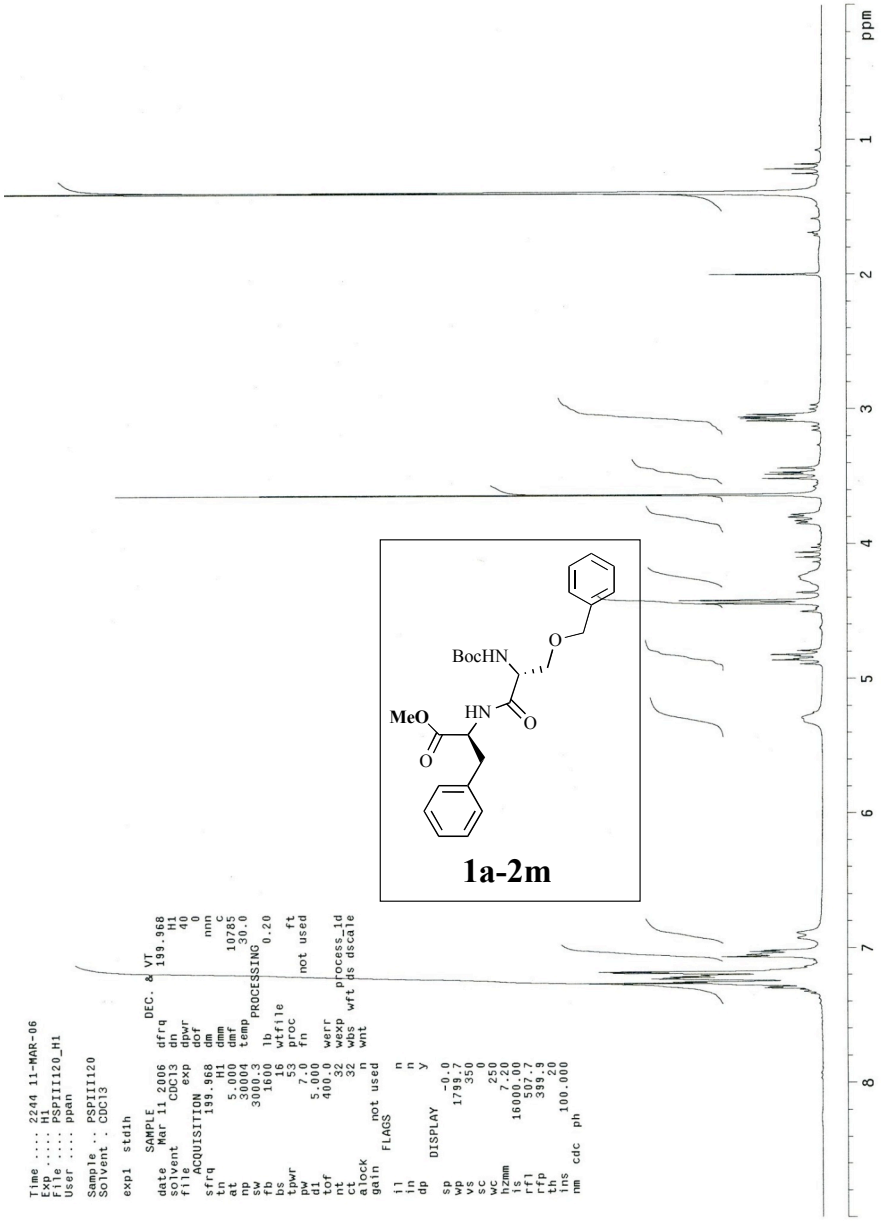

1a-2m

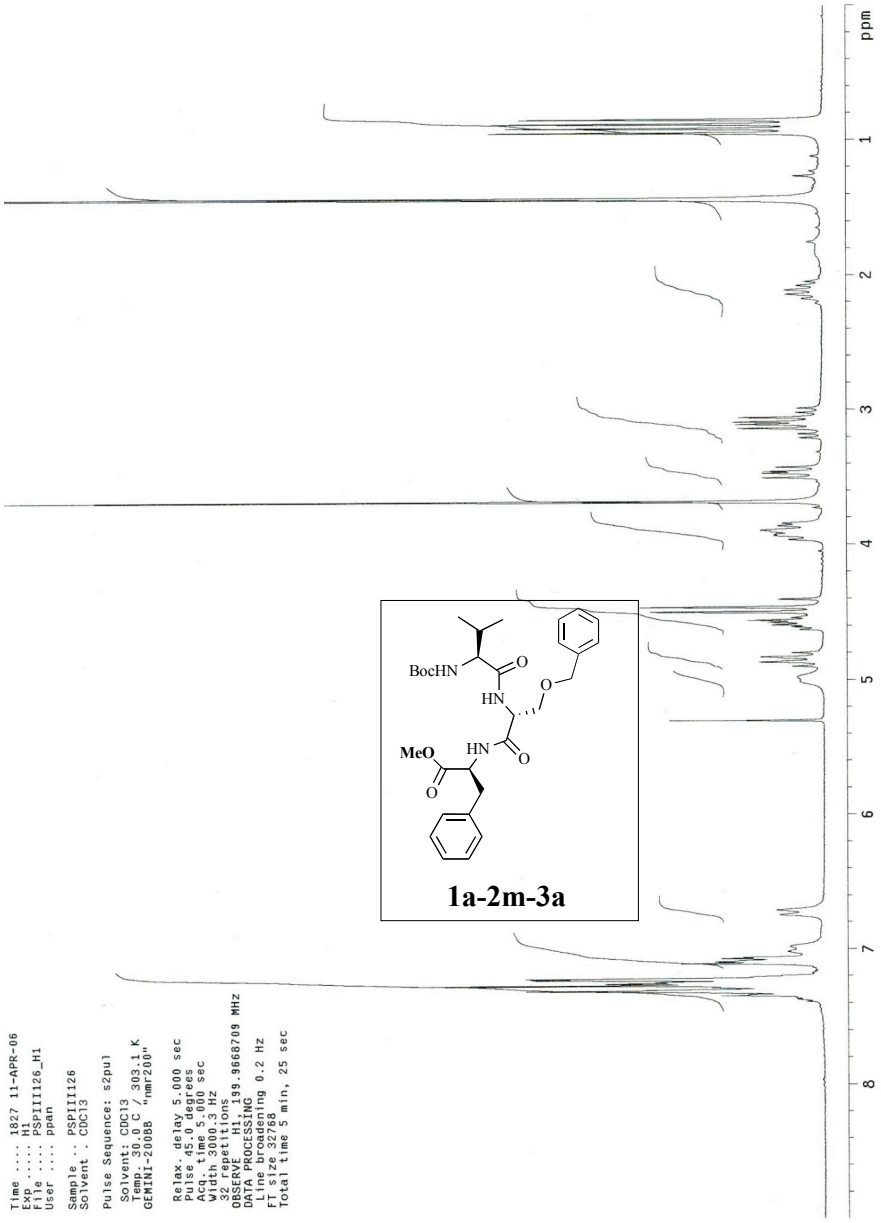
Time 1827 11-APR-06
Exp H1
File ..... PSPIII126_H1
User ..... ppan
Sample .. PSPIII126
Solvent . CDCl3
Pulse Sequence: s2pul
Solvent: CDCl3 303.1 K
Temp 30.0 C / "mm200"
GEMINI-200BB
Relax. delay 5.000 sec
Pulse 45.0 degrees
Acq. time 5.000 sec
Width 3000.3 Hz
32 repetitions
OBSERVE H1, 199.9668709 MHz
DATA PROCESSING
Line broadening 0.2 Hz
FT size 32768
Total time 5 min, 25 sec
BocHN
HN
O
O
HN
O
MeO
O
1a-2m-3a
ppm
1
2
3
4
5
6
7
8

1a-2m-3a

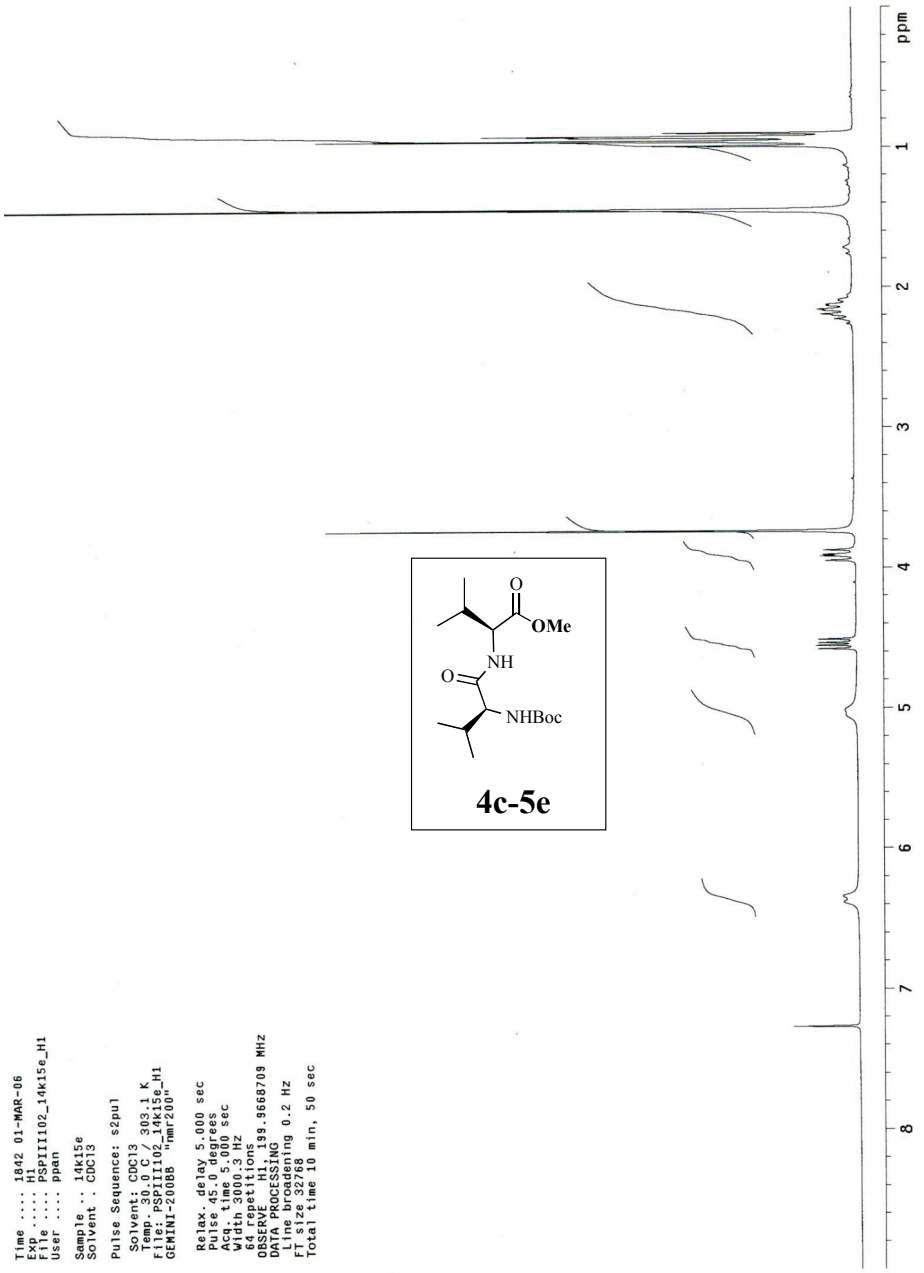
Time 1842 01-MAR-06
Exp H1
File ..... PSPIII102_14k15e_H1
User .... ppan
Sample .. 14k15e
Solvent . CDCl3
Pulse Sequence: s2pul
Solvent: CDCl3
Temp. 30.0 C / 303.1 K
File: PSPIII102_14k15e_H1
GEMINI-200BB "nmr200"
Relax. delay 5.000 sec
Pulse 45.0 degrees
Acq. time 5.000 sec
Width 3000.3 Hz
64 repetitions
OBSERVE H1, 199.9668709 MHz
DATA PROCESSING
Line broadening 0.2 Hz
FT size 32768
Total time 10 min, 50 sec
OMe
NH
O
NHBoc
4c-5e
ppm
1
2
3
4
5
6
7
8

4c-5e

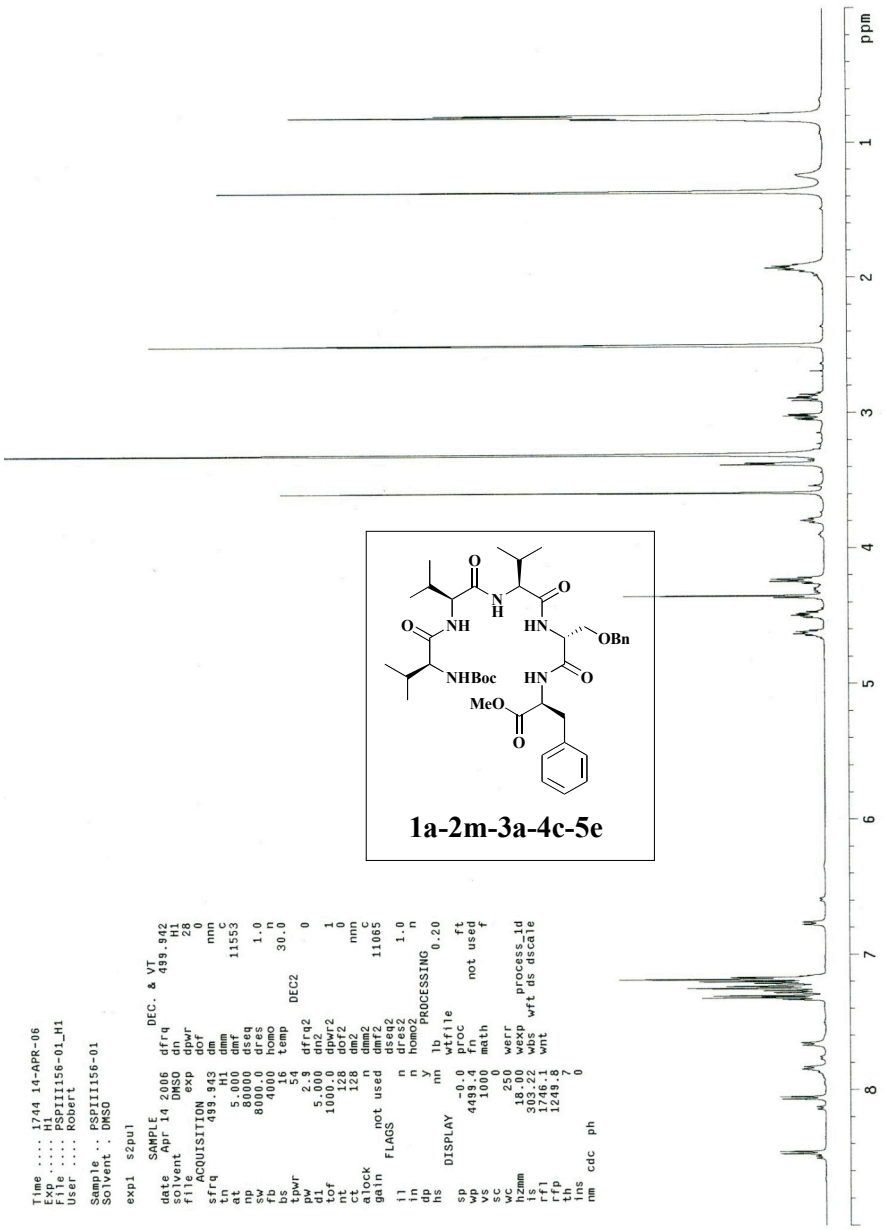
Time 1744 14-APR-06
Exp H1
File .... PSPIII156-01_H1
User .... Robert
Sample .. PSPIII156-01
Solvent . DMSO
exp1 s2pul
SAMPLE
date Apr 14 2006
solvent DMSO
file exp
ACQUISITION
sfrq 499.943
tn H1
at 5.000
np 8000
sw 8000.0
fb 4000
bs 16
tpwr 54
pw 2.9
d1 5.000
tof 1000.0
nt 128
ct 128
alock n
gain not used
FLAGS
il n
in n
dp y
hs nn
DISPLAY
sp -9.0
wp 4449.4
vs 1000
sc 0
wc 250
hzmm 18.00
is 303.22
rfl 1749.1
rfp 1249.7
th 0
ins
nm cdc ph
DEC. & VT
dfrq 499.942
dn H1
dpwr 28
dof 0
dm nnn
dmm c
dmf 11553
dmfeq
dres 1.0
homo n
temp 30.0
DEC2
dfrq2
dn2 0
dpwr2
dof2 1
dm2 0
dmm2 nnn
dmf2 c
dseq2 11065
dres2
homo2 1.0
PROCESSING n
lb n
wtfile 0.20
proc
ftn ft
math not used
werr f
wexp process_1d
wbs wft ds dscale
wnt
ppm
1
2
3
4
5
6
7
8
O
N
H
NH
HN
OBn
NHBoc
MeO
1a-2m-3a-4c-5e

1a-2m-3a-4c-5e

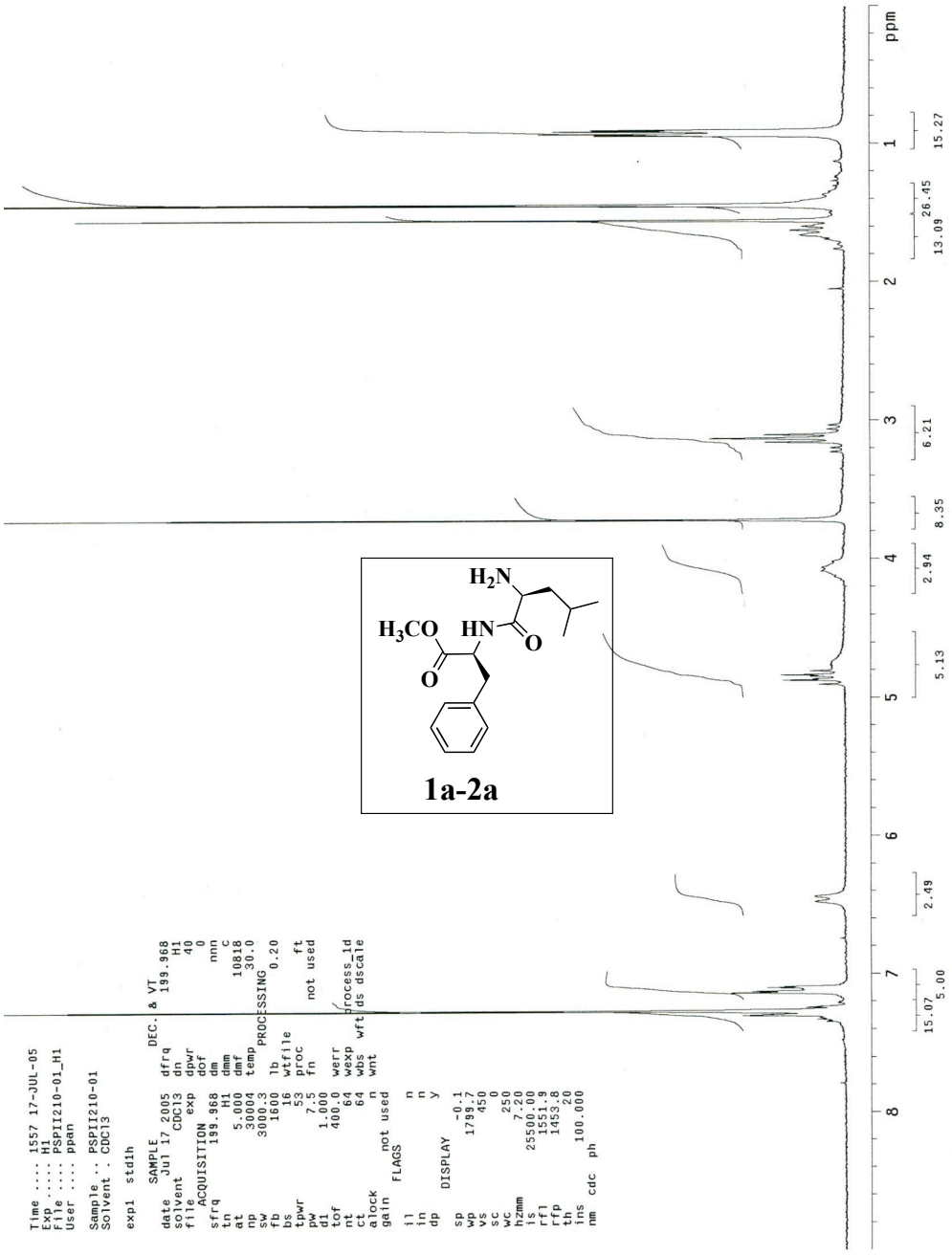
Time 1557 17-JUL-05
Exp H1
File ..... PSPII210-01_H1
User ..... ppan
Sample .. PSPII210-01
Solvent . CDCl3
exp1 std1h
DEC. & VT
SAMPLE 199.968
date Jul 17 2005 dfrq H1
solvent CDCl3 dn 40
file exp dpwr 0
ACQUISITION dof nnn
sfrq 199.968 dm c
tn H1 dmm 10B18
at 5.000 dmf 30.0
np 30004 temp PROCESSING
sw 6000.3 lb 0.20
fb 1600 wtfile
bs 16 proc ft
tpwr 53 fn not used
pw 7.5
d1 1.000 werr
tof 400.0 wexp process_1d
nt 64 wbs wft ds dscale
ct 64 wnt
alock n
gain not used
FLAGS
il n
in n
dp y
DISPLAY
sp -0.1
wp 1799.7
vs 450
sc 0
wc 250
hzmm 7.20
fs 25500.00
rfl 1551.9
rfp 1453.8
th 20
ins 100.000
nm cdc ph
ppm
15.07
5.00
2.49
5.13
2.94
8.35
13.09
26.45
6.21
15.27
1a-2a

1a-2a

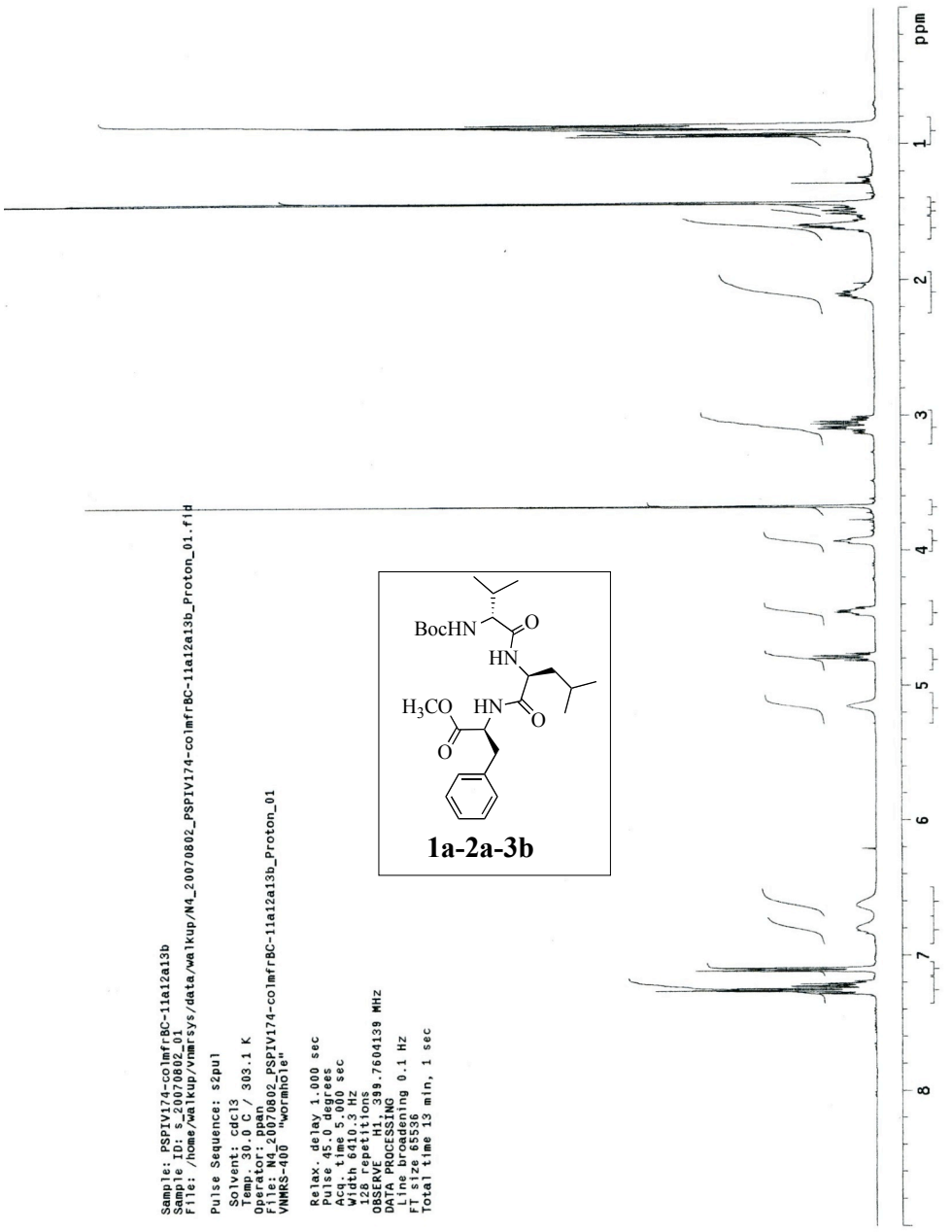
Sample: PSPIV174-colmfrBC-11a12a13b
Sample ID: s_20070802_01
File: /home/walkup/vnmrsys/data/walkup/N4_20070802_PSPIV174-colmfrBC-11a12a13b_Proton_01.fid
Pulse Sequence: s2pul
Solvent: cdcl3
Temp. 30.0 C / 303.1 K
Operator: ppan
File: N4_20070802_PSPIV174-colmfrBC-11a12a13b_Proton_01
VNMRS-400 "wormhole"
Relax. delay 1.000 sec
Pulse 45.0 degrees
Acq. time 5.000 sec
Width 6410.3 Hz
128 repetitions
OBSERVE H1, 399.7604139 MHz
DATA PROCESSING
Line broadening 0.1 Hz
FT size 65536
Total time 13 min, 1 sec
BocHN
O
HN
H3CO
HN
O
O
1a-2a-3b
ppm
1
2
3
4
5
6
7
8

1a-2a-3b

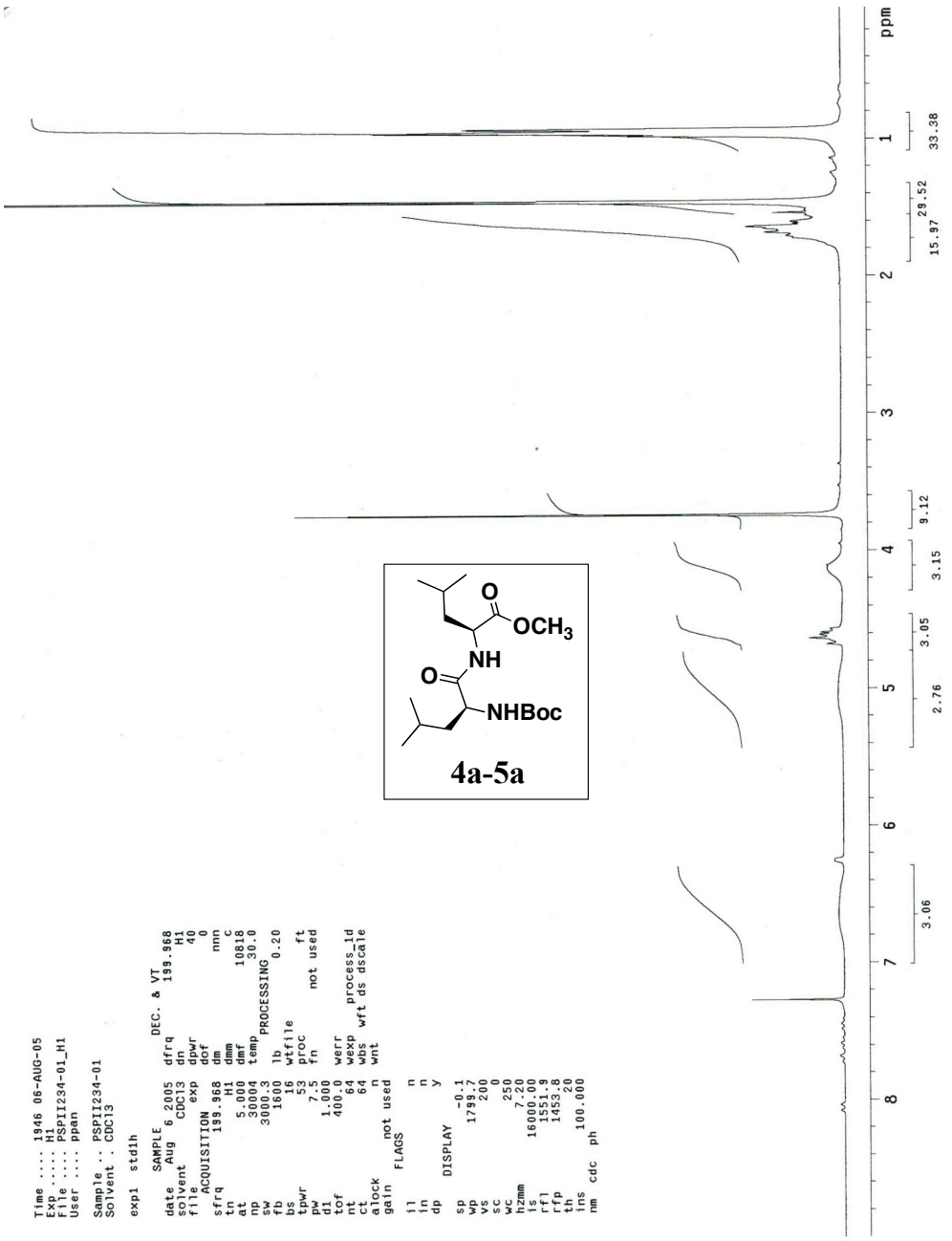
Time 1946 06-AUG-05
Exp H1
File ..... PSPII234-01_H1
User .... ppan
Sample .. PSPII234-01
Solvent . CDCl3
expl stdih
SAMPLE
date Aug 6 2005
solvent CDCl3
file exp
ACQUISITION
sfrq 199.968
tn H1
at 5.000
np 30004
sw 3000.3
fb 1600
bs 16
bwr 53
pw 7.5
d1 1.000
tof 400.0
nt 64
ct 64
alock n
gain not used
FLAGS
il n
in n
dp y
DISPLAY
sp -0.1
wp 1799.7
vs 200
sc 0
wc 250
hzmm 7.20
is 16000.00
rfl 1551.3
rfp 1453.8
th 20
ins 100.000
nm cdc ph
DEC. & VT
dfrq 199.968
dn H1
dpwr 40
dof 0
dm nnn
dmm c
dmf 10818
temp 30.0
PROCESSING
lb 0.20
wtfile
proc ft
fn not used
werr
wexp process_1d
wbs wft ds dscale
wnt
O
OCH3
NH
O
NHBoc
4a-5a
ppm
1
2
3
4
5
6
7
8
29.52
15.97
33.38
9.12
3.15
3.05
2.76
3.06

4a-5a

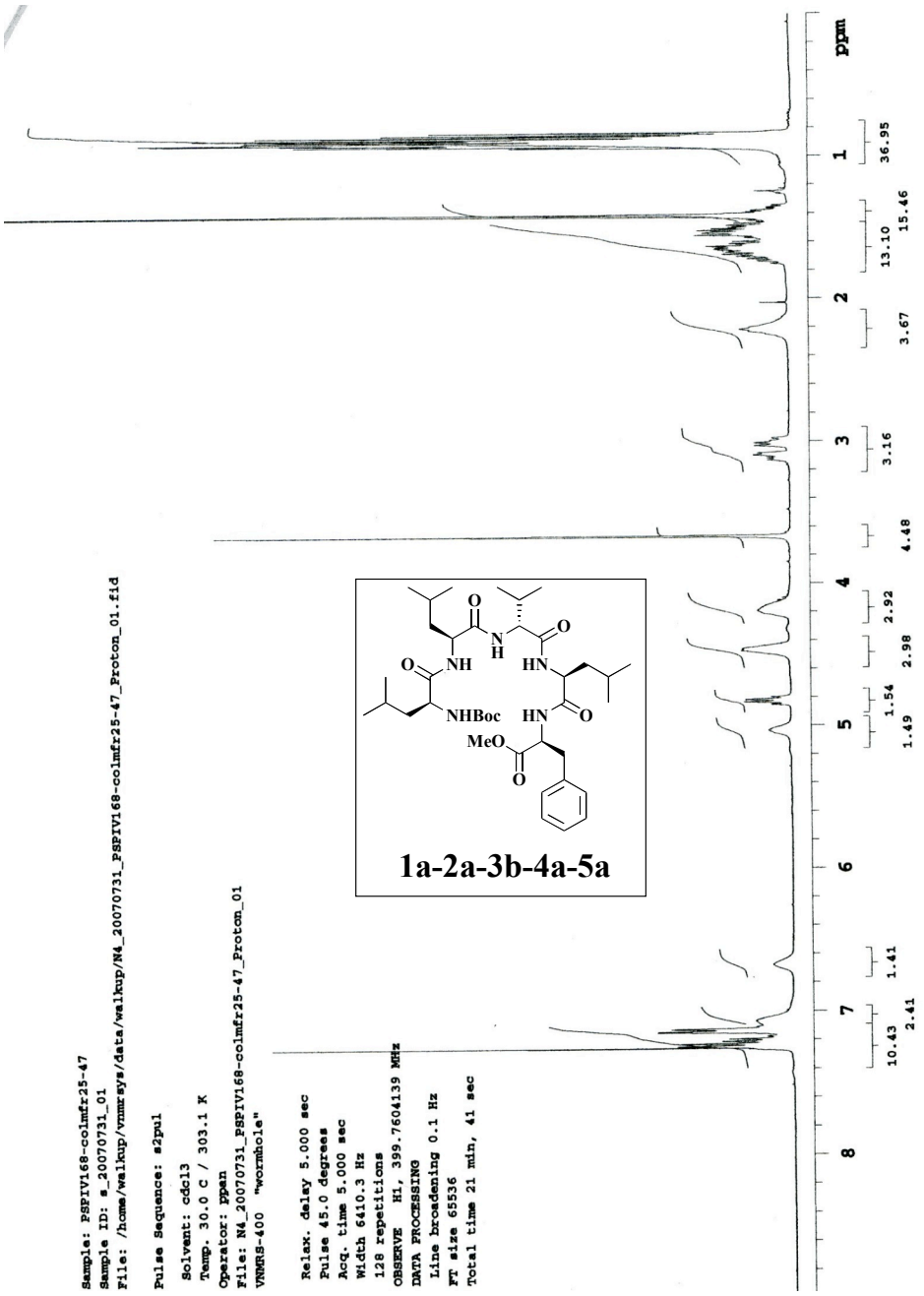
Sample: PSPIV168-colmfr25-47
Sample ID: s_20070731_01
File: /home/walkup/vnmrsys/data/walkup/N4_20070731_PSPIV168-colmfr25-47_Protcon_01.fid
Pulse Sequence: s2pul
Solvent: cdcl3
Temp. 30.0 C / 303.1 K
Operator: ppan
File: N4_20070731_PSPIV168-colmfr25-47_Protcon_01
VNMRS-400 "wormhole"
Relax. delay 5.000 sec
Pulse 45.0 degrees
Acq. time 5.000 sec
Width 6410.3 Hz
128 repetitions
OBSERVE H1, 399.7604139 MHz
DATA PROCESSING
Line broadening 0.1 Hz
FT size 65536
Total time 21 min, 41 sec
NH
NHBoc
HN
MeO
1a-2a-3b-4a-5a
ppm
10.43
1.41
2.41
1.54
1.49
2.92
2.98
3.16
4.48
3.67
13.10
15.46
36.95

1a-2a-3b-4a-5a

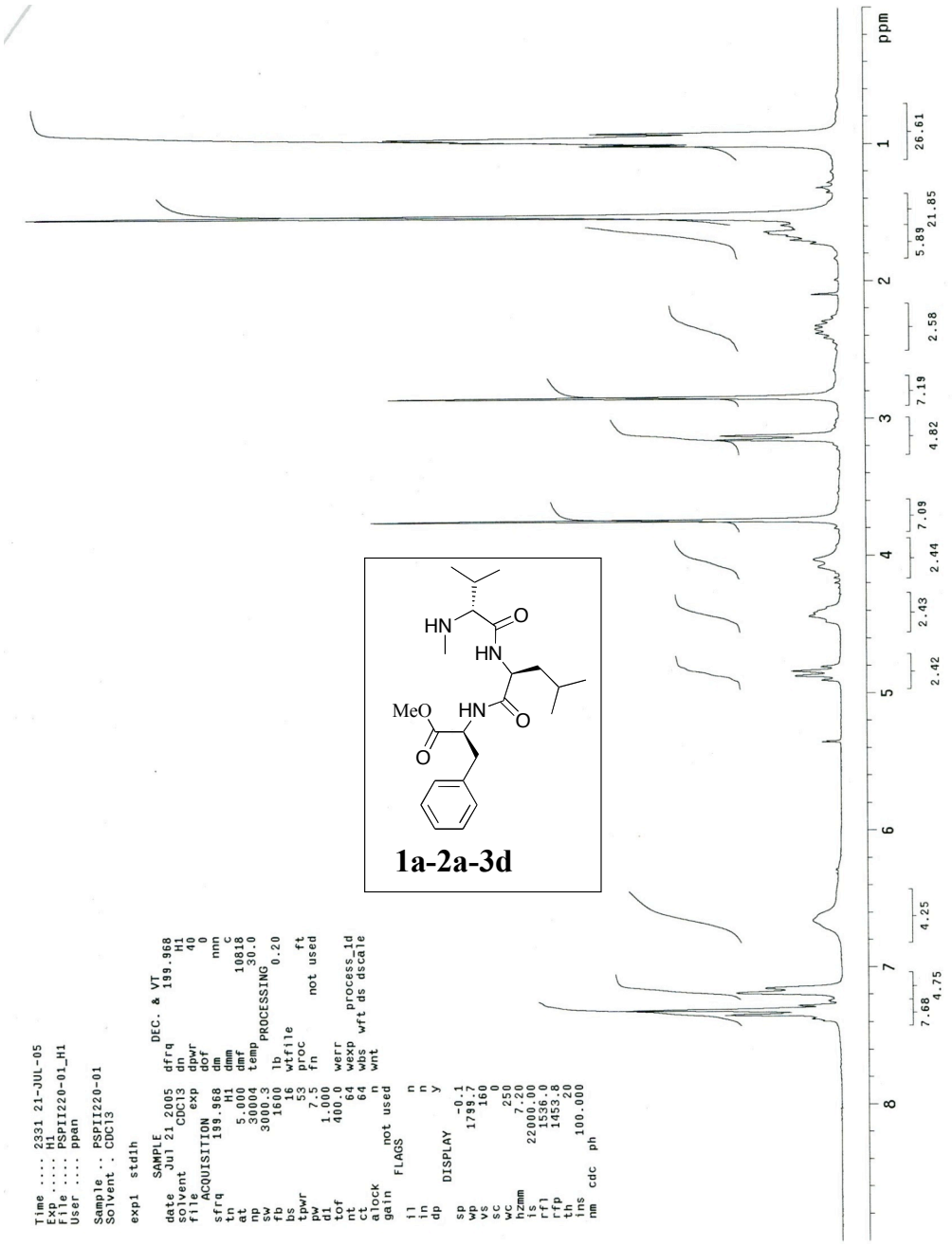
Time 2331 21-JUL-05
Exp H1
File ..... PSPII220-01_H1
User ..... ppan
Sample .. PSPII220-01
Solvent . CDCl3
exp1 std1h
DEC. & VT
SAMPLE
date Jul 21 2005
solvent CDCl3
file exp
ACQUISITION
sfrq 199.968
tn H1
at 5.000
np 30004
sw 3000.3
fb 1600
bs 16
tpwr 53
pw 7.5
d1 1.000
tof 400.0
nt 64
ct 64
alock n
gain not used
FLAGS
il n
in n
dp y
DISPLAY
sp -0.1
wp 1799.7
vs 160
sc 0
wc 250
hzmm 7.20
is 22000.00
rfl 1536.0
rfp 1453.8
th 20
ins 100.000
nm cdc ph
dfrq 199.968
dn H1
dpwr 40
dof 0
dmm nnn
dmf c
temp 10818
PROCESSING 30.0
lb 0.20
wtfile
proc ft
fn not used
werr
wexp process_1d
wbs wft ds dscale
wnt
HN
O
HN
MeO
HN
O
O
1a-2a-3d
ppm
1
2
3
4
5
6
7
8
26.61
5.89
21.85
2.58
7.19
4.82
7.09
2.44
2.43
2.42
4.25
7.68
4.75

1a-2a-3d

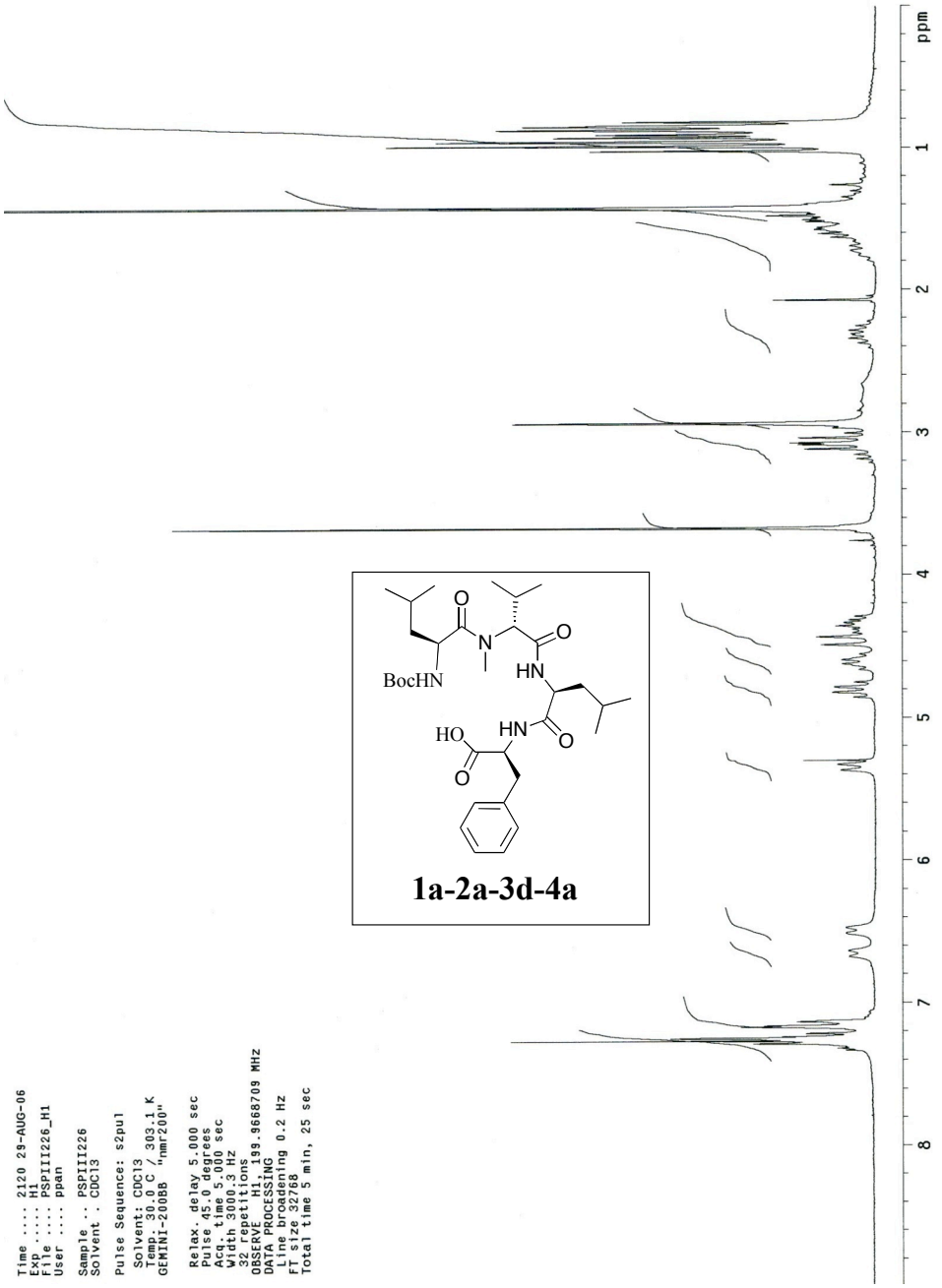
Time 2120 29-AUG-06
Exp H1
File ..... PSPIII226_H1
User .... ppan
Sample .. PSPIII226
Solvent . CDCl3
Pulse Sequence: s2pul
Solvent: CDCl3
Temp. 30.0 C / 303.1 K
GEMINI-200BB "nmr200"
Relax. delay 5.000 sec
Pulse 45.0 degrees
Acq. time 5.000 sec
Width 3000.3 Hz
32 repetitions
OBSERVE H1, 199.9668709 MHz
DATA PROCESSING
Line broadening 0.2 Hz
FT size 32768
Total time 5 min, 25 sec
BocHN
HO
HN
N
O
ppm
1a-2a-3d-4a

1a-2a-3d-4a

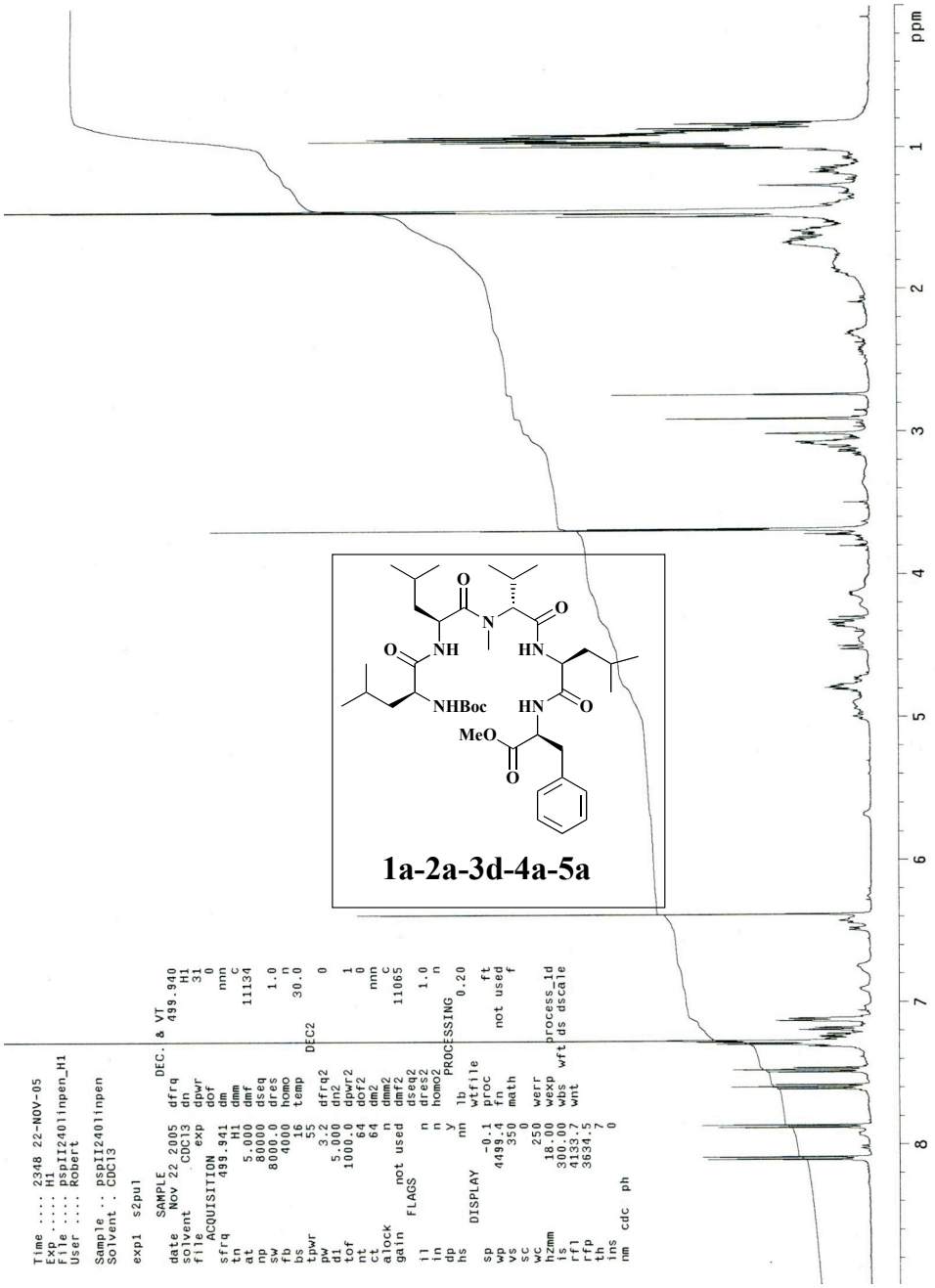

1a-2a-3d-4a-5a

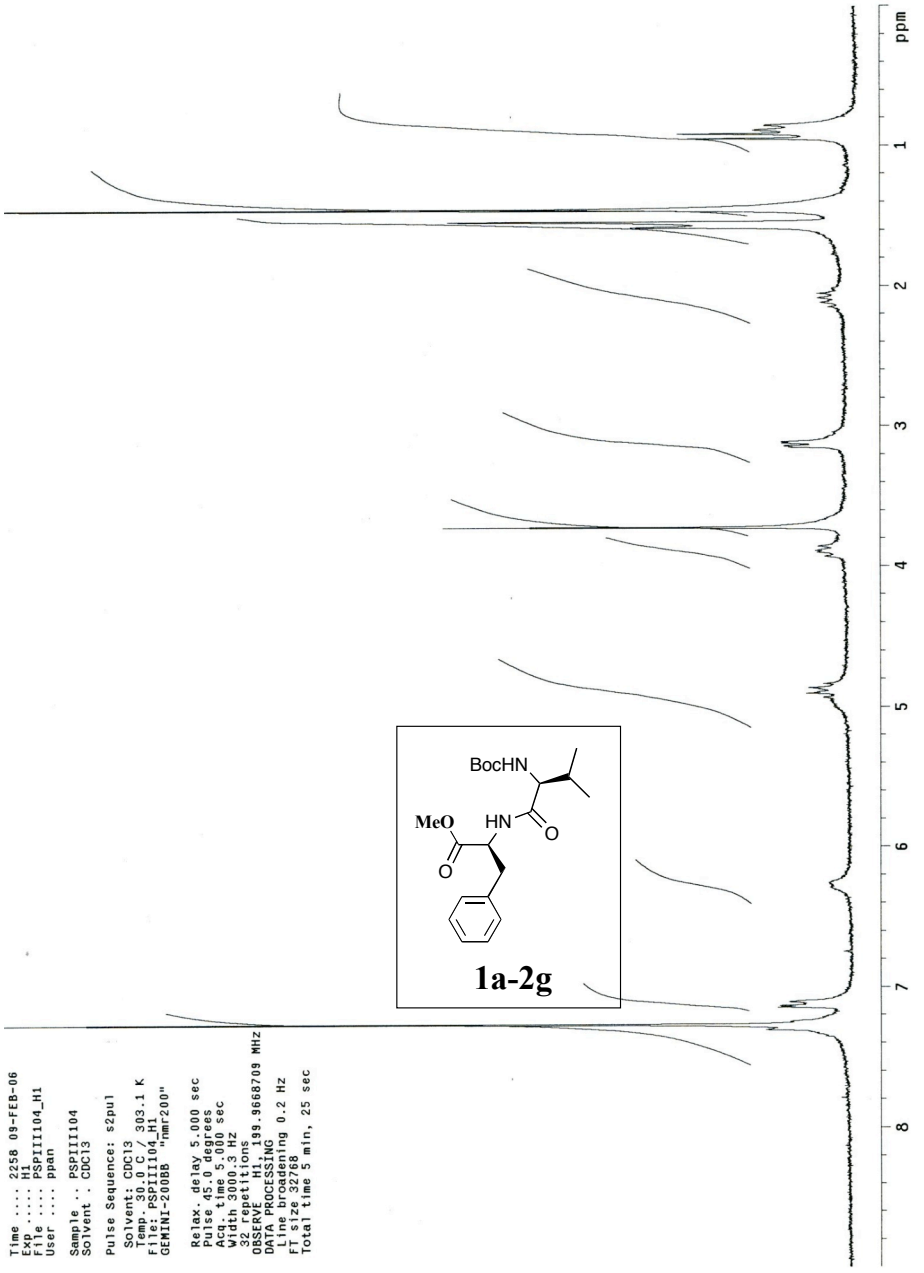
Time 2258 09-FEB-06
Exp H1
File .... PSPIII104_H1
User .... ppan
Sample .. PSPIII104
Solvent . CDCl3
Pulse Sequence: s2pul
Solvent: CDCl3
Temp. 30.0 C / 303.1 K
File: PSPIII104_H1
GEMINI-200BB "nmr200"
Relax. delay 5.000 sec
Pulse 45.0 degrees
Acq. time 5.000 sec
Width 3000.3 Hz
32 repetitions
OBSERVE H1, 199.9668709 MHz
DATA PROCESSING
Line broadening 0.2 Hz
FT size 32768
Total time 5 min, 25 sec
BocHN
MeO
HN
O
O
1a-2g
ppm
1
2
3
4
5
6
7
8

1a-2g

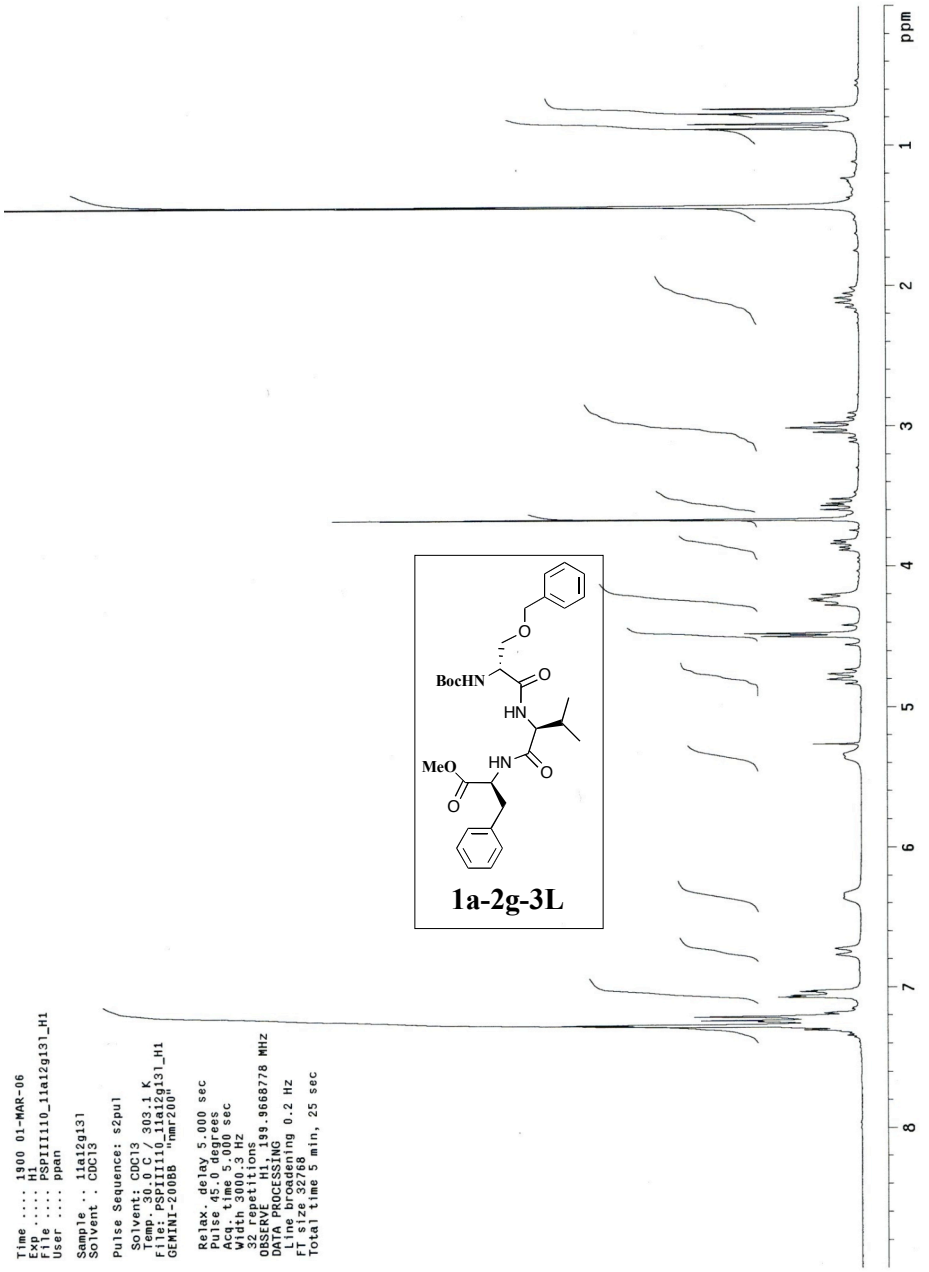
Time 1900 01-MAR-06
Exp H1
File ..... PSPIII110_11a12g131_H1
User ..... ppan
Sample .. 11a12g131
Solvent . CDCl3
Pulse Sequence: s2pul
Solvent: CDCl3
Temp. 30.0 C / 303.1 K
File: PSPIII110_11a12g131_H1
GEMINI-200BB "nmr200"
Relax. delay 5.000 sec
Pulse 45.0 degrees
Acq. time 5.000 sec
Width 3000.3 Hz
32 repetitions
OBSERVE H1, 199.9668778 MHz
DATA PROCESSING
Line broadening 0.2 Hz
FT size 32768
Total time 5 min, 25 sec
BocHN
HN
HN
MeO
O
O
O
O
1a-2g-3L
ppm
1
2
3
4
5
6
7
8

1a-2g-3L

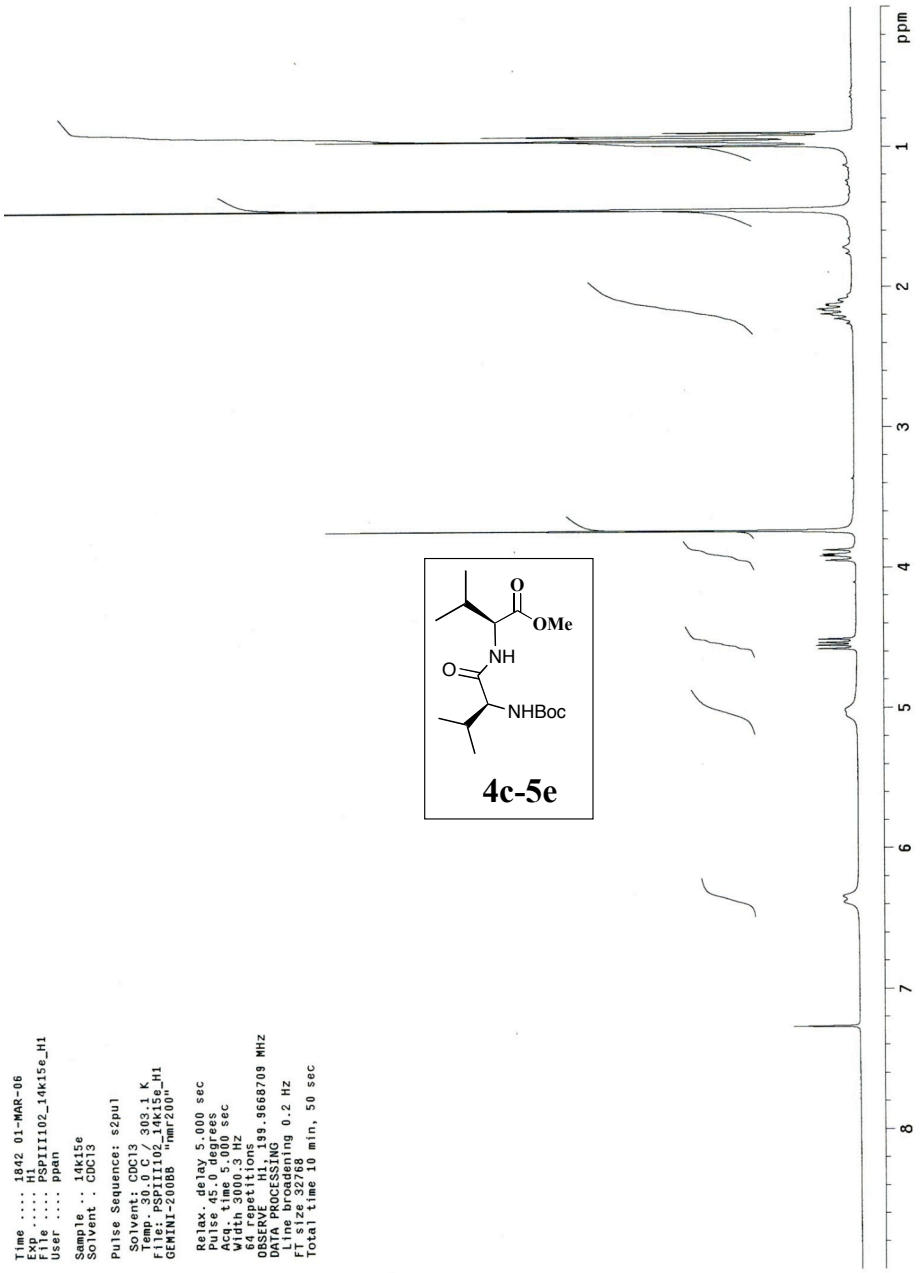
Time 1842 01-MAR-06
Exp H1
File ..... PSPIII102_14k15e_H1
User .... ppan
Sample .. 14k15e
Solvent . CDCl3
Pulse Sequence: s2pul
Solvent: CDCl3
Temp. 30.0 C / 303.1 K
File: PSPIII102_14k15e_H1
GEMINI-200BB "nmr200"
Relax. delay 5.000 sec
Pulse 45.0 degrees
Acq. time 5.000 sec
Width 3000.3 Hz
64 repetitions
OBSERVE H1, 199.9668709 MHz
DATA PROCESSING
Line broadening 0.2 Hz
FT size 32768
Total time 10 min, 50 sec
O
OMe
NH
O
NHBoc
4c-5e
ppm
1
2
3
4
5
6
7
8

4c-5e

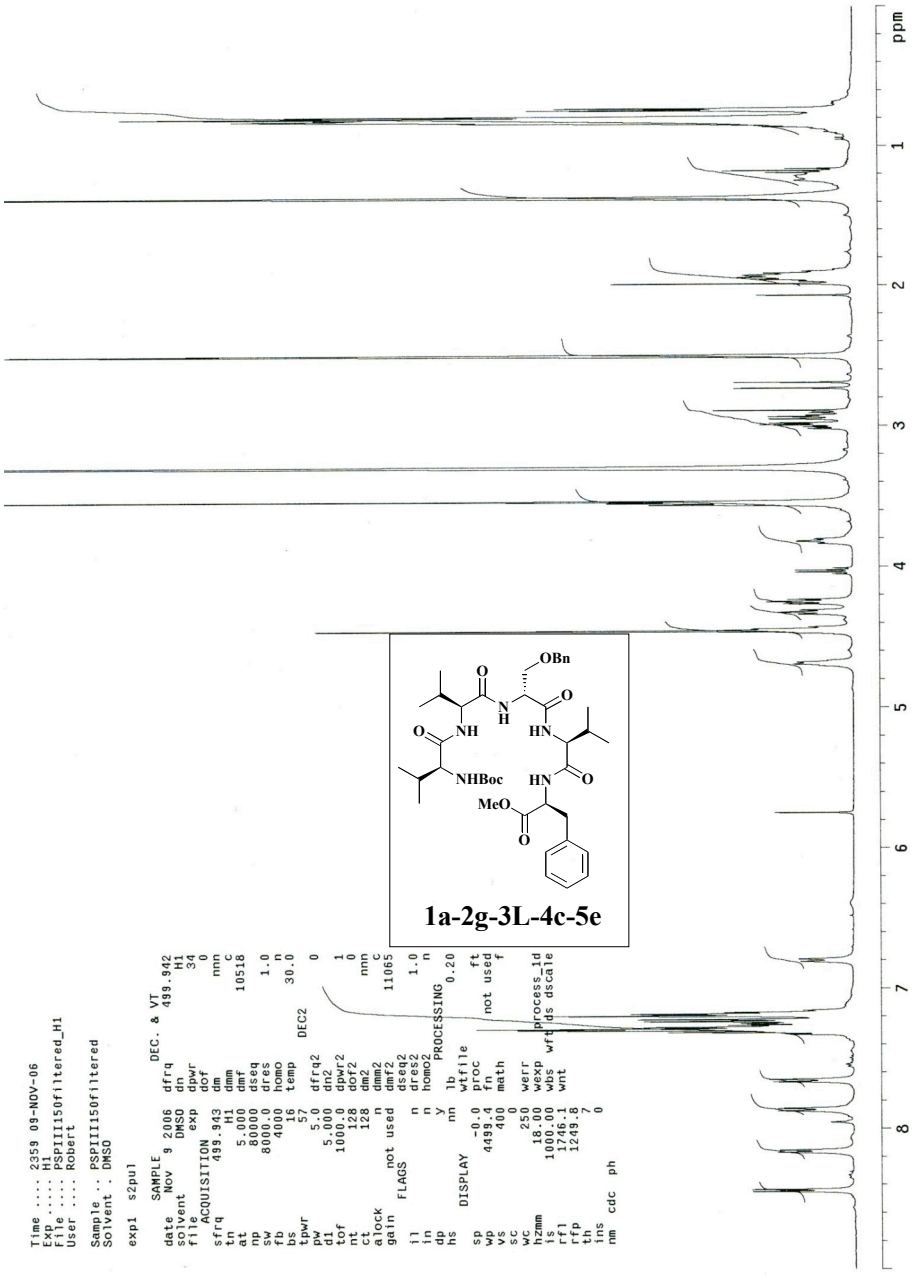
Time 2359 09-NOV-06
Exp H1
File .... PSPIII150filtered_H1
User .... Robert
Sample .. PSPIII150filtered
Solvent . DMSO
exp1 s2pul
SAMPLE
date Nov 9 2006
solvent DMSO
file exp
ACQUISITION
sfrq 499.943
tn H1
at 5.000
np 80000
sw 8000.0
fb 4000
bs 16
tpwr 57
pw 5.000
d1 1000.0
tof 128
nt 128
ct n
alock not used
gain FLAGS n
y
nn
DISPLAY
sp -0.0
wp 4499.4
vs 400
sc 0
wc 250
hzmm 18.00
is 1000.00
rfl 1746.1
rfp 1249.8
th 7
ins 0
nm cdc ph
DEC. & VT
dfrq 499.942
dn H1
dpwr 34
dof 0
dm nnn
dmm c
dmf 10518
dseq
dres
homo
temp 30.0
DEC2
dfrq2 0
dn2
dpwr2 1
dof2 0
dm2 nnn
dmm2 c
dmf2 11065
dseq2
dres2 1.0
homo2 n
PROCESSING
lb 0.20
wtfile
proc ft
fn not used
math f
werr
wexp process_1d
wbs wft ds dscale
wnt
OBn
NHBoc
MeO
1a-2g-3L-4c-5e
ppm

1a-2g-3L-4c-5e

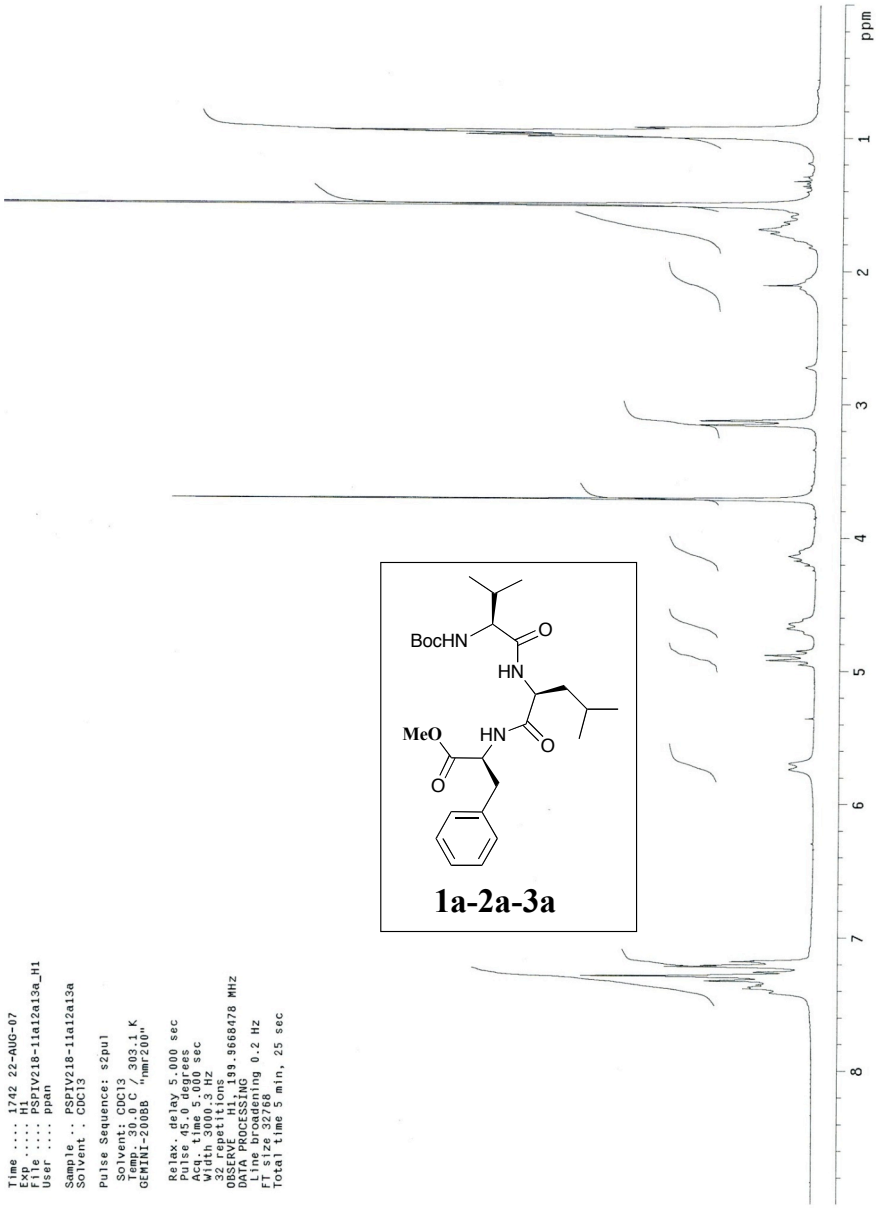
Time 1742 22-AUG-07
Exp. H1
File ..... PSPIV218-11a12a13a_H1
User ..... ppan
Sample .. PSPIV218-11a12a13a
Solvent . CDCl3
Pulse Sequence: s2pul
Solvent: CDCl3
Temp. 30.0 C / 303.1 K
GEMINI-200BB "nmr200"
Relax. delay 5.000 sec
Pulse 45.0 degrees
Acq. time 5.000 sec
Width 3000.3 Hz
32 repetitions
OBSERVE H1 199.9668478 MHz
DATA PROCESSING
Line broadening 0.2 Hz
FT size 32768
Total time 5 min, 25 sec
BocHN
HN
MeO
HN
O
O
O
1a-2a-3a
ppm
1
2
3
4
5
6
7
8

1a-2a-3a

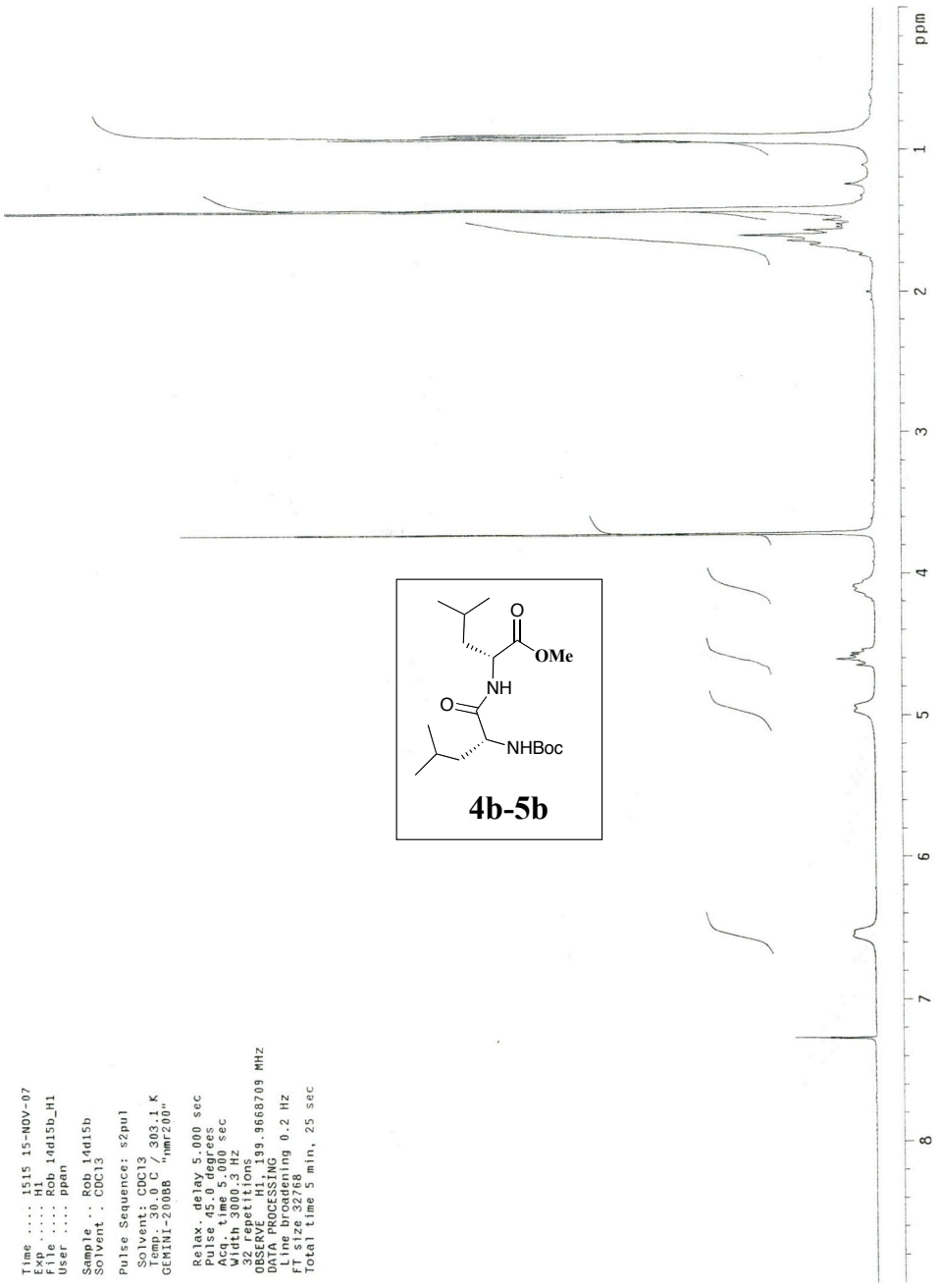
Time 1515 15-NOV-07
Exp H1
File ..... Rob 14d15b_H1
User .... ppan
Sample .. Rob 14d15b
Solvent . CDCl3
Pulse Sequence: s2pul
Solvent: CDCl3
Temp. 30.0 C / 303.1 K
GEMINI-200BB "nmr200"
Relax. delay 5.000 sec
Pulse 45.0 degrees
Acq. time 5.000 sec
Width 3000.3 Hz
32 repetitions
OBSERVE H1, 199.9668709 MHz
DATA PROCESSING
Line broadening 0.2 Hz
FT size 32768
Total time 5 min, 25 sec
OMe
NH
O
NHBoc
4b-5b
ppm
1
2
3
4
5
6
7
8

4b-5b

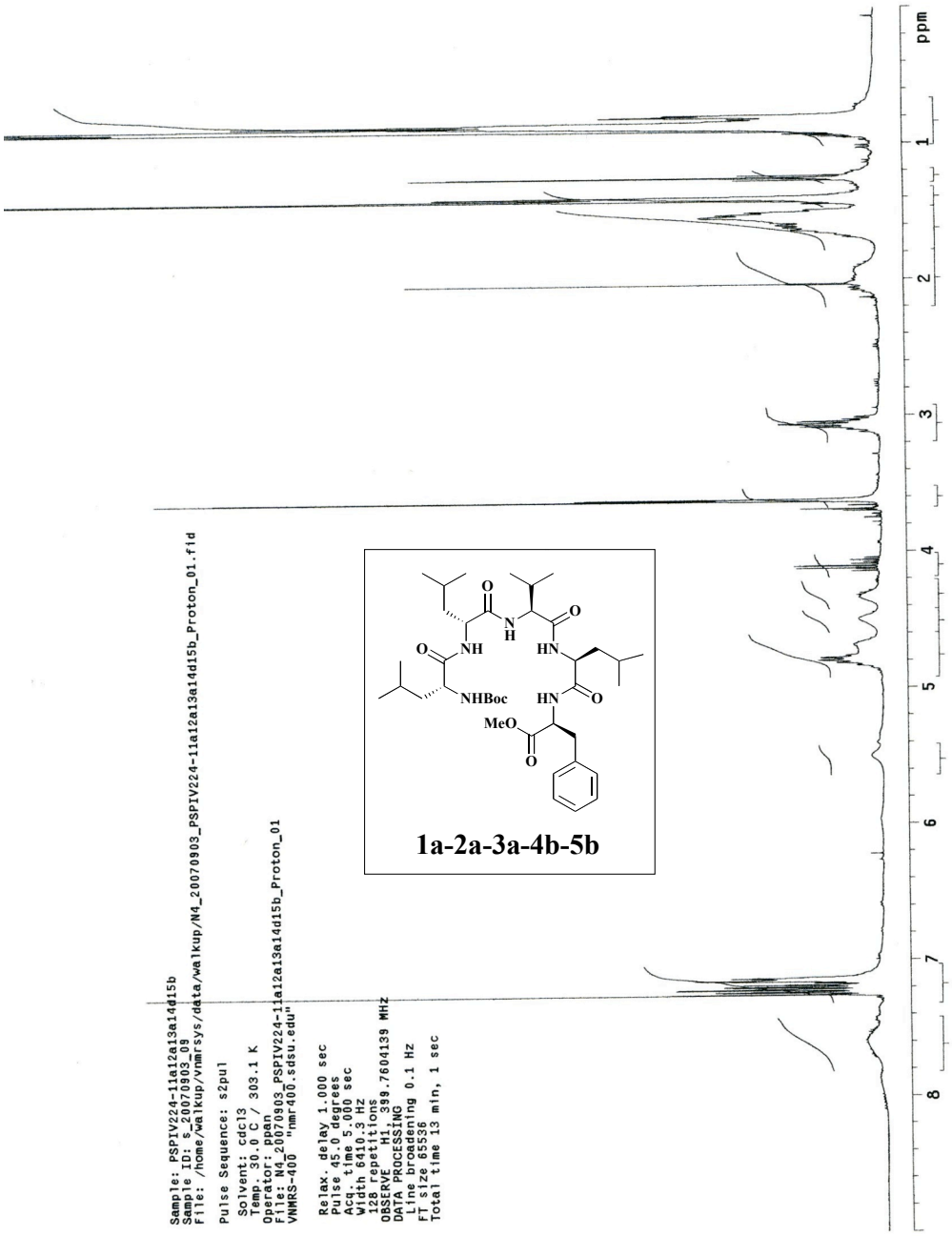
Sample: PSPIV224-11a12a13a14d15b
Sample ID: s_20070903_09
File: /home/walkup/vnmrsys/data/walkup/N4_20070903_PSPIV224-11a12a13a14d15b_Proton_01.fid
Pulse Sequence: s2pul
Solvent: cdcl3
Temp. 30.0 C / 303.1 K
Operator: ppan
File: N4_20070903_PSPIV224-11a12a13a14d15b_Proton_01
VNMRS-400 "nmr400.sdsu.edu"
Relax. delay 1.000 sec
Pulse 45.0 degrees
Acq. time 5.000 sec
Width 6410.3 Hz
128 repetitions
OBSERVE H1, 399.7604139 MHz
DATA PROCESSING
Line broadening 0.1 Hz
FT size 65536
Total time 13 min, 1 sec
NHBoc
MeO
1a-2a-3a-4b-5b
ppm
1
2
3
4
5
6
7
8

1a-2a-3a-4b-5b

^{1}H NMR for Holliday Junction Project

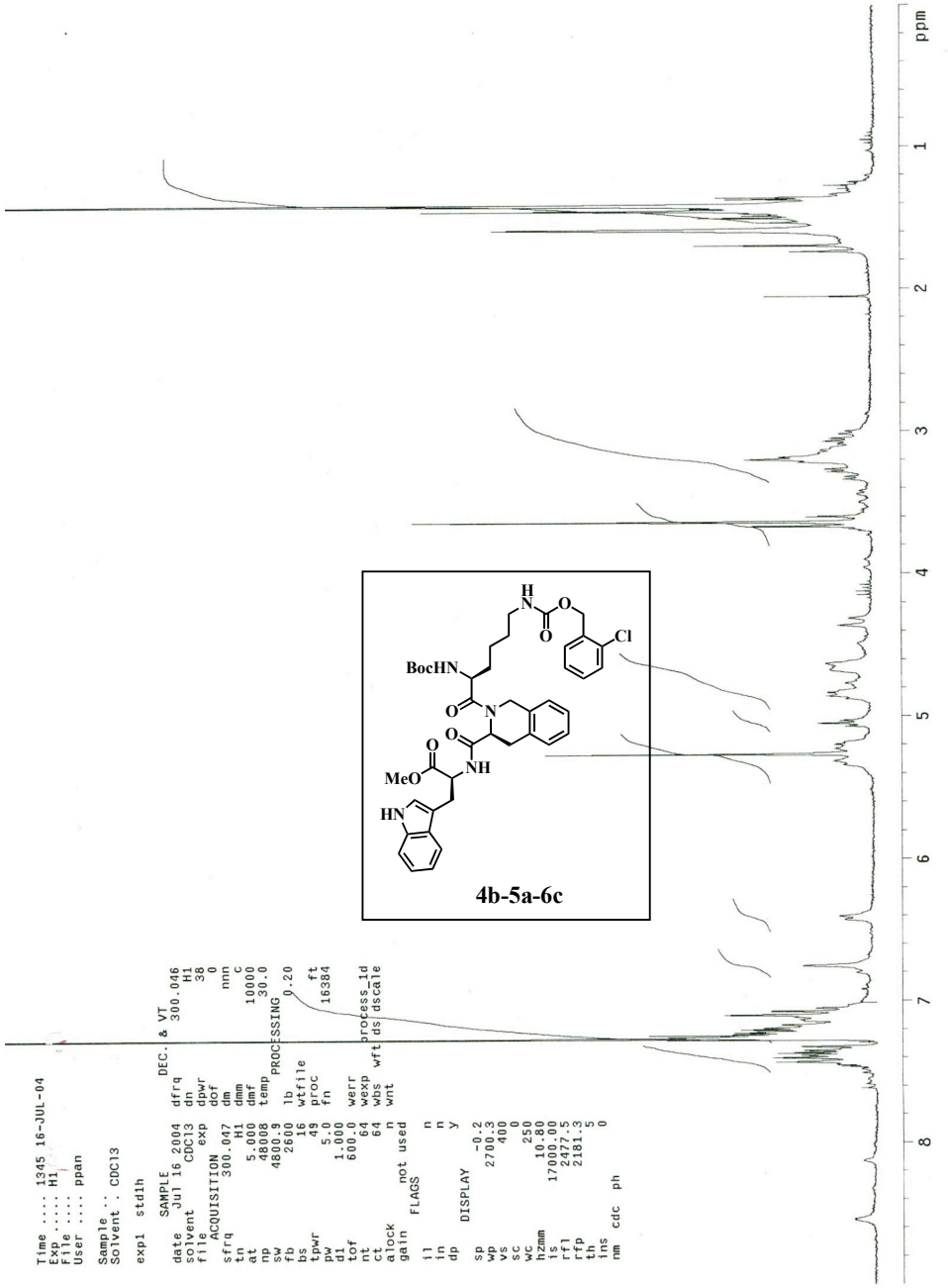

4b-5a-6c

^{1}H NMR for Azatandem

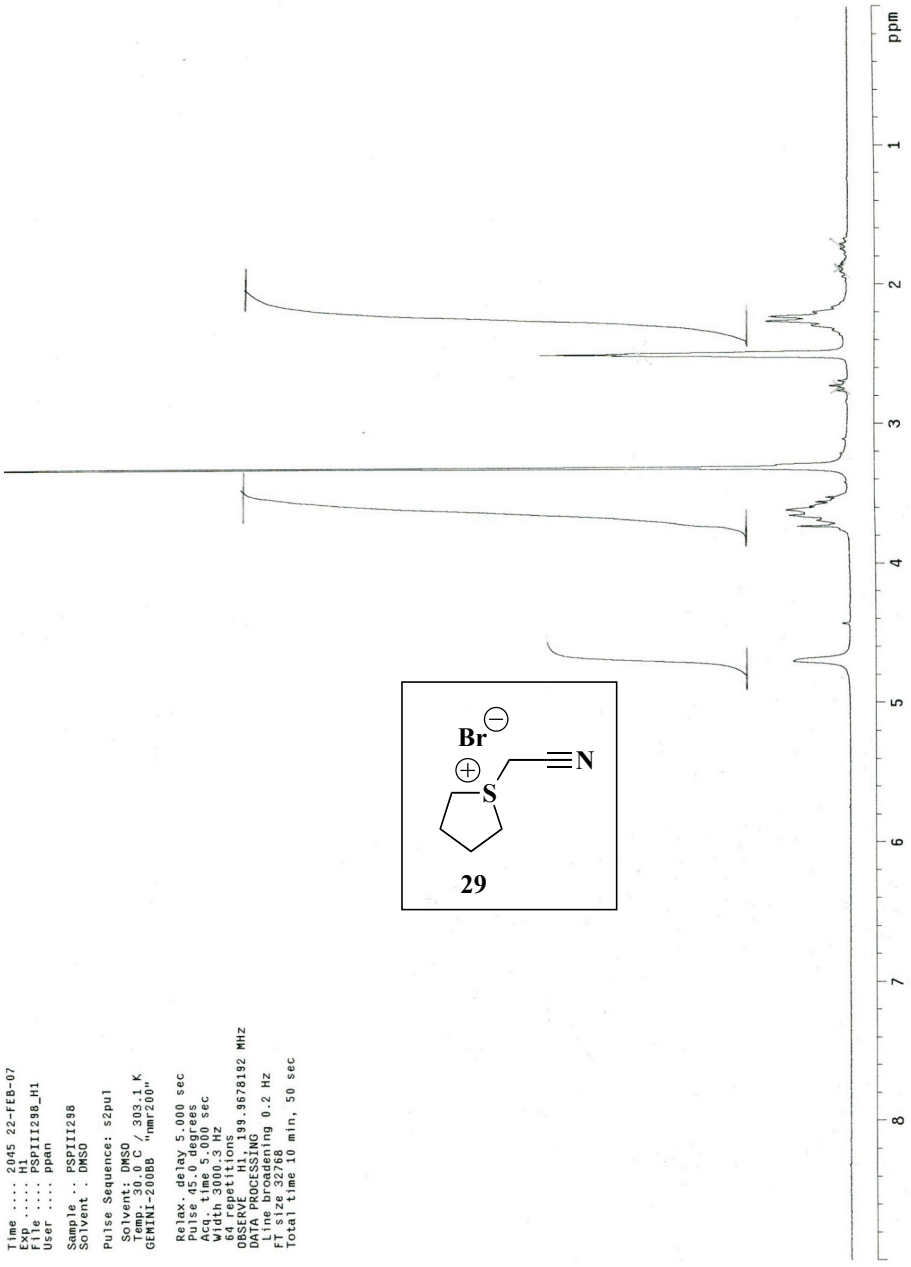

Compound **29**

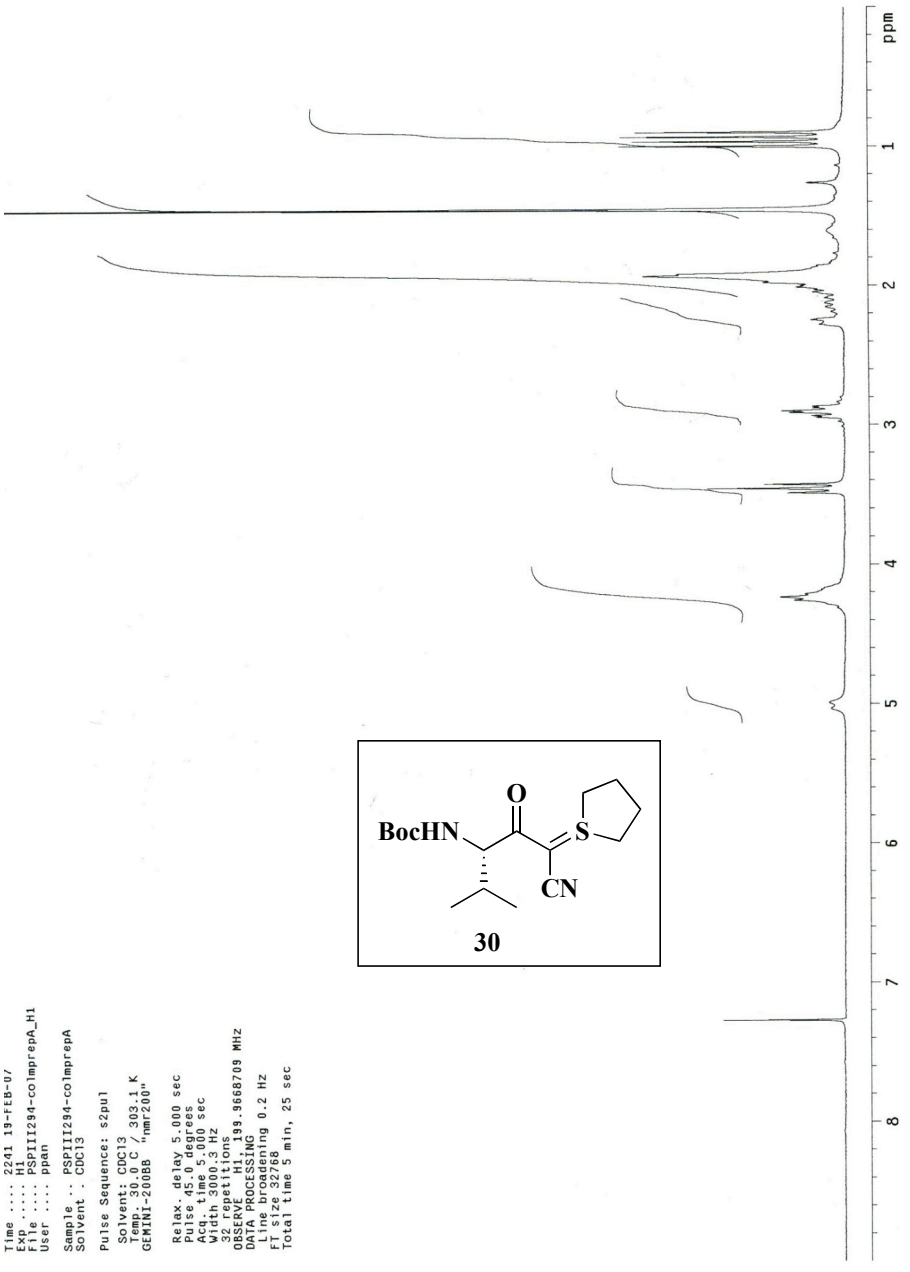
Time 2241 19-FEB-07
Exp H1
File ..... PSPIII294-colmprepA_H1
User ..... ppan
Sample .. PSPIII294-colmprepA
Solvent . CDCl3
Pulse Sequence: s2pul
Solvent: CDCl3
Temp. 30.0 C / 303.1 K
GEMINI-200BB "nmr200"
Relax. delay 5.000 sec
Pulse 45.0 degrees
Acq. time 5.000 sec
Width 3000.3 Hz
32 repetitions
OBSERVE H1, 199.9668709 MHz
DATA PROCESSING
Line broadening 0.2 Hz
FT size 32768
Total time 5 min, 25 sec
BocHN
O
S
CN
30
ppm
1
2
3
4
5
6
7
8

Compound **30**

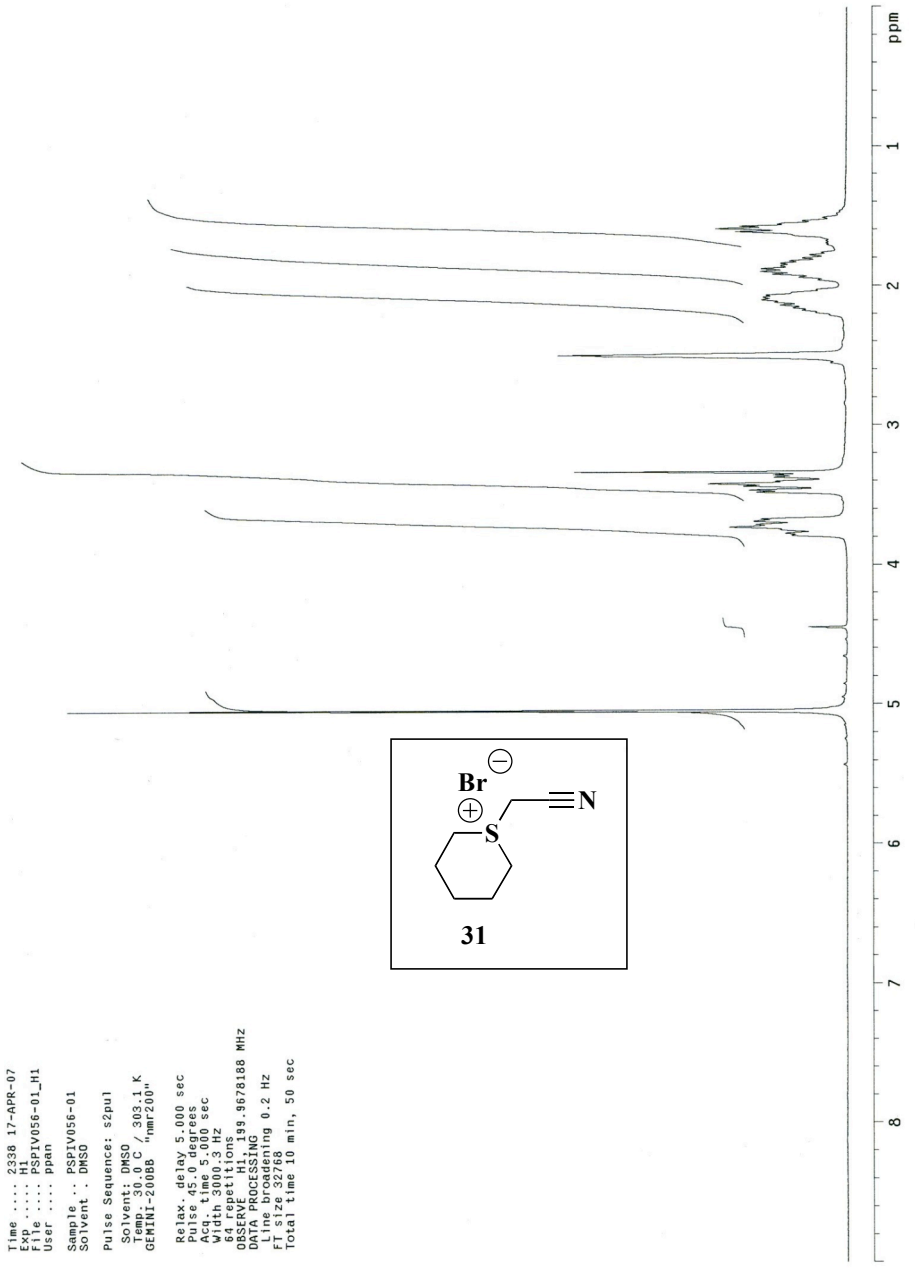
Time 2338 17-APR-07
Exp H1
File ..... PSPIV056-01_H1
User ..... ppan
Sample .. PSPIV056-01
Solvent . DMSO
Pulse Sequence: s2pul
Solvent: DMSO
Temp: 30.0 C / 303.1 K
GEMINI-200BB "mm7200"
Relax. delay 5.000 sec
Pulse 45.0 degrees
Acq. time 5.000 sec
Width 3000.3 Hz
64 repetitions
OBSERVE H1, 199.9678188 MHz
DATA PROCESSING
Line broadening 0.2 Hz
FT size 32768
Total time 10 min, 50 sec
Br
N
S
31
ppm
1
2
3
4
5
6
7
8

Compound **31**

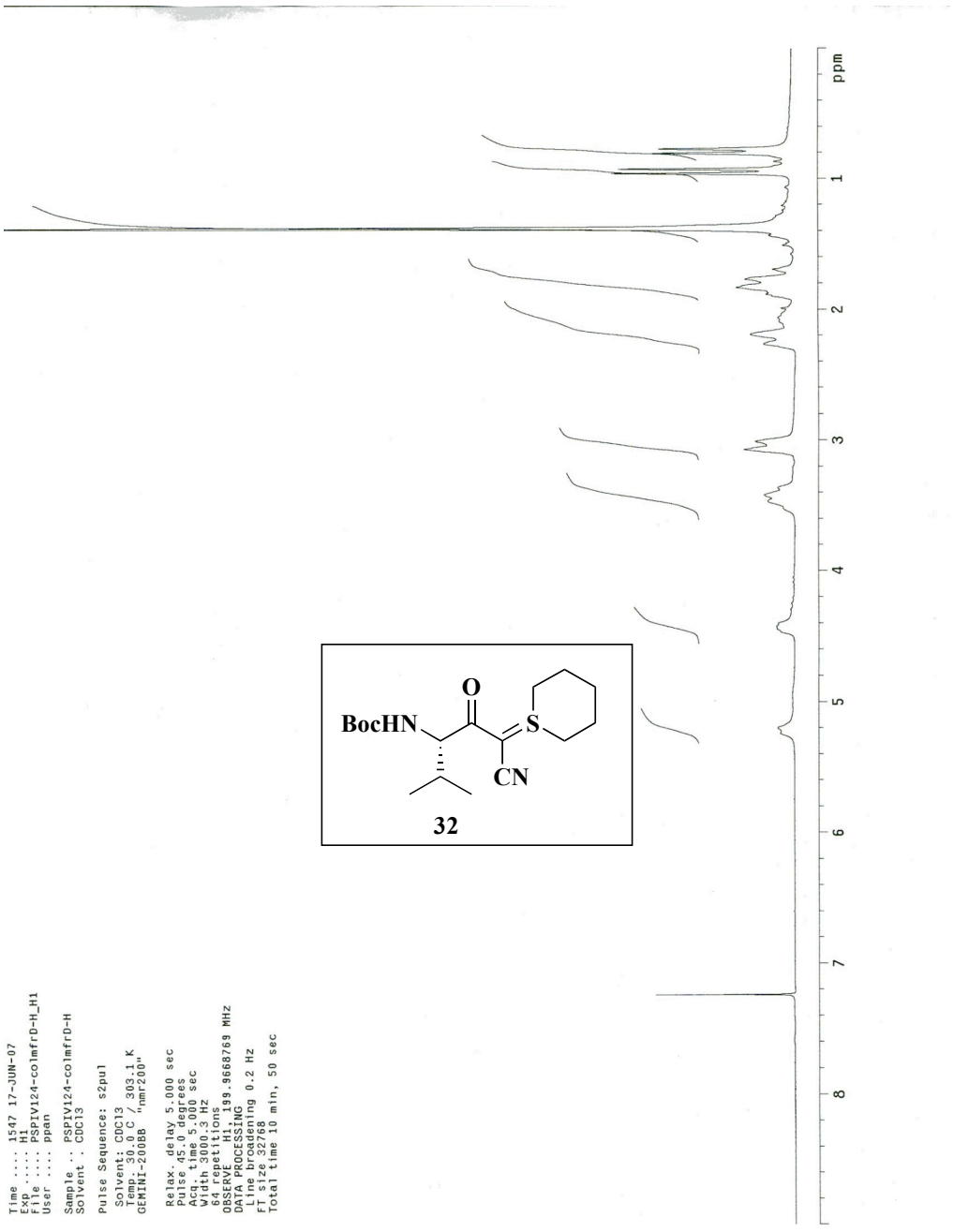
Time 1547 17-JUN-07
Exp H1
File ..... PSPIV124-colmfrD-H_H1
User .... ppan
Sample .. PSPIV124-colmfrD-H
Solvent . CDCl3
Pulse Sequence: s2pul
Solvent: CDCl3
Temp. 30.0 C / 303.1 K
GEMINI-200BB "nmr200"
Relax. delay 5.000 sec
Pulse 45.0 degrees
Acq. time 5.000 sec
Width 3001.2 Hz
64 repetitions
OBSERVE H1, 199.9668769 MHz
DATA PROCESSING
Line broadening 0.2 Hz
FT size 32768
Total time 10 min, 50 sec
BocHN
O
S
CN
32
ppm
1
2
3
4
5
6
7
8

Compound **32**

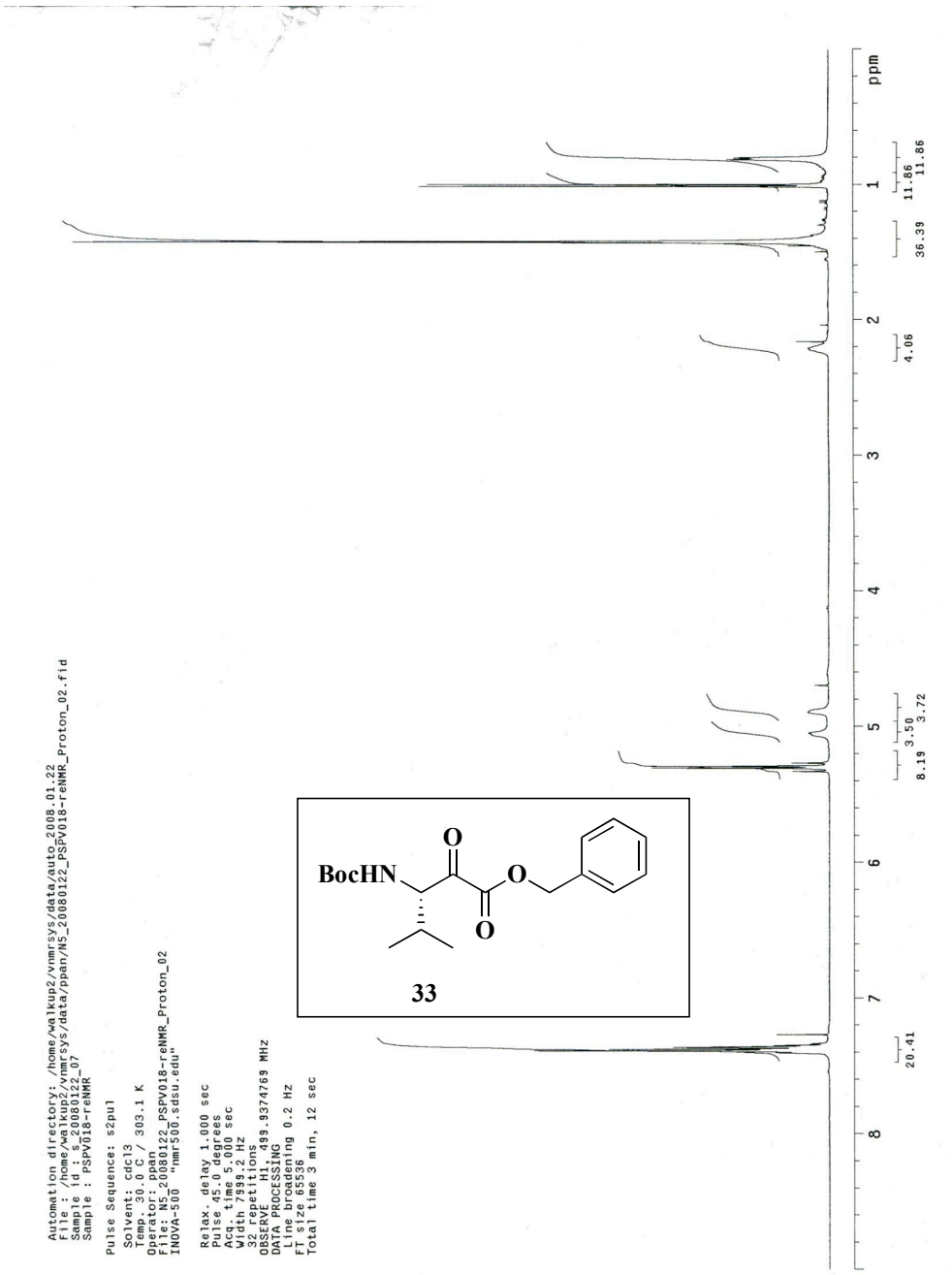
Automation directory: /home/walkup2/vnmrsys/data/auto_0108-01_22
File : /home/walkup2/vnmrsys/data/ppan/N5_20080122_PSPV018-reNMR_Proton_02.fid
Sample id: 20080122_07
Sample : PSPV018-reNMR
Pulse Sequence: s2pul
Solvent: cdcl3
Temp. 30.0 C / 303.1 K
Operator: ppan
File: N5_20080122_PSPV018-reNMR_Proton_02
INOVA-500 "nmr500.sdsu.edu"
Relax. delay 1.000 sec
Pulse 45.0 degrees
Acq. time 5.000 sec
Width 7911.2 Hz
32 repetitions
OBSERVE H1, 499.9374769 MHz
DATA PROCESSING
Line broadening 0.2 Hz
FT size 65536
Total time 3 min, 12 sec
BocHN
O
O
O
33
ppm
20.41
8.19
3.50
3.72
4.06
36.39
11.86
11.86

Compound **33**

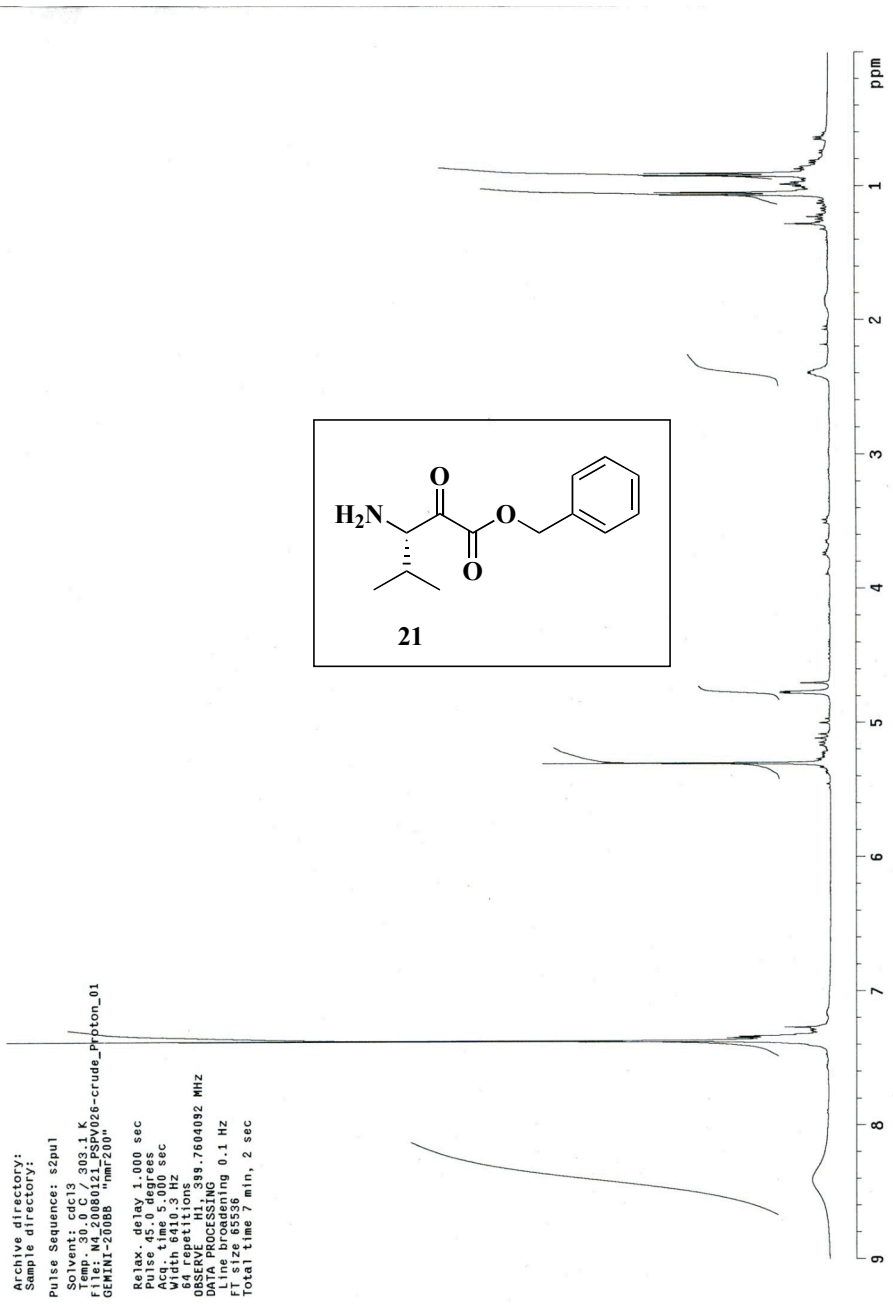
Archive directory:
Sample directory:
Pulse Sequence: s2pul
Solvent: cdcl3
Temp. 30.0 C / 303.1 K
File: N4_20080121_PSPV026-crude_Proton_01
GEMINI-2008B "nmr200"
Relax. delay 1.000 sec
Pulse 45.0 degrees
Acq. time 5.000 sec
Width 6410.3 Hz
64 repetitions
OBSERVE H1, 399.7604092 MHz
DATA PROCESSING
Line broadening 0.1 Hz
FT size 65536
Total time 7 min, 2 sec
ppm
1
2
3
4
5
6
7
8
9
H2N
O
O
O
21

Compound **21**

LCMS for Sansalvamide A derivatives

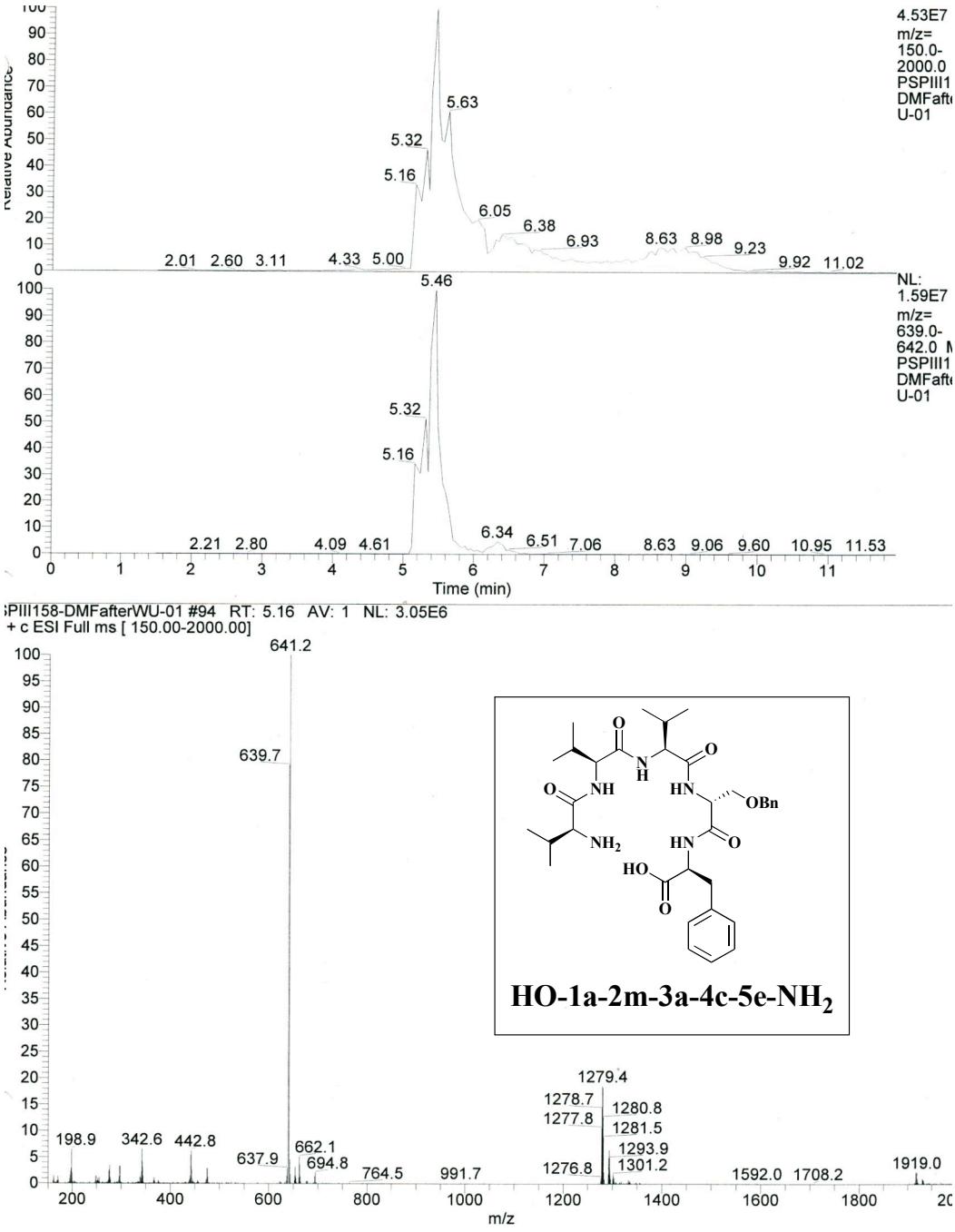

HO-1a-2m-3a-4c-5e-NH_2

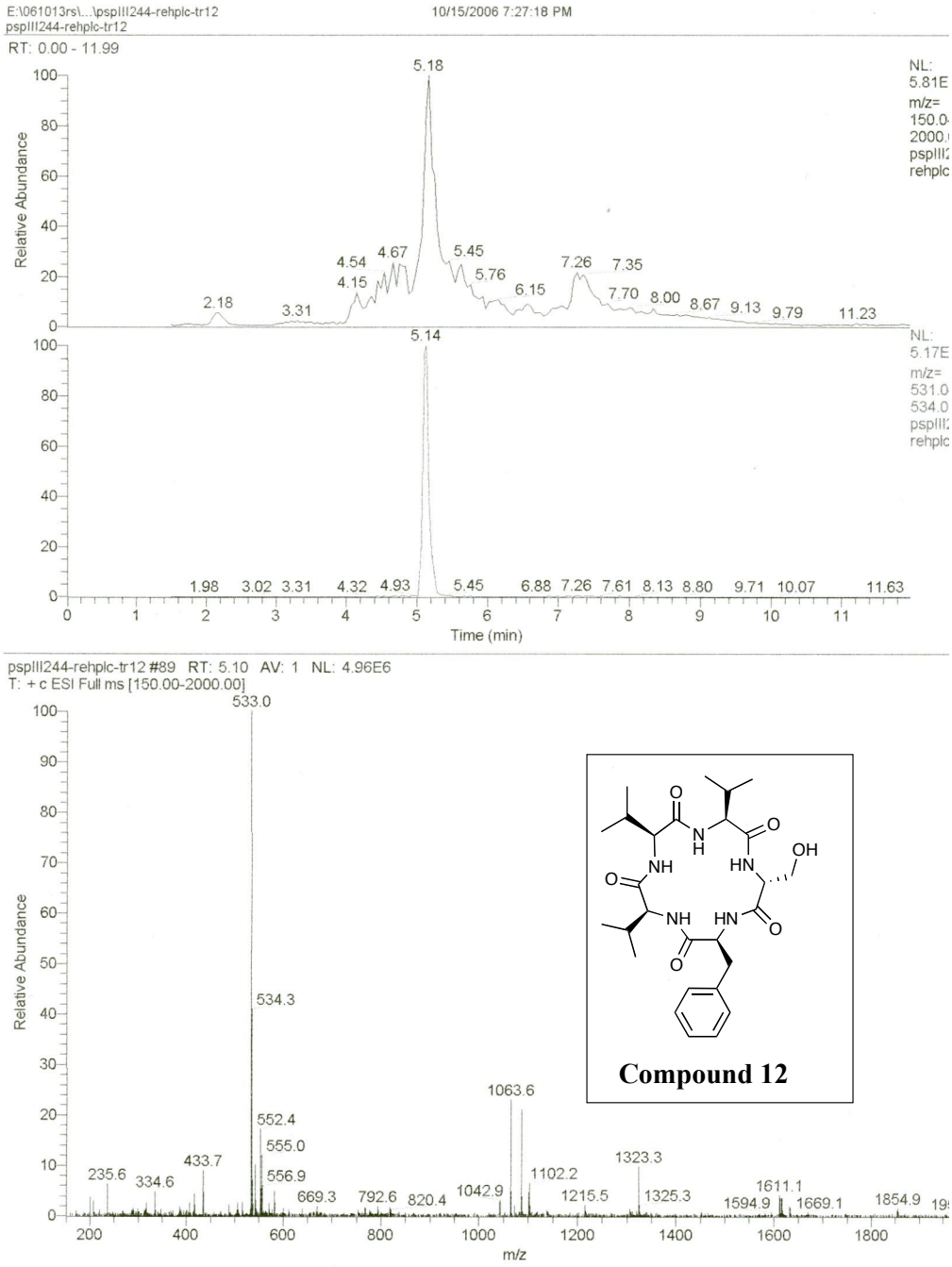
E:\061013rs\...\pspIII244-rehplc-tr12
10/15/2006 7:27:18 PM
pspIII244-rehplc-tr12
RT: 0.00 - 11.99
Relative Abundance
Time (min)
pspIII244-rehplc-tr12 #89 RT: 5.10 AV: 1 NL: 4.96E6
T: + c ESI Full ms [150.00-2000.00]
m/z
Compound 12

Compound 12

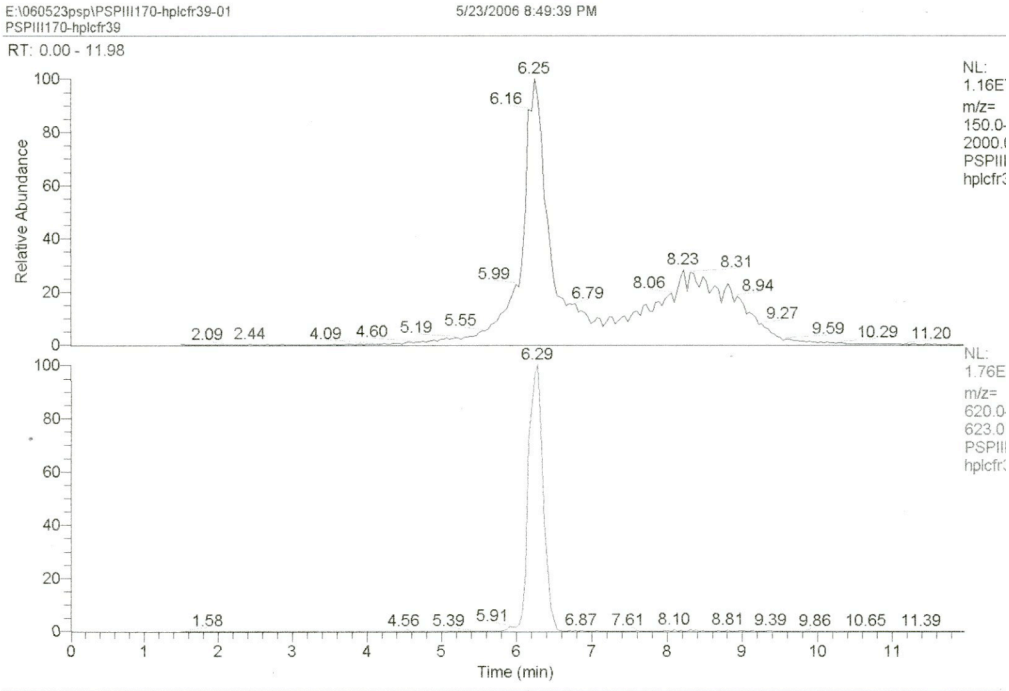
E:\060523psp\PSPIII170-hplcfr39-01
PSPIII170-hplcfr39
5/23/2006 8:49:39 PM
RT: 0.00 - 11.98
Relative Abundance
Time (min)
NL:
m/z=
6.25
6.16
5.99
6.79
8.23
8.31
8.06
8.94
9.27
2.09 2.44
4.09 4.60 5.19 5.55
9.59 10.29 11.20
6.29
1.58
4.56 5.39 5.91
6.87 7.61 8.10 8.81 9.39 9.86 10.65 11.39

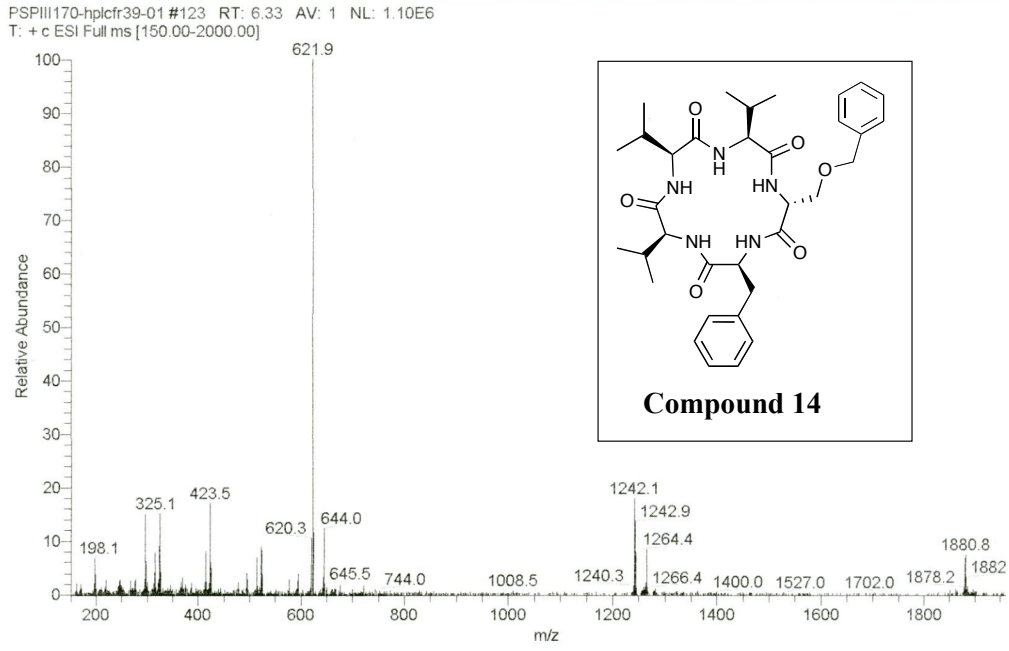
PSPIII170-hplcfr39-01 #123 RT: 6.33 AV: 1 NL: 1.10E6
T: + c ESI Full ms [150.00-2000.00]
Relative Abundance
m/z
621.9
325.1
423.5
620.3
644.0
198.1
645.5
744.0
1008.5
1240.3
1242.1
1242.9
1264.4
1266.4
1400.0
1527.0
1702.0
1878.2
1880.8
1882

Compound 14

Compound 14

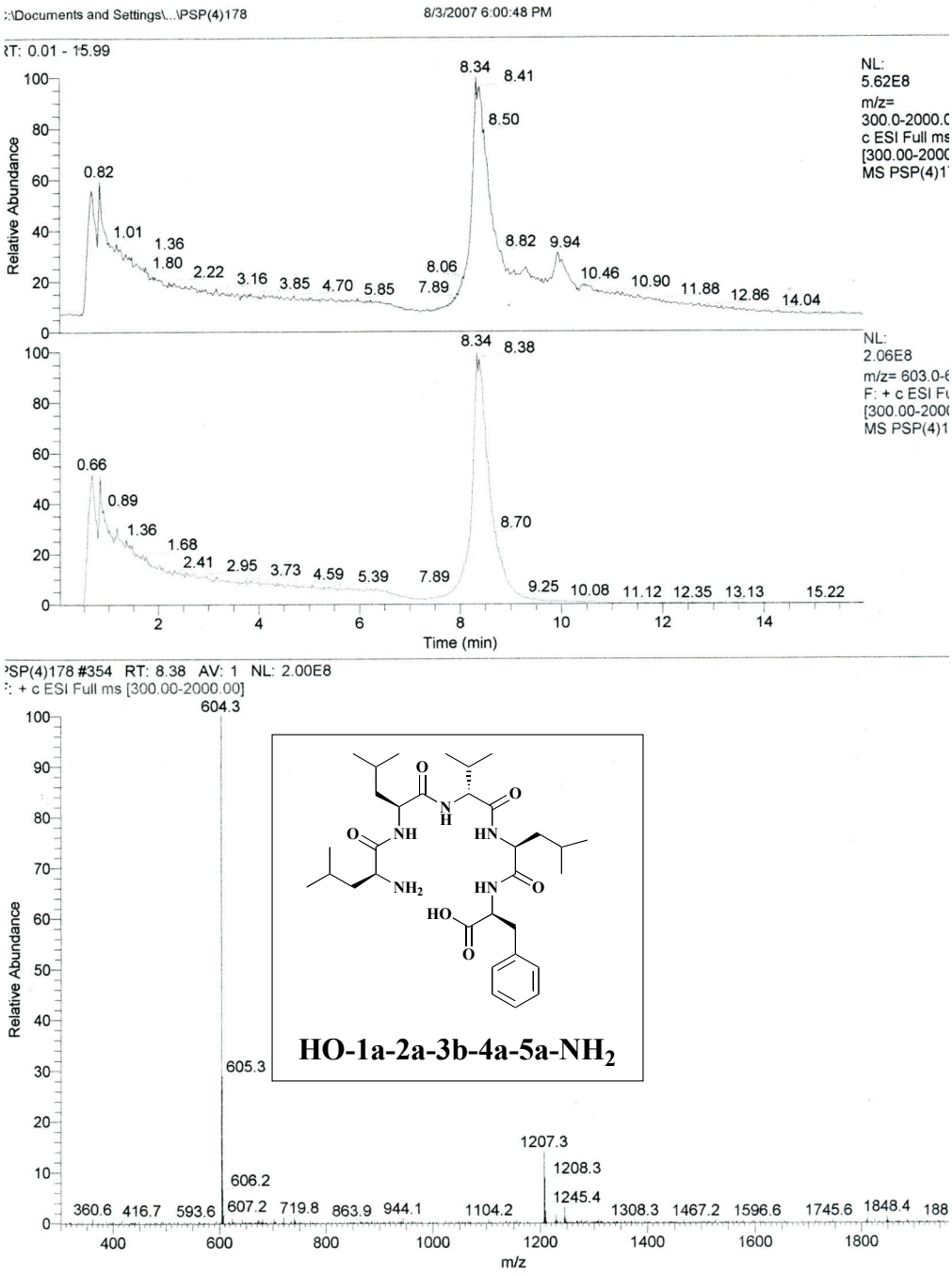

HO-1a-2a-3b-4a-5a-NH_2

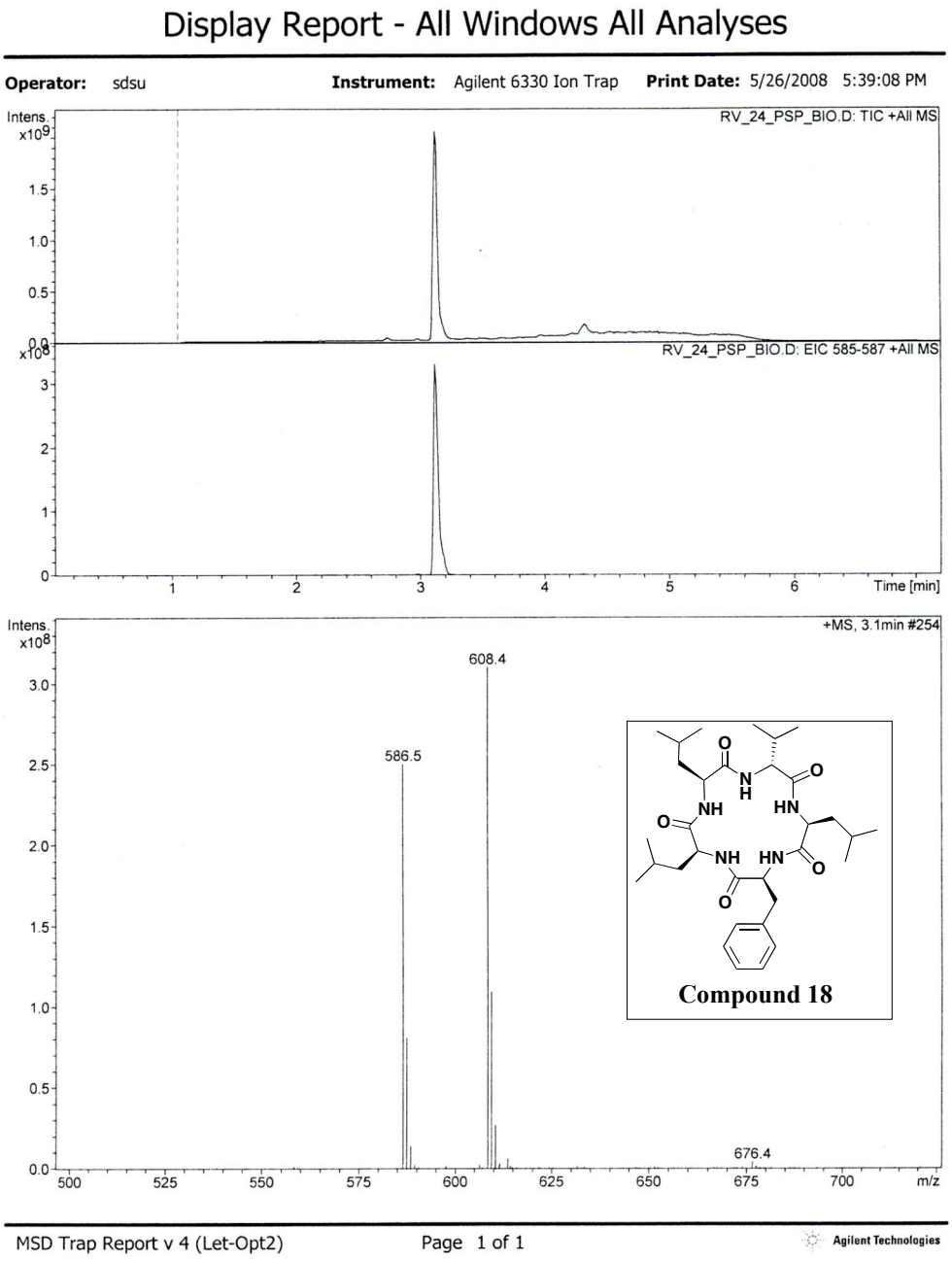
Display Report - All Windows All Analyses
Operator: sdsu
Instrument: Agilent 6330 Ion Trap
Print Date: 5/26/2008 5:39:08 PM
RV_24_PSP_BIO.D: TIC +All MS
RV_24_PSP_BIO.D: EIC 585-587 +All MS
Time [min]
+MS, 3.1min #254
608.4
586.5
676.4
m/z
Compound 18
MSD Trap Report v 4 (Let-Opt2)
Page 1 of 1
Agilent Technologies

Compound 18

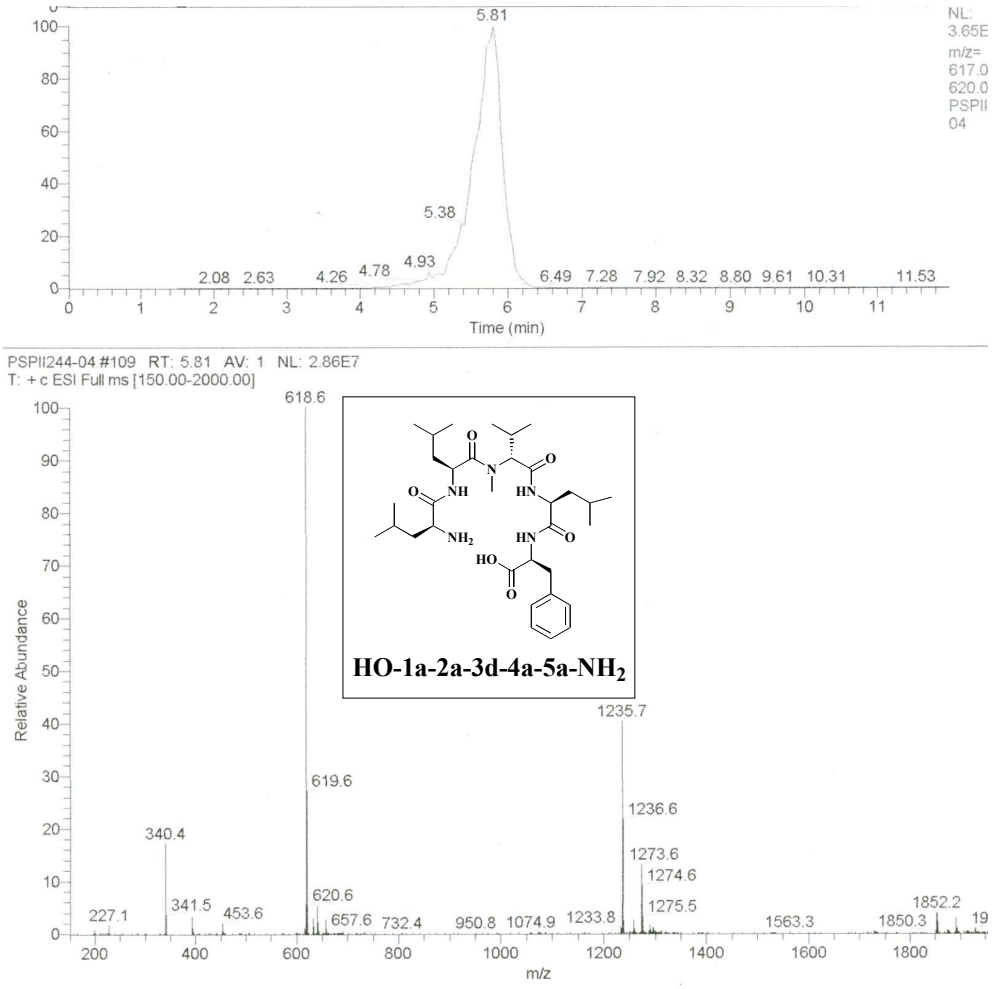

HO-1a-2a-3d-4a-5a-NH_2

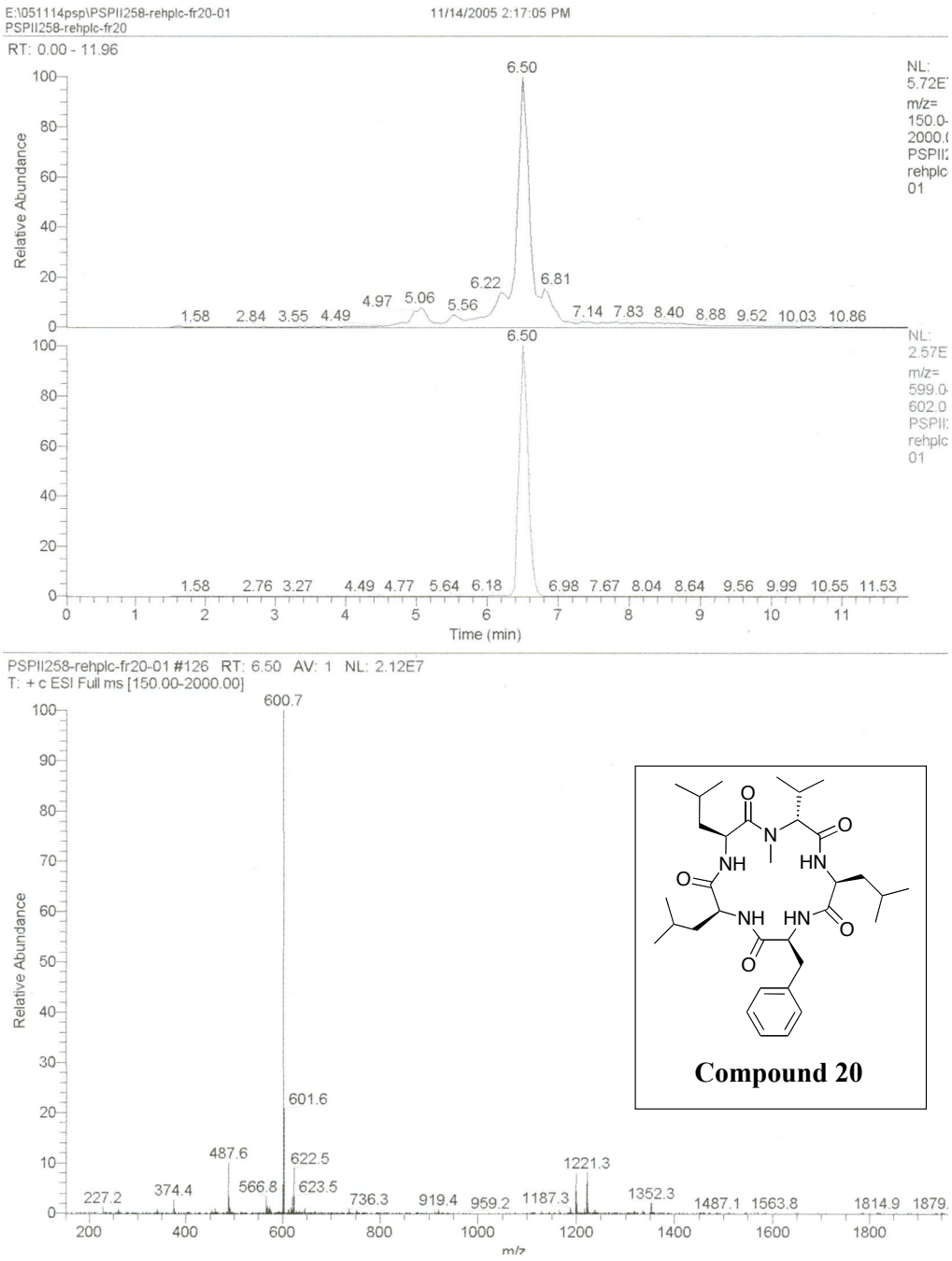
E:\051114psp\PSPII258-rehplc-fr20-01
PSPII258-rehplc-fr20
11/14/2005 2:17:05 PM
RT: 0.00 - 11.96
Relative Abundance
Time (min)
6.50
1.58 2.84 3.55 4.49 4.97 5.06 5.56 6.22 6.81 7.14 7.83 8.40 8.88 9.52 10.03 10.86
1.58 2.76 3.27 4.49 4.77 5.64 6.18 6.98 7.67 8.04 8.64 9.56 9.99 10.55 11.53
PSPII258-rehplc-fr20-01 #126 RT: 6.50 AV: 1 NL: 2.12E7
T: + c ESI Full ms [150.00-2000.00]
600.7
601.6
487.6
622.5
566.8
623.5
227.2
374.4
736.3
919.4
959.2
1187.3
1221.3
1352.3
1487.1
1563.8
1814.9
m/z
Compound 20

Compound 20

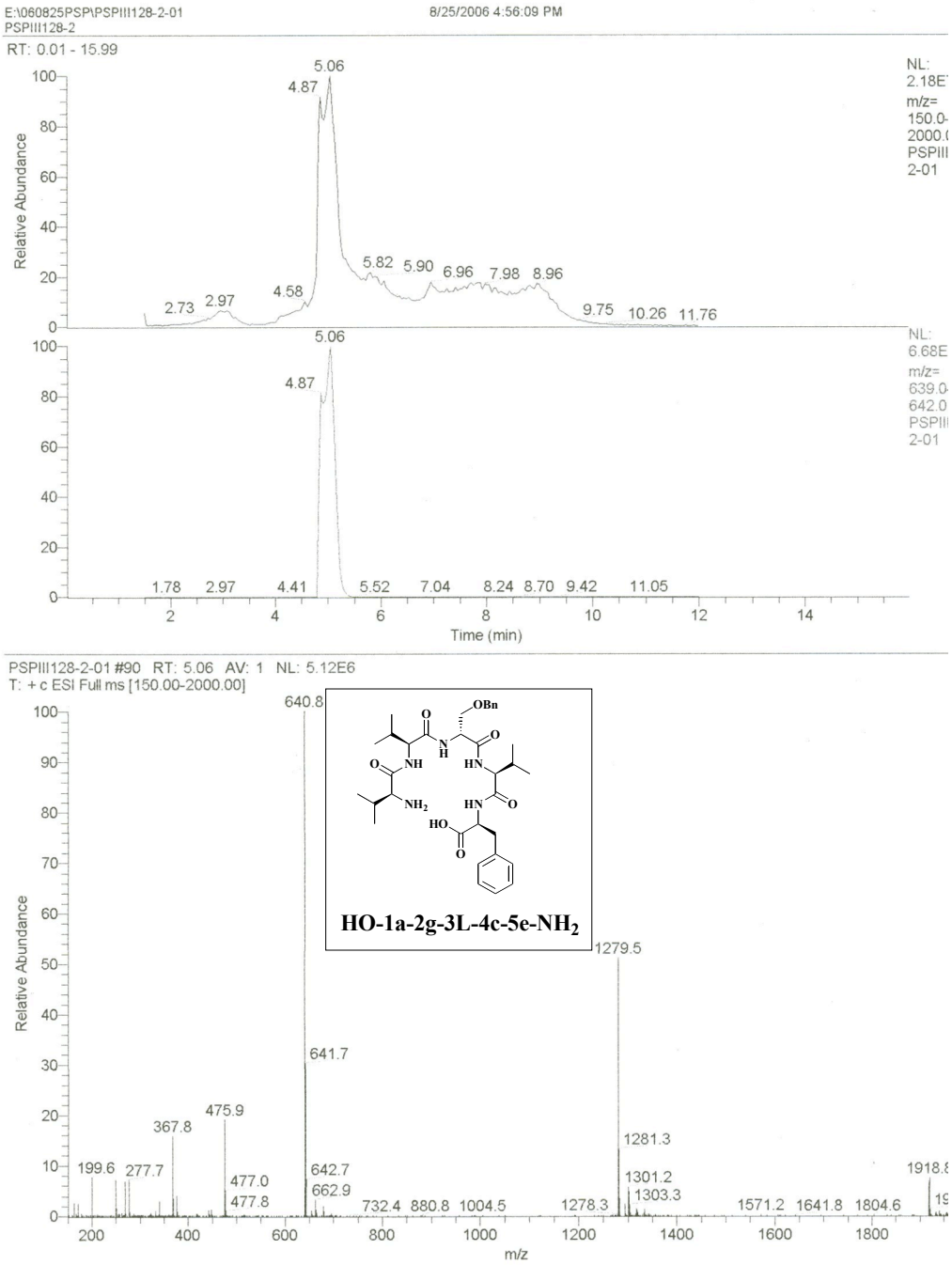

HO-1a-2g-3L-4c-5e-NH_2

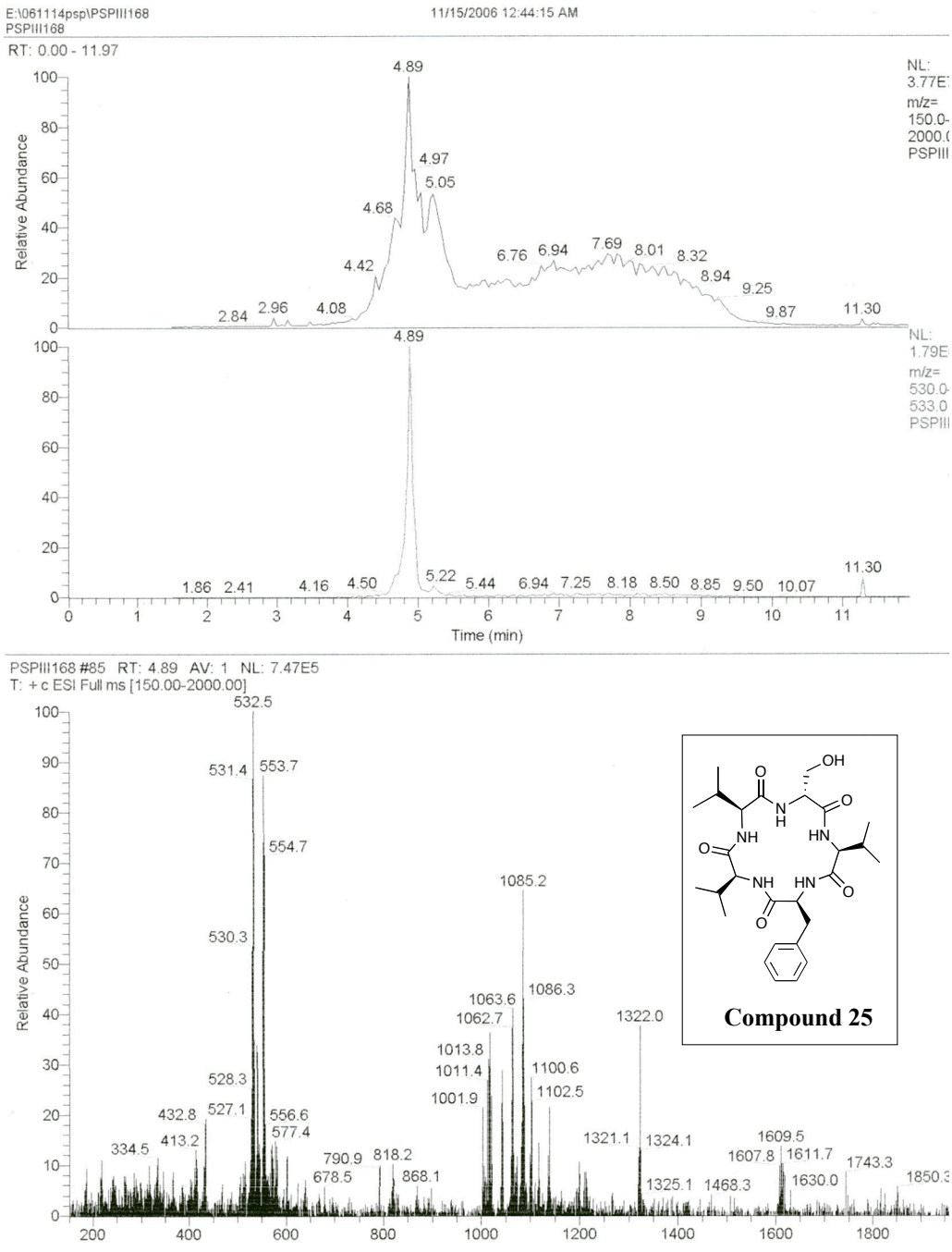
E:\061114psp\PSPIII168
PSPIII168
11/15/2006 12:44:15 AM
RT: 0.00 - 11.97
Relative Abundance
Time (min)
4.89
4.97
5.05
4.68
4.42
2.84
2.96
4.08
6.76
6.94
7.69
8.01
8.32
8.94
9.25
9.87
11.30
1.86
2.41
4.16
4.50
5.22
5.44
6.94
7.25
8.18
8.50
8.85
9.50
10.07
PSPIII168 #85 RT: 4.89 AV: 1 NL: 7.47E5
T: + c ESI Full ms [150.00-2000.00]
532.5
531.4
553.7
554.7
530.3
528.3
527.1
432.8
413.2
334.5
556.6
577.4
790.9
678.5
818.2
868.1
1085.2
1086.3
1063.6
1062.7
1013.8
1011.4
1001.9
1100.6
1102.5
1322.0
1321.1
1324.1
1325.1
1468.3
1609.5
1607.8
1611.7
1630.0
1743.3
1850.3
Compound 25

Compound 25

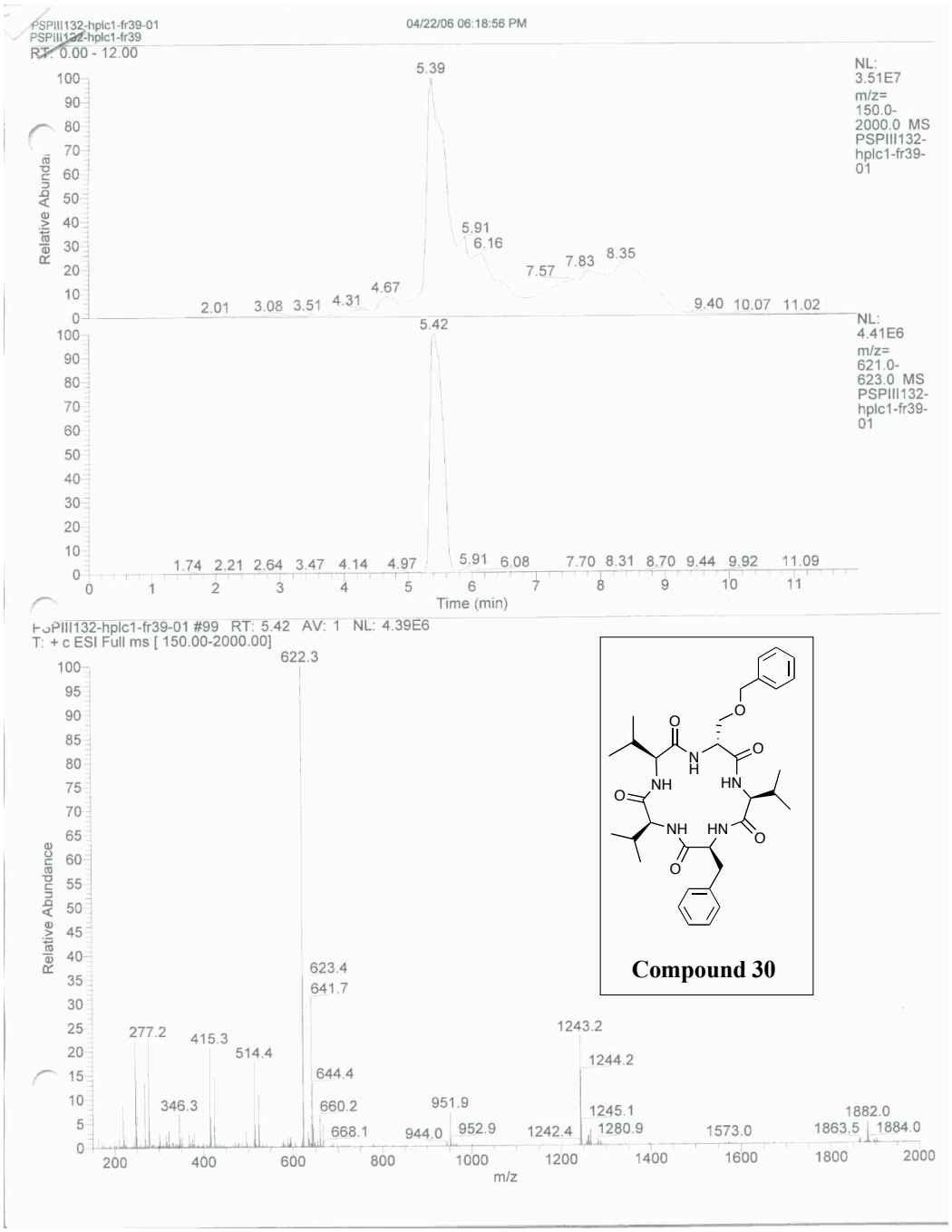
PSPIII132-hplc1-fr39-01
PSPIII132-hplc1-fr39
RT: 0.00 - 12.00
04/22/06 06:18:56 PM
NL: 3.51E7 m/z= 150.0-2000.0 MS PSPIII132-hplc1-fr39-01
NL: 4.41E6 m/z= 621.0-623.0 MS PSPIII132-hplc1-fr39-01
Relative Abundance
Time (min)
PSPIII132-hplc1-fr39-01 #99 RT: 5.42 AV: 1 NL: 4.39E6
T: + c ESI Full ms [150.00-2000.00]
m/z
Compound 30

Compound 30

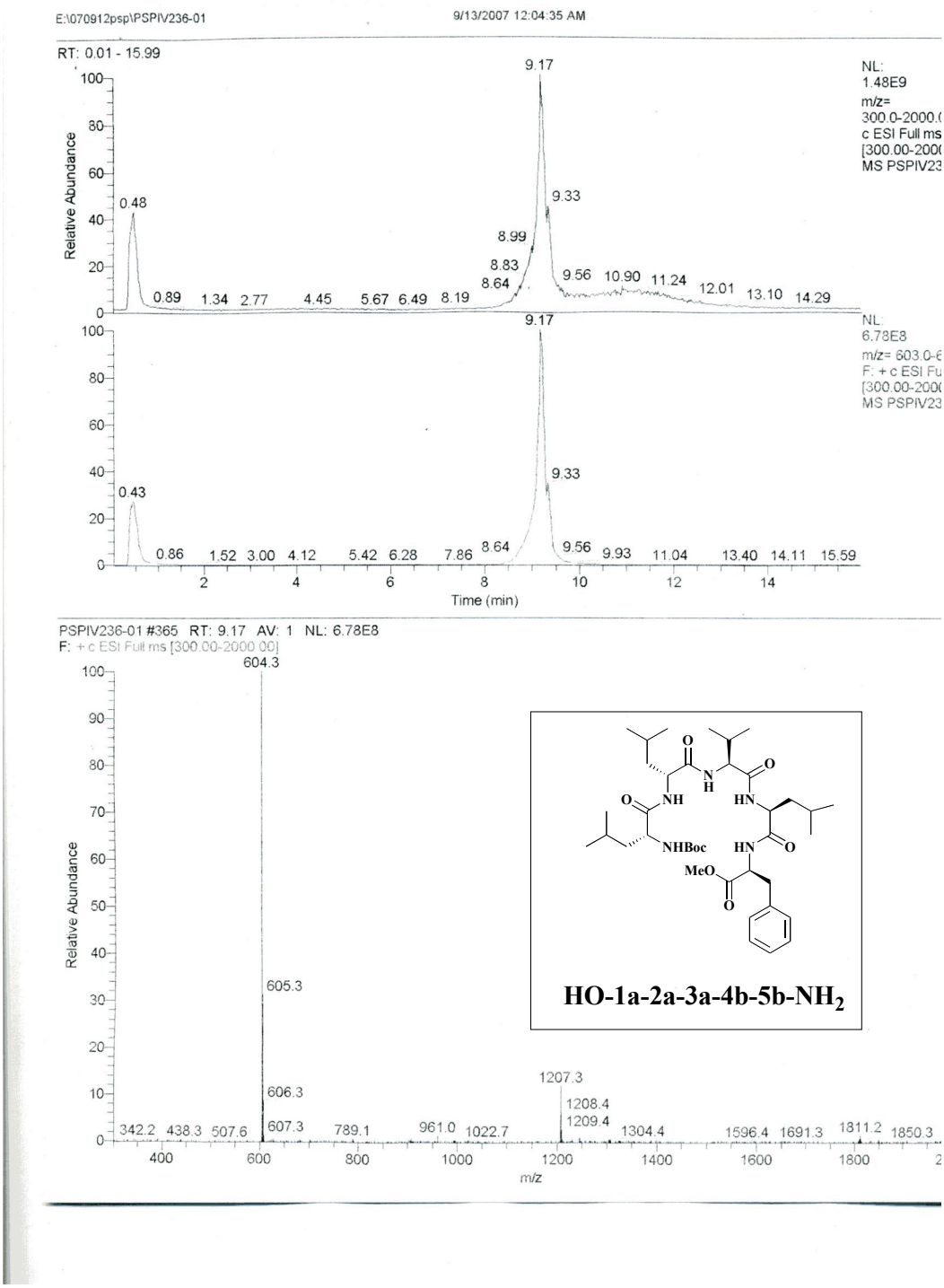

HO-1a-2a-3a-4b-5b-NH_2

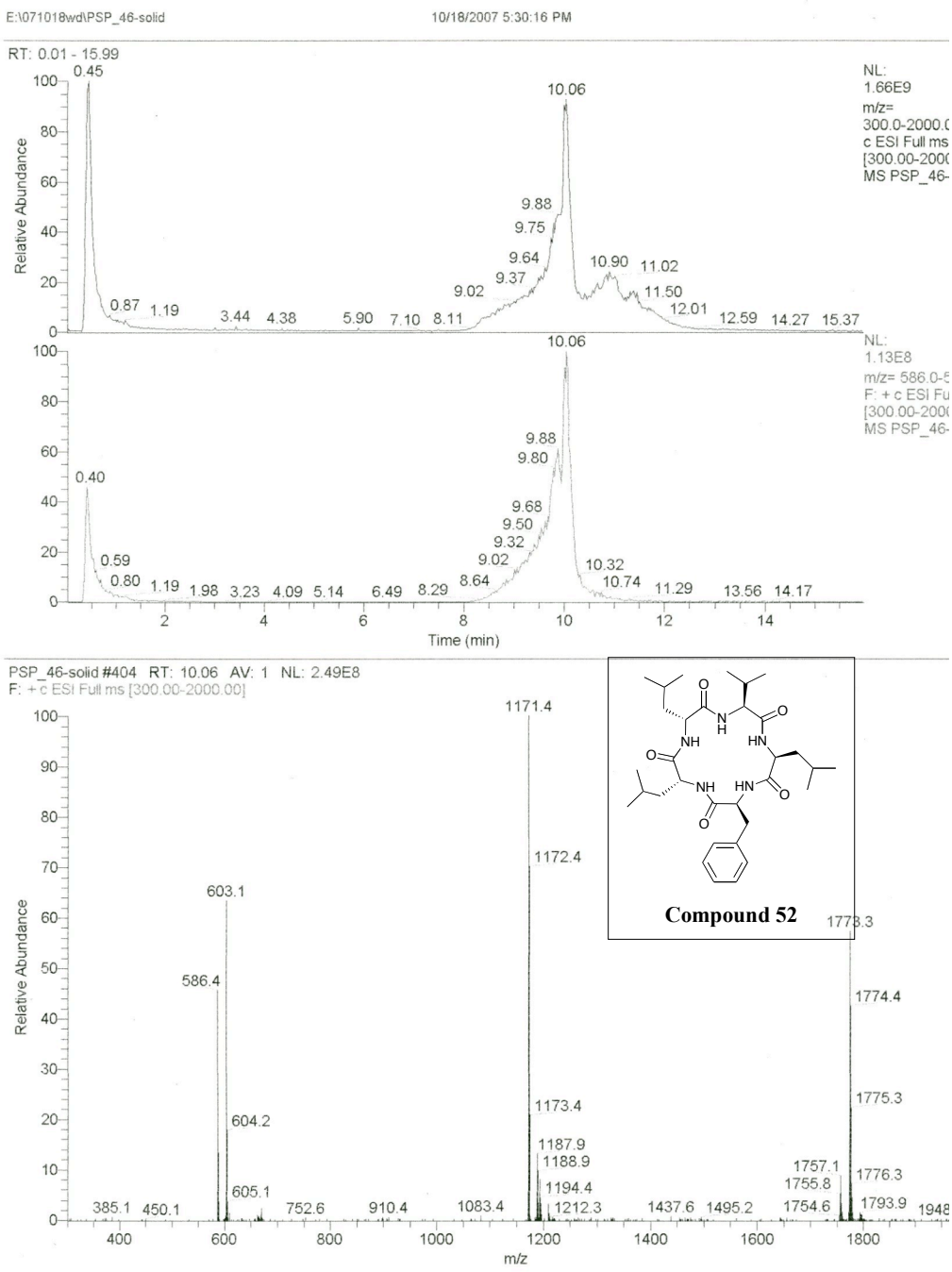
E:\071018wd\PSP_46-solid
10/18/2007 5:30:16 PM
RT: 0.01 - 15.99
Relative Abundance
Time (min)
NL:
1.66E9
m/z=
300.0-2000.0
c ESI Full ms
[300.00-2000
MS PSP_46-
NL:
1.13E8
m/z= 586.0-5
F: + c ESI Fu
[300.00-2000
MS PSP_46-
PSP_46-solid #404 RT: 10.06 AV: 1 NL: 2.49E8
F: + c ESI Full ms [300.00-2000.00]
m/z
Compound 52

Compound 52

LCMS for Holliday Junction Project

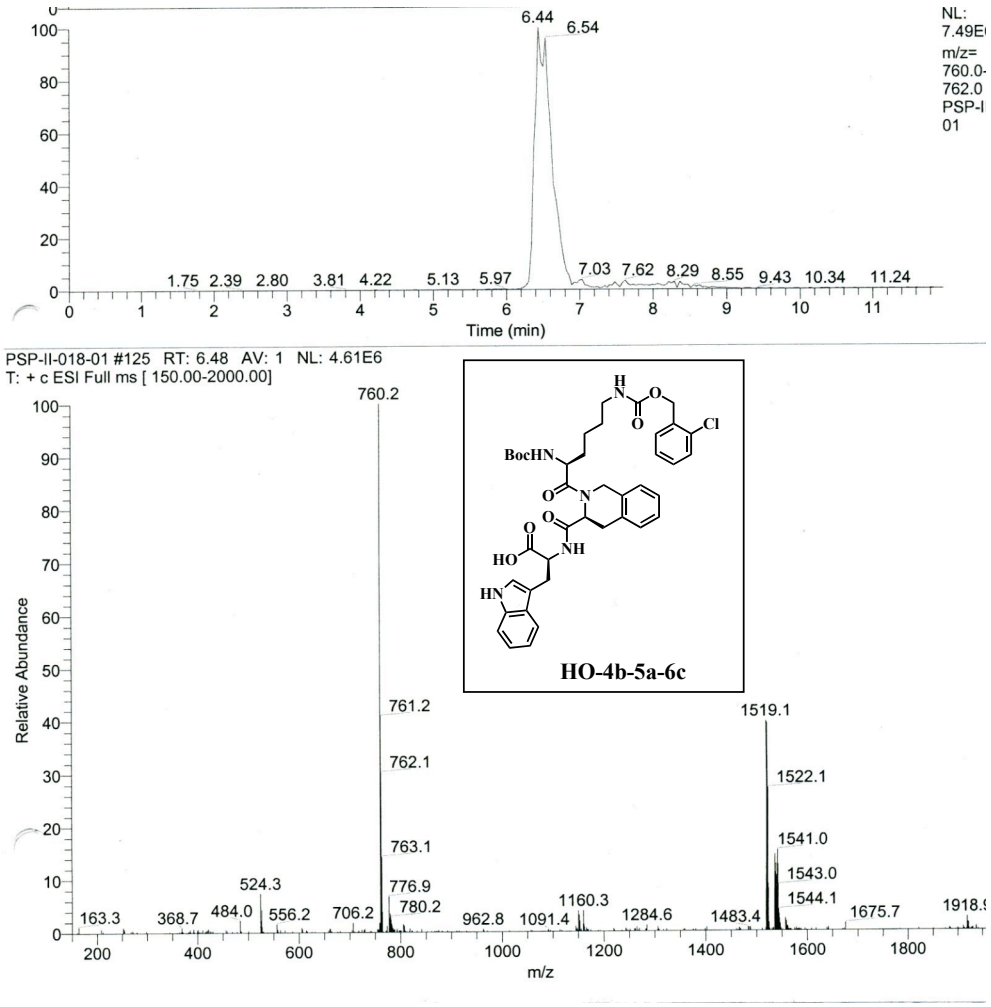

HO-4b-5a-6c

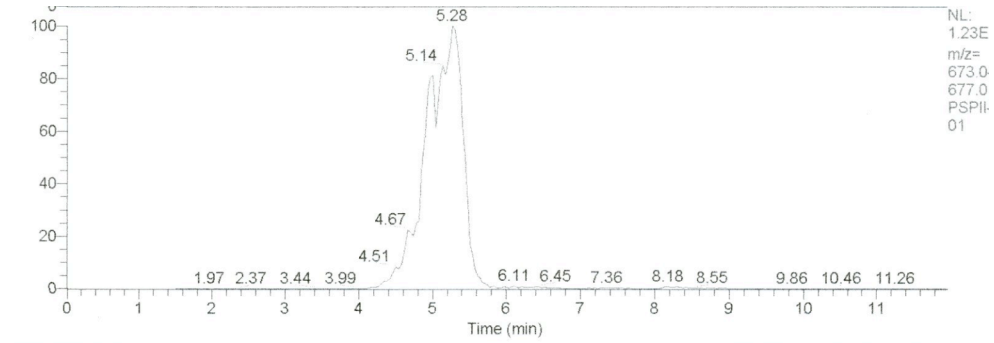
5.28
5.14
4.67
4.51
1.97 2.37 3.44 3.99
6.11 6.45 7.36 8.18 8.55 9.86 10.46 11.26
Time (min)
NL:
1.23E
m/z=
673.0
677.0
PSPII-
01

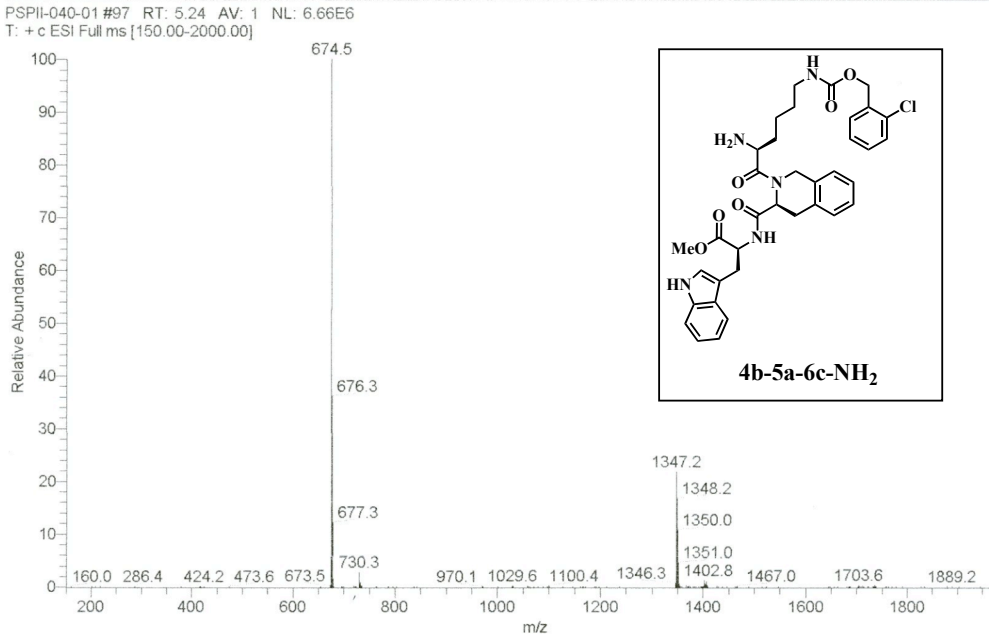
PSPII-040-01 #97 RT: 5.24 AV: 1 NL: 6.66E6
T: + c ESI Full ms [150.00-2000.00]
674.5
676.3
677.3
730.3
1347.2
1348.2
1350.0
1351.0
1402.8
160.0 286.4 424.2 473.6 673.5
970.1 1029.6 1100.4 1346.3
1467.0 1703.6 1889.2
Relative Abundance
m/z
4b-5a-6c-NH2

4b-5a-6c-NH_2

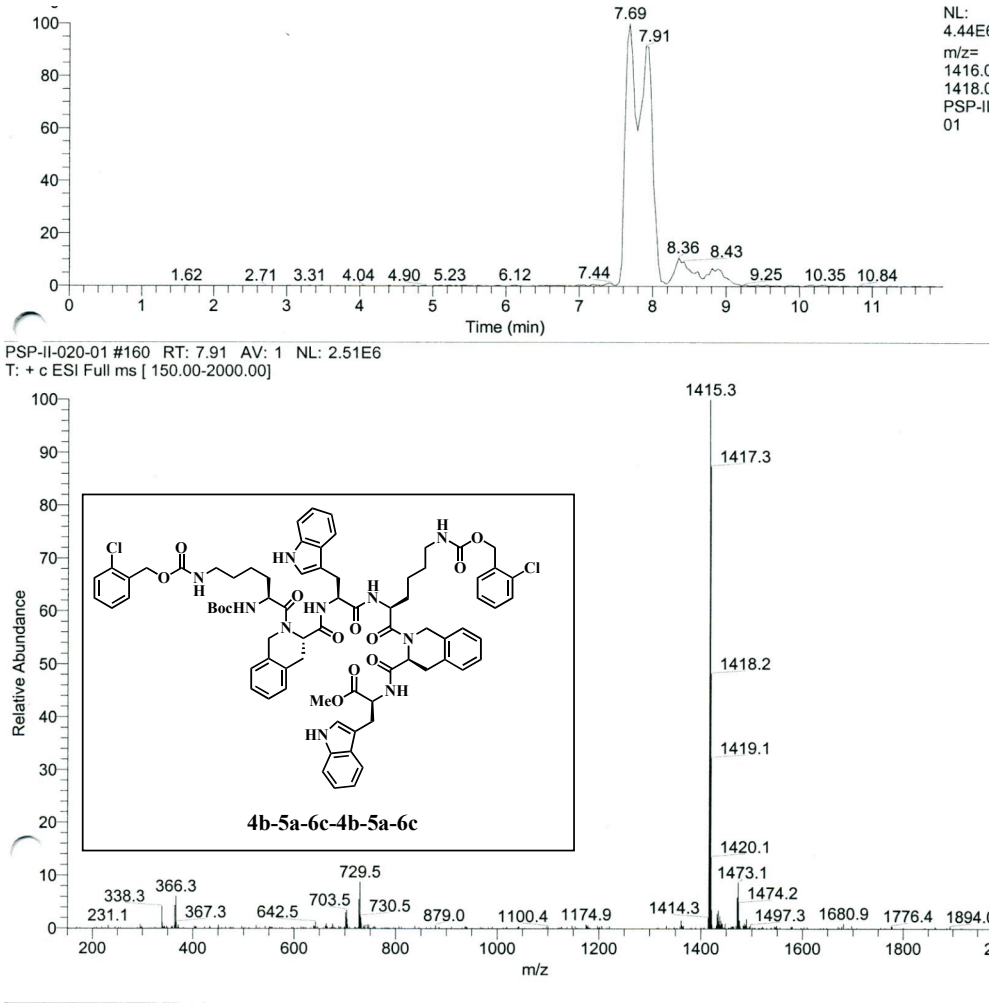

Linear hexapeptide **4b-5a-6c-4b-5a-6c**

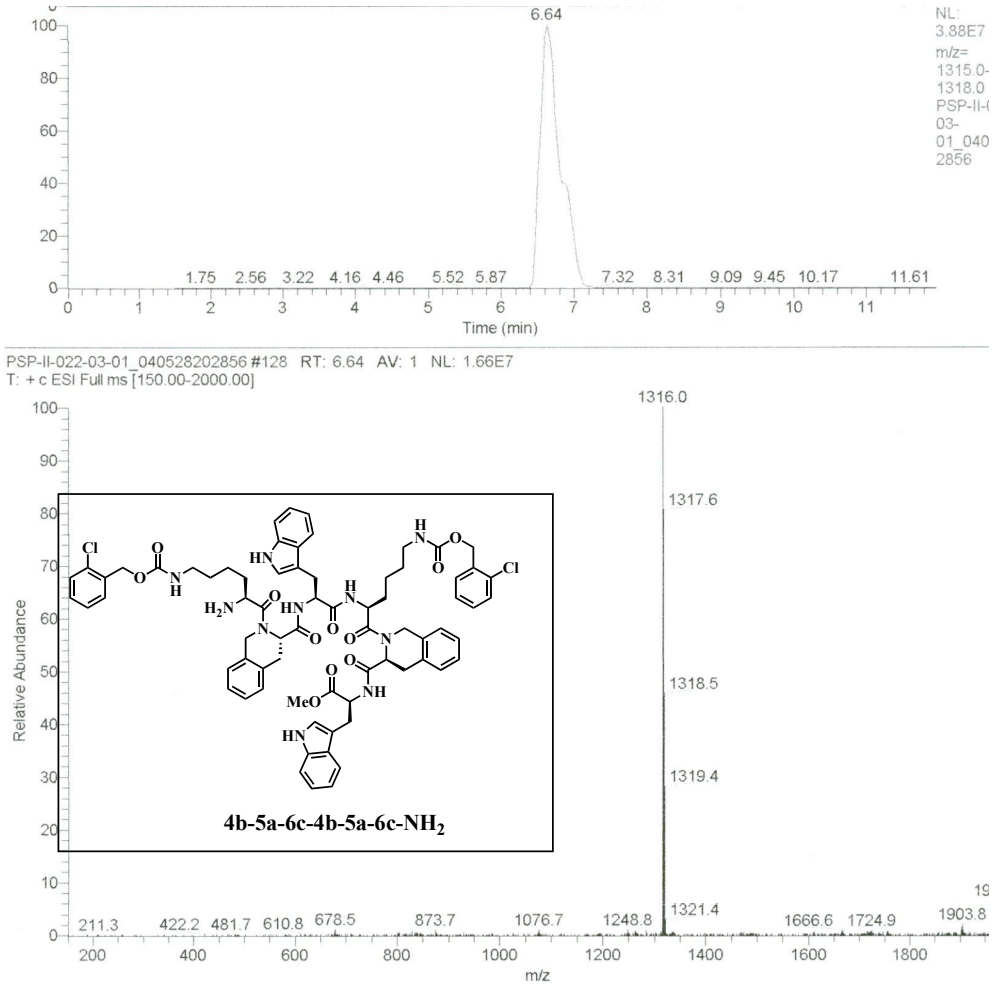

4b-5a-6c-4b-5a-6c-NH_2

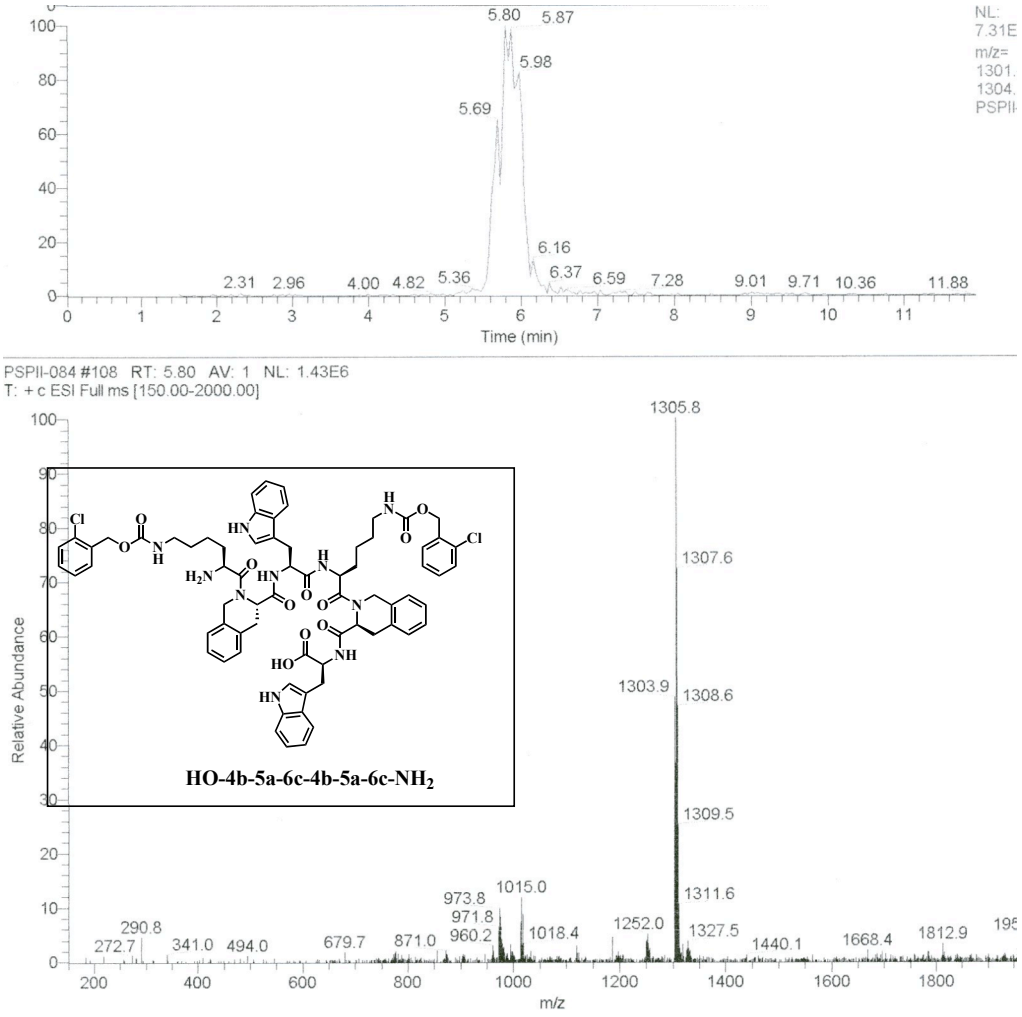

HO-4b-5a-6c-4b-5a-6c-NH_2

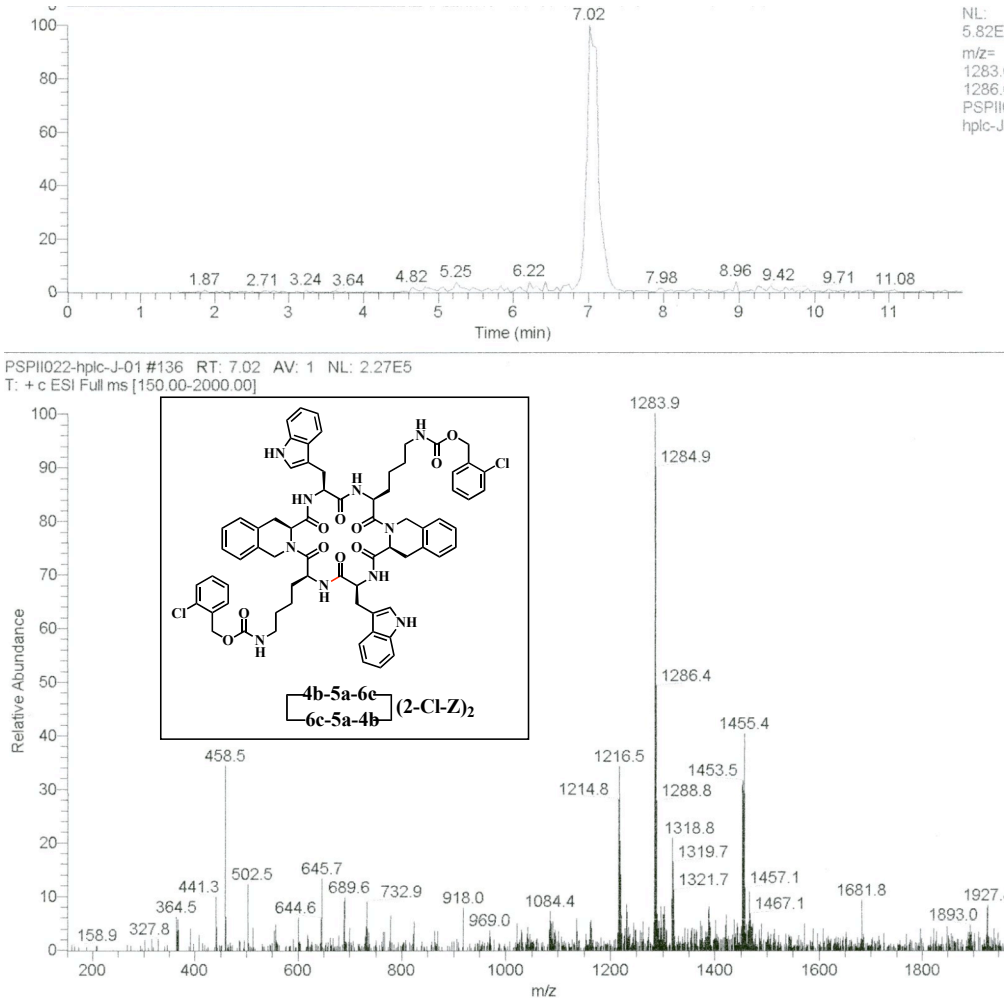

2-Cl-Z protected Cyclized hexapeptide **4b-5a-6c-4b-5a-6c**

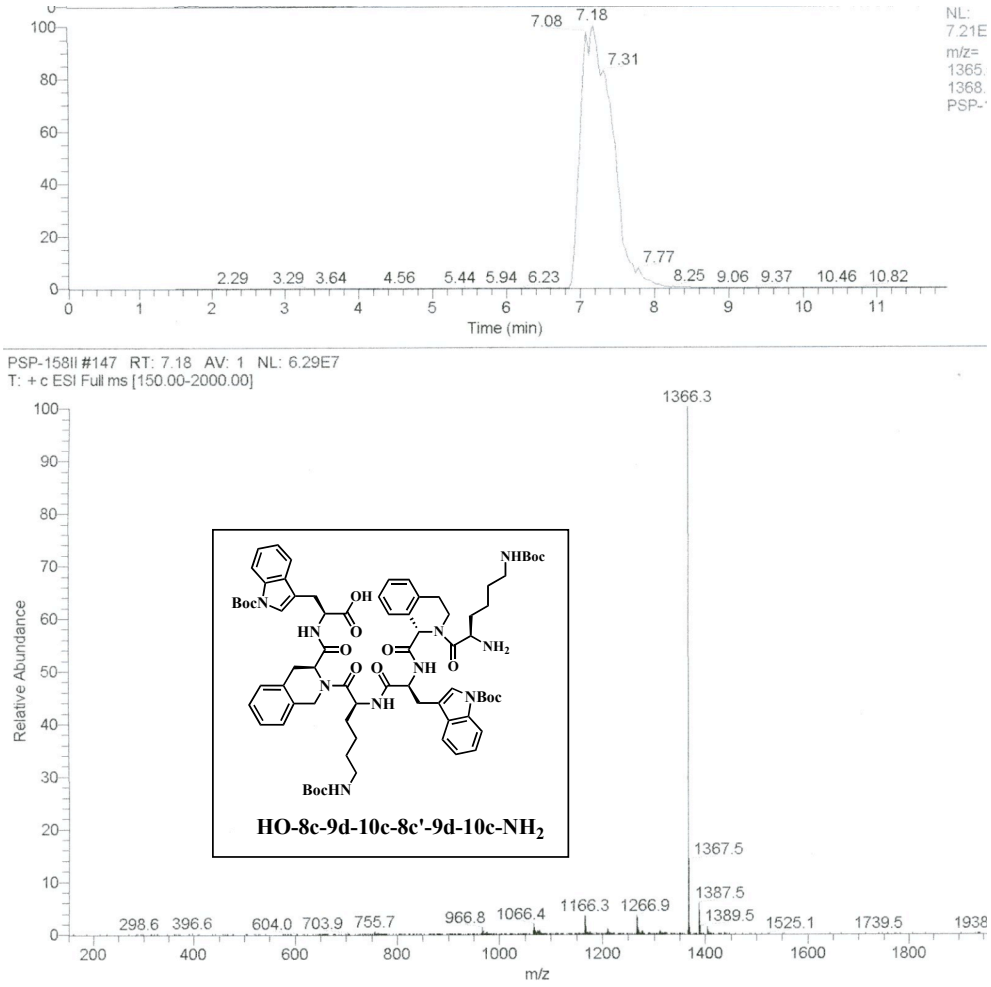

HO-8c-9d-10c-8c’-9d-10c-NH_2

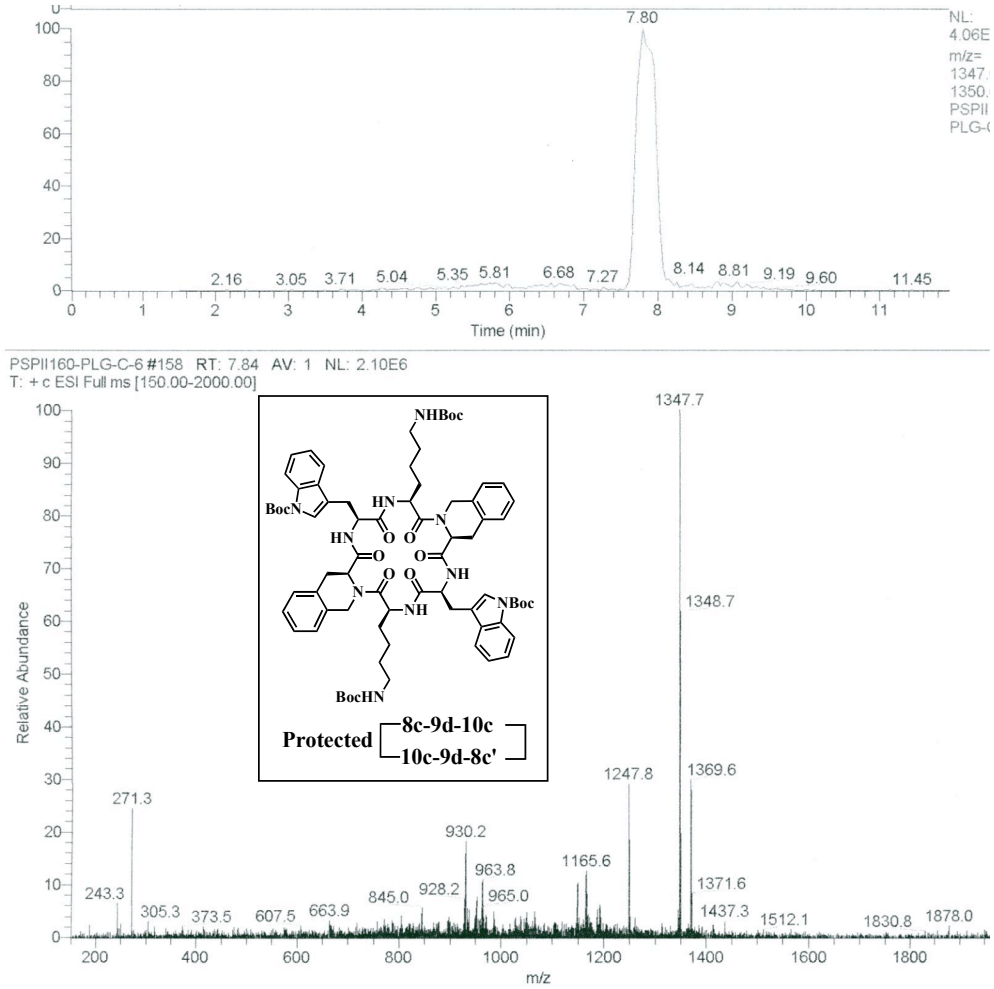

Protected cyclized hexapeptide **8c-9d-10c-8c'-9d-10c**

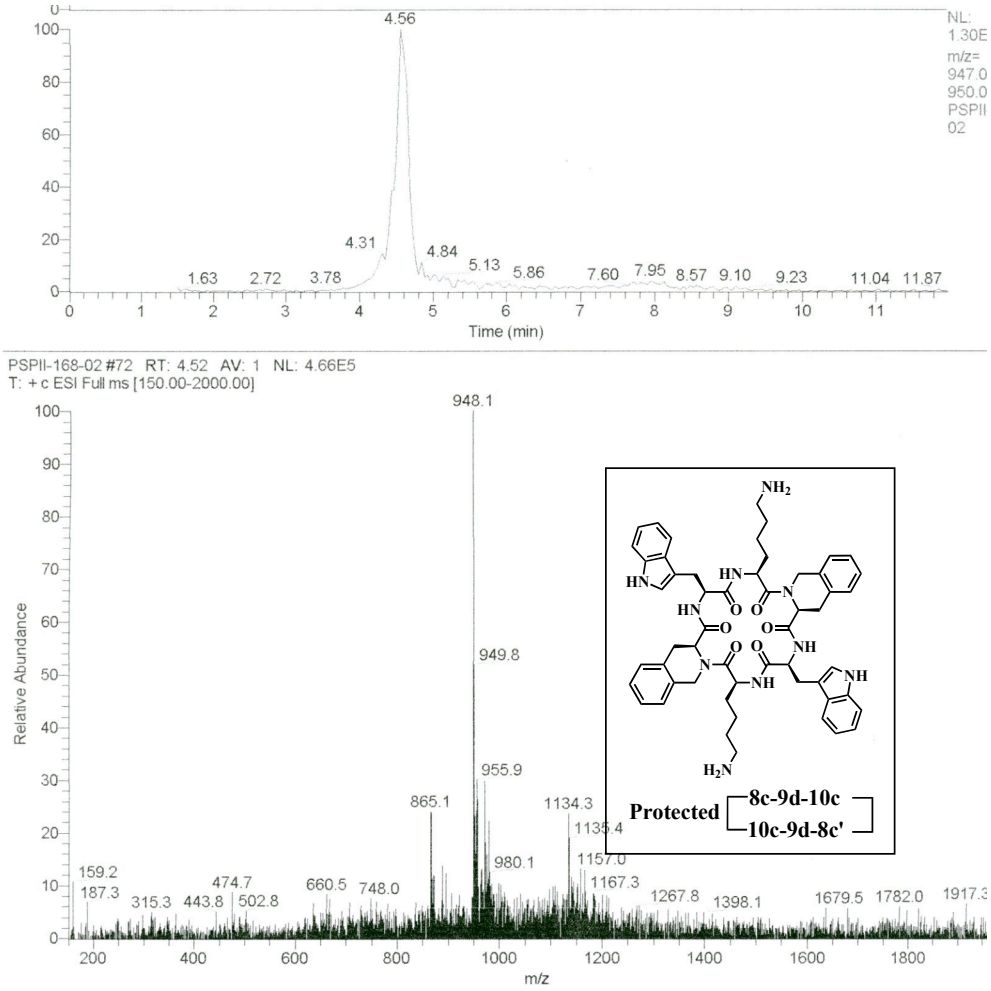
4.56
4.31
4.84
5.13
5.86
1.63
2.72
3.78
7.60
7.95
8.57
9.10
9.23
11.04
11.87
Time (min)
NL:
1.30E
m/z=
947.0
950.0
PSPII
02
PSPII-168-02 #72 RT: 4.52 AV: 1 NL: 4.66E5
T: + c ESI Full ms [150.00-2000.00]
948.1
949.8
955.9
865.1
1134.3
1135.4
980.1
1157.0
1167.3
159.2
187.3
315.3
443.8
474.7
502.8
660.5
748.0
1267.8
1398.1
1679.5
1782.0
1917.3
Relative Abundance
m/z
Protected
8c-9d-10c
10c-9d-8c'

HJ compd 10